Analysis of Fatigue Crack Propagation in Welded Steels

Roberto Angelo DeMarte
Marquette University

ANALYSIS OF FATIGUE CRACK PROPAGATION IN WELDED STEELS

By

Roberto A. DeMarte, B.S.M.E.

A Thesis submitted to the Faculty of the Graduate School,
Marquette University,
In Partial Fulfillment of the Requirements for
the Degree of Master of Science

Milwaukee, Wisconsin

December 2016

ABSTRACT

ANALYSIS OF FATIGUE CRACK PROPAGATION IN WELDED STEELS

Roberto A. DeMarte, B.S.M.E.

Marquette University, 2016

This thesis presents the study of fatigue crack propagation in a low carbon steel (ASTM A36) and two different weld metals (AWS A5.18 and AWS A5.28). Fatigue crack propagation data for each weld wire is of interest because of its use for predicting and analyzing service failures. Fatigue crack growth test specimens were developed and fabricated for the low carbon steel base metal and for each weld wire. Weld specimens were stress relieved prior to fatigue testing. Specimens were tested on a closed-loop servo hydraulic test machine at two different load ratios. Fatigue test data was collected to characterize both Region I and Region II crack propagation for each material. Test materials were characterized and fracture surfaces were analyzed. Experimental test results were compared to fatigue striation measurements taken using a scanning electron microscope (SEM).

Region II fatigue crack propagation data for ASTM A36 was found to be in agreement with existing R=0.05 and R=0.6 data for ferritic-pearlitic steels. Region II fatigue crack propagation data for weld metal was generally the same as ASTM A36 and within the limits of other weld metals. Scanning electron microscopy of the Region II fracture surfaces showed that they all exhibited similar fracture features (striations), indicating that the crack propagation mechanism was the same in all cases.

Region I fatigue crack propagation data resulted in higher ΔK_{th} values for AWS A5.18 as compared to AWS A5.28. ΔK_{th} values for ASTM A36 were in agreement with published values for mild steel. ΔK_{th} values were greater for load ratios R=0.05 as compared to R=0.6. The greater ΔK_{th} values for R=0.05 are thought to be caused by crack closure. ΔK_{th} values for ASTM A36 and AWS A5.18 were greater than those of AWS A5.28. The grain structure of AWS A5.28 was found to be finer than those of ASTM A36 and AWS A5.18 and is thought to be the cause of the lower ΔK_{th} values.

ACKNOWLEDGEMENTS

Roberto A. DeMarte, B.S.M.E.

I express my gratitude to the many people who lent their support and encouragement in completing the requirements for the master's program, especially:

Dr. Raymond Fournelle, my advisor and thesis director, who provided guidance and served as a mentor throughout the course of my graduate studies.

Dr. Matthew Schaefer and Dr. James Rice for taking the time to assist me with this undertaking and serving on my thesis committee.

The many Deere & Co. employees, especially my supervisor Serena Darling, who granted the time and personal support to see this thesis to completion.

My family, Faye, Katrina, and Sarah, who always provided encouragement and sacrificed time together over the course of this academic endeavor. Their faith in me gave me focus and confidence to make this project a success.

TABLE OF CONTENTS

LIST OF FIGURES

LIST OF TABLES

I. INTRODUCTION

Sheet metal structures are prominent in many industrial and consumer vehicle designs. Such structures offer both the design engineer and customer greater flexibility, ease of manufacture, and ease of repair when compared to structures fabricated by other methods. It is often cost prohibitive for manufacturers to fabricate one piece stampings, castings, or forgings for low-annual production structures. As a result, welded sheet metal parts are often used because of their relatively short manufacturing lead time, reduced manufacturing cost, and optimum strength and fatigue properties.

When designing a welded sheet metal structure, an engineer needs to understand strength, hardness, and fatigue properties of the welded material and base material selected. Strength, hardness, and fatigue properties give the engineer necessary information needed to understand how a component will perform in service. Strength and hardness properties can be established with tensile tests and hardness tests. Fatigue properties can be generated using several different methods depending on the design philosophy used. To generate fatigue properties for damage tolerant design fatigue crack propagation testing is performed.

In this study fatigue crack propagation studies were performed to characterize how a fatigue crack grows at a given stress intensity factor range. Fatigue crack propagation studies are important to the design engineer because they serve as a useful tool for understanding the fatigue characteristics of a component design, troubleshooting and predicting component failures. This study is focused on characterizing fatigue crack growth and fatigue crack threshold in a low carbon steel (ASTM A36) and two different weld materials (AWS A5.18 and AWS A5.28). Fatigue crack propagation and threshold are of particular interest in these materials because of the 1) common practice of using welded low carbon steels in sheet metal structures and 2) unexpected fatigue failures that can happen in structures while in service. The results of fatigue crack propagation studies allow the designer to create systems that are designed to tolerate flaws and to understand the rate at which the crack will grow if a crack is detected.

II. LITERATURE REVIEW

2.1. Review of Fatigue

Fatigue is defined as “the process of progressive localized permanent structural change occurring in a material subjected to conditions that produce fluctuating stresses and strains at some point and that may culminate in cracks or complete fracture after a sufficient number of fluctuations.” [1]

There are three factors that are necessary to cause fatigue failure: 1) a maximum tensile stress of sufficiently high value; 2) a large enough cyclical variation or fluctuation in the applied stress; 3) a sufficiently large number of cycles of the applied stress. [2] If any one of these conditions are not present, a fatigue crack will not initiate or propagate.

Fatigue failure can be divided into 5 different stages [3]:

1. Cyclic plastic deformation prior to fatigue crack initiation
2. Initiation of one or more microcracks
3. Propagation or coalescence of microcracks to form one or more macrocracks
4. Propagation of one of more macrocracks
5. Final failure

The division of these five stages are defined by the damage in the fatigued component. Fatigue failures generally start from imperfections in the surface of a component by the formation of cracks at these locations. These fatigue cracks can start very early in the service life of a component and will generally propagate slowly through the material in a direction perpendicular to the main axis of tensile loading. The component ultimately fails when the cross-sectional area becomes small enough to where the load cannot be supported.

Three common features of fatigue failure are [4]:

1. A distinct crack nucleation site or sites
2. Beach marks indicating crack growth
3. A distinct final fracture region

Fatigue is generally categorized into high-cycle or low-cycle fatigue. High-cycle fatigue is failure that occurs at a high number of cycles (typically $N > 10^4$cycles) with an applied stress in the elastic range. High-cycle fatigue is seen in applications such as turbine engines, railroad axles, railroad bridges, and aircraft. Low-cycle fatigue occurs when macroscopic plastic deformation is present during every fatigue cycle. Low-cycle fatigue typically occurs when $N < 10^4$cycles. [3] Applications where low-cycle fatigue designs are typically considered are nuclear pressure vessels, steam turbines, and other types of power equipment.

There are three basic types of approaches used in component design for fatigue:

4. Stress-life $(S - N)$
5. Strain-life $(\varepsilon - N)$
6. Fracture mechanics crack growth $(\frac{da}{dN} - \Delta K)$

The stress-life and strain-life approaches are typically used when a structure is considered to have no flaws. A flaw can be considered to be a crack of any size, a void, or a material discontinuity in the component being evaluated. Stress-life properties are used in infinite-life design which requires local stresses or strains to be elastic and below the fatigue limit of the material. Infinite-life design works well for parts that are exposed to several million cycles but can be impractical for applications where excessive weight and size are factors. Strain-life properties are typically used in safe-life design typically in conjunction with stress-life and fracture mechanic crack growth properties. Safe-life design criteria establishes a finite life for the design component. Establishing a finite life can allow for a much lighter and less costly design and is typically used in automotive and aircraft engineering.

Engineering data for both stress-life and strain-life properties are generated using flawless test specimens. These specimens limit the ability to distinguish between fatigue crack initiation life and fatigue crack propagation life. When flaws are present in structures, these methods offer little information on a quantitative basis for fatigue life assessment. The fracture mechanics approach uses test specimens with pre-existing flaws and offers improved understanding of the fatigue crack initiation and propagation. Conversely, the fracture mechanics approach (referred to as damage tolerant design) can provide further refinement to the safe-life design method by allowing a structure to be designed around pre-existing flaws. [4]

Damage tolerant design philosophies were adopted on many commercial and military aircraft after major fatigue failures in the 1950's. One example of a major fatigue failure was on the F-111A aircraft. On December 22, 1969 an F-111A based out of Nellis Air Force Base was on a mission for operational testing of rockets for the Nellis range. During rocket delivery a wing completely detached from the aircraft during flight. The F-111 was the first production aircraft to utilize variable geometry wings which used a high strength steel wing pivot for the wing box. A defect in the wing pivot fitting was found to have lead to the catastrophic failure of the component and wing detachment. A 22 mm defect in the wing pivot was not observed during inspection and it was found that the fatigue crack grew only 0.38 mm before unstable brittle fracture occurred. The aircraft had only flown 107 flights. This F-111A and others drove changes in aircraft design philosophies to include damage tolerant design principles to prevent in service failures. [5] [6] [7]

Damage tolerant design should not be interpreted as a tool to allow continued safe operation with the known presence of a crack. Damage tolerant design provides the required information to generate an inspection program for a component in service that would not crack under normal conditions. [5]

2.2. Fatigue Crack Growth in Steel

Fatigue crack growth experiments are performed using a specimen with a pre-existing flaw to evaluate fatigue crack growth in materials. These test specimens have mechanically sharpened cracks that are typically subjected to the Mode I type of loading in tension described in Figure 2.2. [8] In this type of test cyclic loads are applied at a specified frequency as shown in Figure 2.1 and crack growth is monitored. Figure 2.1 shows a middle tension specimen loaded in tension with a constant stress amplitude ($\Delta\sigma$), load ratio ($R = \sigma_{min}/\sigma_{max}$), and cyclic frequency (ν). It also shows that crack length (a) increases with the number of fatigue cycles (N). Equation 1 summarizes the relationship among these parameters:

$$\left(\frac{da}{dN}\right)_{R,\nu} = f(\Delta\sigma, a) \tag{1}$$

where f is dependent on the geometry of the specimen and the loading configuration.

During fatigue crack growth testing the crack growth rate $\left(\frac{da}{dN}\right)$ increases as the crack length increases. Also, $\frac{da}{dN}$ is typically higher for any given crack length during tests conducted at high-load amplitudes.

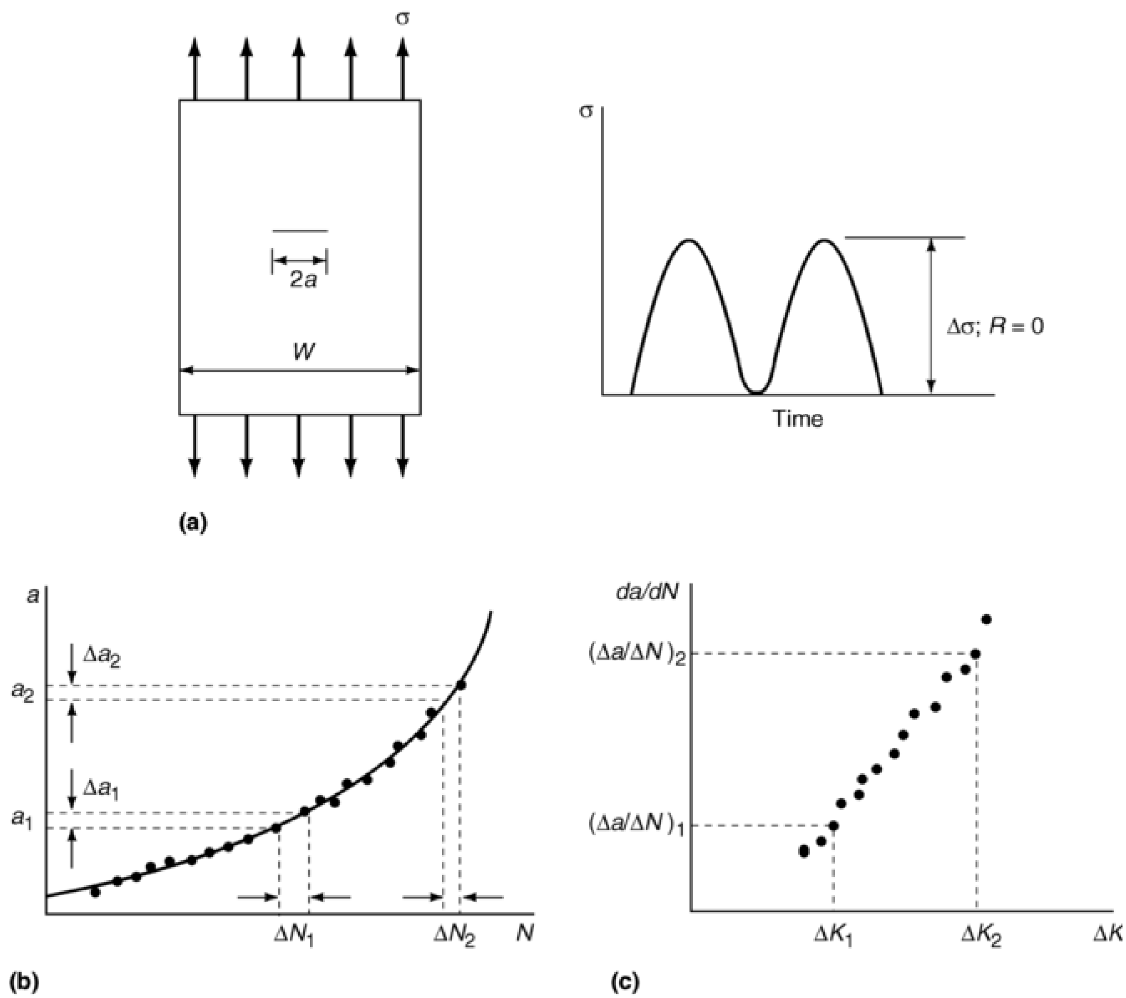

Figure 2.1. Schematic diagram of a middle tension test specimen, test data, and modeling process for generating fatigue crack growth data ($\frac{da}{dN} - \Delta K$) data. (a) Specimen and loading. (b) Measured data. (c) Rate data. [2]

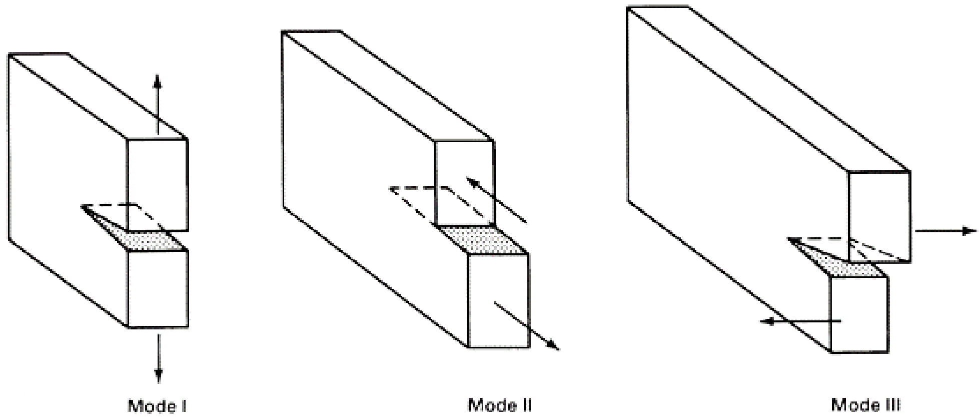

Figure 2.2. Three modes of loading that can be applied to a crack. [8]

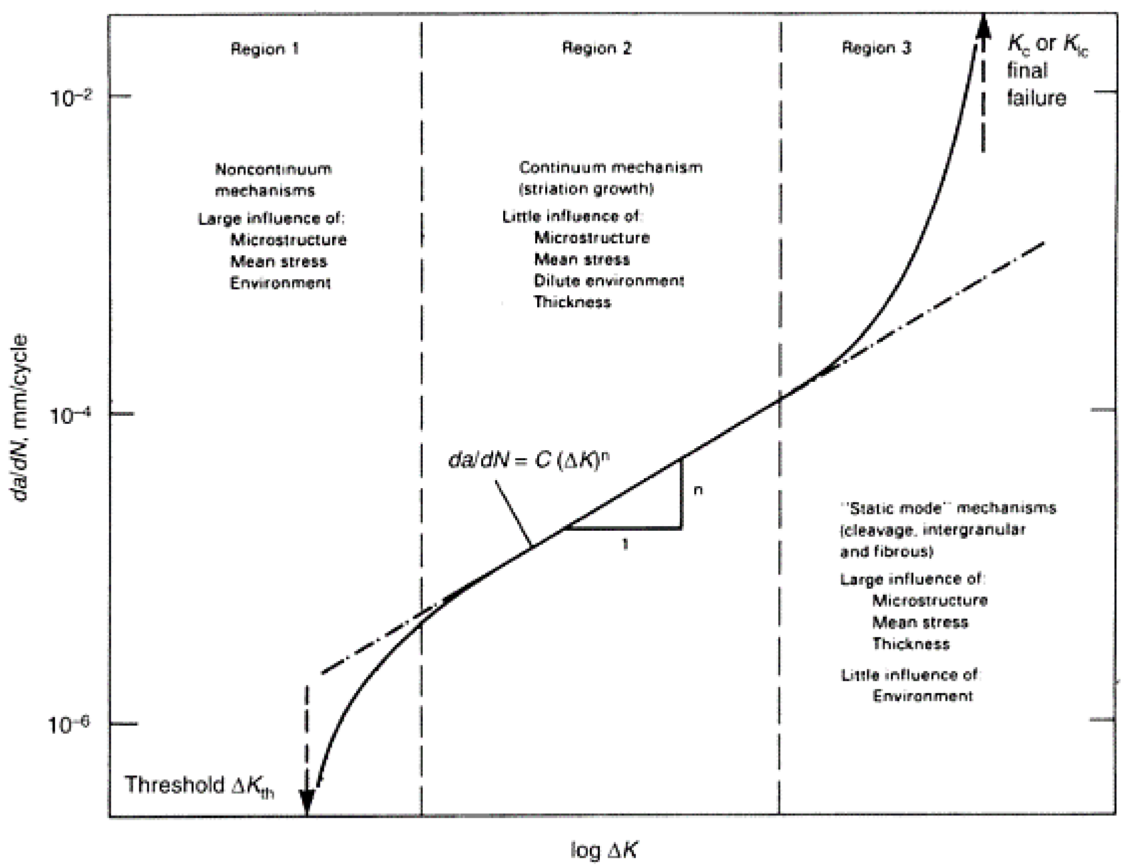

Figure 2.3. Log $\frac{da}{dN}$ vs. Log ΔK plot describing the three regions associated with crack growth rate. [5]

Fatigue crack growth rate test data is summarized in a plot of log $\frac{da}{dN}$ vs. log ΔK. ΔK is the stress intensity factor range defined by Equation 2 [9]:

$$\Delta K = K_{max} - K_{min} \tag{2}$$

where:

K_{max} is the maximum value of the stress intensity factor in a cycle. This value corresponds to σ_{max}.

K_{min} is the minimum value of the stress intensity factor in a cycle. This value corresponds to σ_{min} when R > 0 and is taken be zero when R ≤ 0.

The log $\frac{da}{dN}$ vs. log ΔK plot generally has a sigmoidal shape and is divided into three regions as shown in Figure 2.3. In Region 1 crack growth rate decreases rapidly with decreasing ΔK, approaching the lower threshold, ΔK_{th} where $\frac{da}{dN}$ decreases to zero. Experimentally this is defined as 10^{-10}m/cycle for most materials. It is important to note that crack growth can occur below ΔK_{th}, although it is unlikely that fatigue damage will occur at that range. ΔK_{th} for steel is typically less than 9 MPa $\sqrt{m}$. Mild steel with a tensile strength of 430 MPa has been found to have a ΔK_{th} of 6.6 MPa $\sqrt{m}$ at R=0.13 and 3.2 MPa $\sqrt{m}$ at R=0.64. [4] Region 1 is also extremely sensitive to changes in microstructure, environment, and mean stress. [4] [9] [10]

Region 2 crack growth rate is typically linear on a log-log plot and follows Paris' law defined by Equation 3 [11]:

$$\frac{da}{dN} = A\Delta K^m \tag{3}$$

where:

$\frac{da}{dN}$ = fatigue crack growth rate

ΔK = stress intensity factor range ($\Delta K = K_{max} - K_{min}$)

A, m = experimental constants dependent on external factors such as environment, material variables, frequency, temperature, and stress ratio

One factor affecting crack growth in Region 2 is the stress intensity factor range [2], and Region 2 is typically found in the range from 10 MPa $\sqrt{m}$ to 60 MPa $\sqrt{m}$ for ferritic-pearlitic steels. Region 2 fatigue crack growth corresponds to stable macroscopic crack growth and is typically influenced by environment. [4]

Region 3 involves accelerated crack growth that leads to final failure. In this region K_{max} approaches K_c and final failure occurs at $K_{max} = K_c$, where K_c is defined as fracture toughness. K_c is dependent on material, temperature, strain rate, environment, and specimen geometry. [4]

Fatigue crack growth rate is significantly affected by the stress ratio, $R = K_{min}/K_{max}$, and fatigue crack growth tests are typically done with tensile-tensile loading where $R \geq 0$. Figure 2.4 shows that as stress ratio increases, crack growth rate also increases in all areas of the curve for JIS SS41 steel, which is similar to ASTM A36. Mean stress effects can also affect the shape of the fatigue crack growth rate curve. The Paris equation (Equation 3) is typically modified to the Forman equation (Equation 4) to take into account stress ratio effects. [4]

$$\frac{da}{dN} = \frac{A\Delta K^m}{(1-R)K_c - \Delta K} \tag{4}$$

Mean stress effects are typically small in Region 2 while the effects can be much larger in Regions 1 and 3. Fatigue crack growth rate generally increases as crack length increases. This is very significant because the crack can become longer at a rapid rate which will shorten the life of the component at an alarming rate. This means that most of the loading cycles during the life of a component are during the early stages of crack growth when the crack is very small. [10]

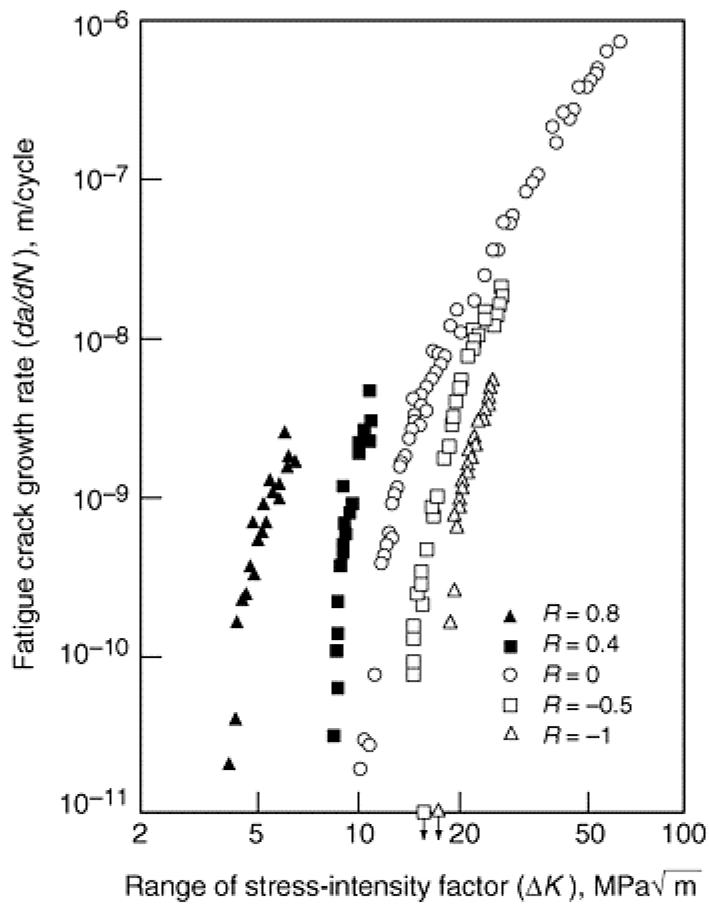

Figure 2.4. Comparison of load ratio (R) effects on fatigue crack growth rate in JIS SS41 steel. Reprinted with Permission from SAE International. [12]

Crack closure can also have an effect on fatigue crack growth rates. Crack closure occurs during cyclic loading when the crack remains closed even though a tensile stress is being applied. The crack will not fully open until a certain opening K level, K_{op}, is applied. The result of this phenomenon is that the only damaging portion of the load excursion occurs when the crack is fully open. This means only the $\Delta K_{eff} = K_{max} - K_{op}$ part of $\Delta K = K_{max} - K_{min}$ causes crack growth. Fatigue crack closure mechanisms in metals are known as plasticity-induced closure, roughness-induced closure, oxide-induced closure, closure induced by a viscous fluid, and transformation-induced closure. Crack closure is most pronounced at lower R-ratios. [13]

Analysis of fracture surfaces after fatigue crack propagation tests is required to determine if any of these crack closure mechanisms affect test results.

Test data from Rolfe and Barsom for ferritic-pearlitic steels have been fit with Equation 5 for Region 2. Here fatigue crack growth rate $\frac{da}{dN}$ is in (m/cycle) and ΔK is in (MPa$\sqrt{m}$). [11]

$$\frac{da}{dN} = 6.8 \times 10^{-12} (\Delta K)^{3.0} \tag{5}$$

Maddox obtained Region 2 crack growth data for weld filler metals with yield strengths ranging from 386 MPa (56 ksi) to 634 MPa (92 ksi). The fatigue crack growth information for these weld metals was generated with a middle tension specimen using a C-Mn base material. Maddox [14] summarized this data with the Paris equation in Equation 6 below. $\frac{da}{dN}$ is in (m/cycle) and ΔK is in (MPa$\sqrt{m}$).

$$\frac{da}{dN} = A(\Delta K)^{3.0} \tag{6}$$

where A ranges from 2.8×10^{-12} to 9.5×10^{-12}

III. EXPERIMENTAL SETUP

3.1. Specimen Materials

The base material being investigated was ASTM A36. ASTM A36 is classified as a low carbon steel (carbon content is less than 0.3). Mechanical property guidelines are listed in Table 3.1 and chemical composition requirements are listed in Table 3.2. [15]

Table 3.1. ASTM A36 mechanical property guidelines

Minimum Tensile Strength (MPa)	400
Minimum Yield Strength (MPa)	250
Minimum Elongation (%)	23

Table 3.2. Chemical requirements for ASTM A36 carbon structural steel (wt. %)

Carbon	**Phosphorus**	**Sulfur**	**Silicon**
0.25 max	0.04 max	0.05 max	0.4 max

The weld wire requirements for one set of welded specimens are given in AWS A5.18 ER70S-6. Mechanical properties are listed in Table 3.3. The brand of wire used is Lincoln Electric SuperArc L-56 with 1.3 mm wire diameter. It is typical to use this AWS A5.18 weld wire with a low carbon structural steel. Chemical requirements for the weld wire are listed in Table 3.4. [16]

Table 3.3. AWS A5.18 Welded Mechanical Property Requirements

Weld Condition	As-welded	Stress Relieved
Minimum Tensile Strength (MPa)	485	485
Minimum Yield Strength (MPa)	400	360
Minimum Elongation (%)	22	26

Table 3.4. AWS A5.18 Weld Wire Chemical Composition Requirements (wt. %)

Carbon	Manganese	Phosphorus	Sulfur	Silicon
0.06-0.15	1.40-1.85	0.025 max	0.035 max	0.80-1.15
Nickel	**Chromium**	**Molybdenum**	**Vanadium**	**Copper**
0.15 max	0.15 max	0.15 max	0.03 max	0.50 max

Weld wire requirements for the second set of welded specimens are given in AWS A5.28 ER100S-G with a 690 MPa (100 ksi) minimum tensile strength. For the 690 MPa weld wire, Lincoln Electric SuperArc LA-100 1.1 mm diameter was used. Typical chemical composition limits for the weld wire are listed in Table 3.5. [17]

Table 3.5. Typical SuperArc LA-100 (AWS A5.28 ER100S-G) Weld Wire Chemical Composition Limits (wt. %)

Carbon	Manganese	Phosphorus	Sulfur	Silicon	Titanium
0.05-0.06	1.63-1.69	0.005-0.009	0.002-0.005	0.46-0.50	0.03-0.04
Nickel	**Chromium**	**Molybdenum**	**Vanadium**	**Copper**	**Aluminum**
1.88-1.96	0.04-0.06	0.43-0.45	≤0.01	0.11-0.14	≤0.01

Chemical and mechanical requirements for AWS A5.28 ER100S-G are agreed to by the purchaser and supplier[1]. [17] The supplier provided material certification of 790 MPa tensile strength, 730 MPa yield strength, and 22% elongation.

[1] Exceptions to the agreement are the minimum tensile strength of 690 MPa and chemical composition requirements of nickel, chromium, and molybdenum.

3.2. Manufacture of ASTM E647 Standard Compact C(T) Tension Specimen for Fatigue Crack Growth Rate Testing

ASTM E647 standard compact C(T) tension specimens were used to study fatigue crack propagation in this study. The dimensions given in Figure 3.1 were used for both the base material and weld materials tested. A specimen thickness of 6 mm was chosen because of its common use for many off-highway structure applications.

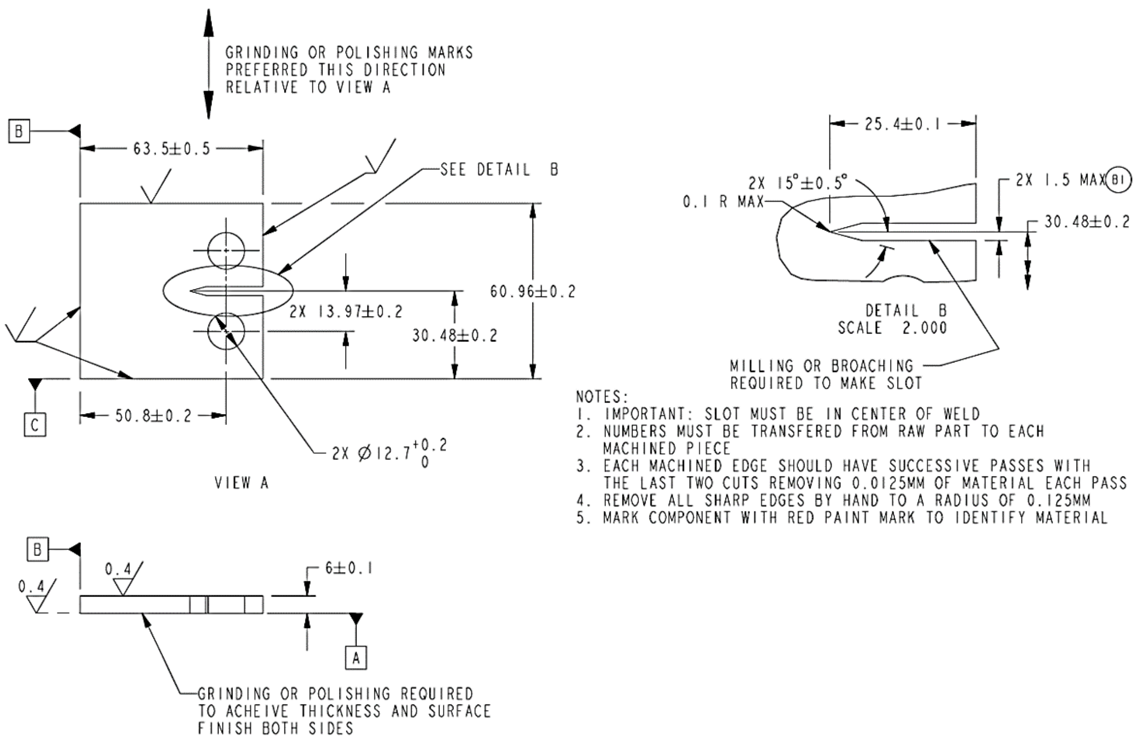

Figure 3.1. Specifications for machining compact specimen (units: mm)

Each specimen started with ASTM A36 plate steel base material with a thickness of 12.7 mm. The plate steel was cut on a Messer Cutting Systems plasma cutting table with each position noted and numbered with a punch after each cut (Figure 3.2). 69.0 mm x 71.5 mm rectangular blanks were cut for the base metal specimens, while 150 mm x 36.5 mm blanks were cut for the weld specimens.

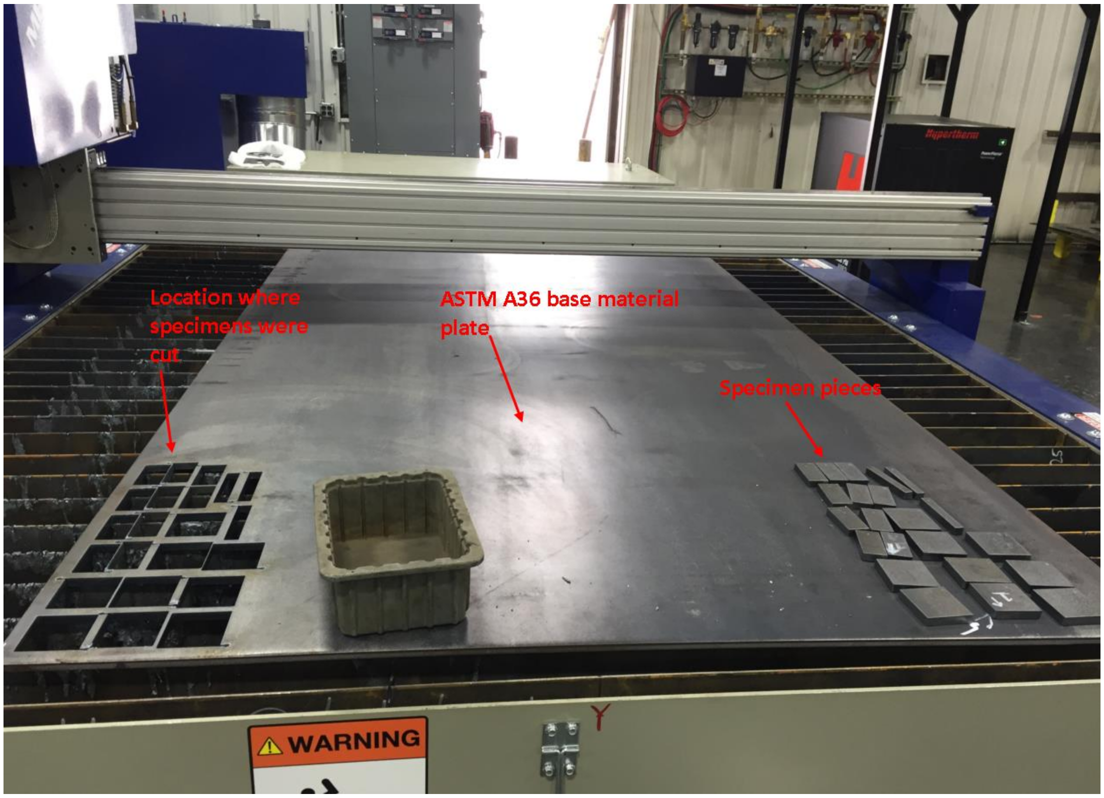

Figure 3.2. Specimen location and numbering on plasma cutter

The welded specimen blanks were joined as shown in Figure 3.3 using a Vizient gas metal arc welding (GMAW) robotic welder (Figure 3.4). Robotic welding was chosen for greater process stability for each welded specimen. As can be seen in Figure 3.3 each weld specimen was fabricated with a 10-13 mm weld gap. This weld gap was chosen for adequate distance from the heat affected zone, overall size of the crack growth region, and ease of manufacture. ASTM A36 base material "backer" plates were also used to aid in the manufacture of welded specimens. Welding parameters are listed in Table 3.6.

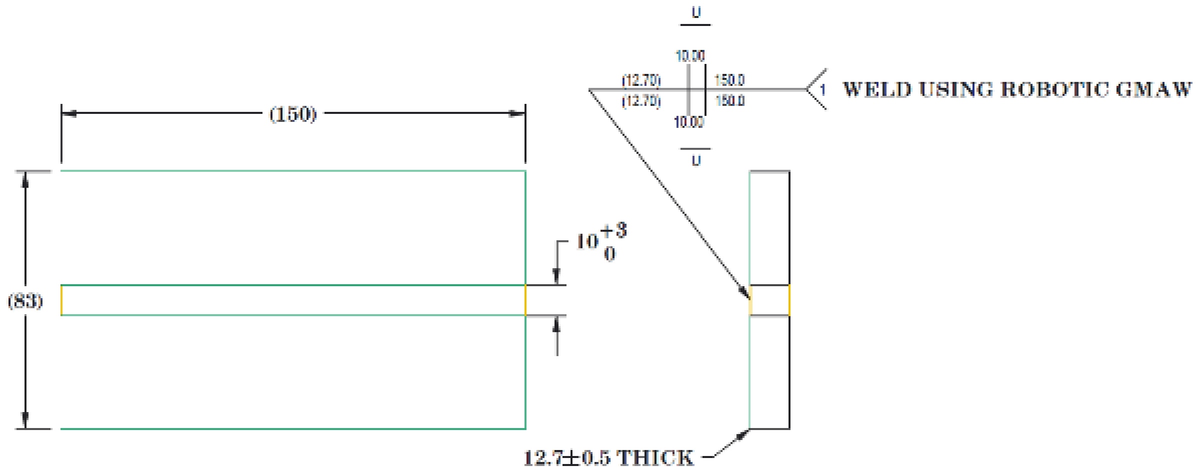

Figure 3.3. Welded specimen geometry after welding (units: mm)

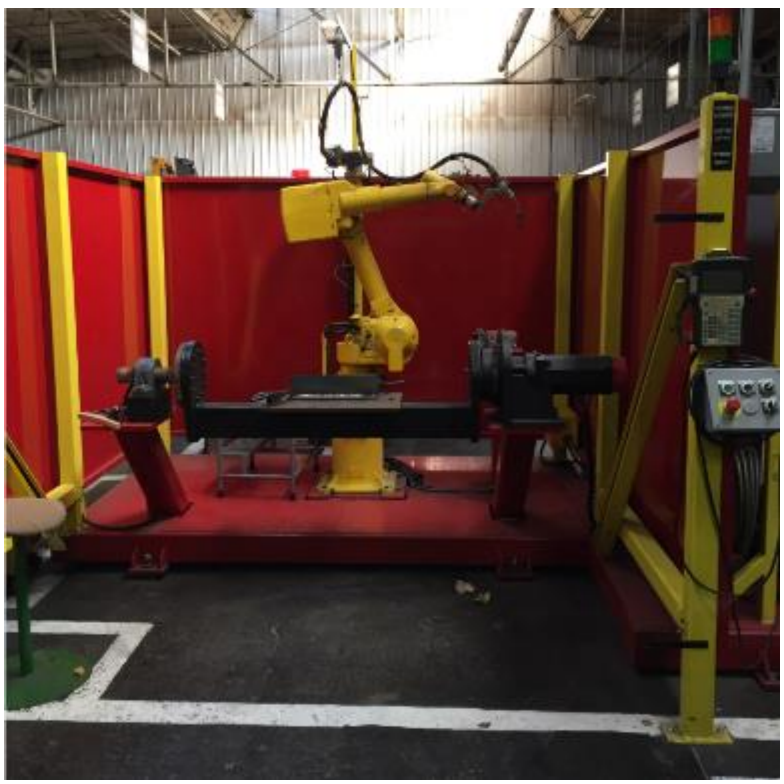

Figure 3.4. Vizient GMAW robot used for making the weld metal specimens

Table 3.6. Welding parameters used to manufacture test specimens

Weld Wire	AWS A5.18	AWS A5.28
Voltage (V)	29	29
Amperage (A)	420	420
Shielding Gas	90/10 Ar/CO_2	90/10 Ar/CO_2
Contact Tip to Work Distance (CTWD) (mm)	19	19
Wire Feed Speed (WFS) (m/min)	11.68	15.62
Tip Travel Speed (m/min)	0.38-0.51	0.38-0.51

Following cutting of base metal specimens on the plasma table and welding of the weld specimens, they were machined. Machining was completed on a CNC mill to achieve the dimensions, slot, and grip pin holes required by ASTM E647 and a thickness of 6.0 mm**.** The compact specimen notch was created using wire electrical discharge machining (EDM) or using a broach. Several grinding/polishing operations were completed to achieve a 1.6μm finish or better.[2] Figure 3.5 shows a weld specimen after welding. Figure 3.1 shows the requirements for machining the weld specimen with the notch of the compact tension specimen in the center of the weld. Figure 3.6 shows the finished compact specimen.

[2] For some specimens a final pass with 320 grit silicon carbide sand paper was done for a better view of the crack during testing.

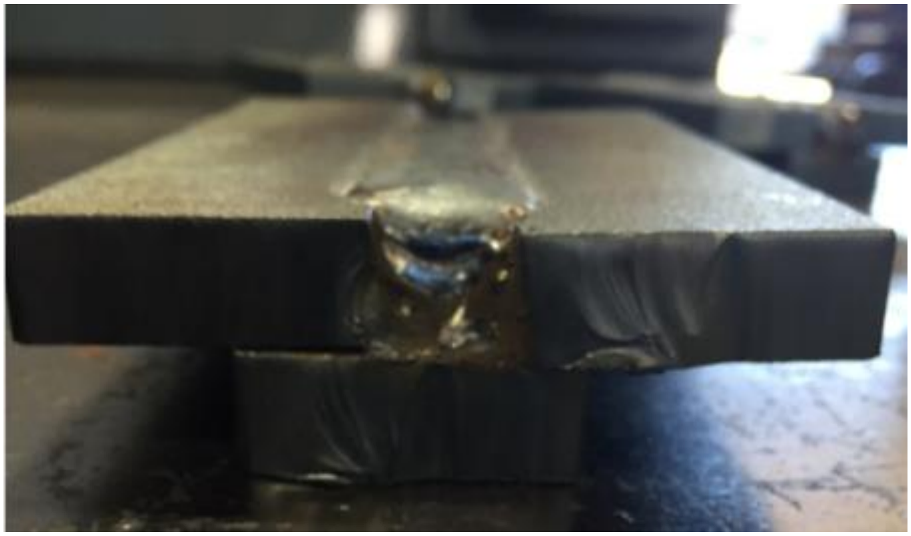

Figure 3.5. Specimen as welded (end view)

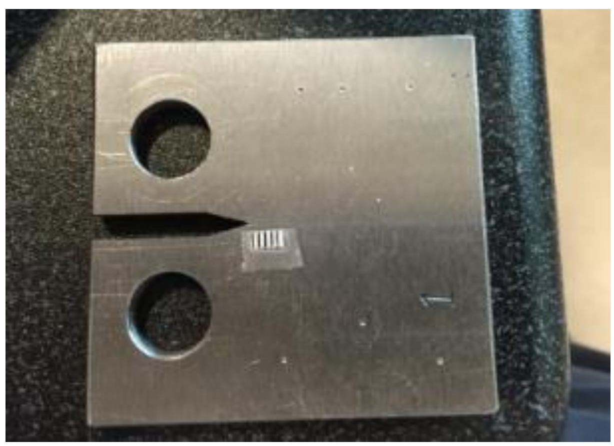

Figure 3.6. Finished compact C(T) specimen (after machining)

Welded specimens were stress relieved to remove any manufacturing induced stresses. Stress relieving was done in a Lindberg Hevi-Duty Box Furnace. The stress relieving procedure was derived from the requirements for post weld stress relief treatment of a low carbon steel as listed in AWS D1.1 and is given below [18]:

1. Furnace preheated to 315°C.
2. Specimens placed into furnace and maintained at temperature for 1 hour.
3. Furnace temperature increased to 535°C and maintained at temperature for 1 hour.
4. Furnace temperature increased to 625°C and maintain temperature for 15 minutes once temperature is achieved.
5. Furnace temperature reduced to 535°C and maintained at temperature for 1 hour.
6. Furnace temperature reduced to 315°C and maintained at temperature for 1 hour.
7. Specimens allowed to cool in still air until room temperature was achieved.

A tensile test specimen was also stress relieved with every batch of stress relieved compact C(T) tension specimens. This was done to verify any effects on mechanical properties for the compact C(T) tension specimens.

3.3. Test Procedures

3.3.1. Fatigue Crack Growth Measurements

Fatigue tests were completed according to ASTM E647-15 “Standard Test Method for Measurement of Fatigue Crack Growth Rates.” They were conducted under load control on an 89 kN (20,000 lb_f) closed loop servo-hydraulic MTS machine (MTS Model 312.21). The test environment was 68°F-72°F and 30%-50% humidity. Load application followed a sinusoidal waveform with test frequencies of 10Hz, 25Hz, and 60Hz. Testing was originally started at 10Hz but the length of time to complete Region I and Region II test was almost 300 hours. The 60Hz test frequency was chosen to perform almost all tests because of resource availability and test time. Load ratios tested were R = 0.05 and R = 0.6. Load ratio R is defined in Equation 7 [9]:

$$R = \frac{P_{min}}{P_{max}} \tag{7}$$

where:

P_{min} = the lowest applied force during a cycle

P_{max} = the highest applied force during a cycle

The stress intensity factor range (ΔK) at the crack tip is defined in Equation 8 [9]:

$$\Delta K = \frac{\Delta P}{B\sqrt{W}} \frac{(2+\alpha)}{(1-\alpha)^{3/2}} \left(0.886 + 4.64\alpha - 13.32\alpha^2 + 14.72\alpha^3 - 5.6\alpha^4\right) \tag{8}$$

where:

$\alpha = a/W$

$\Delta P = P_{max} - P_{min}$

B, a, and W are defined in Figure 3.7; B is thickness and a is crack length.

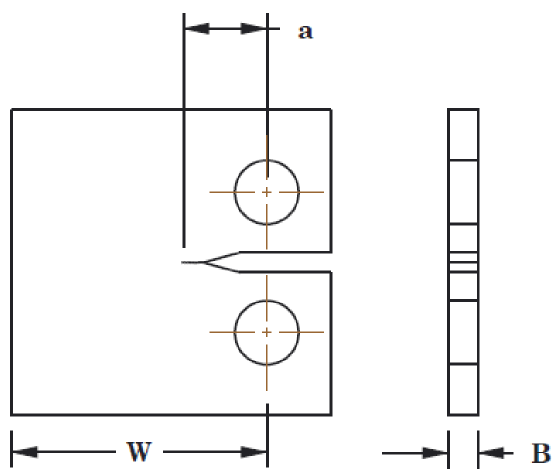

Figure 3.7. Compact C(T) specimen dimension used to calculate stress intensity range

Prior to test specimens being installed in the MTS machine critical dimensions (B, W, and a uncracked) were measured along with overall size. A measurement calibration scale was added to each side of the specimen. Detailed instructions that were used for setting up the test machine are included in Appendix B.

Prior to the start of every test the test specimen was fatigue pre-cracked. Fatigue pre-cracking was accomplished using pre-determined loads P_{max} and P_{min} for starting the test. The loads were determined based on the availability of test data collected and what crack growth region the data was targeted. For all tests the pre-crack loads were the same as the first targeted data point for each test. A minimum pre-crack of 1 mm is required for this specimen geometry prior to starting the test. Once the test was started the following parameters were monitored:

- P_{max} and P_{min}
- Cycle count
- Crack length (a) on both sides of the specimen

Key inputs for the MTS machine were:

- P_{mean} and P_{amp}
- Test Cycle Frequency
- Machine tuning (P/I Gain)

Machine tuning varied based on R ratio and test load. It is very important to monitor test loads throughout the test since test specimen response can change, especially at the high frequency (60 Hz) used. The machine tuning variables require adjustment to maintain a constant load. This can be monitored in various ways. The method used was a scope display of axial force command versus axial force response and a meter measurement of P_{max} and P_{min}.

Data recording frequency was dependent on test procedure. After performing several tests it was determined that two different test procedures were required: 1) K-increasing and 2) K-decreasing. The K-increasing test procedure requires the maximum test load to be increased by no more than 10% of the previous test load. A crack growth extension of approximately 0.25 mm was allowed before changing test loads. Both load increase and crack extension guidelines are used to minimize transient crack growth rate effects. Crack growth measurements were targeted for every 0.1 mm. In some cases this was not achieved because of the variation in crack growth rate. K-increasing tests are only recommended for crack growth rates greater than 10^{-8} m/cycle and they were used to cover a large portion of Region II for the materials tested. In contrast, K-decreasing tests are recommended for crack growth rates less than 10^{-8} m/cycle and are used to define Region I. K-decreasing tests can be executed using a constant force shedding technique or step force shedding. To define Region I for these fatigue crack growth tests step force shedding was used. Step force shedding requires 0.5 mm of crack growth before the next reduction in force. This technique also requires that P_{max} be reduced no more than 10% with each reduction in force. Based on these requirements measurements were performed at every 0.5 mm crack growth increment after a reduction in force and measured at the next 0.1 mm until the next reduction in force.

Since K-decreasing and K-increasing tests are required to define Region I and Region II a minimum of two test specimens were required for each material and load ratio. These tests were planned to have data overlap for each specimen at approximately 12 MPa√m stress intensity factor range. Therefore K-decreasing tests started with a test force that generated a stress intensity range greater than 12 MPa√m. For K-increasing tests the initial test load used generated a stress intensity range lower than 12 MPa√m and was increased from the starting load. Several test specimens were used to determine the appropriate test loads within this stress intensity factor range because there was no available data to estimate beginning test loads.

The crack length (a) was determined by measuring the distance from the tip of the machined notch to the tip of the crack and adding the distance from the centerline of the loading pin holes to the tip of the machined notch. The distance from the tip to the machined notch to the crack tip was measured using DinoCapture 2.0 software from pictures (Figure 3.8) taken with two Dino-Lite Pro microscopic cameras, one on each side of the specimen. A calibration was made using a section of a photocopied ruler attached to each side of the compact C(T) specimen (Figure 3.8). Measurements from the front and back sides were taken on each specimen. Differences between the measurements of the front and back sides of the specimen are not allowed to exceed $0.25B$ or as a rule of thumb 1.5 mm for these specimens. Any deviation from this requirement indicates a potential problem with the test set-up or test specimen. In addition to this requirement the crack was required to maintain a plane of symmetry of ±20° over a distance of $0.1W$ according to ASTM E647. The overall crack length for both front and back sides along with these requirements were verified after images were taken to determine 1) if a load change was required 2) if additional data was needed at this load point and 3) if the test needed to be stopped. It was sometimes necessary to adjust microscope camera position for ideal lighting and picture position. Camera adjustment should be avoided and was used only when necessary. Every time the camera was moved a new calibration was required to ensure measurement accuracy. The crack length (a) was taken to be the average for both the front and back sides of the test specimen.

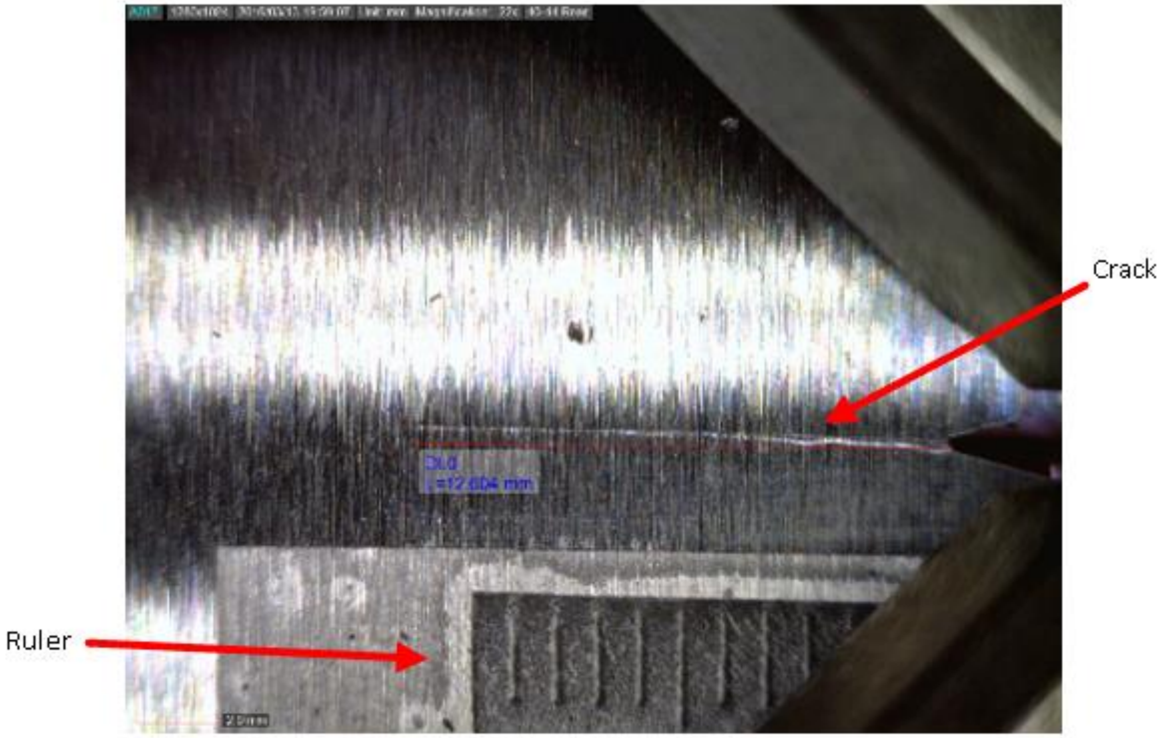

Figure 3.8. Crack measurement photo showing crack and calibration ruler in mm.

3.3.2. Tensile Testing

Tensile testing was completed in accordance to ASTM E8/E8M – 15a "Standard Test Methods for Tension Testing of Metallic Materials." Testing was completed on a 44.5 kN (10,000 lb_f) Instron Model 5500 Test Machine using round tensile test specimens with threaded ends. Fabrication of the round test specimens was completed on a CNC lathe using the same base material (from the same sheet of steel) as the compact C(T) specimens. Additional details on specimen requirements are detailed in Figure A.1 in Appendix A: Tensile Specimen Dimensions and Manufacture. Test set-up and procedures are detailed in Appendix B: Instron Model 5500R Test Machine Set-up. Figure 3.9 shows the Instron Test Machine and set-up.

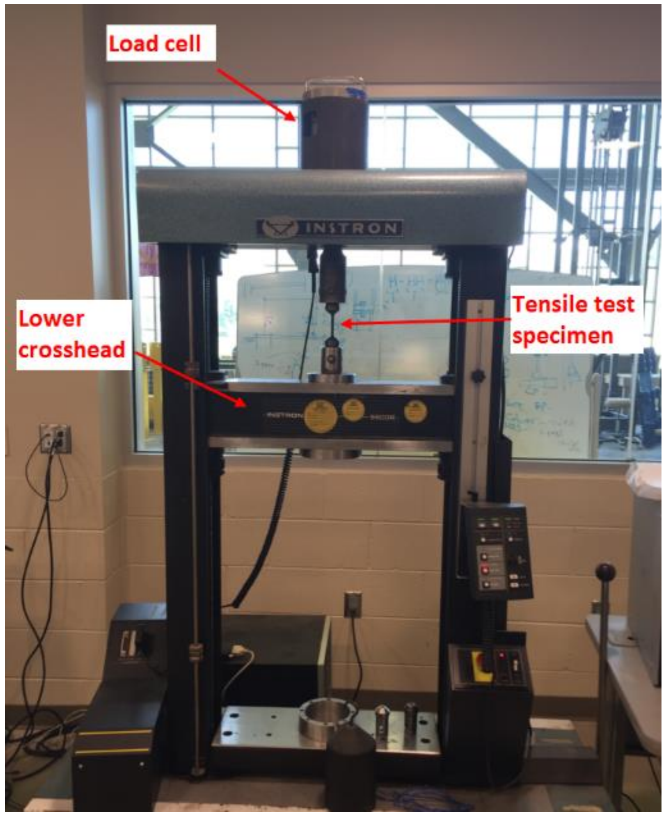

Figure 3.9. Instron Tensile Test Machine

3.3.3. Hardness Testing

The Rockwell B hardness was checked using a Wilson/Rockwell Series 500 (Model 523T) hardness testing machine. Prior to testing the machine calibration was checked with Rockwell B standard. Hardness was checked perpendicular to the intended crack growth path with a measurement every 2 mm. Details of the measurements are given in Appendix E, where Figure E.1 shows measurement locations for AWS A5.18 and Figure E.2 shows the measurement locations for AWS A5.28. Results from these measurements are listed in Table E.1 for AWS A5.18 and in Table E.2 for AWS A5.28. Weld zones were approximately 14 mm in height with a relatively short transition in mechanical properties from base material to weld metal. This information indicates there is a relatively uniform weld region for fatigue crack growth data to be measured.

3.4. Characterization of Fracture Surfaces

The fracture surfaces of the broken fatigue crack propagation specimens were examined macroscopically and microscopically to characterize the fracture features and correlate them with the crack propagation rate measurements. First, macro photography was performed using a Canon Rebel XT camera with a Canon Macro Lens to show overall crack appearance. Next, fracture surface regions of selected C(T) specimens were cut from broken specimens to fit into the scanning electron microscope and cleaned ultrasonically in methanol. These were then examined in a JEOL JSM6510 scanning electron microscope operated at 20kV in the secondary electron imaging mode.

3.5. Characterization of Microstructures

Metallography was used to characterize the microstructure of an untested fatigue crack propagation test specimen. Weld specimens are sectioned to characterize base material, weld material along the crack growth plane, and weld material perpendicular to the crack growth plane. Each specimen was mounted in LECOSET 100, ground through 600 grit SiC, polished with 1.0μm Al_2O_3 and etched with 3% nitric acid in methanol for 10 seconds. Each was then examined with an Olympus PME 3 metallograph using bright field illumination and objective lenses up to 50X. Photomicrographs were obtained with a Spot Insight Camera and software.

IV. RESULTS & DISCUSSION

4.1. Chemical Composition of Base and Weld Metals

Chemical composition of each material was verified using an Angstrom optical emission spectrometer (OES) test machine. Table 4.1 displays results for the base material chemical composition. These values meet the requirements given in Table 3.2 for ASTM A36. Table 4.2 and Table 4.3 present the compositions of the AWS A5.18 and AWS A5.28 weld metals. The percentages of the elements in these two weld metals were close to the values specified for Lincoln SuperArc L-56 and SuperArc LA-100 in Table 3.4 and Table 3.5, respectively.

Table 4.1. Chemical composition of ASTM A36 steel base plate.

Fe (%)	**C (%)**	**Mn (%)**	**P (%)**	**S (%)**	**Si (%)**	**Ni (%)**	**Cr (%)**	**Mo (%)**
99	0.195	0.697	0.006	0.01	0.009	0.016	0.027	0.001
Al (%)	**Cu (%)**	**Ti (%)**	**Nb (%)**	**V (%)**	**B (%)**	**W (%)**	**Sn (%)**	**Pb (%)**
0.038	0.019	0.02	0.001	0	0.002	0.033	0.004	0.027

Table 4.2. Chemical composition of AWS A5.18 weld metal (Lincoln Electric SuperArc L-56).

Fe (%)	**C (%)**	**Mn (%)**	**P (%)**	**S (%)**	**Si (%)**	**Ni (%)**	**Cr (%)**	**Mo (%)**
98	0.109	1.132	0.038	0.013	0.502	0.017	0.035	0
Al (%)	**Cu (%)**	**Ti (%)**	**Nb (%)**	**V (%)**	**B (%)**	**W (%)**	**Sn (%)**	**Pb (%)**
0.018	0.111	0.02	0.008	0	0	0	0.006	0

Table 4.3. Chemical composition of AWS A5.28 weld metal (Lincoln Electric SuperArc LA-100).

Fe (%)	C (%)	Mn (%)	P (%)	S (%)	Si (%)	Ni (%)	Cr (%)	Mo (%)
97	0.084	1.304	0.046	0.011	0.286	1.332	0.043	0.287
Al (%)	**Cu (%)**	**Ti (%)**	**Nb (%)**	**V (%)**	**B (%)**	**W (%)**	**Sn (%)**	**Pb (%)**
0.014	0.081	0.02	0.009	0.003	0.0003	0.005	0.006	0

4.2. Metallography

The microstructure of the ASTM A36 base metal (Figure 4.1) showed that it was mostly ferrite (light etching constituent) with some pearlite (dark etching constituent). This microstructure is typical of a low carbon steel and is what one would expect for ASTM A36. [19]

Figure 4.1. ASTM A36 base metal microstructure consisting of proeutectoid ferrite and pearlite.

Macro photographs like that in Figure 4.2 and in Appendix D of polished and etched specimens show very similar appearance for the AWS A5.18 and AWS A5.28 specimens. As can be seen in Figure 4.2 there is a fairly uniform region of weld metal about 10 mm wide in the center of the 15 mm wide weld bead. This is the region through which fatigue cracks propagated during testing.

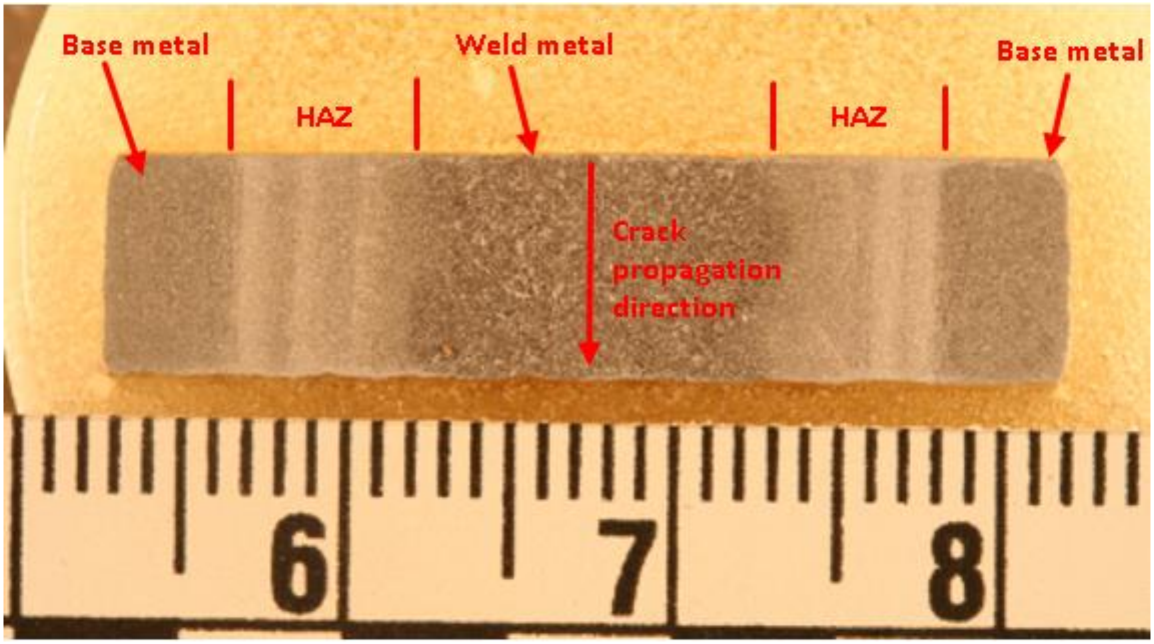

Figure 4.2. Macroscopic view of a polished and etched section of the weld zone cut from an AWS A5.18 weld fatigue specimen parallel to the surface of the specimen showing the 15 mm weld zone through which a crack propagates. HAZ = heat affected zone.

As can be seen in Figure 4.3 the microstructure of the base metal outside of the heat affected zone (HAZ) on the weld is the same as that for the base metal specimen shown in Figure 4.1.

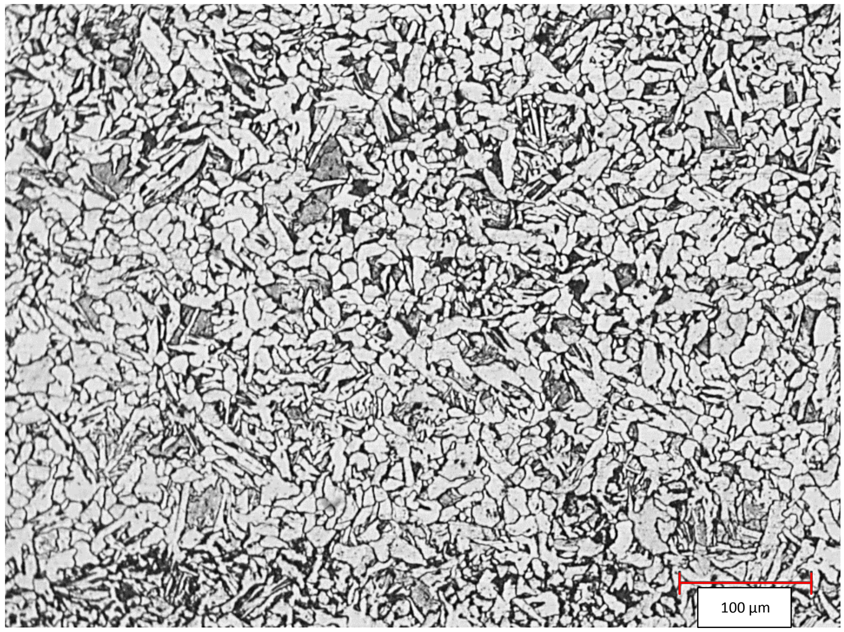

Figure 4.3. AWS A5.28 test specimen base metal microstructure. Microstructure is identical to base metal microstructure as shown in Figure 4.1.

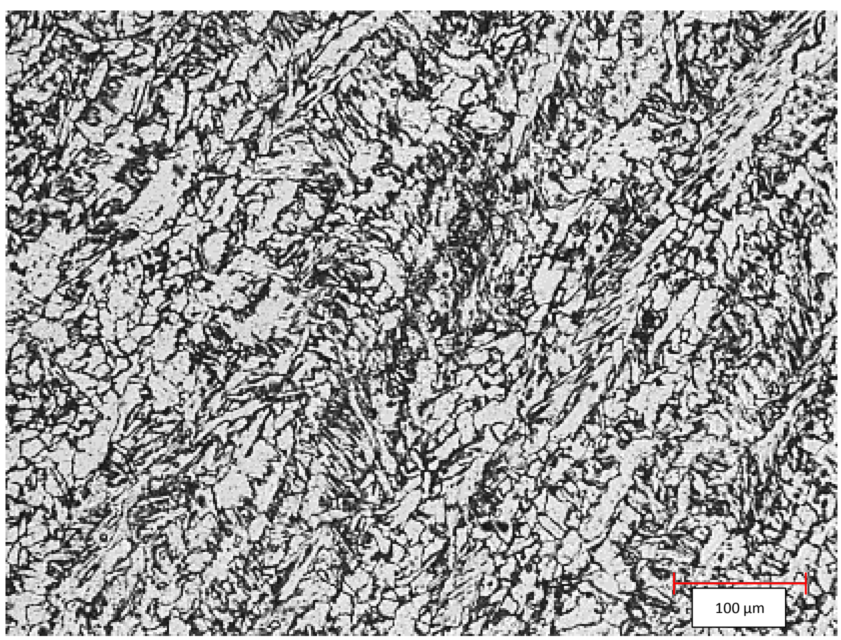

Figure 4.4. AWS A5.18 microstructure consisting of acicular ferrite and carbides.

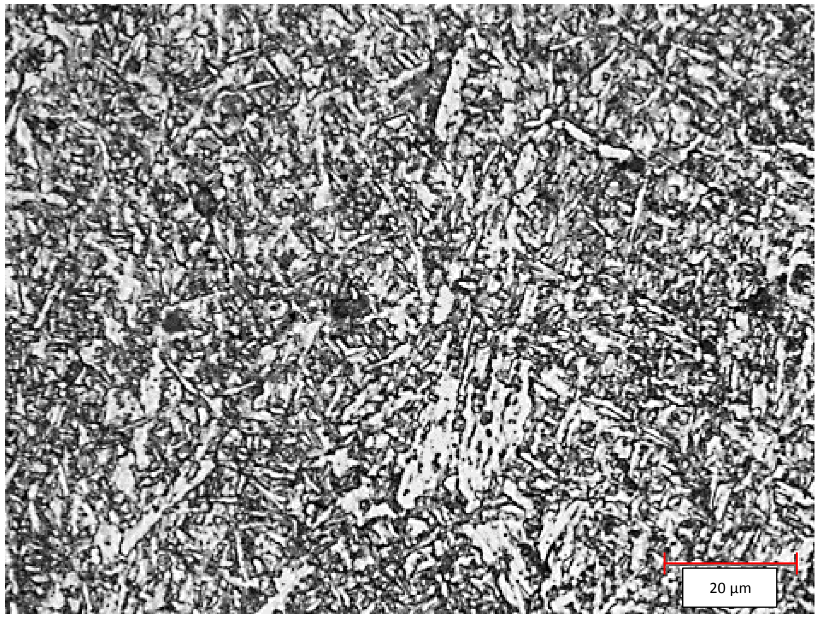

Figure 4.5. Image of etched AWS A5.28 weld metal specimen at high magnification showing it to consist of fine acicular grains of ferrite with some fine carbides.

Figure 4.4 and Figure 4.5 present the microstructures of AWS A5.18 and AWS A5.28 weld metal. Figure 4.4 shows that the microstructure of AWS A5.18 is primarily a mixture of fine acicular ferrite and some carbides. Figure 4.5 and Figure 4.6 shows the microstructure of AWS A5.28 to consist of a fine mixture of ferrite grains and carbides with some larger acicular ferrite regions.

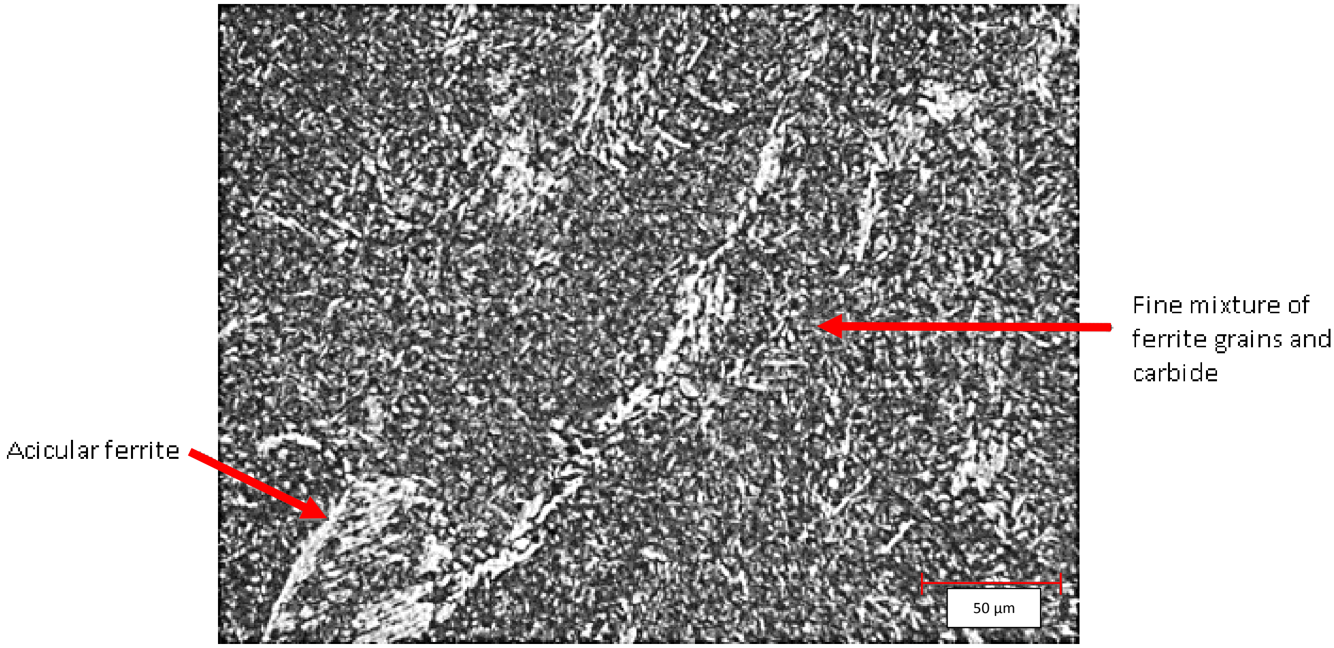

Figure 4.6. AWS A5.28 microstructure consisting of a fine mixture of ferrite grains and carbides as well as a small mixture of acicular ferrite.

4.3. Mechanical Properties

Tensile tests were performed on the as-manufactured ASTM A36 base metal and dedicated stress relieved specimens. The results are summarized in Table 4.4 and the details are presented in Appendix C. Tensile test Specimens #1-#3 were from the as-manufactured steel and Specimens #4-#6 were from steel stress relieved using the process described in Section 3.3 Test Procedures. As can be seen the as-fabricated tensile test specimens generally had strength values that were greater than those for the stress relieved specimens. In all cases the strength and ductility values exceeded the minimum requirements for ASTM A36 steel given in Table 3.1.

The load-elongation curves, presented in Figure C.1 and Figure C.2 in Appendix C show that both the as-manufactured steel and the stress relieved steel had upper and lower yield points, with the lower yield point being defined as the material yield strength.

Table 4.4. Tensile Test Summary for ASTM A36 Base Metal

Material State	Specimen #	Yield Strength (MPa)	Ultimate Tensile Strength (MPa)	Elongation	Reduction Area
As-manufactured	1	295	462	37%	63%
As-manufactured	2	307	465	30%	65%
As-manufactured	3	299	466	30%	68%
Stress-relieved	4	280	455	25%	59%
Stress-relieved	5	286	453	26%	60%
Stress-relieved	6	296	459	27%	62%
	Average and ASTM Requirement				
	#1-#3	300	465	32%	65%
	#4-#6	287	456	26%	61%
	Guideline	250	400	23%	-

Tensile tests were also performed on the weld metals. The tensile test specimens were made from large weld beads following the same weld parameters to make the compact C(T) tension specimens. The weld tensile test specimens were manufactured to the requirements shown in Figure A.1 and stress relieved. The tensile test results are given in Table 4.5.

Table 4.5. Tensile Test Summary – stress relieved weld metals

Specimen #	Ultimate Tensile Strength (MPa)	Yield Strength (MPa)	Reduction Area	Elongation
Specimen #1 - AWS A5.28	693	622	56%	17%
Specimen #2 - AWS A5.28	677	596	61%	20%
Specimen #4 - AWS A5.18	530	404	44%	22%
Specimen #6 - AWS A5.18	516	387	59%	23%
Average and AWS Requirement				
AWS A5.18	523	396	52%	23%
AWS A5.18 Requirement	485	360	-	26%
AWS A5.28	685	609	59%	18%
AWS A5.28 Requirement	690	-	-	-

Tensile test results from the weld metals result in higher yield and ultimate tensile strengths for AWS A5.28. They show that both weld metals meet their respective requirements for AWS A5.18 and AWS A5.28. The load-elongation curves for both weld metals presented in Figure C.4 in Appendix C. Figure C.4 show that both AWS A5.18 and AWS A5.28 had upper and lower yield points, with the lower yield point being defined as the material yield strength.

Rockwell B hardness profiles across weld regions like that shown in Figure 4.2 were generated to characterize mechanical properties of welds on the welded compact tension specimens. The results of these measurements, which are presented in detail in Appendix E, show that the hardness values are fairly uniform in the base metal and in the center of the weld metal. The base metal for AWS A5.18 had an average Rockwell B harness of 72; the base material for AWS A5.28 had an average Rockwell B hardness of 74. Both averages are very close as was expected. Average hardness for the weld metal measured 96 HRB for AWS A5.28 and 79 HRB for AWS A5.18. The higher value for the AWS A5.28 weld metal is consistent with the much finer grain size and higher strength for this weld metal (Figure 4.6).

4.4. Fatigue Test Results and Fractography

4.4.1. Region II Fatigue Crack Growth

Figure 4.7 through Figure 4.12 show Region II crack propagation and ΔK_{th} results for each material studied along with comparisons to published fatigue crack propagation data. Table 4.6 and Table 4.7 summarize the Paris Law equation fits of Region II data in comparison to published equations. Table 4.8 summarizes the ΔK_{th} results. Figure 4.20 through Figure 4.22 present the scanning electron micrographs for Region II for all materials studied and Table 4.9 and Table 4.11 summarize the fatigue striation measurements from them. The tabulated and graphical results for all of the individual fatigue measurements made and presented in this section are given in Appendix H.

As can be seen in Figure 4.7 and Figure 4.8 the crack propagation data for the ASTM A36 base metal are in agreement with the published Paris Law fit equations to existing data for ferritic-pearlitic steels for both R=0.05 and R=0.6. [11] As can also be seen the data for the stress ratio R=0.05 had a steeper slope (m) than that for the stress ratio R=0.6. This is reflective of the drop off in $\frac{da}{dN}$ for low ΔK values for R=0.05 data, and this may, in turn, be the result of crack closure at the lower ΔK values. Crack closure is expected to be more pronounced for low R values.

As can be seen in Figure 4.9 through Figure 4.12 the test results show that the fatigue crack growth rate data for each weld metal for Region II is generally the same as that of the ASTM A36 base material and falls within the limits observed for other steel welds. [14] Again there is a more rapid drop off in the $\frac{da}{dN}$ values at low ΔK values for the specimens tested at R=0.05. Again this is thought to result from the effective ΔK being lower than the actual ΔK because of the greater amount of crack closure.

As can be seen in Table 4.6, which summarizes the Region II crack growth data in the form of Paris law equations, the experimental exponents (m) are in most cases, especially for the R=0.05 ratio tests, greater than the accepted value of 3. This is most likely due to the drop off in $\frac{da}{dN}$ values for low ΔK, which as mentioned above may be due to crack closure effects. As can be seen in Table 4.7, which present the Paris law equations for the individual crack growth tests for AWS A5.18 weld metal for R=0.05, the test conducted at high ΔK resulted in a value of m=3.3, while tests at lower ΔK values resulted in values over 5. Comparison of the $\frac{da}{dN}$ versus ΔK data for the ASTM A36 base materials and the two weld metals presented in Figure 4.7 through

Figure 4.12 shows that it all falls within a narrow band in Region II. This is expected for Region II crack growth, which is relatively insensitive to microstructure and mean stress (R ratio).

As can be seen in Figure 4.12 some of the $\frac{da}{dN}$ versus ΔK values deviate from the general trend of the data. This is especially true for the data for Specimen #55-66 which exhibits anomalously low growth rates for ΔK less than about 13 MPa√m. This may be due to changes in the weld microstructure. Figure 4.13 shows the fracture surface of Specimen #55-66. This low magnification picture highlights the region where there is an apparent difference in microstructure.

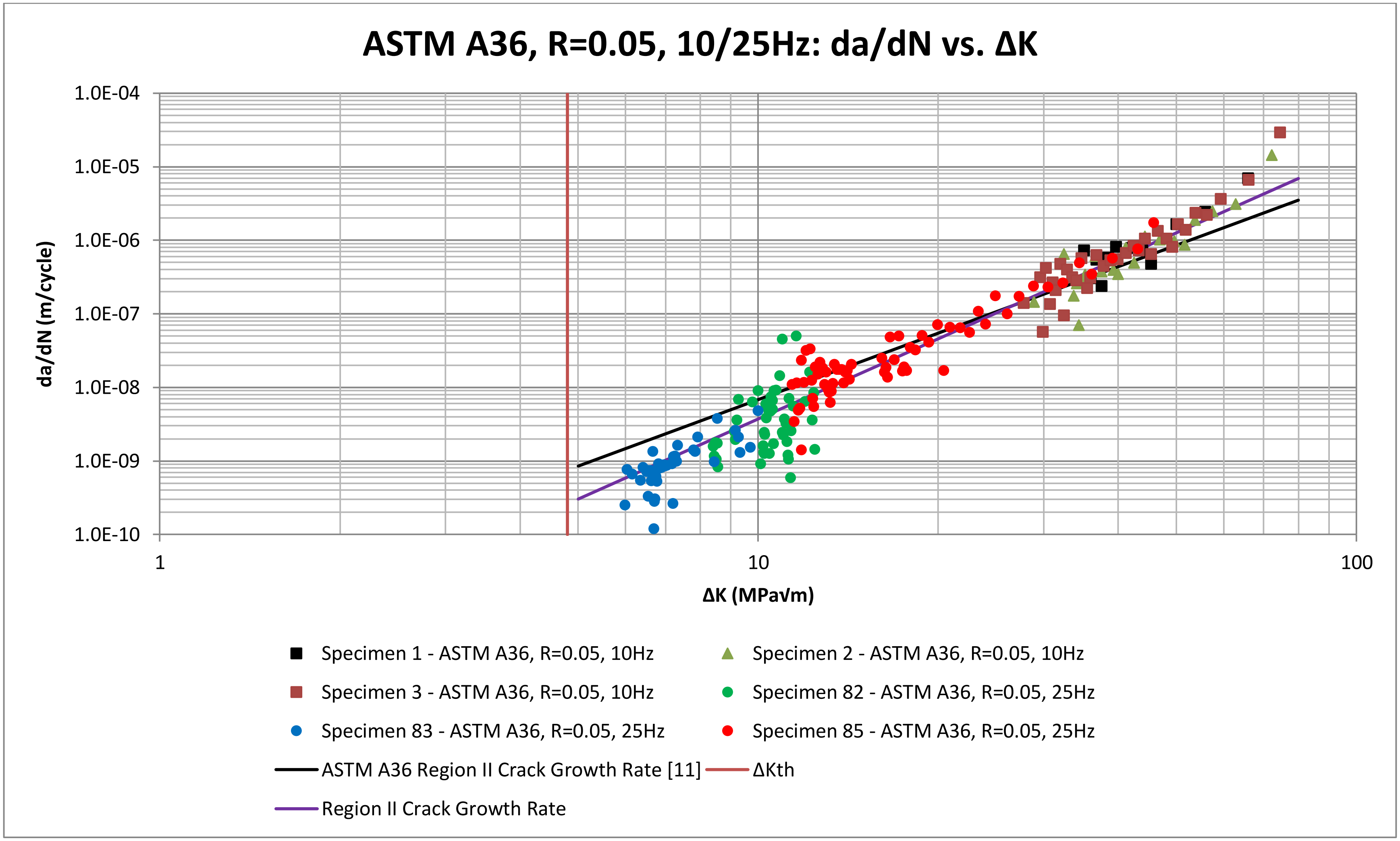

Figure 4.7. ASTM A36 fatigue crack propagation data for R=0.05.

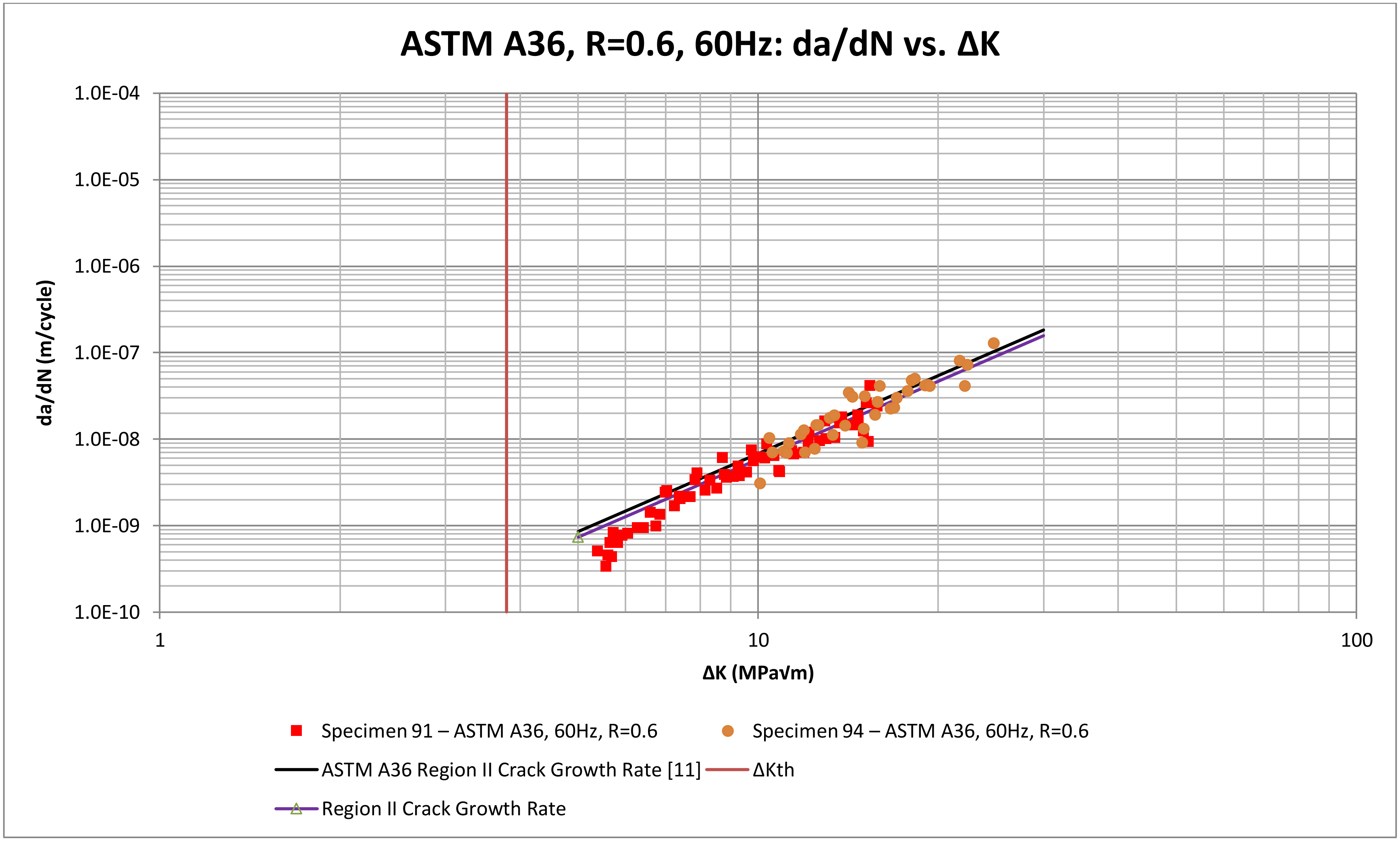

Figure 4.8. ASTM A36 fatigue crack propagation data for R=0.6.

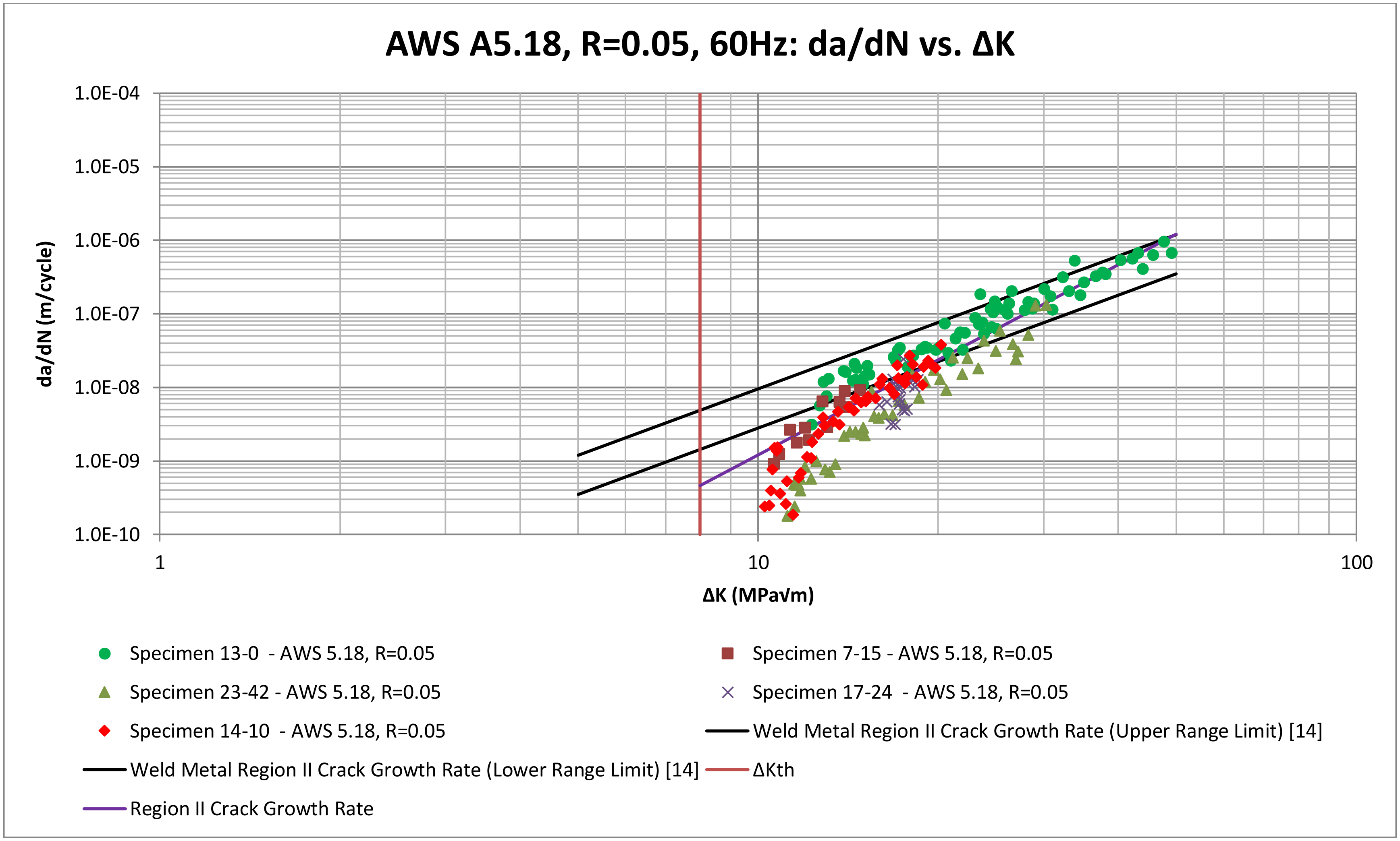

Figure 4.9. AWS A5.18 fatigue crack propagation results for R=0.05.

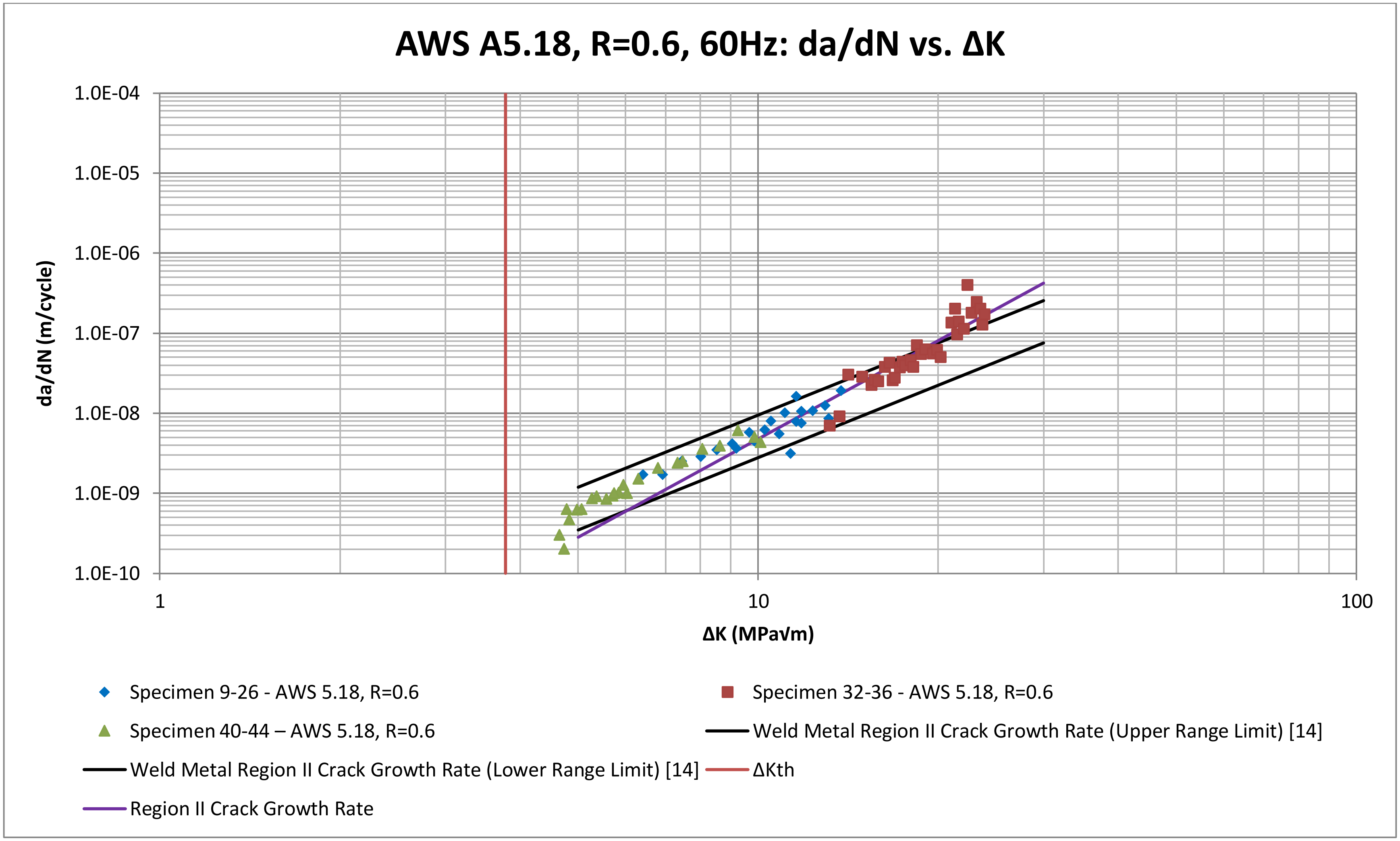

Figure 4.10. AWS A5.18 fatigue crack propagation results for R=0.6.

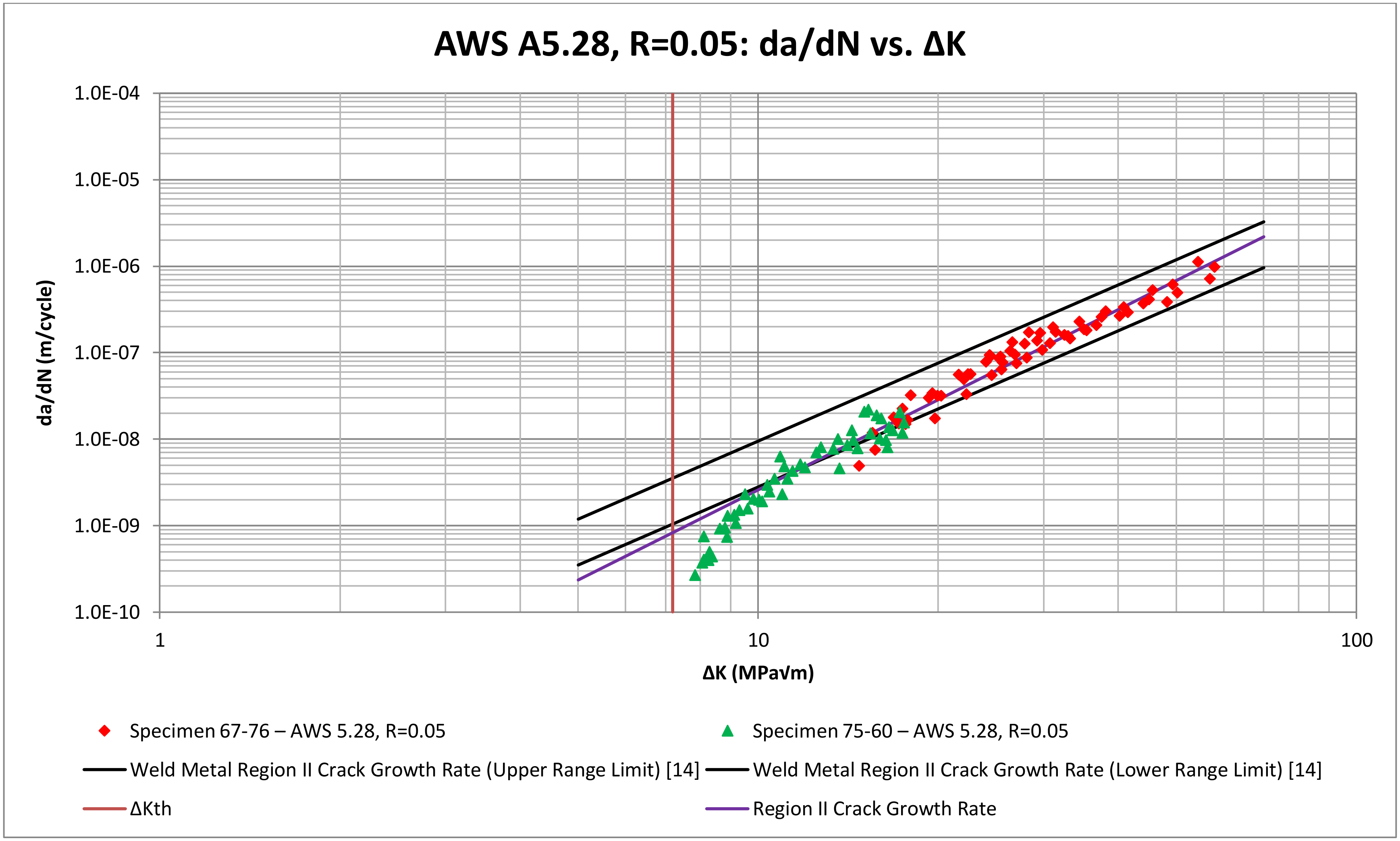

Figure 4.11. AWS A5.18 fatigue crack propagation results for R=0.05.

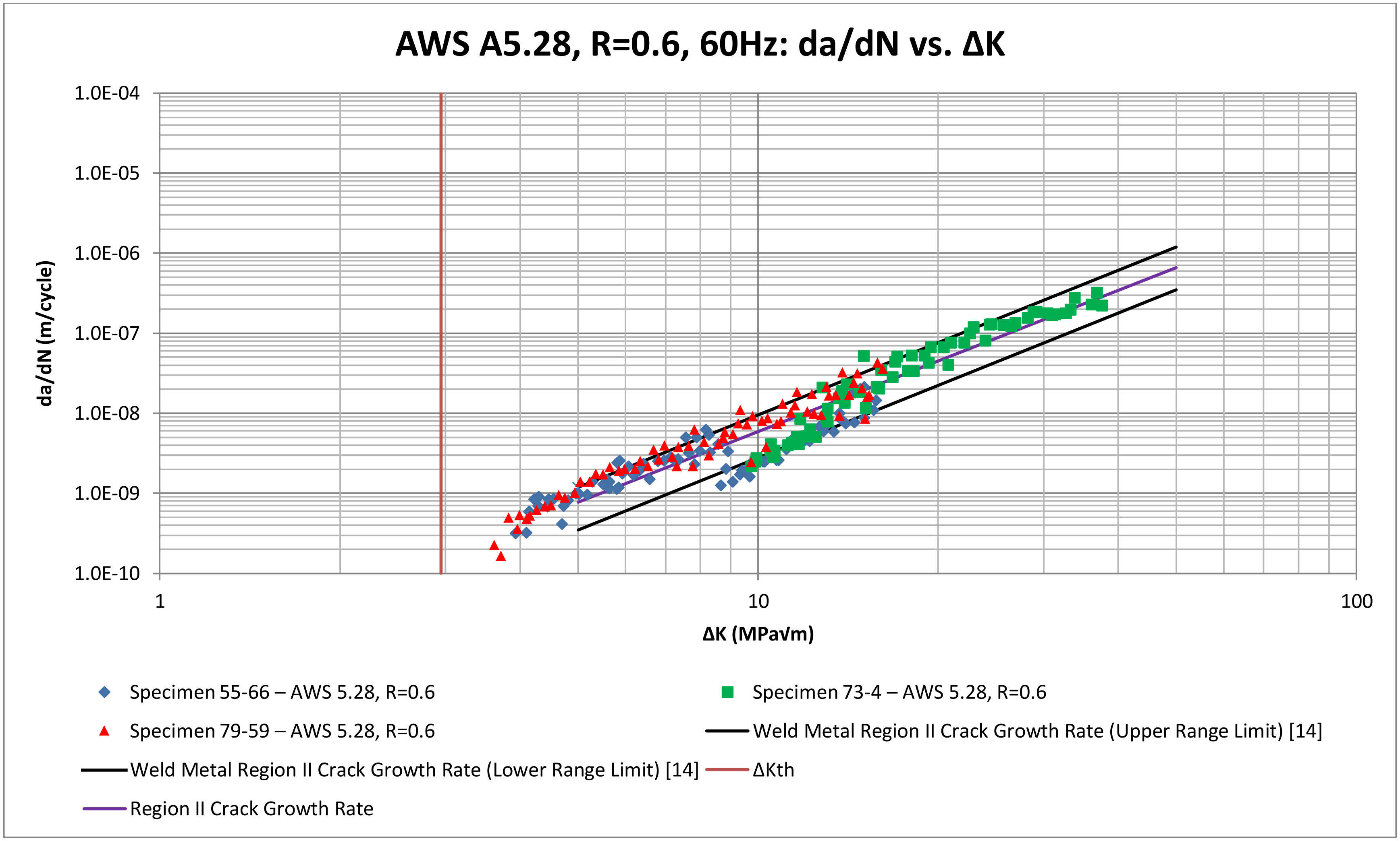

Figure 4.12. AWS A5.18 fatigue crack propagation results for R=0.6.

Table 4.6. Summary of Paris Law equations for Region II fatigue crack propagation data for all specimens tested.

Material	Paris Equation	R^2	R - ratio
ASTM A36 Base Material	$9 \times 10^{-13} (\Delta K)^{3.6}$	0.93	0.05
ASTM A36 Base Material	$6 \times 10^{-12} (\Delta K)^{3.0}$	0.89	0.6
ASTM A36 [11]	$6.8 \times 10^{-12} (\Delta K)^{3.0}$	-	-
AWS A5.18 Weld Wire	$6 \times 10^{-14} (\Delta K)^{4.3}$	0.87	0.05
AWS A5.18 Weld Wire	$4 \times 10^{-13} (\Delta K)^{4.0}$	0.90	0.6
AWS A5.28 Weld Wire	$9 \times 10^{-13} (\Delta K)^{3.5}$	0.97	0.05
AWS A5.28 Weld Wire	$7 \times 10^{-12} (\Delta K)^{2.9}$	0.86	0.6
Weld Wire (Upper Limit) [14]	$9.5 \times 10^{-12} (\Delta K)^{3.0}$	-	-
Weld Wire (Lower Limit) [14]	$2.8 \times 10^{-12} (\Delta K)^{3.0}$	-	-

**Units - m/cycle and MPa√m*

Table 4.7. Summary of Paris Law equations for Region II fatigue crack propagation data for AWS A5.18 R=0.05.

Material	Paris Equation	R^2	R - ratio
Specimen 14-10	$2 \times 10^{-15} (\Delta K)^{5.5}$	0.89	0.05
Specimen 13-0	$2 \times 10^{-12} (\Delta K)^{3.3}$	0.93	0.05
Specimen 23-42	$5 \times 10^{-15} (\Delta K)^{5.0}$	0.92	0.05
AWS A5.18 Weld Wire	$6 \times 10^{-14} (\Delta K)^{4.3}$	0.87	0.05
Weld Wire (Upper Limit) [14]	$9.5 \times 10^{-12} (\Delta K)^{3.0}$	-	-
Weld Wire (Lower Limit) [14]	$2.8 \times 10^{-12} (\Delta K)^{3.0}$	-	-

**Units - m/cycle and MPa√m*

Figure 4.13. Fracture surface of AWS A5.28 material test Specimen #55-66. Measurement units are mm.

4.4.2. Region I Fatigue Crack Propagation and Fatigue Crack Threshold (ΔK_{th})

The details of the K-decreasing crack growth tests are presented in the $\frac{da}{dN}$ versus ΔK graphs in Figure 4.15 through Figure 4.19, and the resulting ΔK_{th}values are summarized in Table 4.8. Best-fit lines were used between the values of 10^{-9} and 10^{-10} m/cycle on the log $\frac{da}{dN}$ versus log ΔK plots to generate ΔK_{th}values. ΔK_{th}values for all materials tested are within the guideline of less than 9 MPa $\sqrt{m}$.

As can be seen in Table 4.8 ΔK_{th}values for R=0.6 are established at 3.8 MPa√m for both ASTM A36 and AWS A5.18, and 2.95 MPa√m for AWS A5.28. The increase in ΔK_{th} values for ASTM A36 and AWS A5.18 is likely due to the larger grain size as compared to AWS A5.28

(reference Figure 4.1, Figure 4.4, and Figure 4.6.) Low strength steels (< 500 MPa yield strength) with fine grain structures have lower ΔK_{th} values than steels with coarse grain structures. [20] Fine grain materials promote a flatter crack path that tends to promote higher crack growth rates whereas coarse grain materials tend to promote a rougher crack path. The rougher crack path offers greater resistance to macro-crack growth through crack closure and crack tip deflection mechanisms. [4]

As can be seen in Table 4.8 the ΔK_{th} for each material was, as expected, greater for a load ratio of R=0.05 than for a ratio of R=0.6. [13] Higher ΔK_{th} values for R=0.05 are typical for steels [20] because of crack closure as discussed in Section 2.2. Crack closure effects typically do not occur at high stress ratios (R > 0.5). Differences in microstructure and the effect of crack closure likely contribute to the change in values of ΔK_{th} for R=0.05.

As can be seen in Figure 4.15 through Figure 4.19 there is a significant amount of scatter in Region I data which resulted in low R^2 values for the least square fits used to determine ΔK_{th}. Additional data points and lower $\frac{da}{dN}$ values would likely increase the R^2 values. This will also generate a ΔK_{th} value with higher refinement. Generating these data points will add a significant amount time to each test because of the low $\frac{da}{dN}$ values.

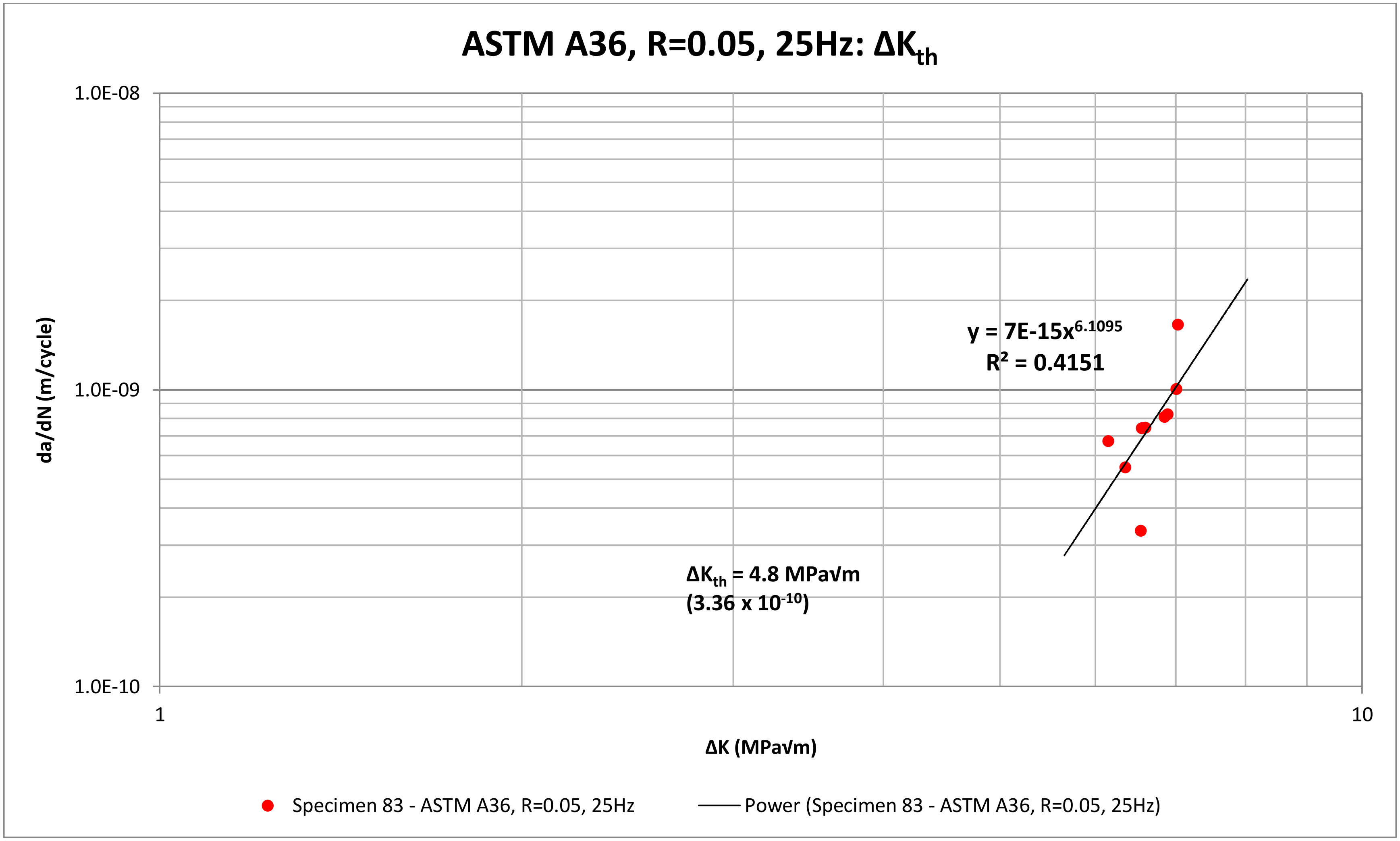

Figure 4.14. ΔK_{th} data for ASTM A36 at stress ratio R=0.05 with a test frequency of 25Hz.

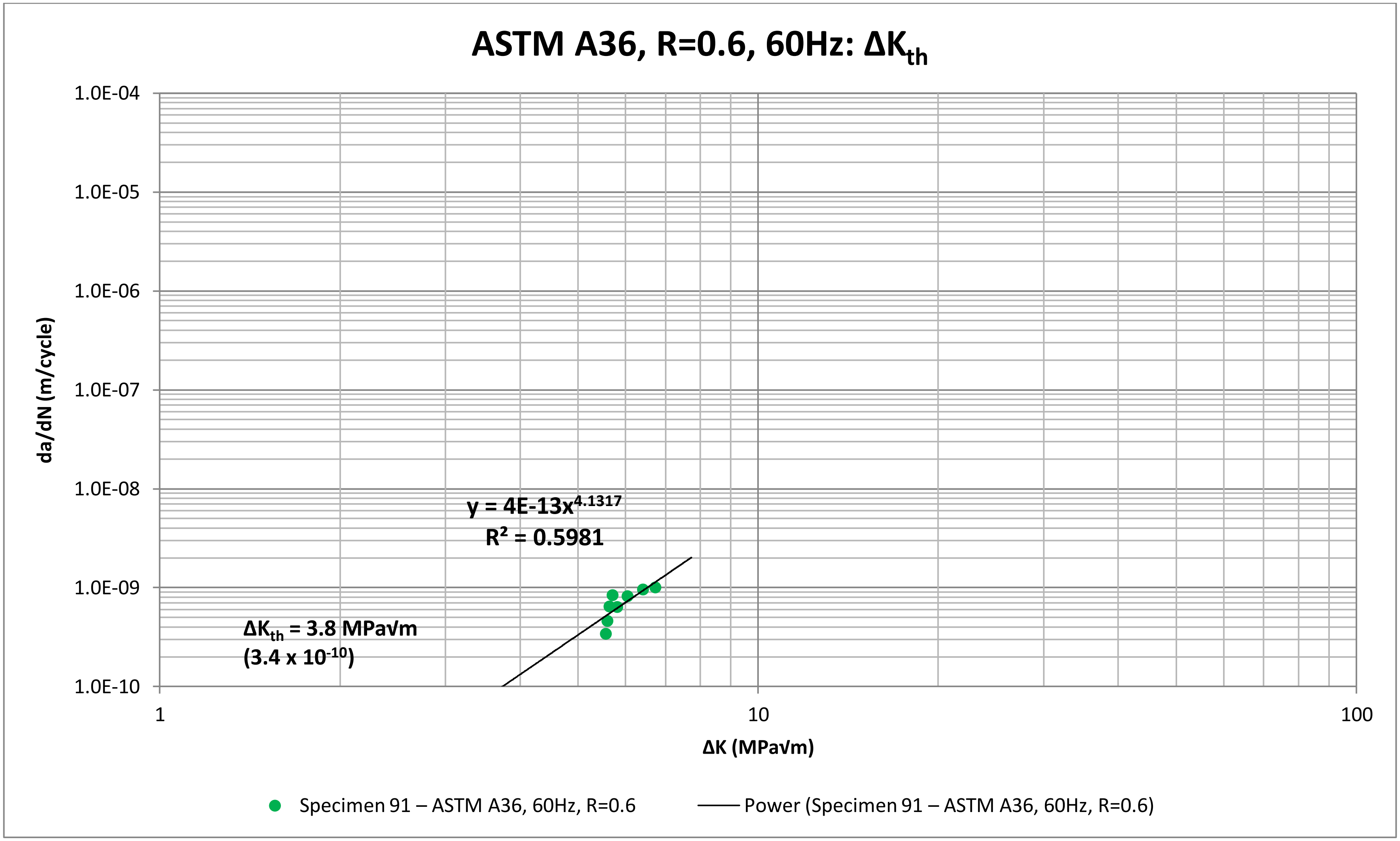

Figure 4.15. ΔK_{th} data for ASTM A36 at stress ratio R=0.6 with a test frequency of 60Hz.

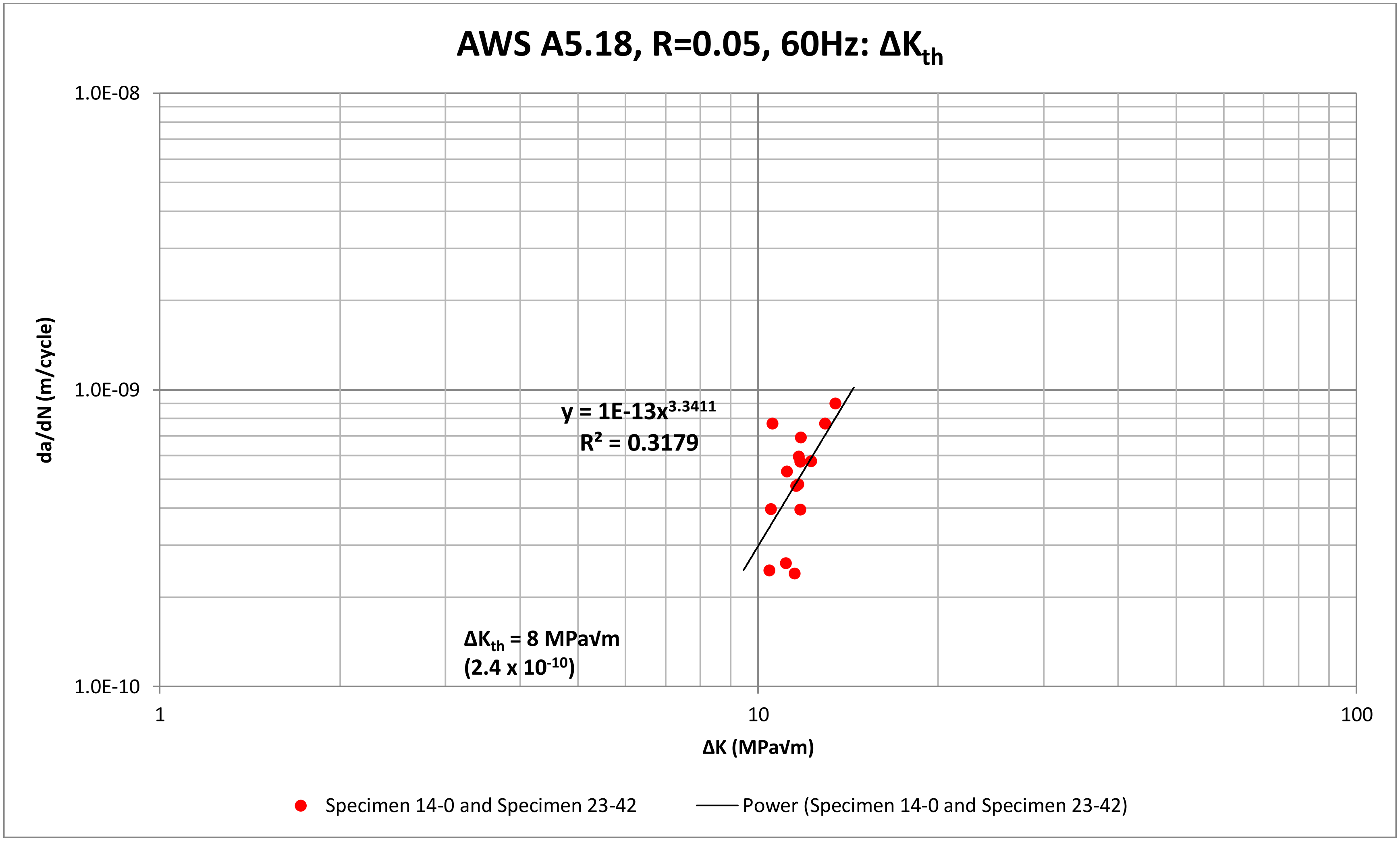

Figure 4.16. ΔK_{th} data for AWS A5.18 at stress ratio R=0.6 with a test frequency of 60Hz.

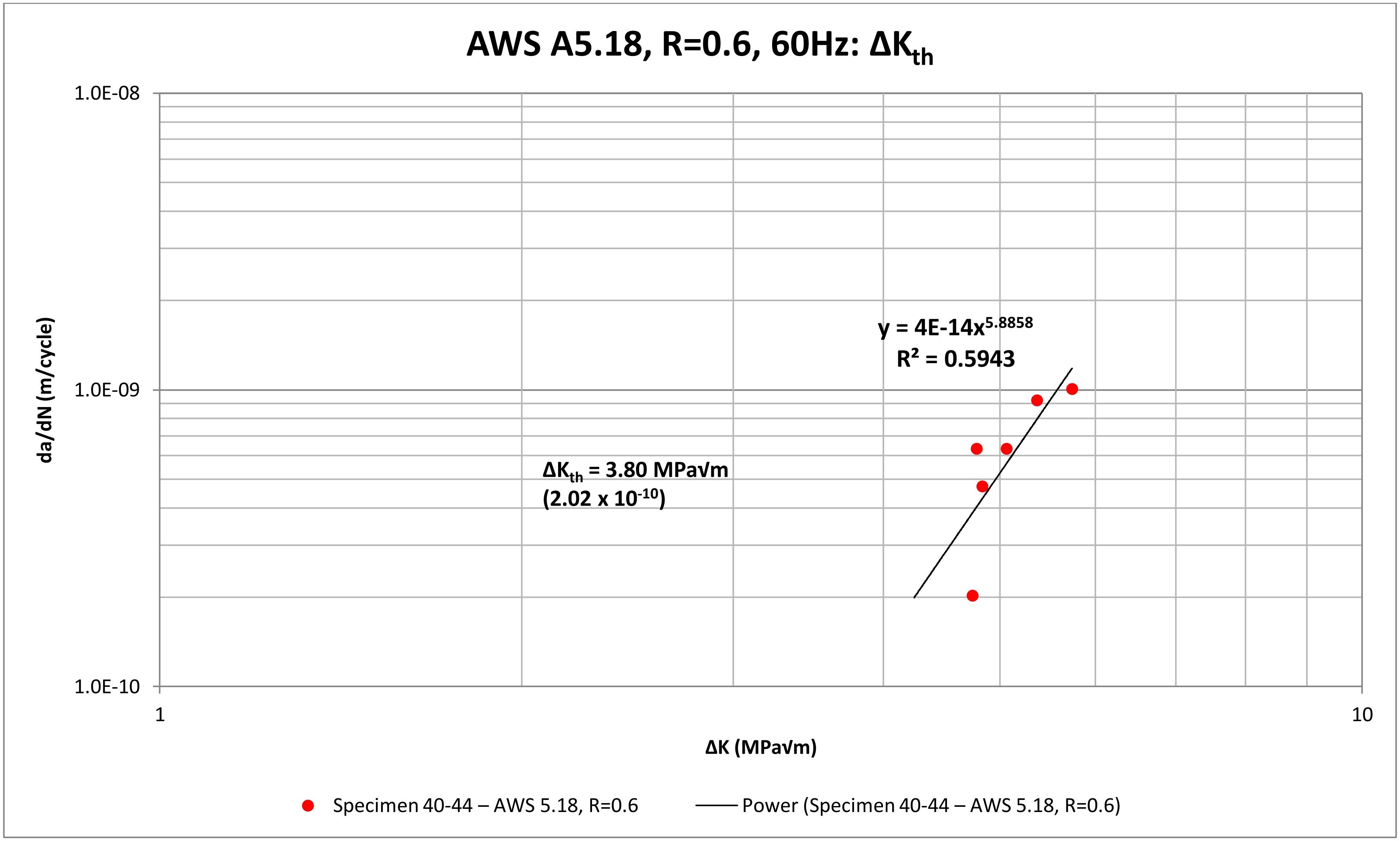

Figure 4.17: ΔK_{th} data for AWS A5.18 at stress ratio R=0.6 with a test frequency of 60Hz.

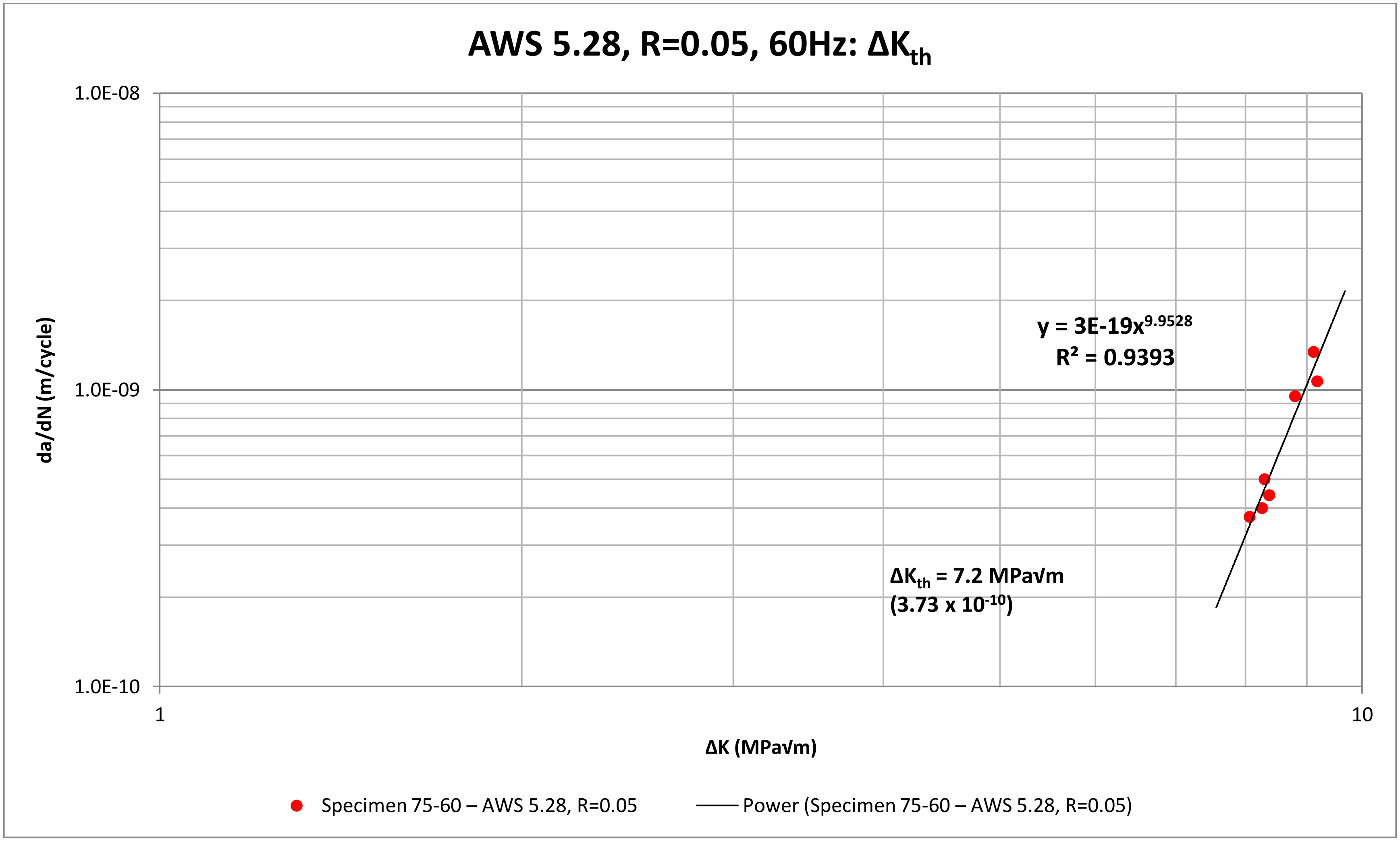

Figure 4.18. ΔK_{th} data for AWS A5.28 at stress ratio R=0.05 with a test frequency of 60Hz.

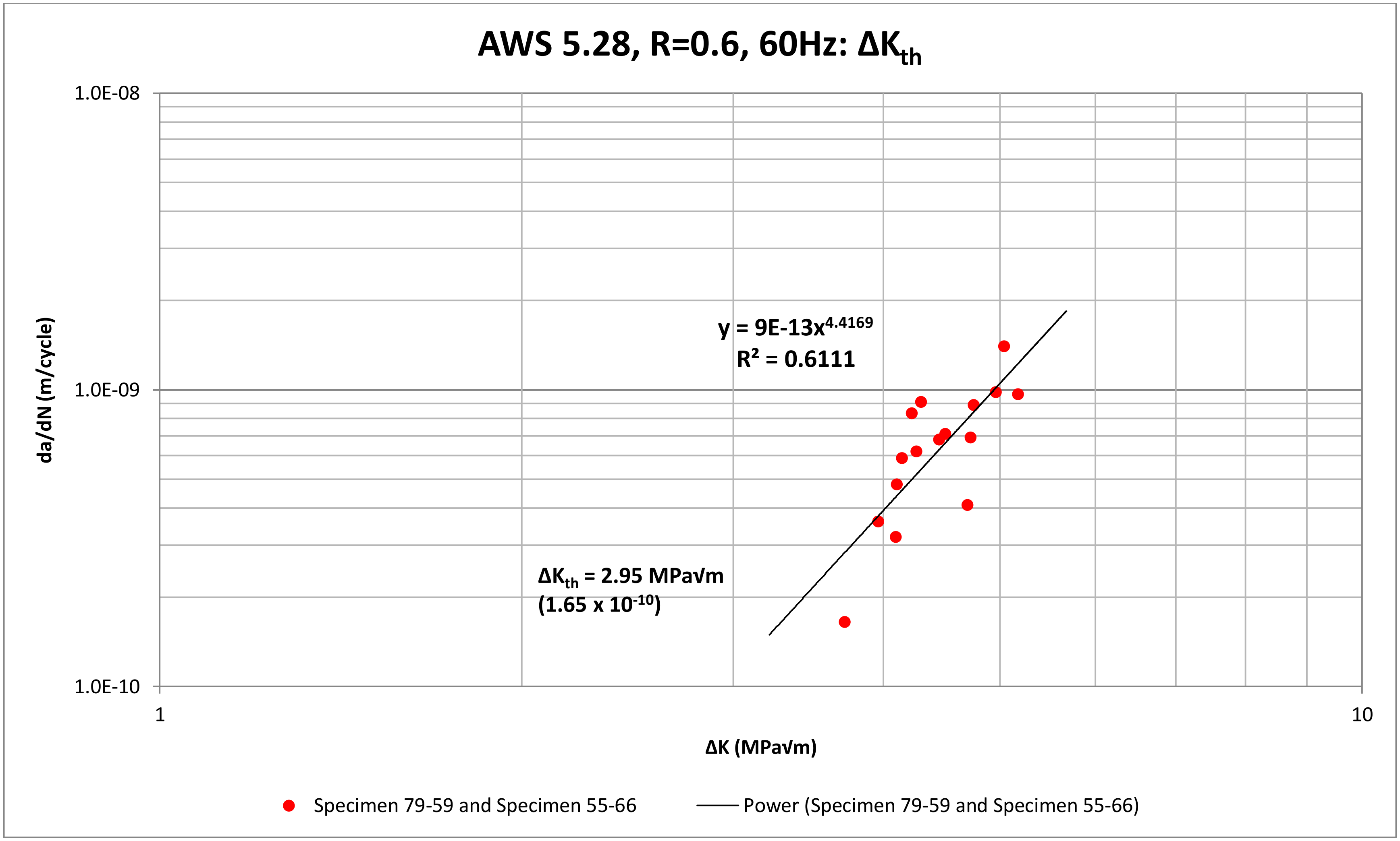

Figure 4.19. ΔK_{th} data for AWS A5.28 at stress ratio R=0.6 with a test frequency of 60Hz.

Table 4.8. Summary of Region I test data for all materials and load ratios.

Material	**ΔK_{th}***	**Lowest da/dN***	**R^2**	**R - ratio**
ASTM A36 Base Material	4.80	3.36×10^{-10}	0.42	0.05
ASTM A36 Base Material	3.80	3.4×10^{-10}	0.60	0.6
Mild Steel 430 MPa UTS** [4]	6.60	-	-	0.13
Mild Steel 430 MPa UTS** [4]	3.20	-	-	0.64
AWS A5.18 Weld Wire	8.00	2.4×10^{-10}	0.32	0.05
AWS A5.18 Weld Wire	3.80	1.65×10^{-10}	0.61	0.6
AWS A5.28 Weld Wire	7.20	3.73×10^{-10}	0.94	0.05
AWS A5.28 Weld Wire	2.95	2.02×10^{-10}	0.59	0.6

**Units - m/cycle for* $\frac{da}{dN}$ *and MPa√m for* ΔK_{th}

***Ultimate tensile strength (UTS)*

4.4.3. Fractography

Overall the fatigue crack front for all of the test specimens was parallel to the machined notch. All test materials displayed ratchet marks where fatigue crack initiation occurred at the machined notch, indicating multiple initiation sites. With the exception of crack growth in Specimen #55-66 the crack growth through each weld material appears to be very smooth without any change in fracture behavior. With the exception of the anomaly shown in Figure 4.13 the fracture surfaces do not show any significant weld inclusions or variations. Several specimens examined at low magnification exhibited very consistent and straight crack growth.

As can be seen in the scanning electron micrographs in Figure 4.20 through Figure 4.22 Region II crack growth regions are characterized by well-defined fatigue striations and occasional secondary cracking for the base metal and two weld metals. This indicates that the mechanism of Region II crack growth was the same for these materials even though the microstructures for the base metal (Figure 4.1) and the weld metals (Figure 4.4 and Figure 4.5) are different. Table 4.9 through Table 4.11 show the average striation spacing measurements obtained from the scanning micrographs. These correlate well with measured $\frac{da}{dN}$ values for the crack locations examined. As can be seen the greatest difference between striation spacing and crack growth rate was about 16% for the AWS A5.28 specimen.

It should be noted that the fatigue crack growth specimens and the locations on their fracture surfaces chosen for scanning microscopy and striation spacing measurement were well within Region II. Specimen #3 was used for the base metal, and the scanning electron micrograph in Figure 4.20 was obtained at a crack length of a = 23.6 mm, which corresponds to (See Table H.3) a stress intensity factor range of 48.2 MPa√m. The test specimen was tested at crack growth rates of 2.0×10^{-7} to 5.0×10^{-5} m/cycle. Weld specimens #13-0 and #67-76 were used to characterize the fracture surfaces for AWS A5.18 and AWS A5.28, respectively. Figure 4.21 displays the fracture surface for Specimen #13-0 at a crack length of a = 22.6 mm, which corresponds to a stress intensity factor range of 26.5 MPa√m. Figure 4.22 displays the fracture surface for Specimen #67-76 at a crack length of a = 22.5 mm which corresponds to a stress intensity factor range of 32.5 MPa√m.

Table 4.10 and Table 4.11 summarize the striation spacing measurements for both weld metals. These pictures have very good resolution for counting fatigue striations and have good correlation to test measurement. Crack growth rate measurement with the microscope cameras for AWS A5.18 are within 2% of measured SEM values and within 16% for AWS A5.28.

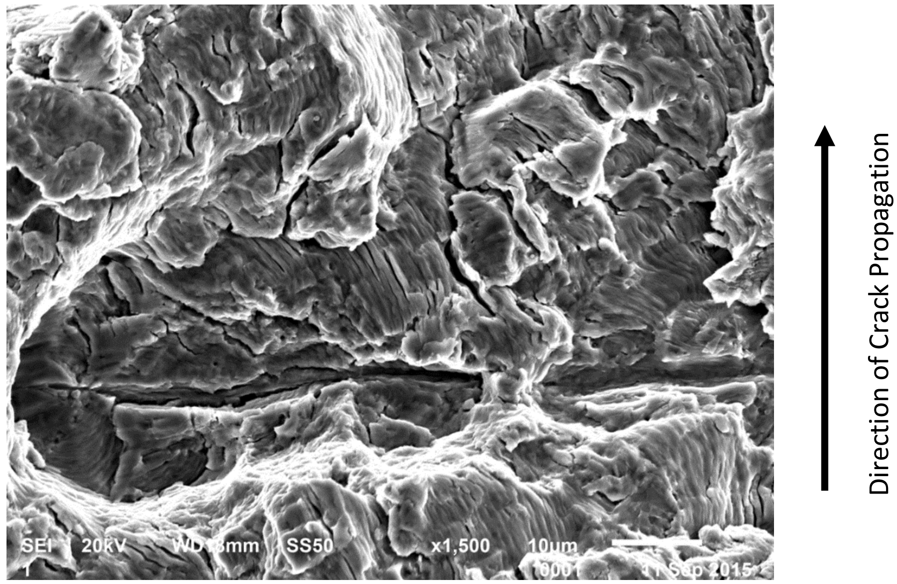

Figure 4.20. High magnification image of fracture surface for Specimen #3 – ASTM A36. Image taken at a=23.6 mm and showing well defined fatigue striations and secondary cracks. Average striation spacing is 1.0 µm.

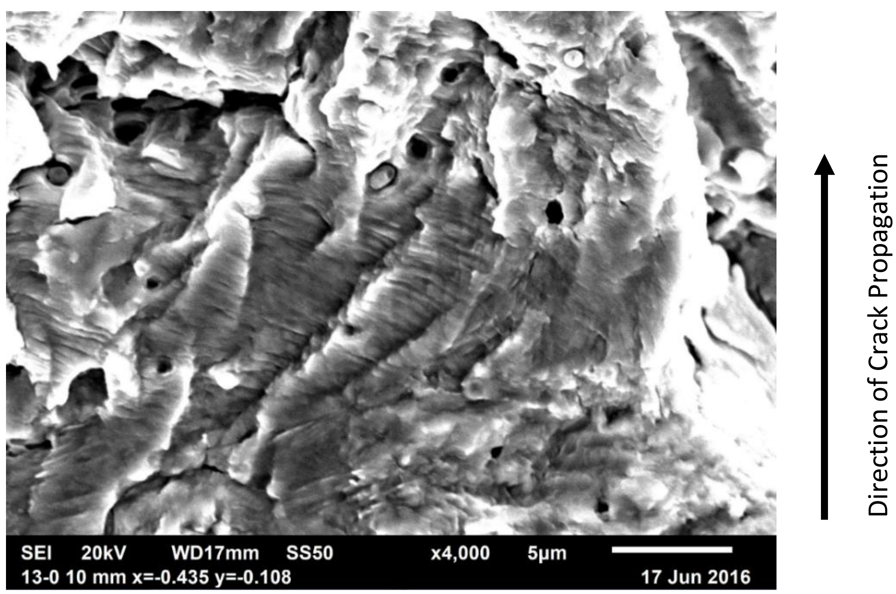

Figure 4.21. High magnification image of fracture surface at for Specimen #13-0 - AWS A5.18 taken at a=22.6 mm and showing well defined fatigue striations. Average striation spacing is 0.2 µm.

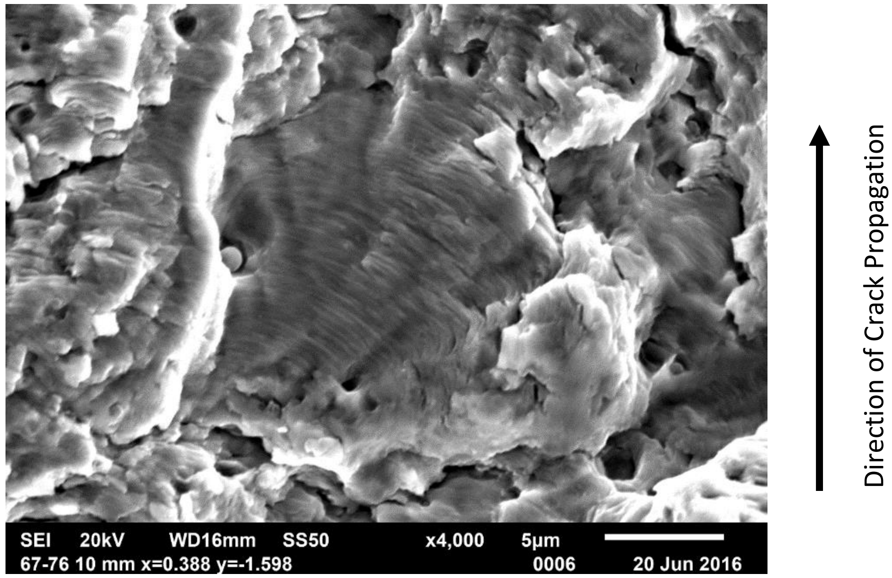

Figure 4.22. High magnification image of fracture surface for Specimen #67-76 - AWS A5.28 taken at a=22.5 mm and showing well defined fatigue striations. Average striation spacing is 0.18 µm.

Table 4.9. Striation spacing measurements from Figure 4.21 for the ASTM A36 base metal versus $\frac{da}{dN}$ measurement for a = 23.6 mm.

Specimen 3 - ASTM A36 - 23.6 mm	
	SEM Measurement (da/dN in m/cycle)
Location 1 Spacing (m)	9.44E-07
Location 2 Spacing (m)	1.06E-06
Location 3 Spacing (m)	9.73E-07
Average (m/cycle)	9.91E-07
Test Measurement (m/cycle)	1.06E-06
Error (%)	6.51%

Table 4.10. Striation spacing measurements from Figure 4.21 for the AWS A5.18 weld metal versus $\frac{da}{dN}$ measurement for a = 22.6 mm.

Specimen 13-0 - AWS 5.18 - 22.6 mm	
	SEM Measurement (da/dN in m/cycle)
Location 1 Spacing (m)	2.00E-07
Location 2 Spacing (m)	2.08E-07
Location 3 Spacing (m)	1.92E-07
Average (m/cycle)	2.00E-07
Test Measurement (m/cycle)	2.03E-07
Error (%)	1.37%

Table 4.11. Striation spacing measurements from Figure 4.22 for the AWS A5.18 weld metal versus $\frac{da}{dN}$ measurement for a = 22.5 mm.

Specimen 67-76 - AWS 5.28 - 22.5 mm	
	SEM Measurement (da/dN in m/cycle)
Location 1 Spacing (m)	2.38E-07
Location 2 Spacing (m)	1.38E-07
Location 3 Spacing (m)	1.79E-07
Average (m/cycle)	1.85E-07
Test Measurement (m/cycle)	1.60E-07
Error (%)	15.54%

V. SUMMARY AND CONCLUSION

A summary of the test results for both stress ratios for all materials studied is shown in Figure 5.1 and Figure 5.2. As can be seen the Region II $\frac{da}{dN}$ versus ΔK values were about the same to slightly higher for R=0.05 as compared to R=0.6. Greater $\frac{da}{dN}$ versus ΔK values indicate lower resistance to crack growth.

Crack propagation data for the ASTM A36 base metal are in agreement with the published Paris Law fit equations to existing data for ferritic-pearlitic steels for both R=0.05 and R=0.6. The data for the stress ratio R=0.05 had a steeper slope (m) than that for the stress ratio R=0.6. This is reflective of the drop off in $\frac{da}{dN}$ for low ΔK values for R=0.05 data may be the result of crack closure at the lower ΔKvalues.

Fatigue crack growth rate data for each weld metal for Region II is generally the same as that of the ASTM A36 base material and falls within the limits observed for other steel welds. Again there is a more rapid drop off in the $\frac{da}{dN}$ values at low ΔK values for the specimens tested at R=0.05. Again this is thought to result from the effective ΔK being lower than the actual ΔK because of the greater amount of crack closure.

ΔK_{th}values for R=0.6 are established at 3.8 MPa√m for both ASTM A36 and AWS A5.18, and 2.95 MPa√m for AWS A5.28. The higher ΔK_{th} values for ASTM A36 and AWS A5.18 is thought to be due to the larger grain size as compared to AWS A5.28. Steel with finer grain structures exhibit lower ΔK_{th} as compared to steel with coarse grain structures. ΔK_{th} for each material was greater for load ratios R=0.05 versus R=0.6 as expected. Differences in microstructure and the effect of crack closure are thought to contribute to the change in values of ΔK_{th} for R=0.05.

The test results also show that is Region I AWS A5.18 has greater fatigue resistance than AWS A5.28. This is due to the greater ΔK_{th} values for both stress ratios. A greater ΔK_{th} indicates that the material can tolerate a longer crack length (a) or greater stress range Δσ. This also indicates that AWS A5.28 could be less tolerant to flaws and defects as compared to AWS A5.18.

Inspection of the fracture surfaces showed Region II crack growth regions are characterized by well-defined fatigue striations and occasional secondary cracking for the base metal and two weld metals. This indicates that the mechanism of Region II crack growth was the same for these materials even though the microstructures for the base metal and the weld metals are different. The average striation spacing measurements obtained from the scanning micrographs which correlate within 16% of measured $\frac{da}{dN}$ values for the crack locations examined.

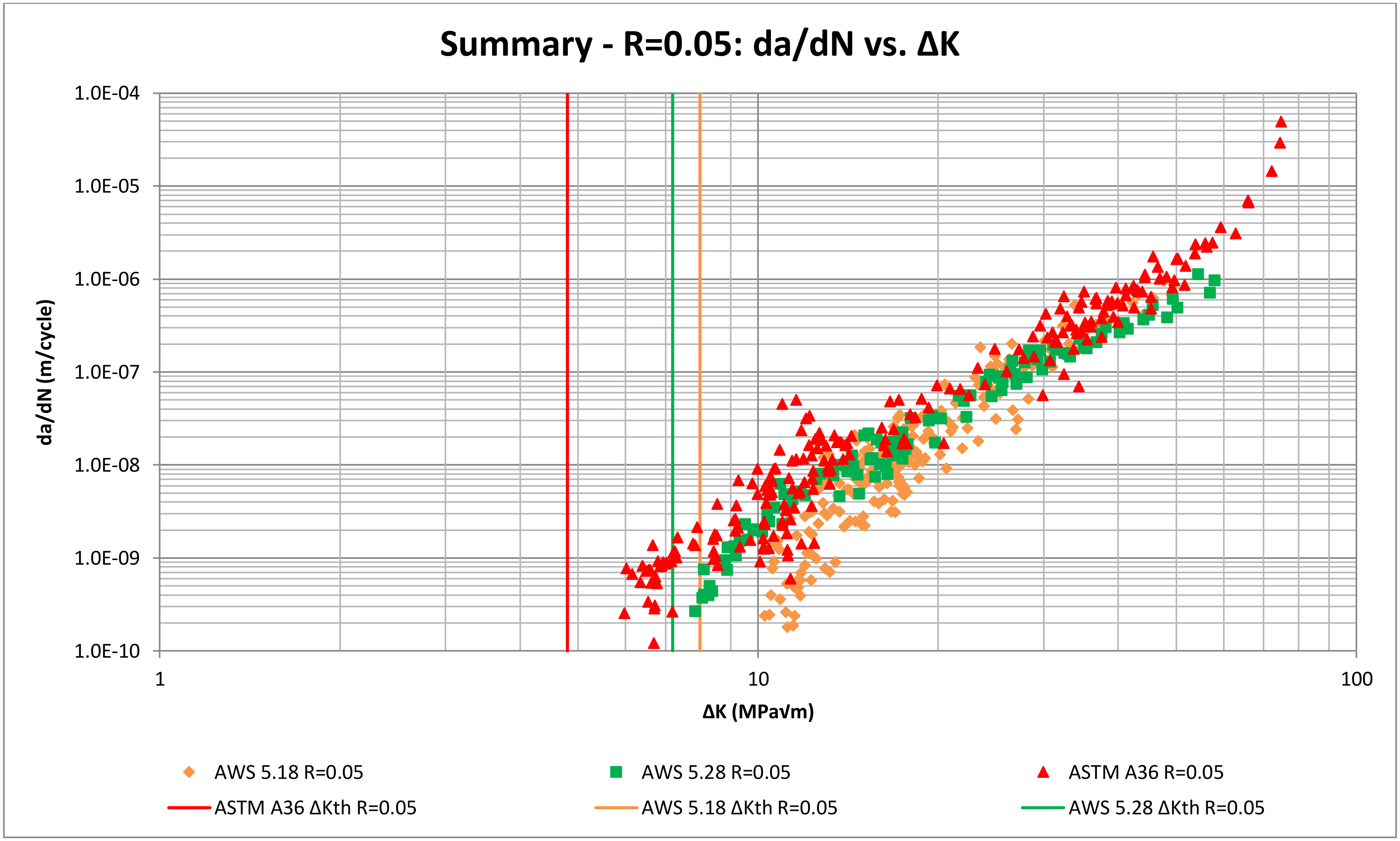

Figure 5.1. Summary of all fatigue crack propagation results for R=0.05.

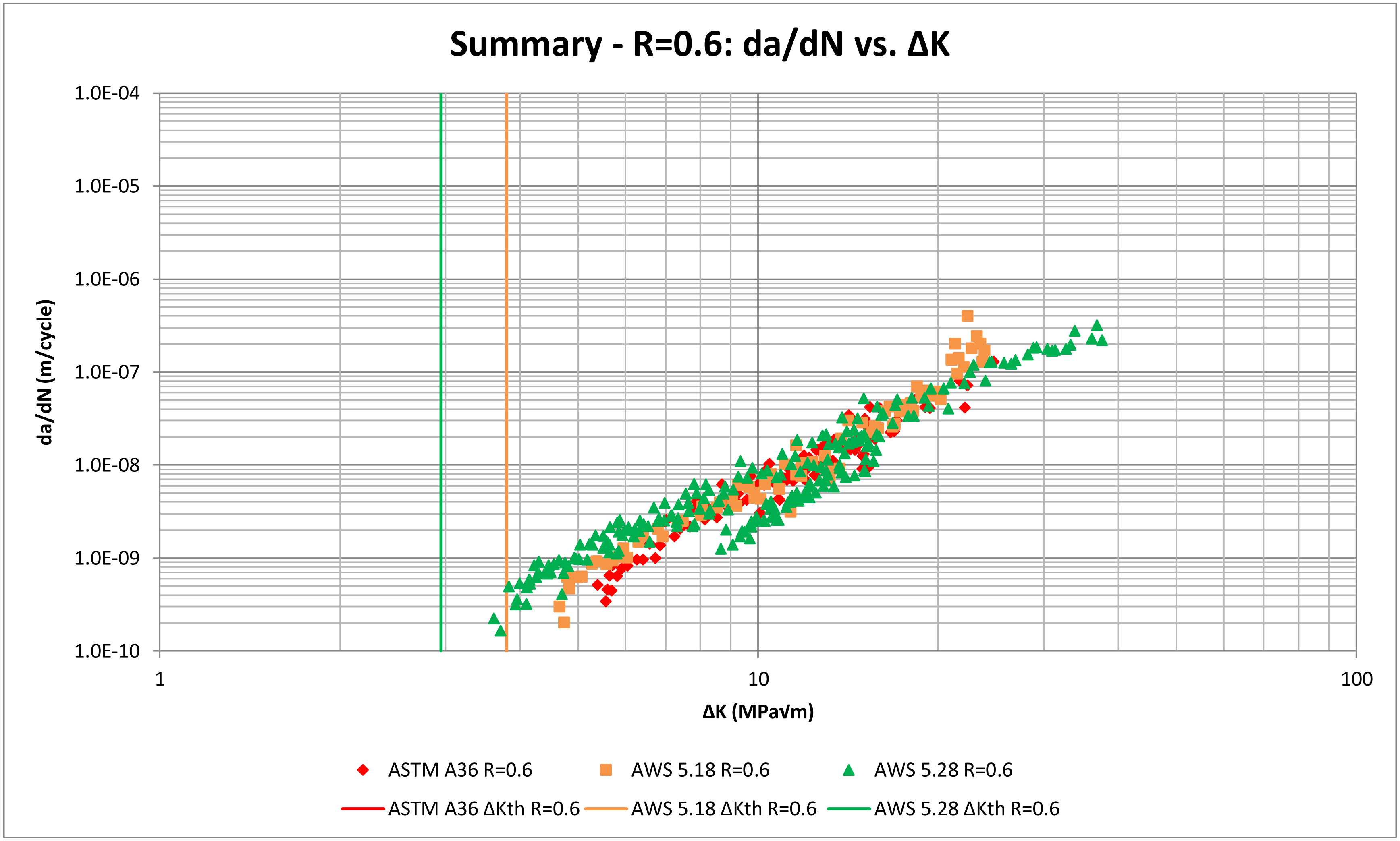

Figure 5.2. Summary of all fatigue crack propagation results for R=0.6. ΔK_{th}= 3.80 for both ASTM A36 and AWS A5.18.

VI. RECOMMENDATIONS FOR FUTURE WORK

Additional testing for each weld metal should be conducted to completely characterize crack growth in Regions I. As-welded condition fatigue crack propagation tests should be completed to understand residual stress impact on fatigue crack growth rates. This testing would also give additional insight on service life of welded joints not stress relieved.

VII. BIBLIOGRAPHY AND REFERENCES

[1] F. C. Campbell, Fatigue and Fracture: Understanding the Basics, Materials Park, OH: ASM International, 2012, pp. 1-17.

[2] ASM International, Fatigue and Fracture, vol. 19, Materials Park, OH: ASM International, 1996, pp. 15-26, 63-72.

[3] ASM International, Mechanical Testing and Evaluation, vol. 8, Materials Park, OH: ASM International, 2000, pp. 681-685.

[4] R. I. Stephens, A. Fatemi, R. R. Stephens and H. O. Fuchs, Metal Fatigue in Engineering, New York, New York: John Wiley & Sons, Inc., 2001, pp. 19-56, 122-175, 454.

[5] ASM International, Failure Analysis and Prevention, vol. 11, Materials Park, OH: ASM International, 2002, pp. 227-242, 559-586.

[6] A. S. Network, "ASN Aircraft accident 22DEC1969 - General Dynamics F111A67-0049," Aviation Safety Network, 27 January 2013. [Online]. Available: https://aviation-safety.net/wikibase/wiki.php?id=60449. [Accessed 4 April 2016].

[7] N. R. C. (U.S.), "Aging of U.S. Air Force aircraft: Final report," National Academy Press, Washington, D.C, 1997.

[8] ASM International, Fractography, vol. 12, Materials Park, OH: ASM International, 1987, pp. 12-71.

[9] International, ASTM, ASTM E647, West Conshohocken: Online at IHS Standards Expert, 2015.

[10] R. A. Smith, " Proceedings of a Conference on Fatigue Crack Growth, Crambirdge, UK, 20 September 1984," in *Fatigue Crack Growth: 30 Years of Progress*, Oxford, 1986.

[11] J. M. B. Stanley T. Rolfe, Fracture and Fatigue Control in Structures, Englewood Cliffs, New Jersey: Prentice-Hall, Inc., 1977, pp. 232-264.

[12] R. C. Rice, B. N. Leis, D. Nelson, & Society of Automotive Engineers, Fatigue Design Handbook, Warrendale, PA: Society of Automotive Engineers, 1988, p. 42.

[13] T. L. Anderson, Fracture Mechanics, Fundamentals and Applications, Third Edition ed., Boca Raton, Florida: Taylor & Francis Group, 2005.

[14] S. Maddox, Assessing the Significance of Flaws in Welds Subject to Fatigue, Miami: American Welding Society, 1974, pp. 401-409.

[15] International, ASTM, ASTM A36/A36M - 14: Standard Specification for Carbon Structural Steel, West Conshohocken: ASTM International, 2014.

[16] A. Society, AWS A5.18/A5.18M:2005, Miami, FL: American Welding Society, 2005.

[17] A. Society, AWS A5.28/A5.28M:2005 (R2015), Miami, FL: American Welding Society, 2015.

[18] A. W. Society, AWS D1.1, USA: American Welding Society, 2015.

[19] ASM International, Metallography and Microstructures, vol. Volume 9, Materials Park, OH: ASM International, 2004, pp. 588-607.

[20] R. O. Ritchie, "Near-threshold fatigue-crack propagation in steels," *International Metals Reviews,* vol. 5 & 6, pp. 205-230, 1979.

VIII. APPENDICES

This page intentionally left blank.

Appendix A: Tensile Specimen Dimensions and Manufacture

All steel for specimens was cut at the John Deere Dubuque Works Experimental Shop. The tensile test specimens were made from the same base plate as that for all standard compact C(T) tension specimens for fatigue crack growth studies. The plate first was cut into a 16 mm x 16 mm x 108 mm sections. Then the tensile test specimens were machined to the dimensions shown in Figure A.1 using a CNC lathe (onsite at Marquette University and at a machine shop in Dubuque, IA). Welded tensile test specimens were created with a 19 mm x 19 mm x 108 mm weld section using the same machining method. The welded tensile test specimens material were created using several subsequent weld passes just as was done to create weld C(T) specimens to create material section to be machined. They were also stress relieved in the same manner as the C(T) specimens.

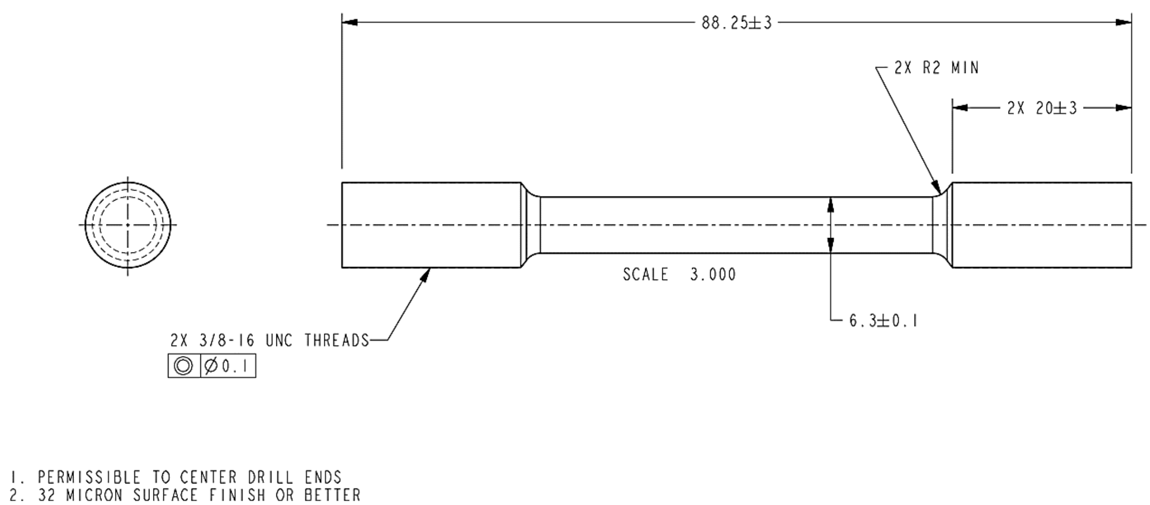

Figure A.1. Manufacturing specifications for tensile test specimen

Appendix B: Instron Model 5500R Test Machine Set-up for Tensile Tests

Tensile test specimen installation into Instron Model 5500R test machine and test start are summarized below. Figure B.1 identifies the different machine controls.

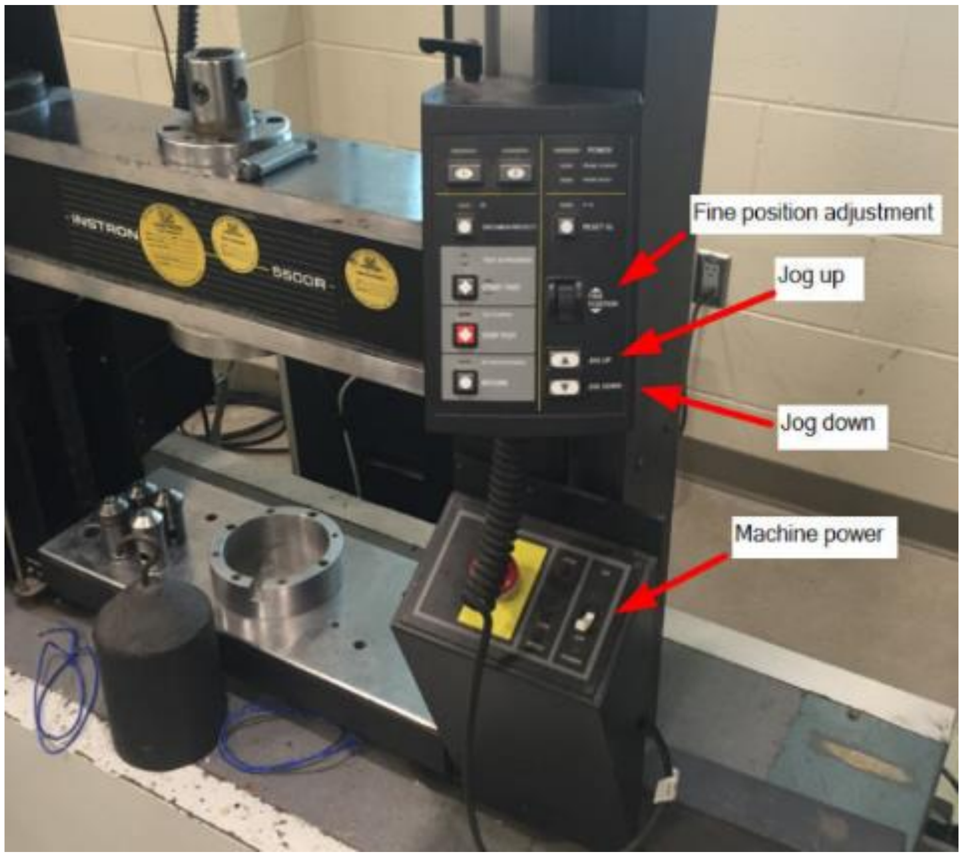

Figure B.1. Instron machine system controls

1. Insure that the 10,000 lb_f load cell is installed. Figure B.2 shows the load cell identification.

Figure B.2. 10,000 lb_f load cell identification

2. Verify that the threaded grips are installed (see Figure B.3).

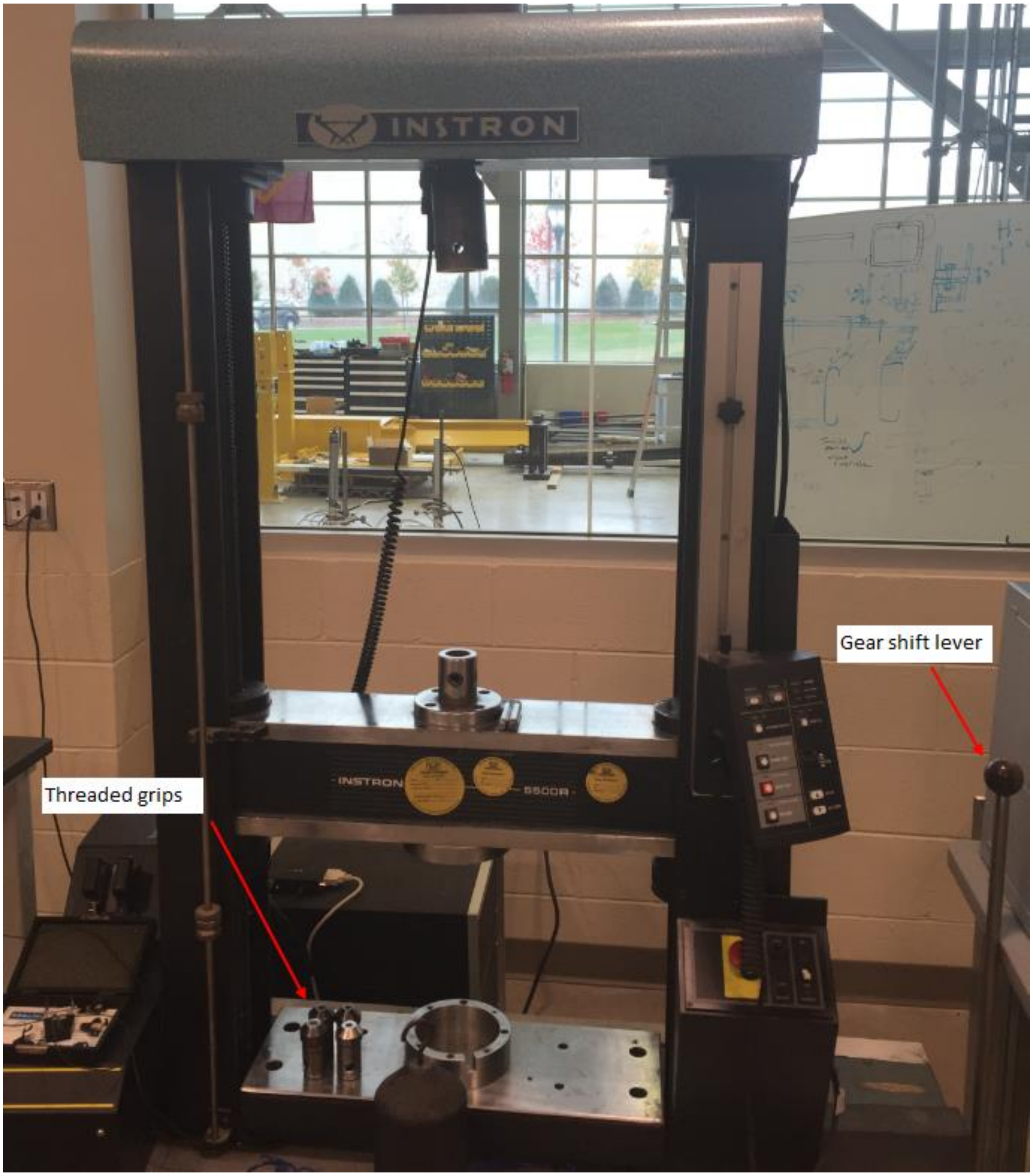

Figure B.3. Grip and gear shift lever identification

3. Verify that the gear shift level is in the fully back (high cross head speed) position (see Figure B.3).
4. Verify that the load cell is connected to the testing machine.

5. Log in to computer:
    a. Username: Instron
    b. Password: instron
6. Using the computer mouse, double-click Instron Bluehill to open the Bluehill 2 (version 2.16) software.
7. Select Tensile Test
8. Balance and calibrate the load cell
    a. Left click the Balance Load key or left click the Load Cell icon
    b. Balance is achieved when the Load Cell readout is ± 1.0 lb.
    c. Left click the Load Cell icon in the upper right hand corner and then left click the Calibrate key in the dialog box.
    d. After the calibration is complete, hang a 25 lb weight from the lower grip.
    e. The calibration is acceptable if the load cell readout is 25.0 ± 1.0 lb
9. Screw tensile test specimen into the upper grip
10. Screw the lower grip onto the bottom of the tensile specimen.
11. Use the Jog Up and Jog Down Buttons and the Fine Adjust dial to position the lower crosshead and pin the lower grip to it.
12. Use the Fine Adjust dial to apply a tensile preload of about 20 lbs.
13. Clock the Reset Gage Length icon on the top of the screen.
14. Press the Start button to run the test.
15. Adjust the X and Y scales on the load vs. strain plot to refine the plot of P versus ΔL.

Appendix C: Tensile Load-Elongation Curves

This page intentionally left blank.

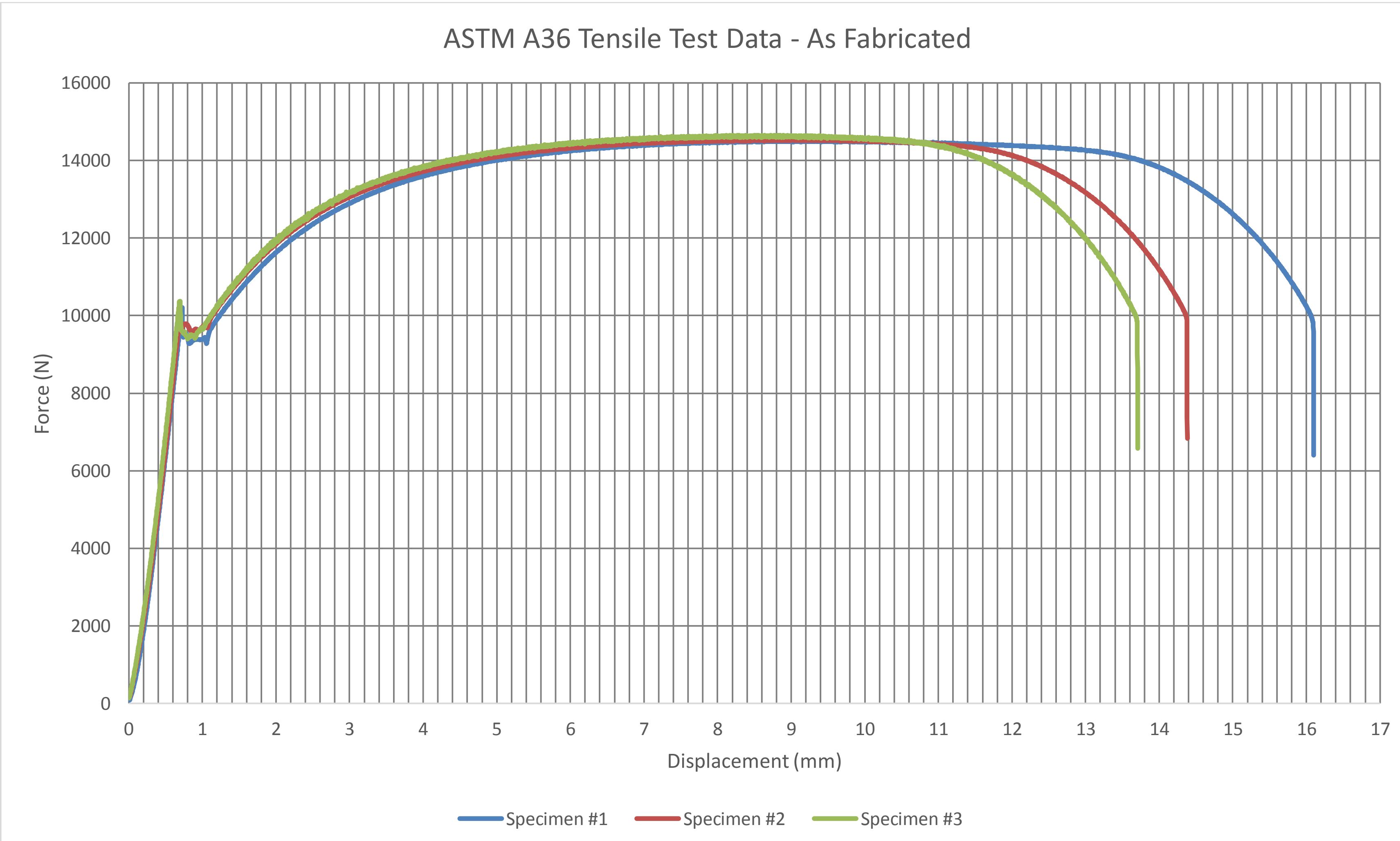

Figure C.1. Tensile test data from as fabricated tensile test specimens – ASTM A36

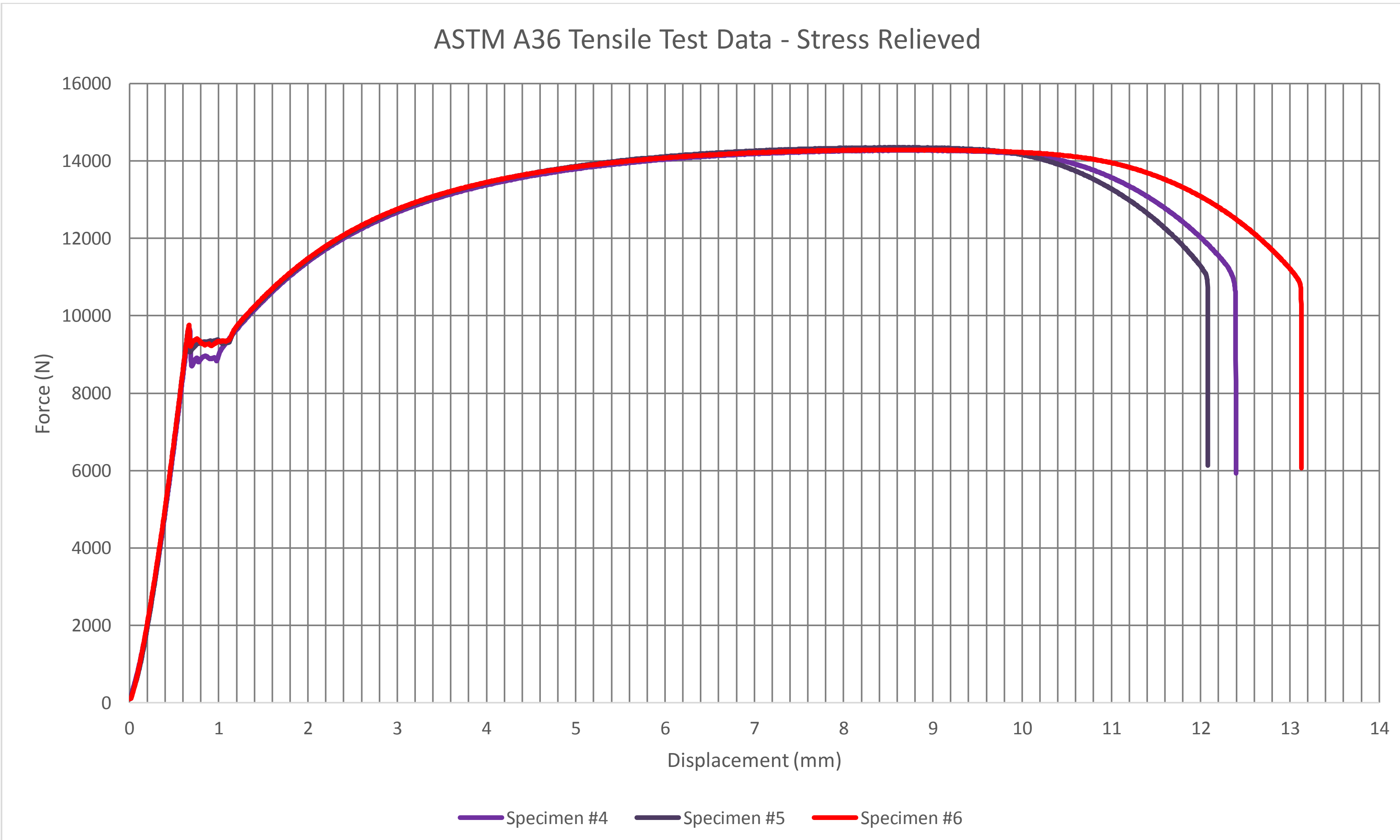

Figure C.2. Tensile test data of stress relieved specimens – ASTM A36

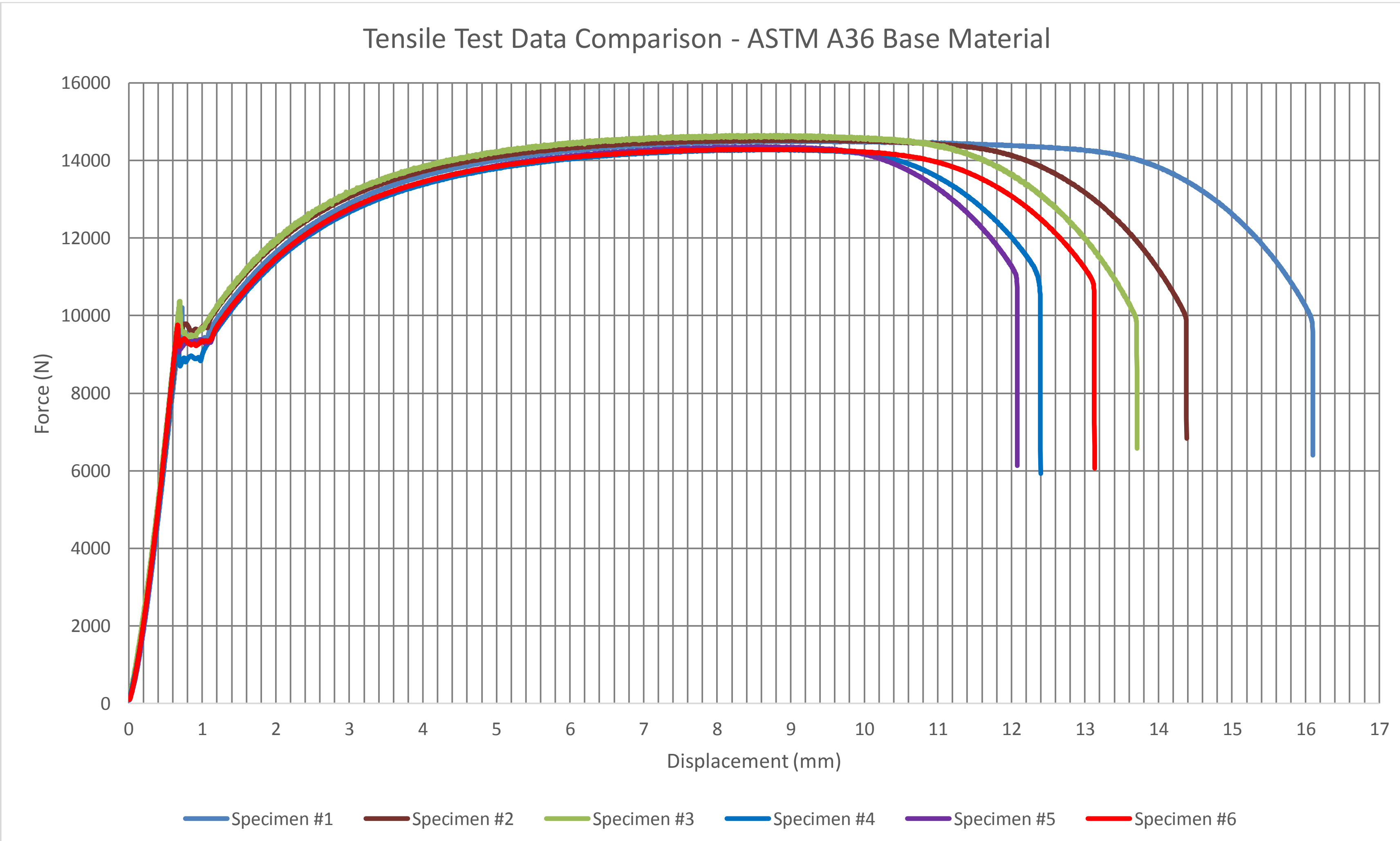

Figure C.3. Tensile test data comparison for ASTM A36 base material

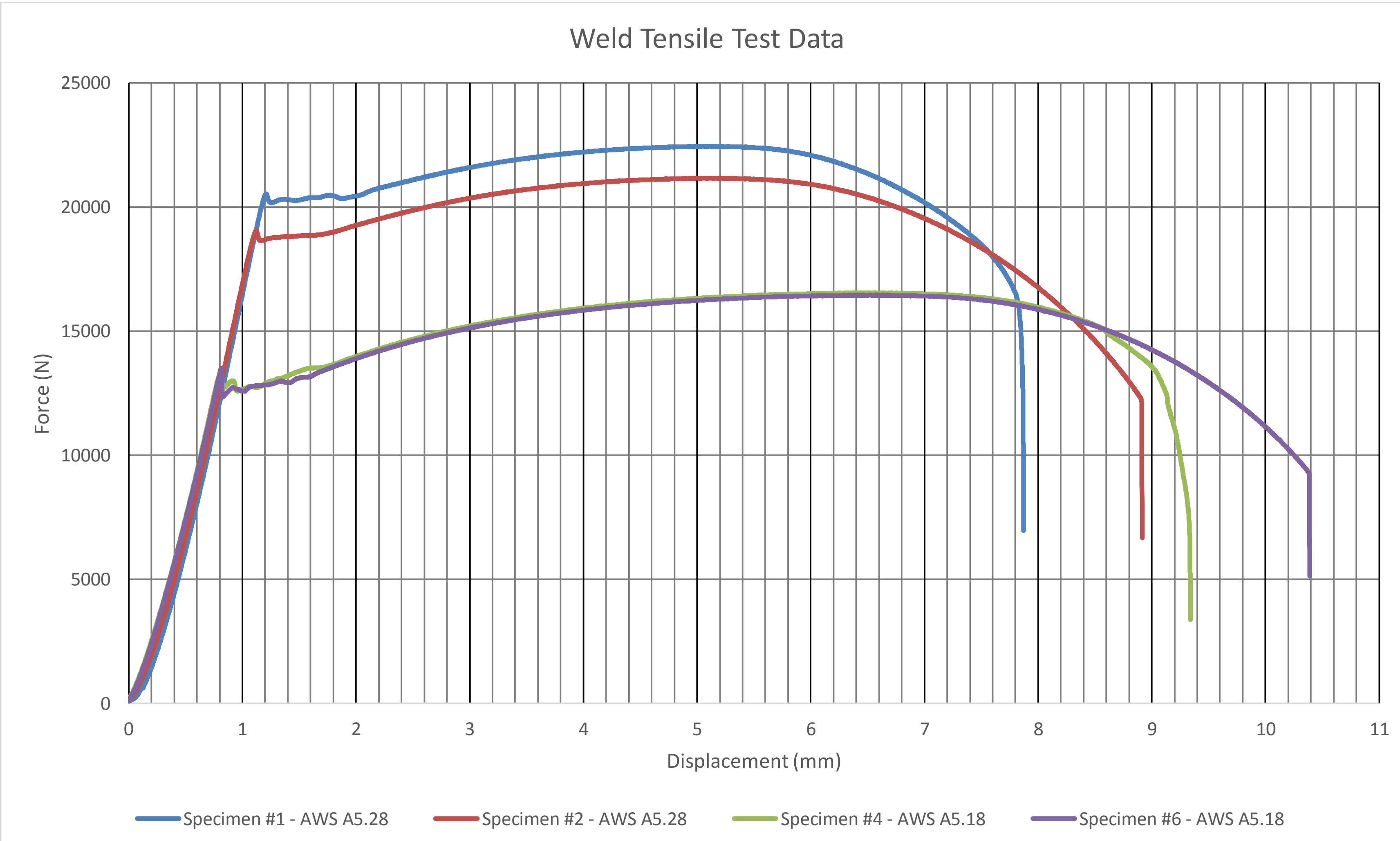

Figure C.4. Tensile test data for weld metal AWS A5.18 and AWS A5.28

Appendix D: Metallography

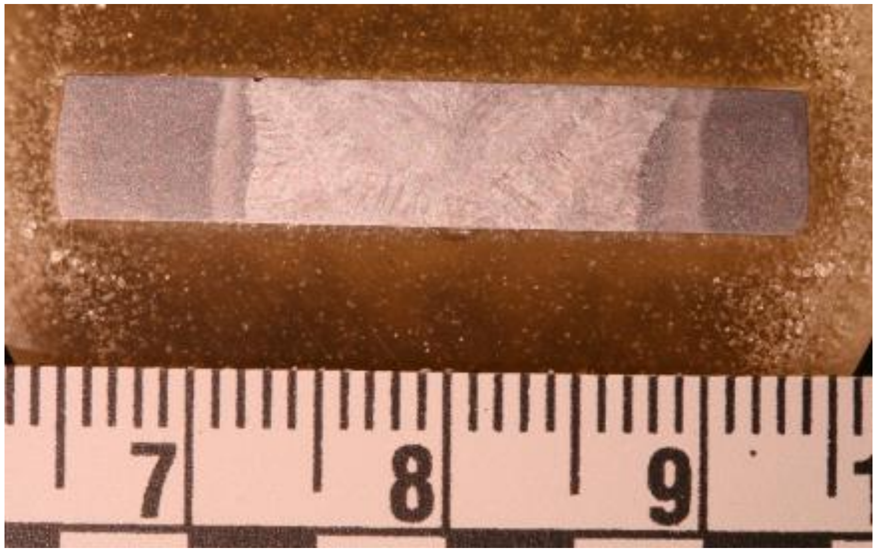

Figure D.5. AWS A5.28 metallographic specimen. Specimen was mounted in orientation for which the crack would grow perpendicular into the specimen.

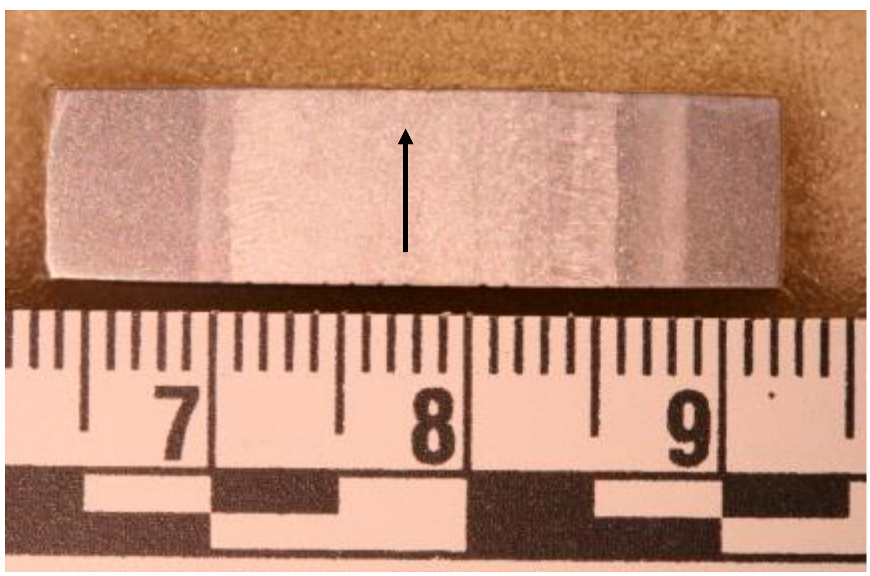

Figure D.6. AWS A5.28 metallographic specimen. Specimen was mounted in orientation for which the crack would grow in the direction of the arrow.

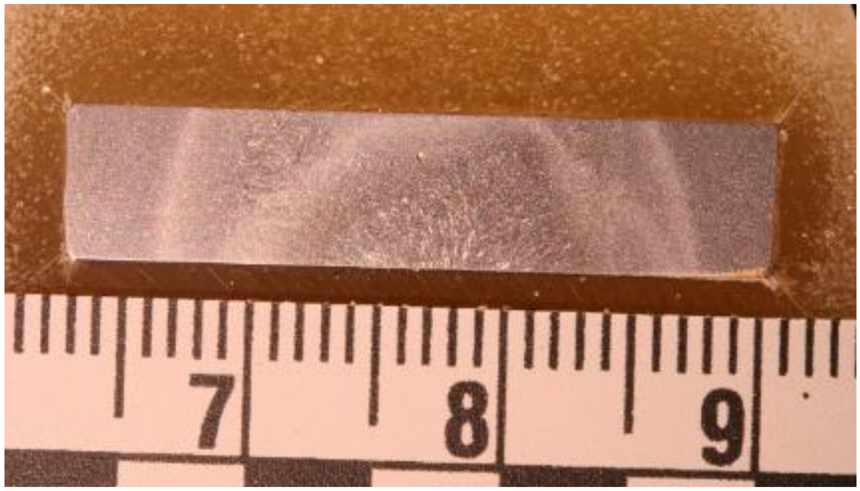

Figure D.7. AWS A5.18 metallographic specimen. Specimen was mounted in orientation for which the crack would grow perpendicular into the specimen.

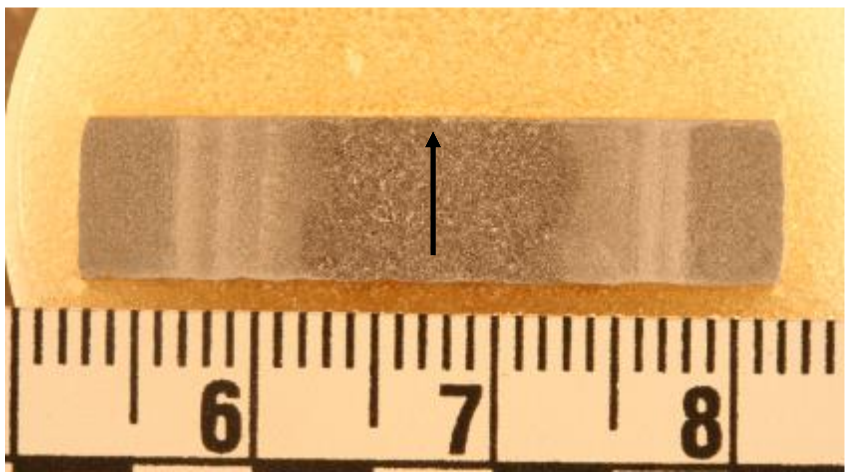

Figure D.8. AWS A5.18 metallographic specimen. Specimen was mounted in orientation where the crack would grow in the direction of the arrow.

Appendix E: Rockwell B Hardness Measurements

Figure E.1. Hardness gradient measurement profile on chemically etched test specimen - Specimen #37-31 AWS A5.18.

Table E.1. AWS A5.18 Rockwell B Harness Gradient

#	Left (HRB)	Right (HRB)
1	67.9	70.7
2	71.4	71.9
3	72.2	72.4
4	72.1	71.7
5	72.5	71.6
6	72.6	72.1
7	72.9	72.8
8	72.4	71.1
9	71.9	71.4
10	73.3	73.2
11	74.1	73.0
12	77.6	76.9
13	78.9	79.0
14	80.6	80.5
15	80.0	79.7
16	81.9	80.0
17	78.0	78.0
18	79.4	79.1
19	74.0	73.4
20	72.0	72.0
21	69.7	69.4
22	71.7	70.6
23	72.4	71.4
24	72.2	71.8
25	72.6	71.7
26	72.0	70.7
27	71.8	68.8
28	71.2	71.7
29	71.4	71.1

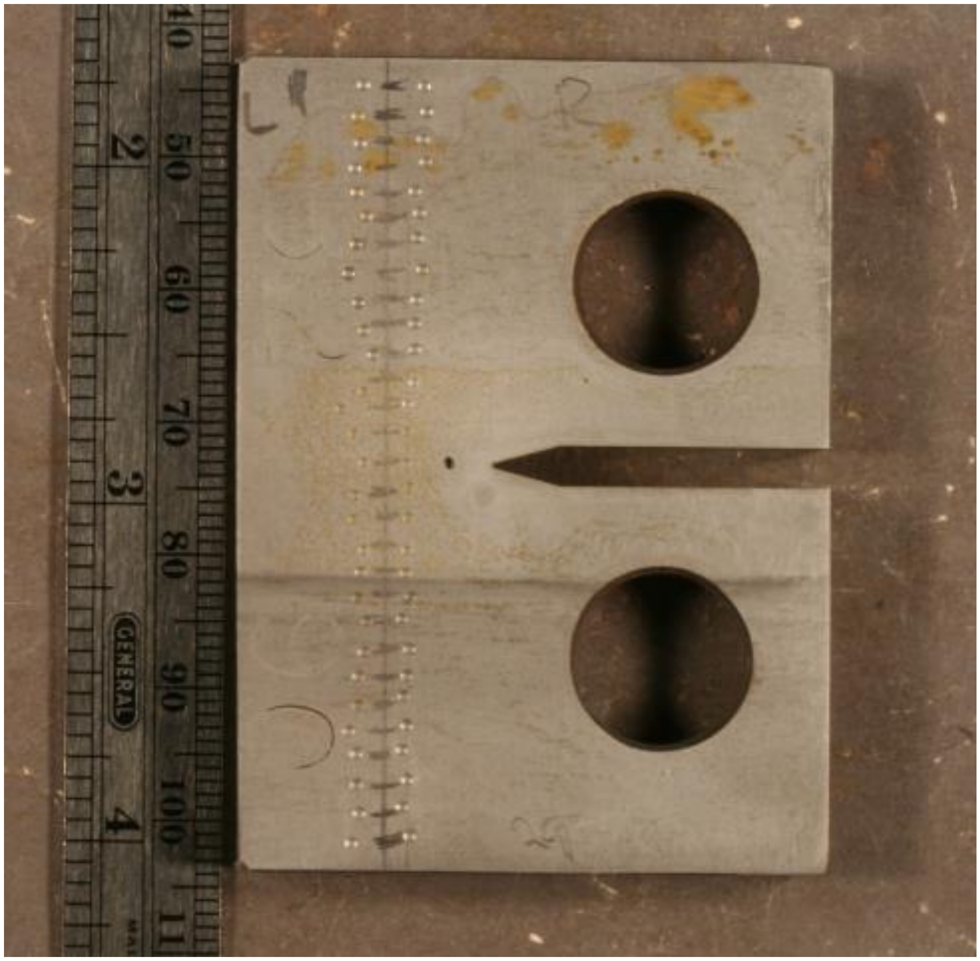

Figure E.2. Hardness gradient measurement profile on chemically etched test specimen - Specimen #52-90 AWS A5.28.

Table E.2. AWS A5.28 Rockwell B Hardness Gradient

#	Left (HRB)	Right (HRB)
1	73.4	72.8
2	73.3	73.4
3	73.9	73.2
4	74.1	74.5
5	73.9	73.1
6	75.4	73.9
7	74.8	73.3
8	73.8	73.5
9	75.2	73.5
10	75.9	74.1
11	75.9	75.4
12	97.5	96.4
13	96.3	96.1
14	96.7	95.7
15	97.7	97.8
16	96.4	99.0
17	95.5	96.3
18	97.1	97.2
19	87.5	87.4
20	77.6	77.4
21	73.7	73.5
22	73.5	72.4
23	74.3	73.6
24	74.3	75.7
25	74.2	73.6
26	72.1	72.8
27	70.4	70.9
28	72.0	70.8
29	73.2	73.1

Appendix F: Set-up, Start and Operation of 20,000 lb_f MTS Test Machine for the Fatigue Crack Growth Tests

Detailed instructions for the removal and installation of standard compact C(T) specimens into the MTS Model 312.21 20,000 lb_f test machine and the start and running of fatigue crack growth tests are summarized below.

Standard Compact C(T) Specimen Removal and Installation

Removal and installation basically involves setting the testing machine software for manual load control, setting the load to zero, removing a specimen or specimen pieces, changing to displacement control, installing the specimen in the pinned connector grips, and setting up the cameras for monitoring crack growth. To do this one must:

1. Log in to computer:
    a. Username: .\c2e2
    b. Password: Engineering 1
2. Using the computer mouse, double-click Station Manager.

3. Select and Open Fatigue Crack Propagation file.

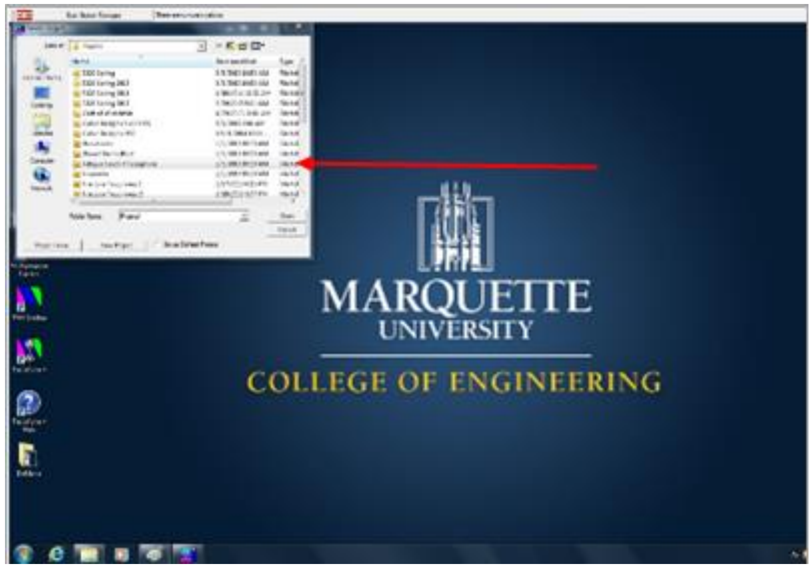

4. Select 20 KIP FRAME in Open Station window.

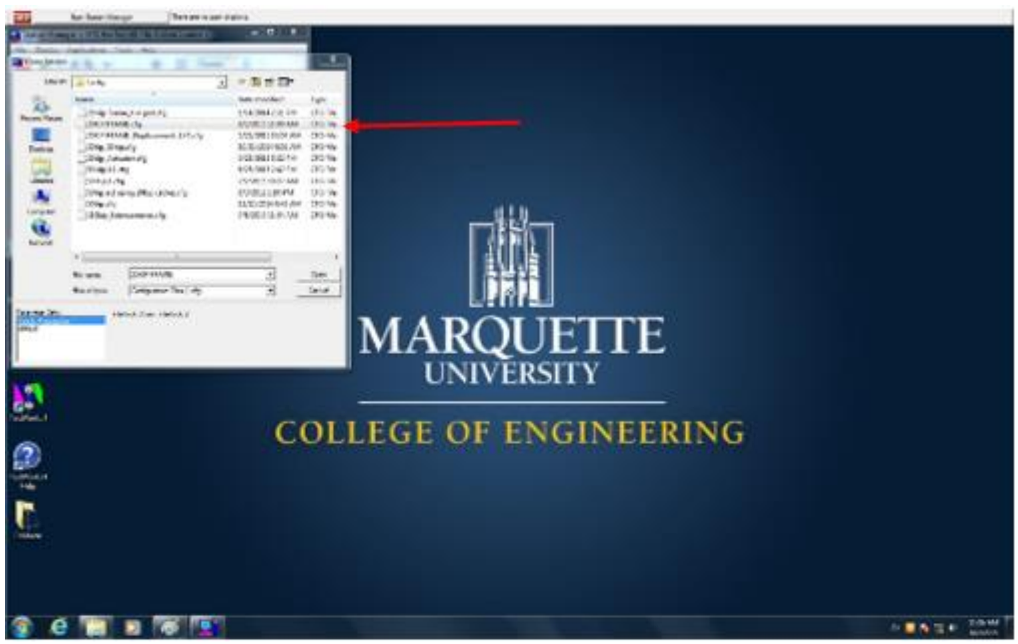

5. Click Open button in Open Station window.

6. Select Exclusive Control in the Station Manager window

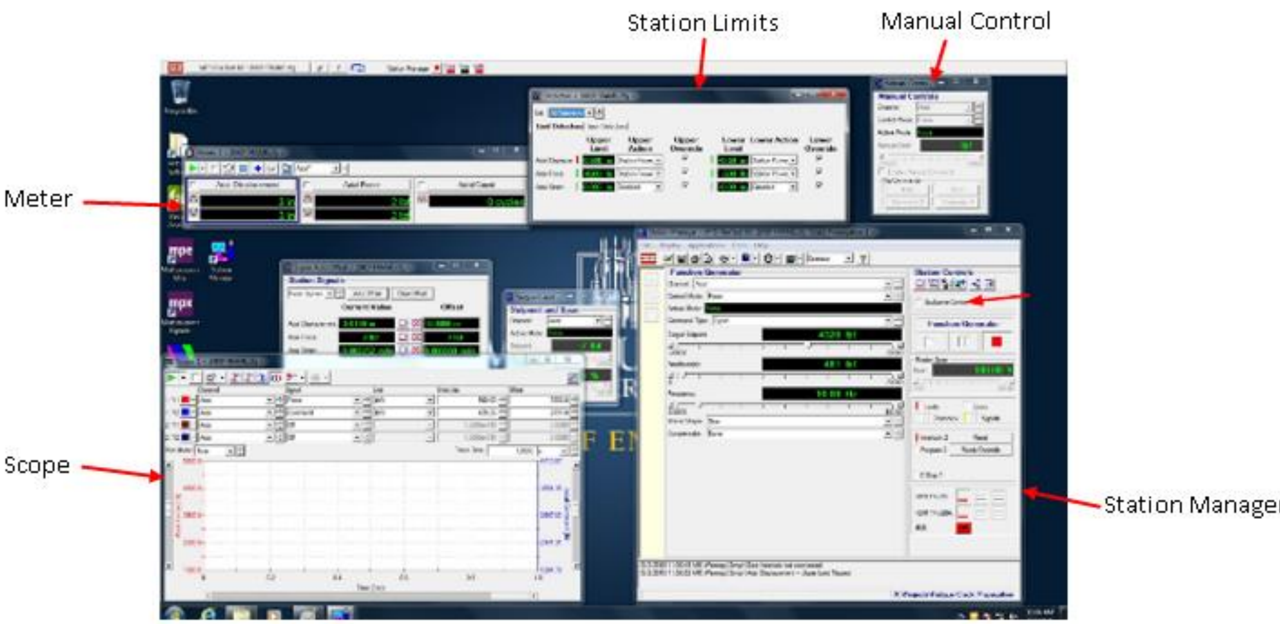

7. To remove a specimen, disable the following detectors:
   - Axial displacement
   - Axial force

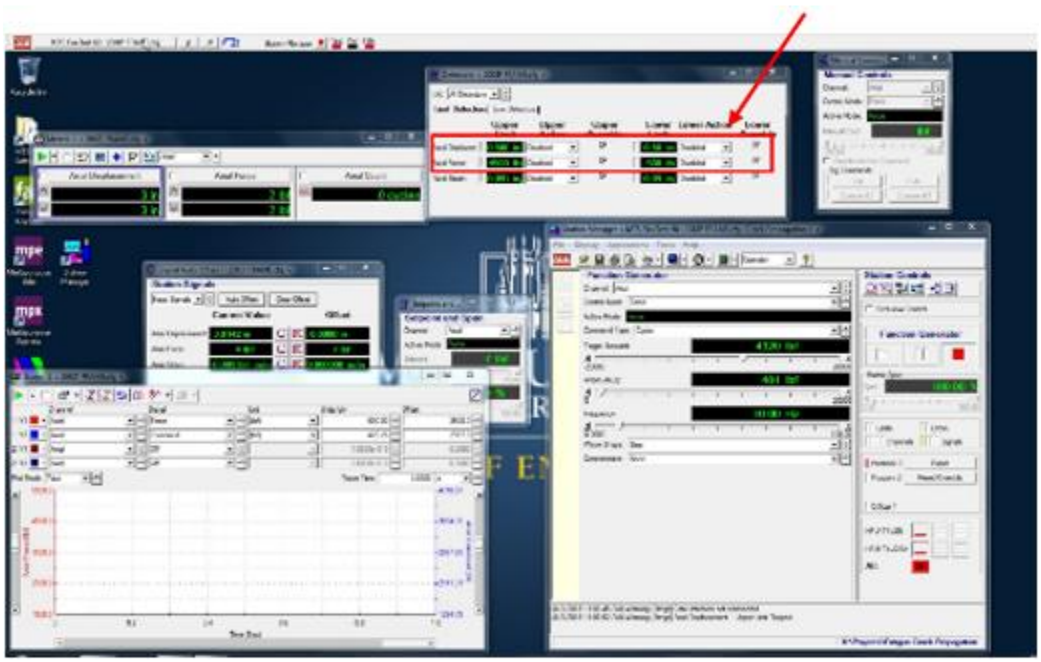

8. Enable Manual Command

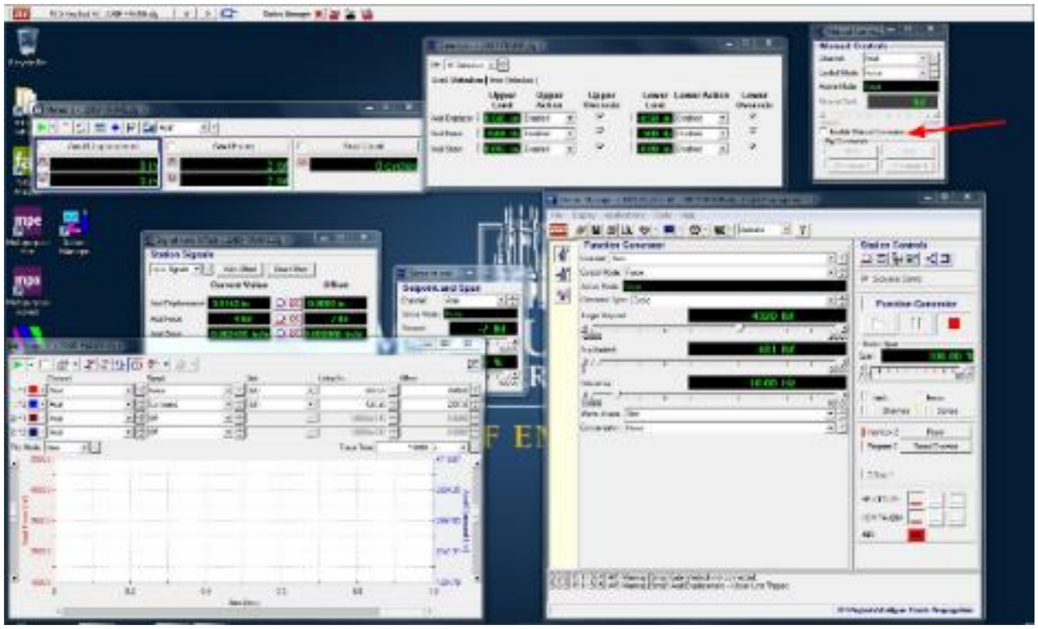

9. Select control mode Force

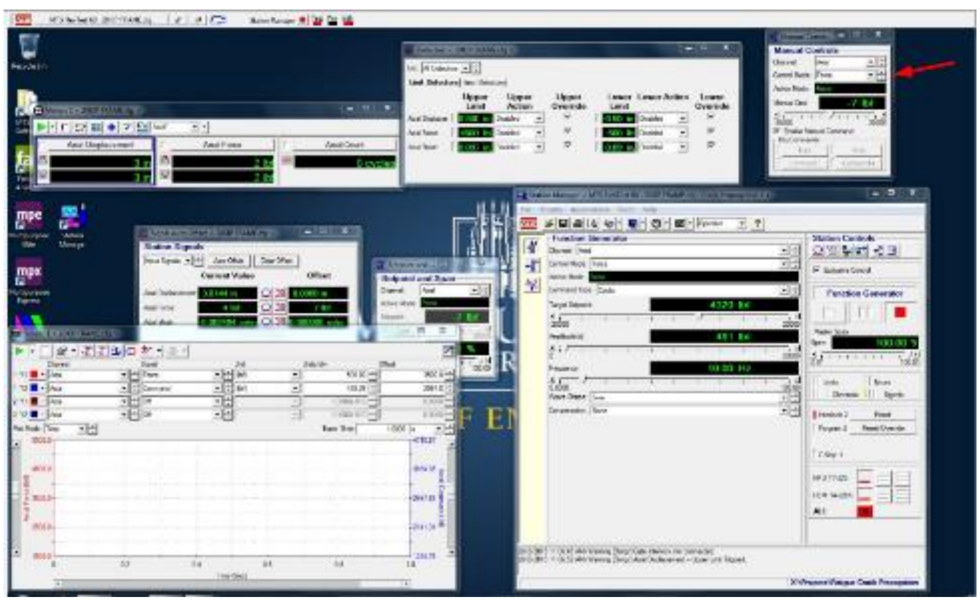

10. Enable hydraulics in the Station Manager window:
    - Reset Interlock 2
    - Turn on hydraulic pump (HPU T7-J25) to low pressure (Middle Button)
    - Turn on station power (HSM T4-J28A) to low pressure (Middle Button)

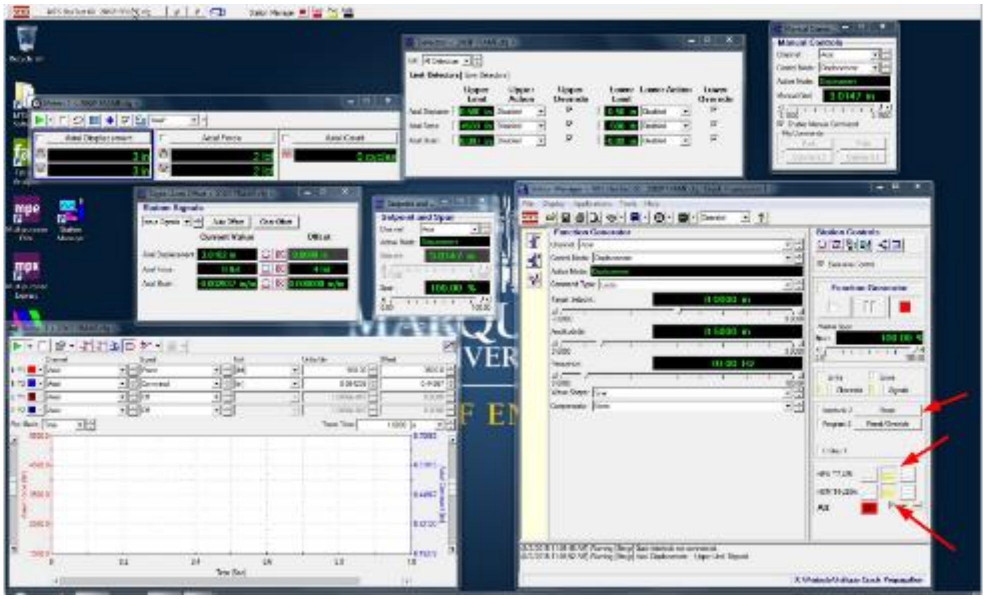

11. Move the Manual Command Slider bar until the Axial Force value (listed in Station Signals) reads 0 lb_f.

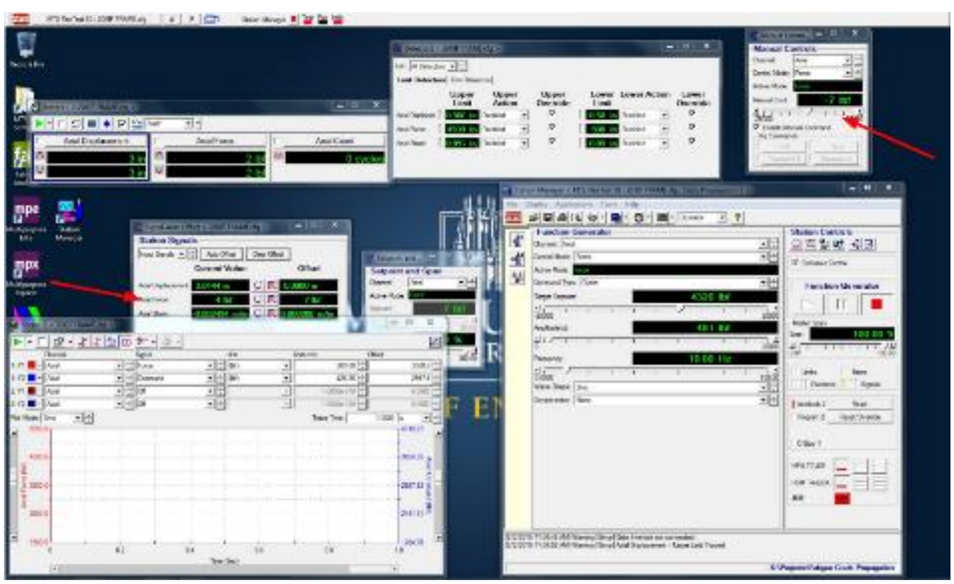

12. Remove test specimen from lower grip by remove (2) cotter pins, grip pin, and (2) spacers.

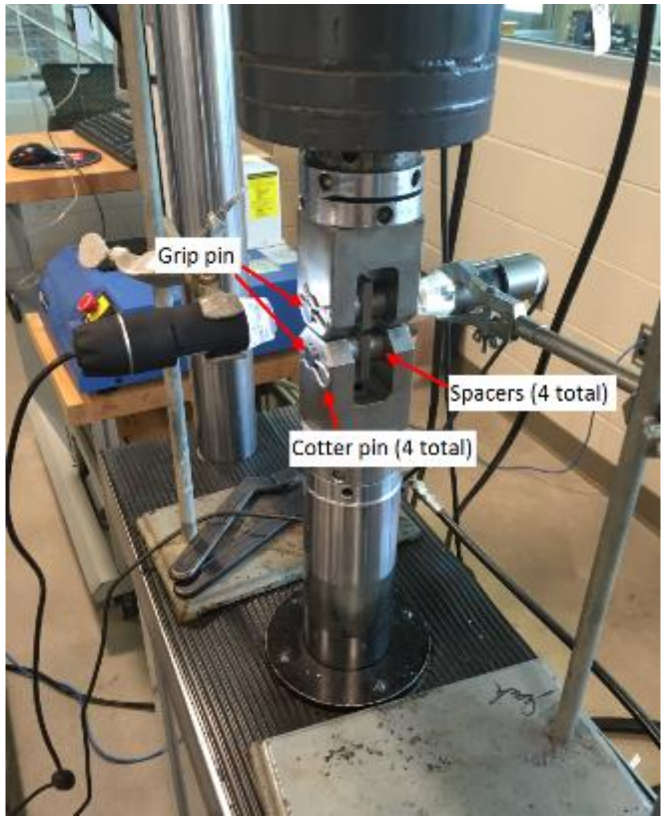

13. Under Manual Controls select the Displacement control mode and move the slider bar to the maximum slider value.

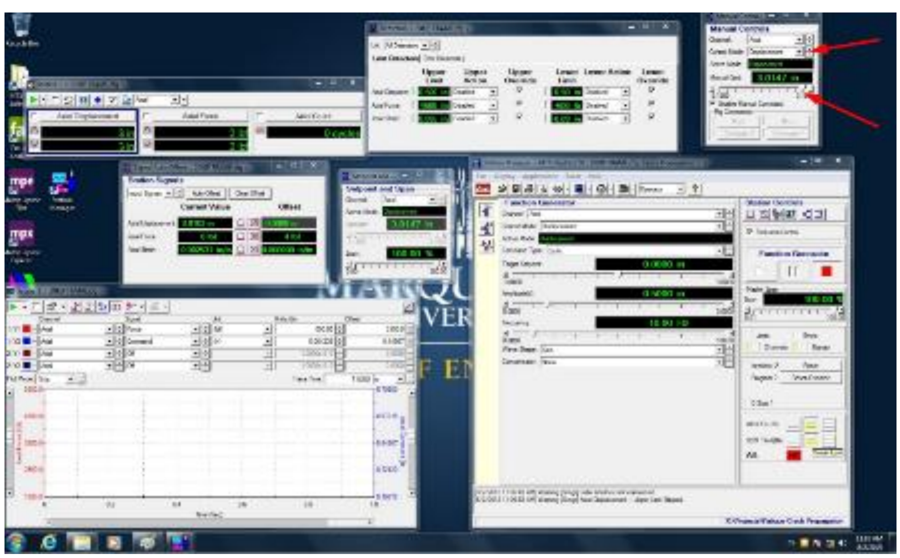

14. Follow the same procedure as Step 12 for the upper grip to remove the compact specimen.
15. In the Signal Auto Offset window:
    - Clear offsets
    - Click Auto Offset for Axial Force

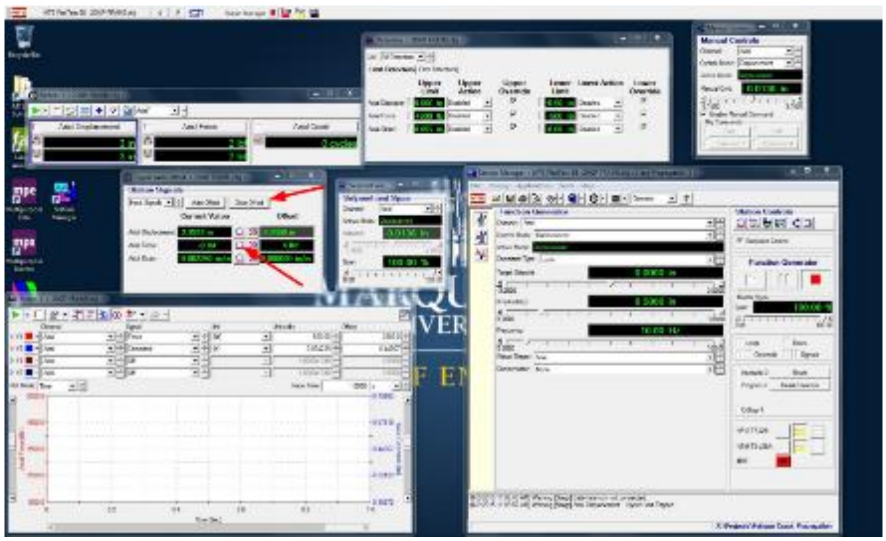

16. Install specimen in upper grip with (2) spacers, grip pin, and (2) cotter pins with compact specimen centered between both spacers.

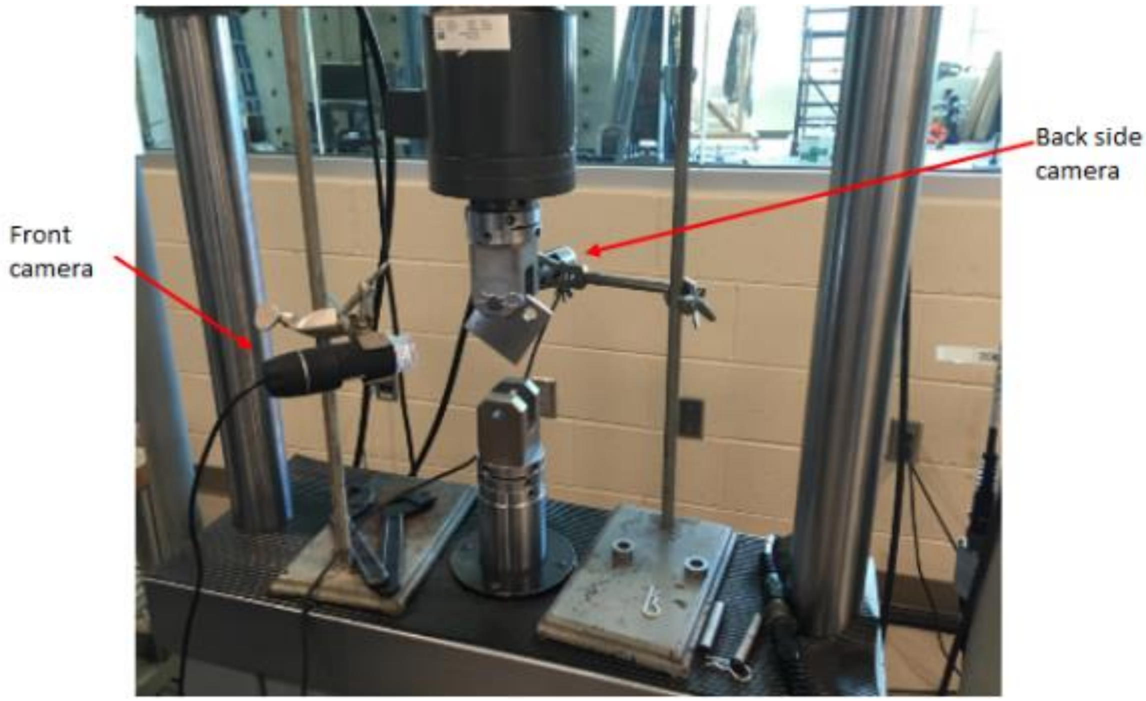

17. Move the lower grip into a position where it is possible to install the lower grip pin. The lower grip is moved with the Manual Control slide bar. Ensure that specimen remains clear of lower grip as it approached the upper grip.

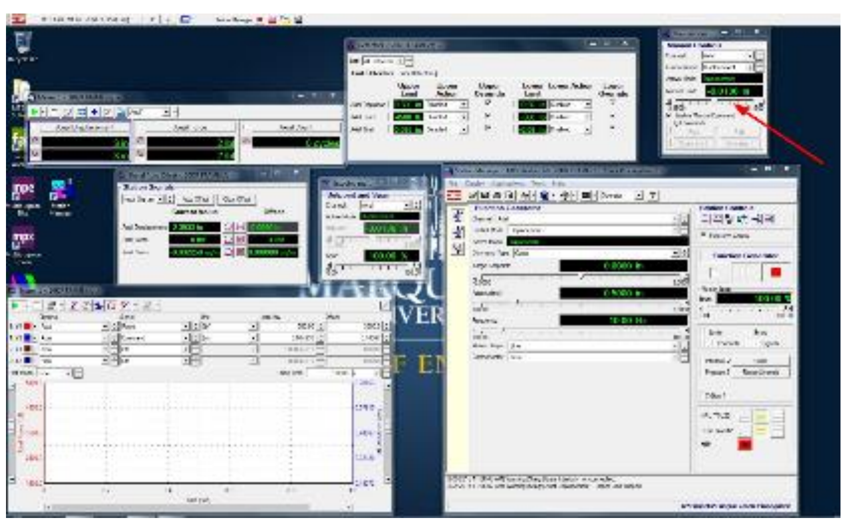

18. Install the grip pin, spacers, cotter pins into the lower grip. Final assembly should appear as the pictures below:

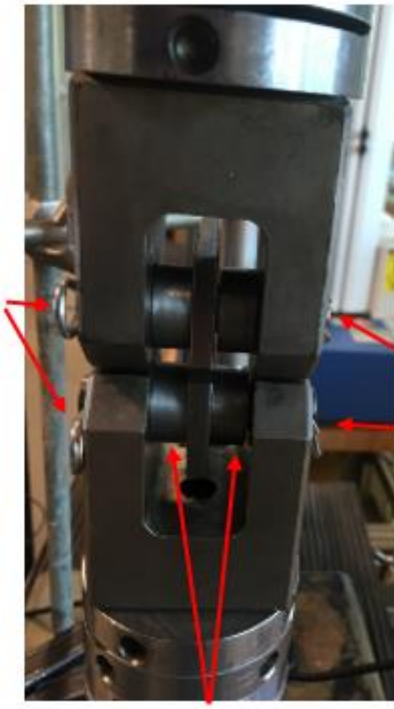

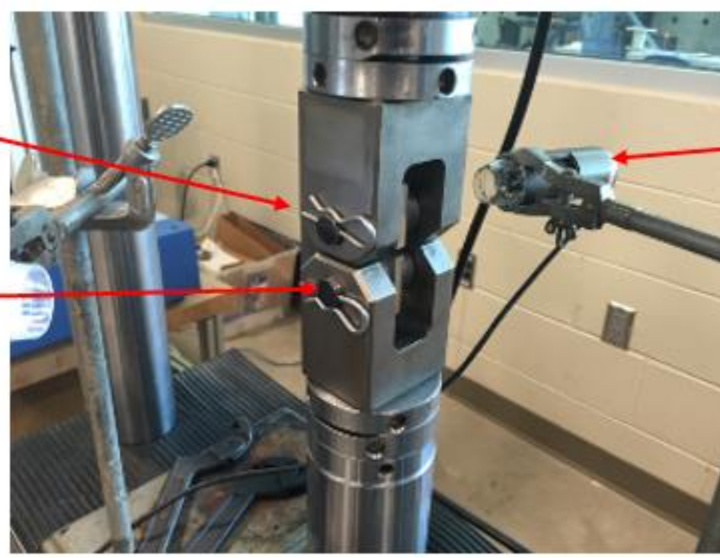

Start of Test

1. Install and align microscope cameras. Ensure that the cameras are in a position to capture the entire crack length and focused. Take baseline picture with each camera.

Front camera

Back side camera

Ruler

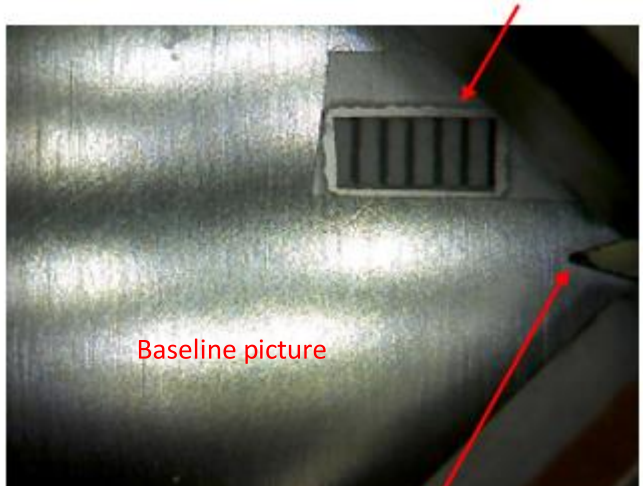

Machined notch - compact C(T) tension

2. In the Manual Control window change the Control Mode to Force. Un-check Enable Manual Command.

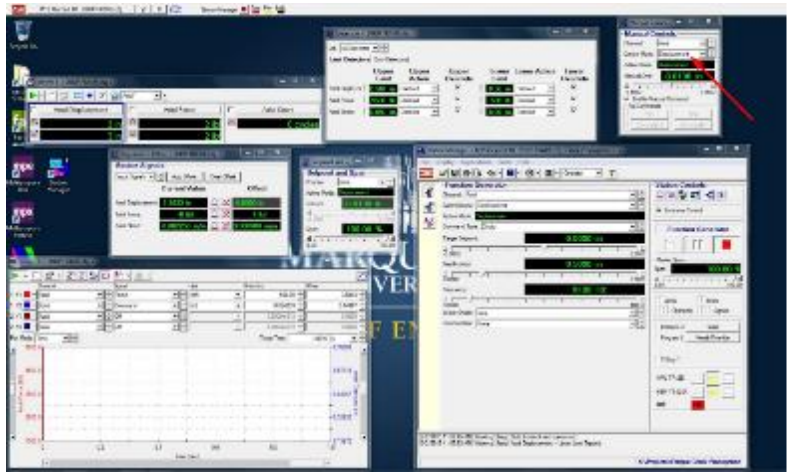

3. In the Station Manager window:
    - Select Function Generator
    - Set the mean load with Target Set Point
    - Set load amplitude with Amplitude
    - Set the Frequency

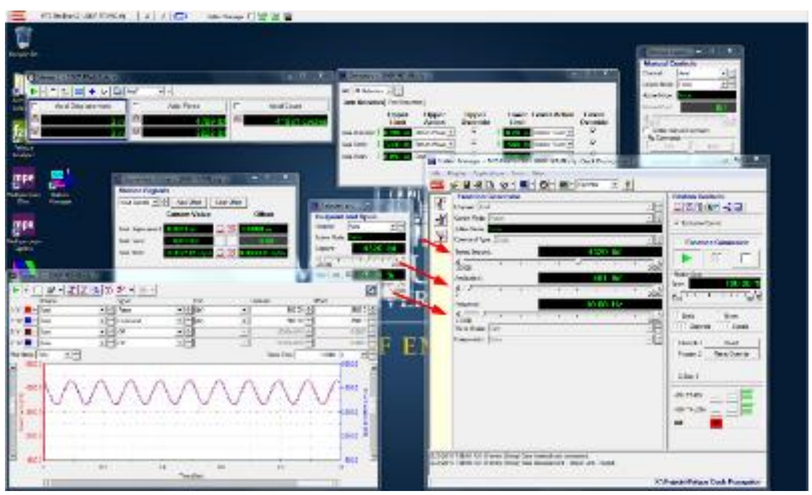

4. In the Detectors window:
   - Set Axial Force values +500lbs of the maximum load and -500lbs of the minimum load.
   - Set Axial Displacement values to +0.200 inches and -0.200 inches.
   - Set the Upper and Lower Action for Axial Displacement to Station Power.

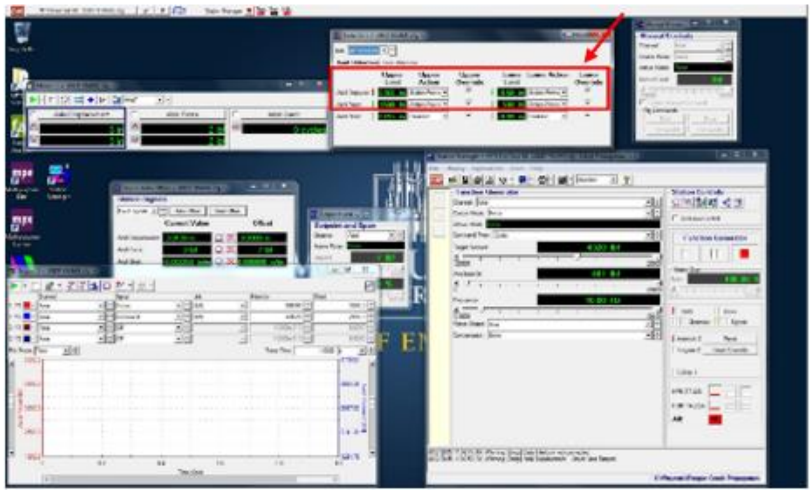

5. If MTS machine has not been running for 30 minutes, allow unit to run for 30 minutes prior to running a test.

6. In the Station Manager window:
   - Select Function Generator
   - Set HPU T7-J25 to high pressure (right button)
   - Set HSM T4-J28A to high pressure (right button)

7. Start test. Monitor Axial Force and Axial Commanded Force for convergence (both traces should follow each other within several lb_f).

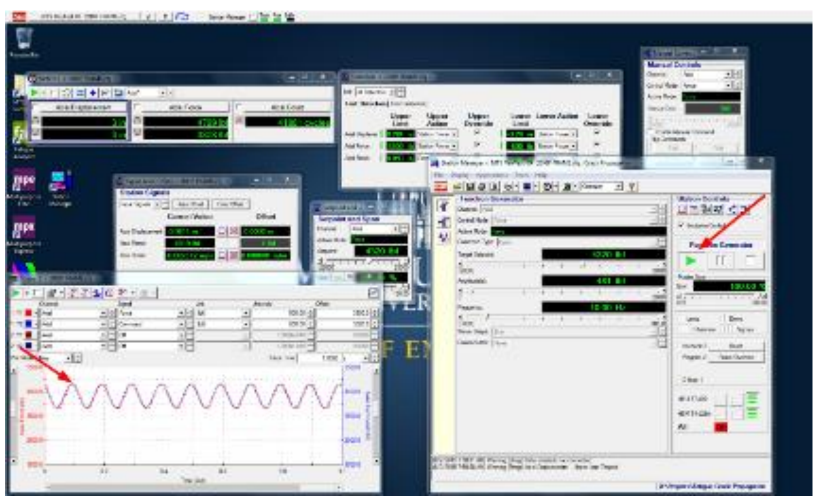

Running of Test

1. Once crack is visible, simultaneously collect the following:
   - Both front and rear pictures of the specimen
   - Maximum and minimum axial force values
   - Cycle count (listed under Axial Count)

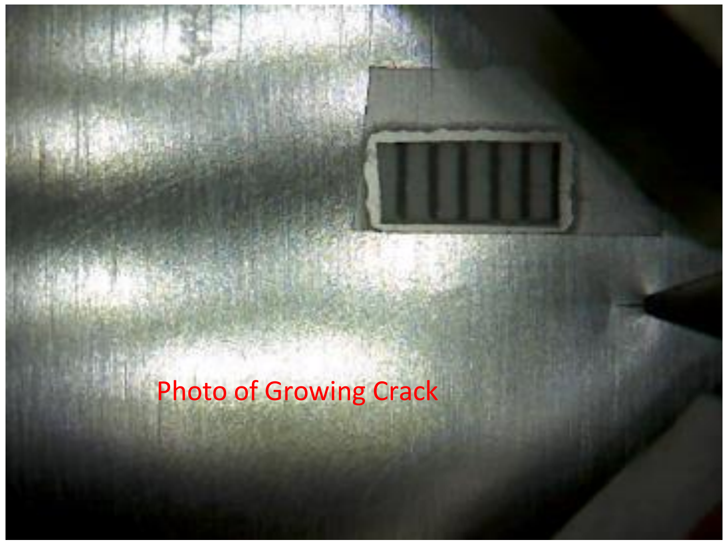

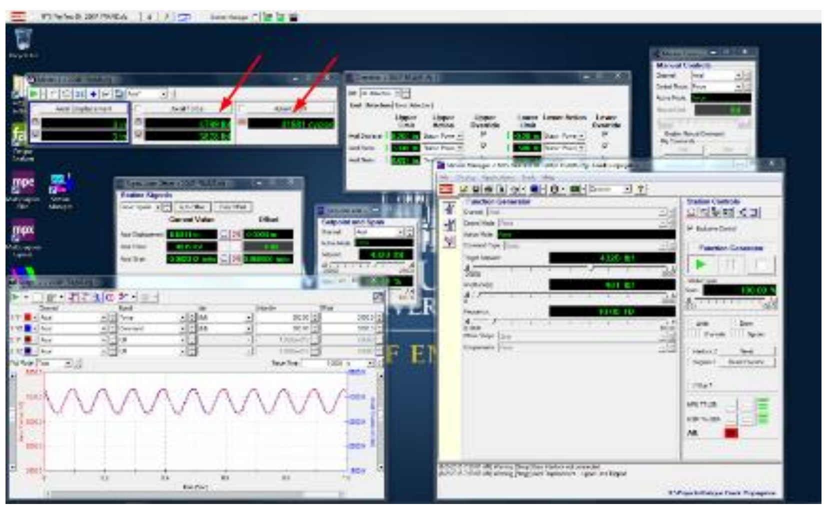

2. Collect data at frequency required for test.
3. Test machine will automatically shutdown when specimen can no longer support load or displacement.

Appendix G: Instructions for Measuring Crack Length with DinoLite Camera

Instructions for taking pictures and making crack length measurements with DinoLite cameras and DinoCapture 2.0 camera software are given in detail below.

Selecting storage location:

1. Open DinoCapture 2.0 software.
2. Verify camera is connected to computer. In this case the camera is connected using a USB port.
3. Select Folder.

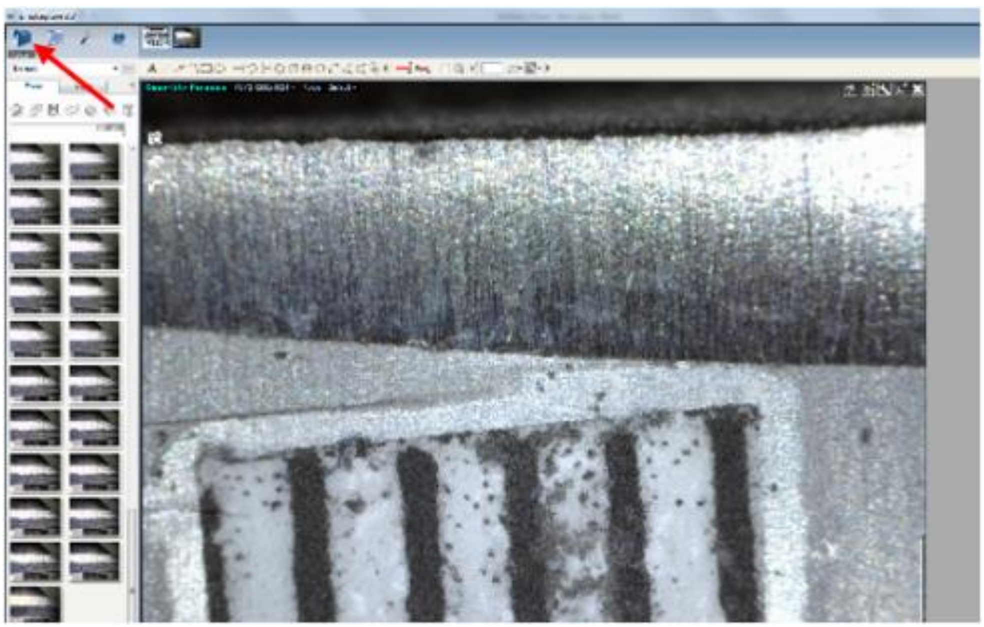

4. Select New.

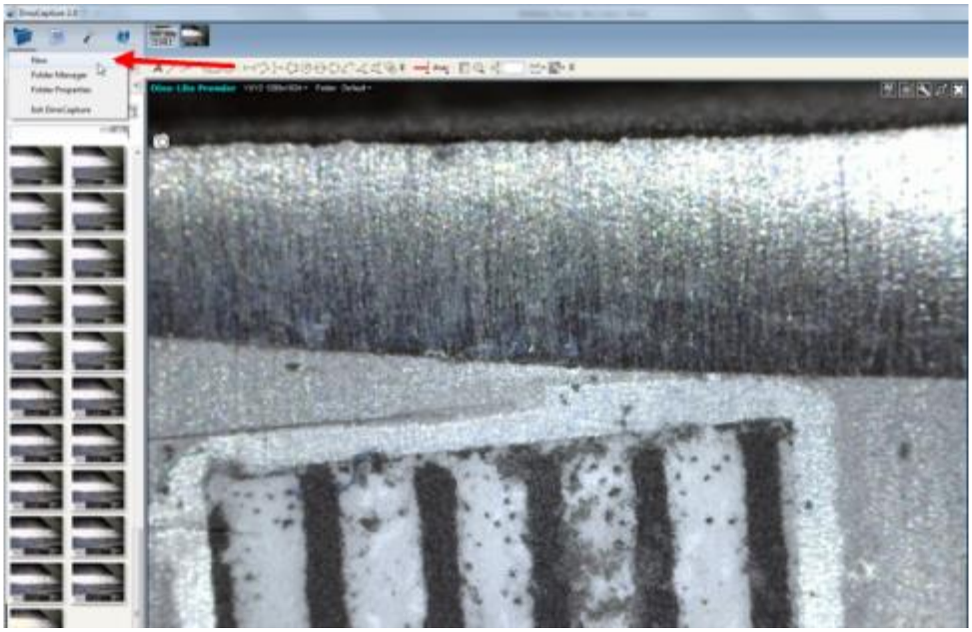

5. Select storage location on computer and enter title for storage folder. When complete press Select.

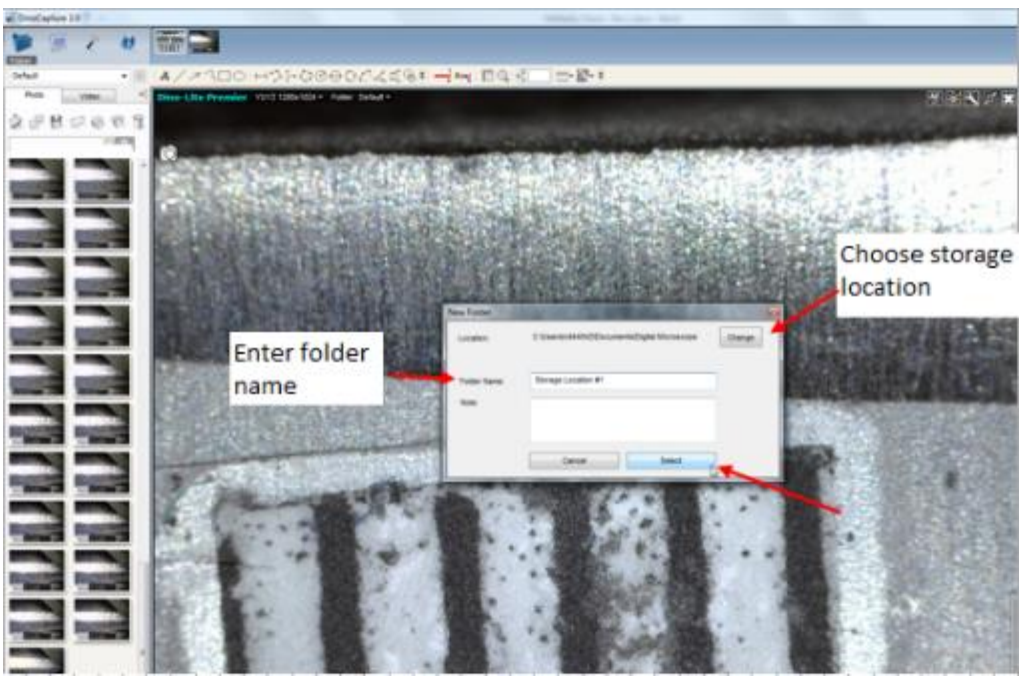

6. In the scenario where the storage folder is already existing select the Folder icon → Folder Manager.

7. Select desired storage location. Click Open.

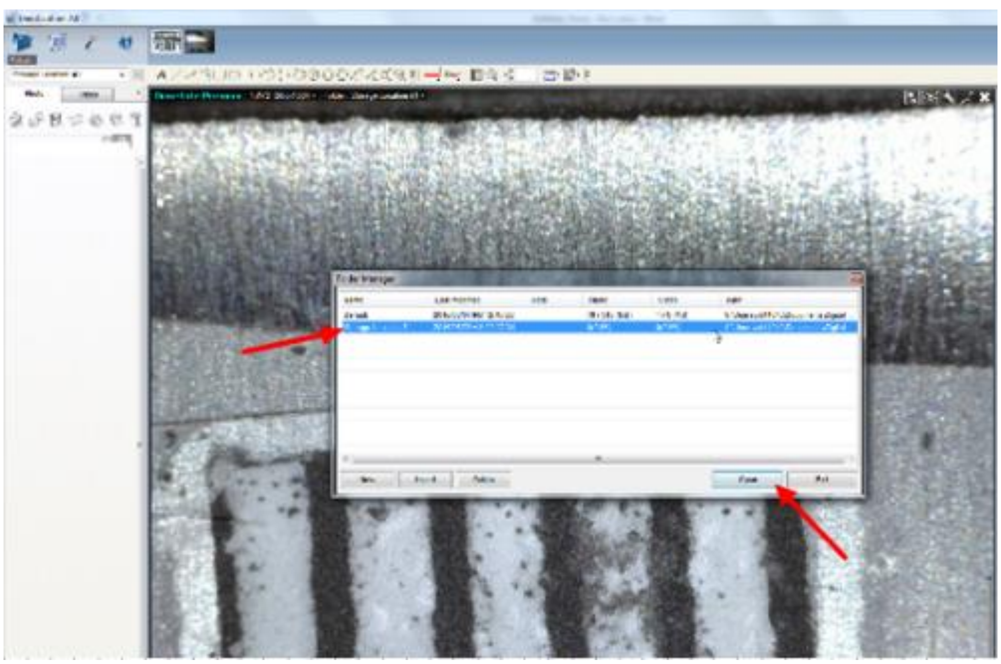

<u>Taking Pictures</u>

1. With DinoCapture 2.0 open and proper storage location selected, double click on the camera icon.

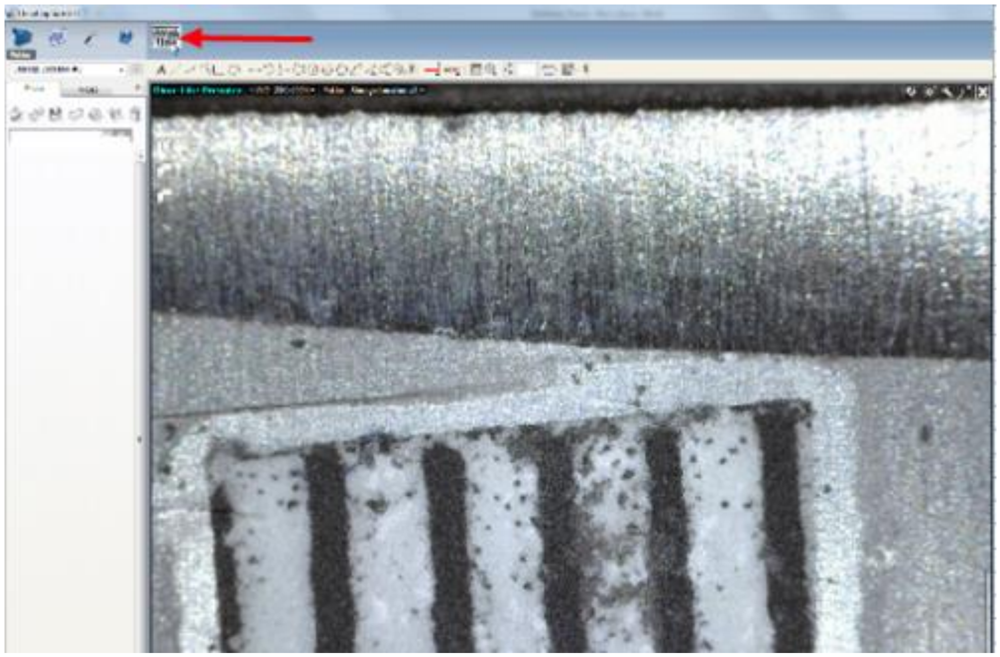

2. Microscope is now viewable. Adjust camera magnification and position until the desired picture is achieved. Select camera icon to take snapshot. Note: if measurement value is desired on picture it is most efficient to perform calibration and add measurement before taking picture. The measurement can always be added after the picture has been taken.

3. Snapshot is now viewable under the photo tab.

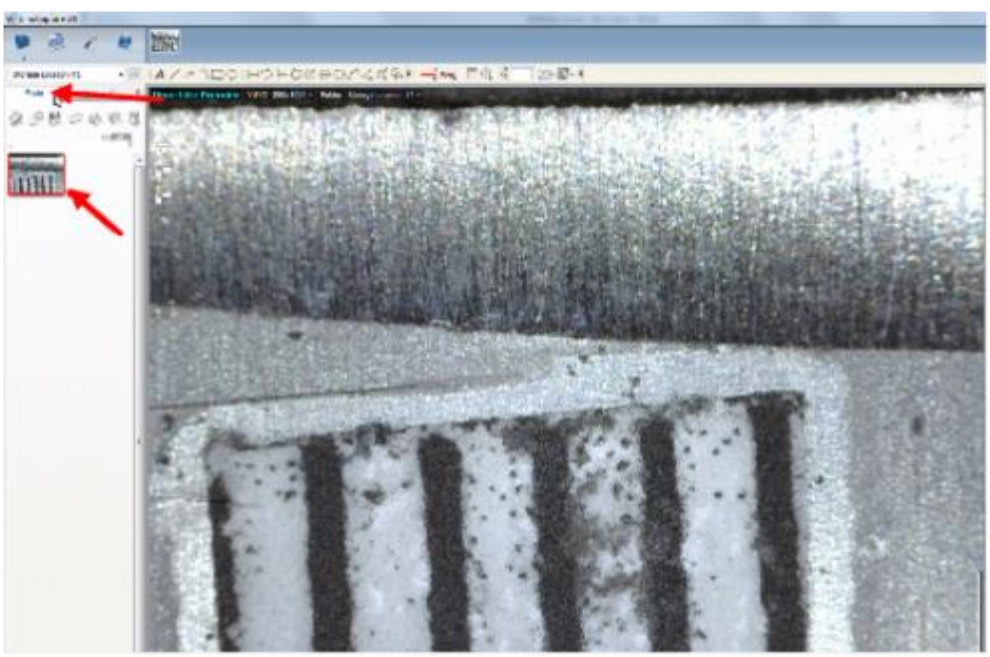

Calibrating and adding measurements

1. With DinoCapture 2.0 open and camera active, select the Calibration icon → New Calibration Profile

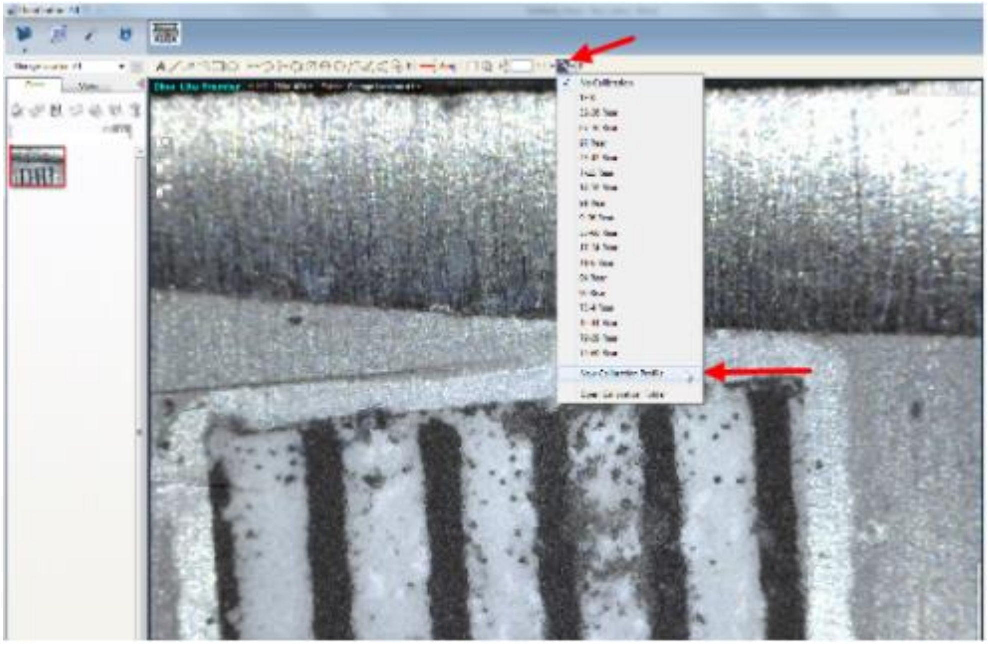

2. Enter Calibration Profile name. Select Continue Calibration.

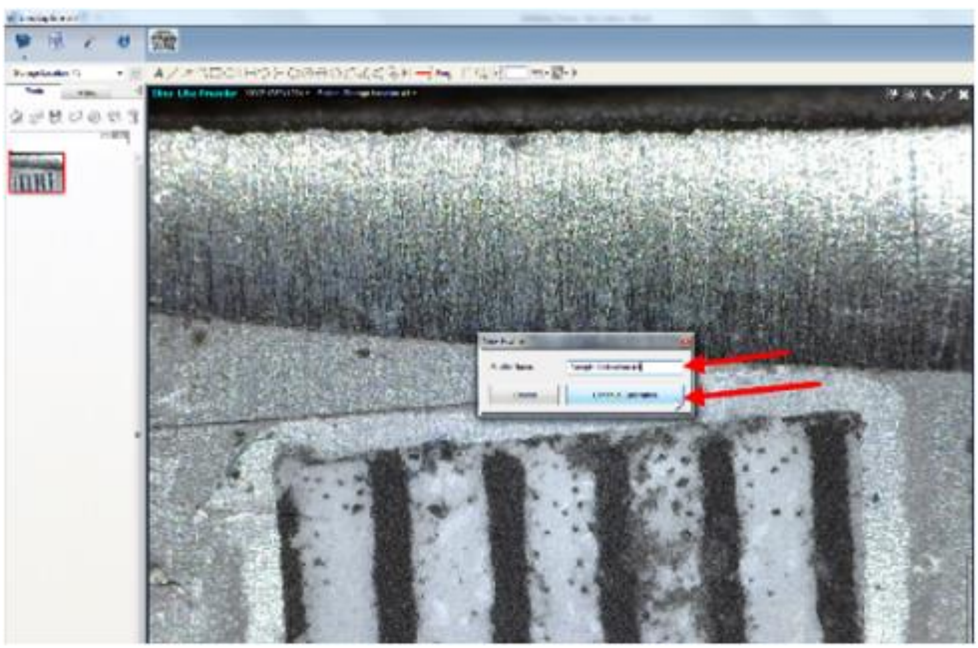

3. Press F8 or select Freeze. Enter the magnification of the camera (located on the side of the camera). Press enter when complete.

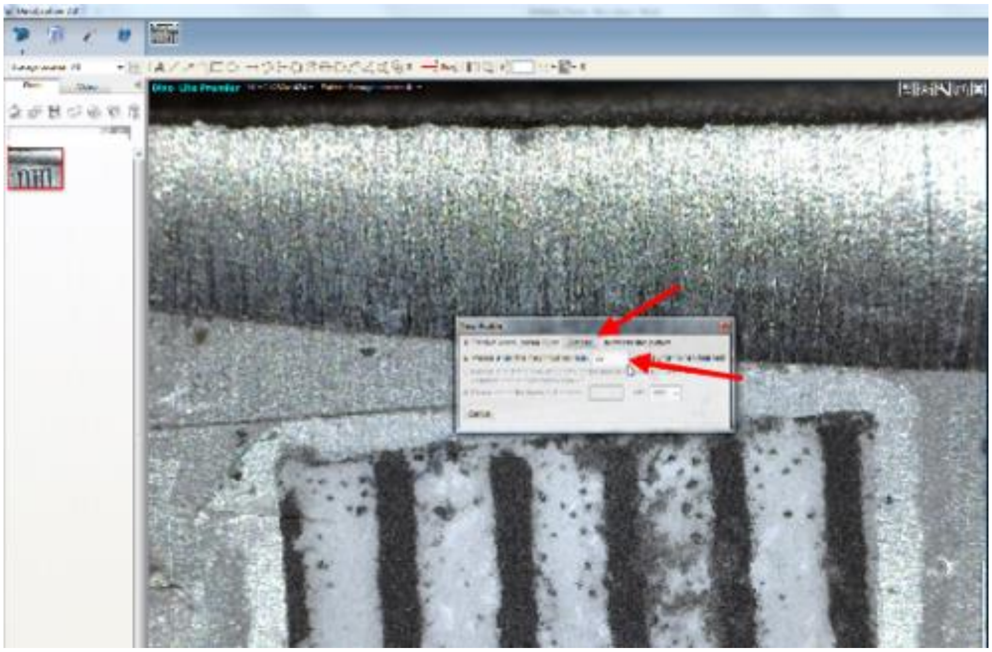

4. Align the H-frame around the ruler. Make the H-frame as wide as possible and utilize the ends of each mark for a precise calibration. To move the H-frame click the small box where the vertical and horizontal lines intersect. To place click on desired location.

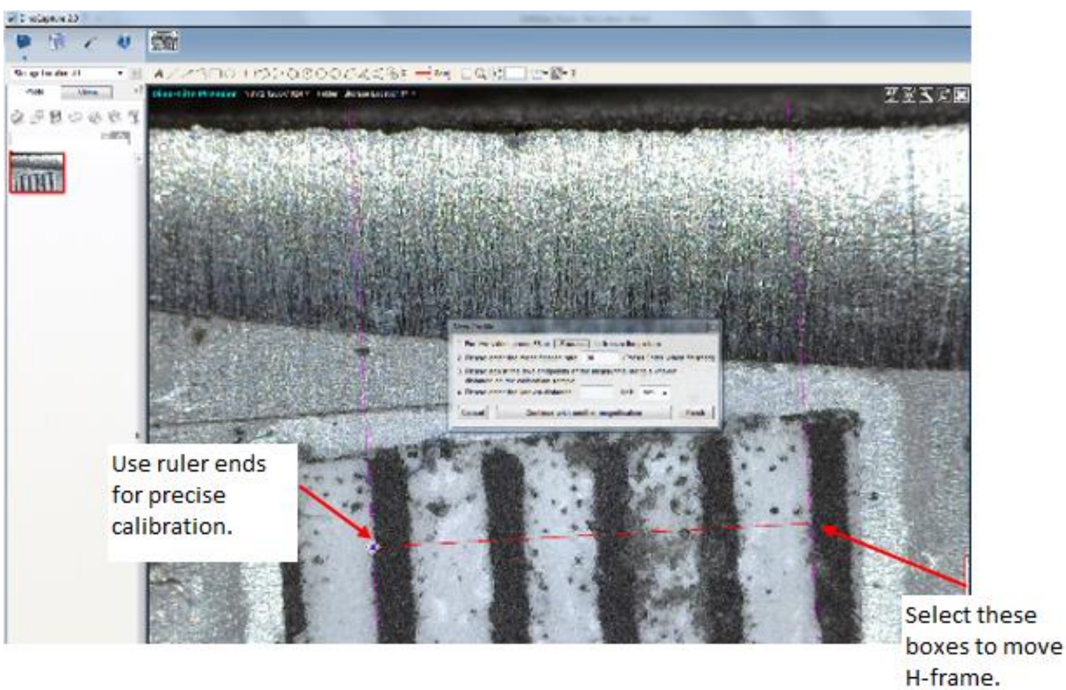

5. Enter the known distance. When complete select finish.

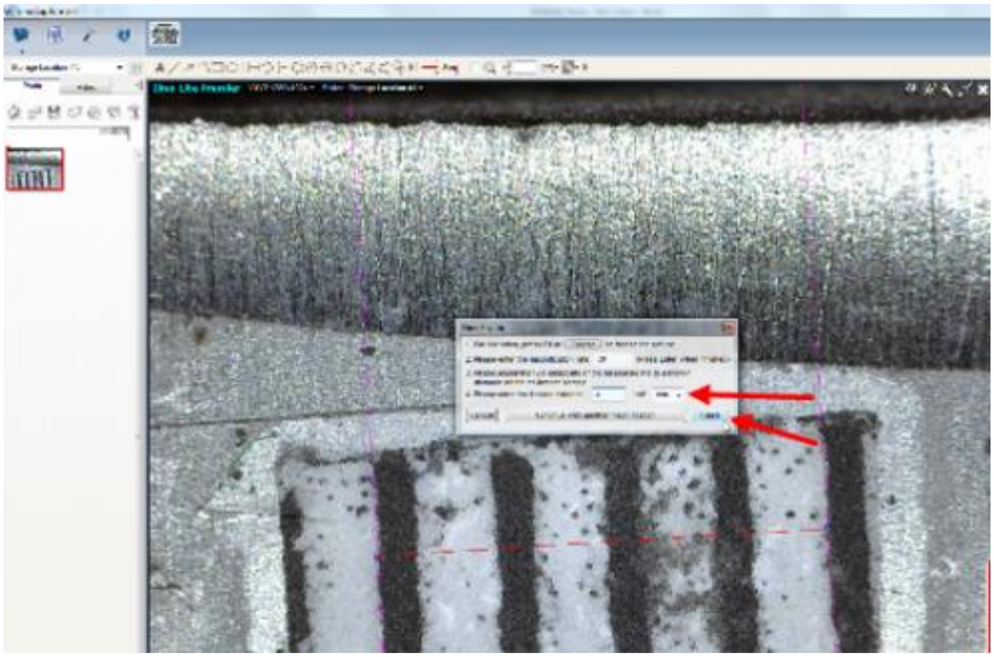

6. Enter magnification (value located on side of camera).

7. Select Line Measurement icon.

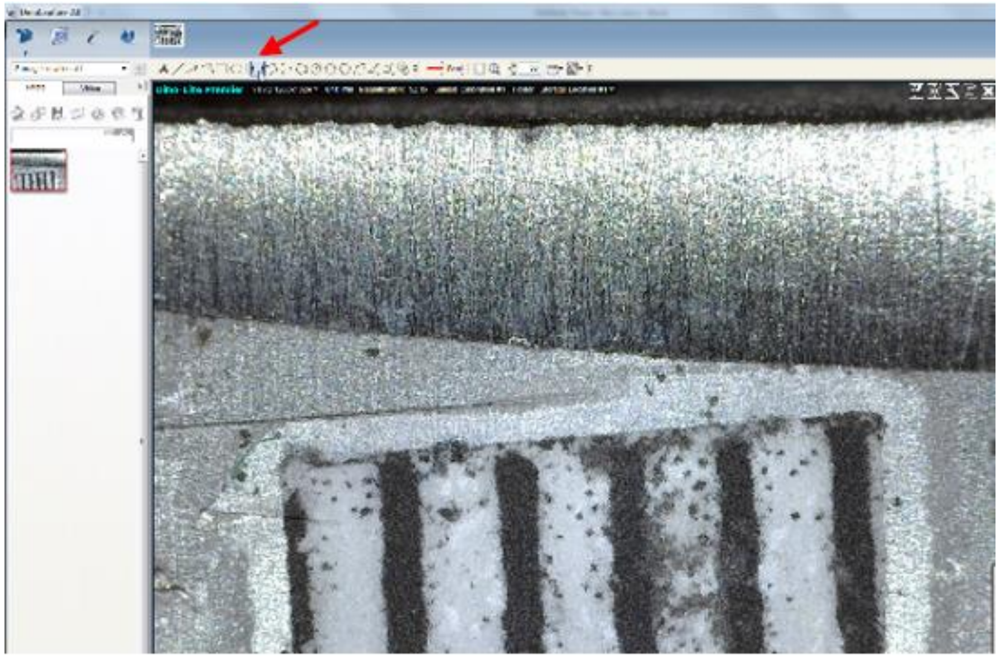

8. Select two point to measure. Click on the first position and click on the second position to complete the measurement.

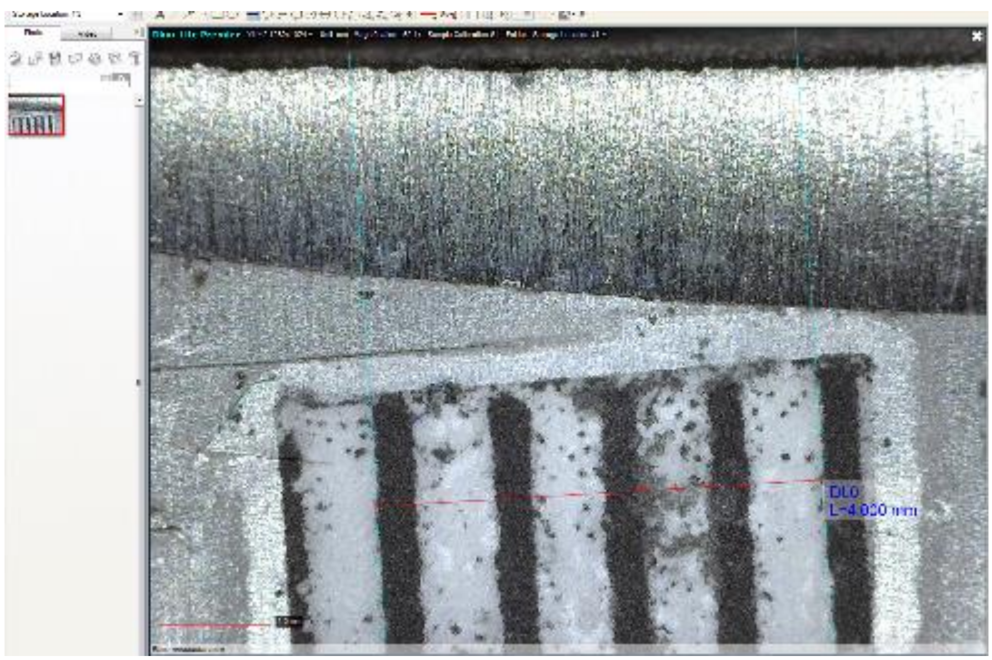

Saving pictures

Note: pictures will automatically be stored to this location selected in the Folder Manager. This process renames the pictures and saves in the desired format.

1. Take snapshot. Right click on picture to be saved.

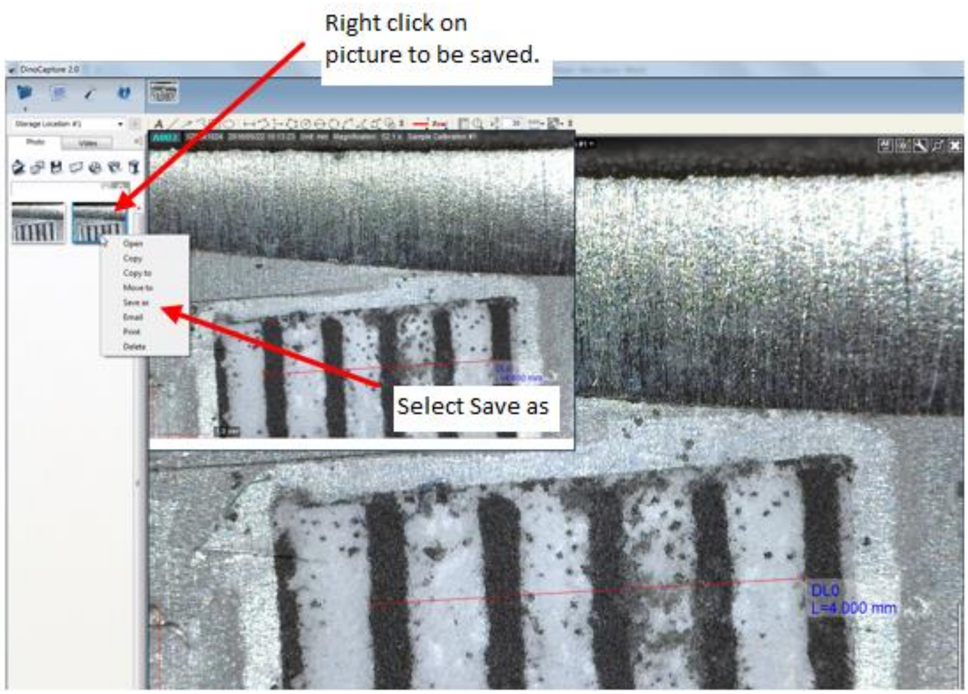

2. Select preferences for saved picture. Select Continue when complete.

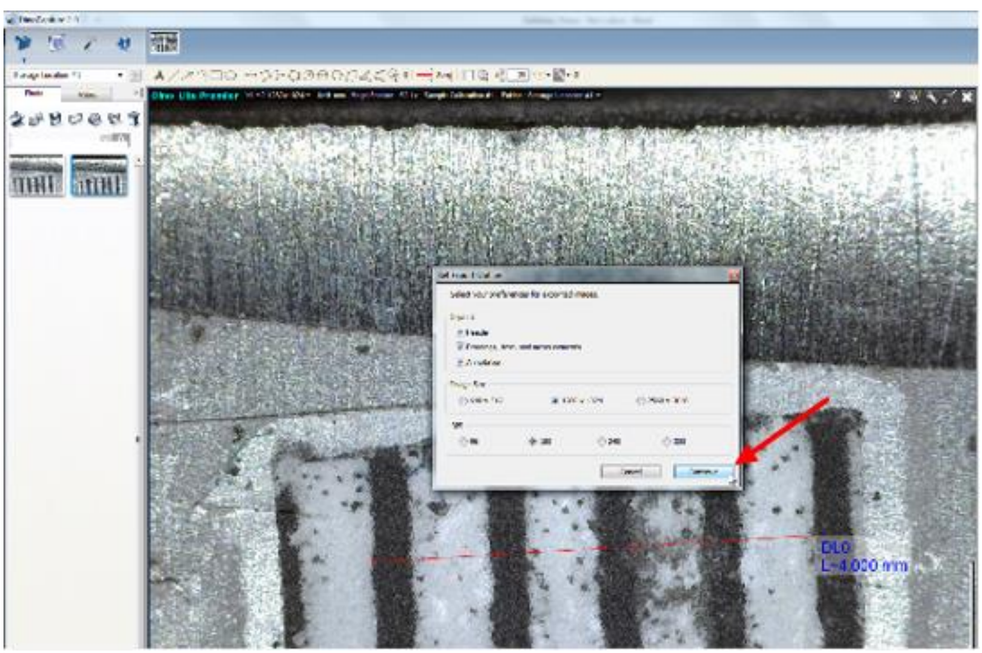

3. Navigate to the correct file storage location. Enter desired file name for picture. Select Save when complete.

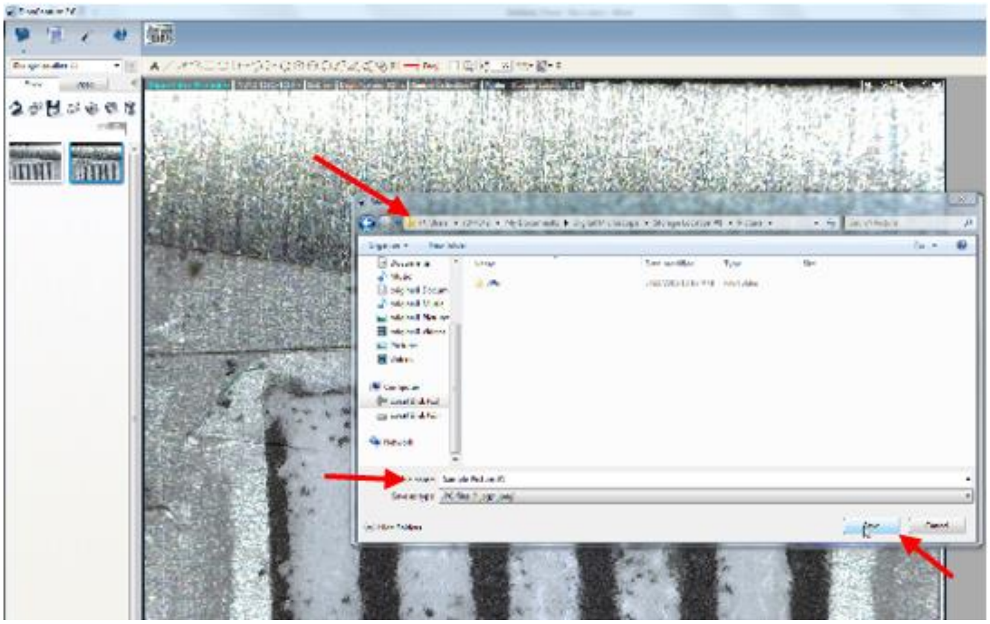

Appendix H: Fatigue Crack Growth Test Results

This page intentionally left blank.

Table H.1. Fatigue crack growth data for test Specimen #1 – ASTM A36, R=0.05, 10Hz.

Fatigue Crack Growth Rate Calculations

Secant Method

Specimen 1 - ASTM A36, R=0.05, 10Hz

B (m)	0.006
W (m)	0.05029
a_0 (mm)	11.4

N (cycles)	a (mm)	da/dN (m/cycle)	log(da/dN)	ΔP (N)	a_{avg} (mm)	$\alpha = a_{avg}/W$ (≥0.2)	ΔK (MPa√m)	log (ΔK) (MPa√m)	W-a	$(4/\pi)*(K_{max}/\sigma_F)^2$
	11.40									
15102	14.57	2.10E-07	-3.68	8452	12.99	0.26	31.6	1.50	0.036	0.010
16094	15.30	7.32E-07	-3.14	8452	14.93	0.30	35.0	1.54	0.035	0.012
17112	15.61	3.07E-07	-3.51	8452	15.45	0.31	36.0	1.56	0.035	0.013
18026	16.11	5.48E-07	-3.26	8452	15.86	0.32	36.7	1.57	0.034	0.013
19187	16.39	2.38E-07	-3.62	8452	16.25	0.32	37.5	1.57	0.034	0.014
20430	17.11	5.85E-07	-3.23	8452	16.75	0.33	38.4	1.58	0.033	0.014
21016	17.59	8.12E-07	-3.09	8452	17.35	0.35	39.6	1.60	0.033	0.015
22115	18.16	5.18E-07	-3.29	8452	17.87	0.36	40.7	1.61	0.032	0.016
23167	18.99	7.90E-07	-3.10	8452	18.57	0.37	42.2	1.63	0.031	0.017
24051	19.64	7.31E-07	-3.14	8452	19.31	0.38	43.8	1.64	0.031	0.019
25438	20.30	4.81E-07	-3.32	8452	19.97	0.40	45.4	1.66	0.030	0.020
26070	20.94	1.01E-06	-3.00	8452	20.62	0.41	47.0	1.67	0.029	0.021
27102	22.64	1.65E-06	-2.78	8452	21.79	0.43	50.0	1.70	0.028	0.024
28027	24.90	2.44E-06	-2.61	8452	23.77	0.47	55.9	1.75	0.025	0.030
28474	28.02	6.98E-06	-2.16	8452	26.46	0.53	65.9	1.82	0.022	0.042
28487	28.66	4.93E-05	-1.31	8452	28.34	0.56	74.8	1.87	0.022	0.054

Table H.2. Fatigue crack growth data for test Specimen #2 – ASTM A36, R=0.05, 10Hz.

Fatigue Crack Growth Rate Calculations

Secant Method

Specimen 2 - ASTM A36, R=0.05, 10Hz

B (m)	0.006
W (m)	0.05207
a_0 (mm)	12.77

N (cycles)	a (mm)	da/dN (m/cycle)	log(da/dN)	ΔP (N)	a_{avg} (mm)	$\alpha = a_{avg}/W$ (≥0.2)	ΔK (MPa√m)	log (ΔK) (MPa√m)	W-a	$(4/\pi)*(K_{max}/\sigma_F)^2$
0	12.77									
18016	15.40	1.46E-07	-3.84	7606	14.09	0.27	28.9	1.46	0.037	0.008
21016	16.07	2.24E-07	-3.65	7606	15.74	0.30	31.4	1.50	0.036	0.010
22017	16.73	6.53E-07	-3.19	7606	16.40	0.31	32.5	1.51	0.035	0.010
23014	17.04	3.16E-07	-3.50	7606	16.88	0.32	33.2	1.52	0.035	0.011
24124	17.24	1.77E-07	-3.75	7606	17.14	0.33	33.7	1.53	0.035	0.011
25259	17.53	2.60E-07	-3.58	7606	17.39	0.33	34.1	1.53	0.035	0.011
26055	17.59	7.04E-08	-4.15	7606	17.56	0.34	34.4	1.54	0.034	0.011
27165	17.89	2.74E-07	-3.56	7606	17.74	0.34	34.7	1.54	0.034	0.012
28017	18.19	3.41E-07	-3.47	7606	18.04	0.35	35.2	1.55	0.034	0.012
29112	18.53	3.18E-07	-3.50	7606	18.36	0.35	35.7	1.55	0.034	0.012
30149	19.17	6.12E-07	-3.21	7606	18.85	0.36	36.6	1.56	0.033	0.013
31015	19.49	3.78E-07	-3.42	7606	19.33	0.37	37.5	1.57	0.033	0.014
32024	20.03	5.28E-07	-3.28	7606	19.76	0.38	38.3	1.58	0.032	0.014
33015	20.42	3.92E-07	-3.41	7606	20.22	0.39	39.2	1.59	0.032	0.015
34043	20.77	3.45E-07	-3.46	7606	20.59	0.40	40.0	1.60	0.031	0.015
35045	21.56	7.89E-07	-3.10	7606	21.17	0.41	41.1	1.61	0.031	0.016
36036	22.05	4.95E-07	-3.30	7606	21.81	0.42	42.5	1.63	0.030	0.017
37022	23.16	1.12E-06	-2.95	7606	22.61	0.43	44.3	1.65	0.029	0.019
38045	24.20	1.02E-06	-2.99	7606	23.68	0.45	47.0	1.67	0.028	0.021
39046	25.18	9.73E-07	-3.01	7606	24.69	0.47	49.7	1.70	0.027	0.024
39477	25.55	8.69E-07	-3.06	7606	25.36	0.49	51.6	1.71	0.027	0.026
40012	26.56	1.89E-06	-2.72	7606	26.05	0.50	53.7	1.73	0.026	0.028
40514	27.80	2.47E-06	-2.61	7606	27.18	0.52	57.5	1.76	0.024	0.032
41013	29.35	3.10E-06	-2.51	7606	28.57	0.55	62.9	1.80	0.023	0.038
41182	31.80	1.45E-05	-1.84	7606	30.57	0.59	72.2	1.86	0.020	0.050

Table H.3. Fatigue crack growth data for test Specimen #3 – ASTM A36, R=0.05, 10Hz.

Fatigue Crack Growth Rate Calculations

Secant Method

Specimen 3 - ASTM A36, R=0.05, 10Hz

B (m)	0.006
W (m)	0.0508
a_0 (mm)	11.7

N (cycles)	a (mm)	da/dN (m/cycle)	log(da/dN)	ΔP (N)	a_{avg} (mm)	$\alpha = a_{avg}/W$ (≥0.2)	ΔK (MPa√m)	log (ΔK) (MPa√m)	W-a	$(4/\pi)*(K_{max}/\sigma_F)^2$
0	11.7									
15001	13.82	1.41E-07	-3.85	7606	12.76	0.25	27.8	1.44	0.037	0.007
16002	14.13	3.14E-07	-3.50	7606	13.97	0.28	29.6	1.47	0.037	0.008
17038	14.19	5.65E-08	-4.25	7606	14.16	0.28	29.9	1.48	0.037	0.009
18062	14.62	4.22E-07	-3.37	7606	14.41	0.28	30.3	1.48	0.036	0.009
19043	14.75	1.35E-07	-3.87	7606	14.69	0.29	30.7	1.49	0.036	0.009
20014	15.01	2.67E-07	-3.57	7606	14.88	0.29	31.0	1.49	0.036	0.009
21000	15.22	2.10E-07	-3.68	7606	15.12	0.30	31.4	1.50	0.036	0.010
22001	15.70	4.78E-07	-3.32	7606	15.46	0.30	32.0	1.50	0.035	0.010
23055	15.80	9.54E-08	-4.02	7606	15.75	0.31	32.4	1.51	0.035	0.010
24057	16.20	3.98E-07	-3.40	7606	16.00	0.31	32.9	1.52	0.035	0.010
25207	16.56	3.16E-07	-3.50	7606	16.38	0.32	33.5	1.53	0.034	0.011
26003	16.79	2.85E-07	-3.55	7606	16.68	0.33	34.0	1.53	0.034	0.011
27082	17.40	5.70E-07	-3.24	7606	17.10	0.34	34.7	1.54	0.033	0.012
28003	17.61	2.25E-07	-3.65	7606	17.51	0.34	35.5	1.55	0.033	0.012
29008	17.92	3.11E-07	-3.51	7606	17.77	0.35	35.9	1.56	0.033	0.012
30005	18.55	6.31E-07	-3.20	7606	18.24	0.36	36.8	1.57	0.032	0.013
31002	19.00	4.47E-07	-3.35	7606	18.78	0.37	37.8	1.58	0.032	0.014
32003	19.54	5.39E-07	-3.27	7606	19.27	0.38	38.8	1.59	0.031	0.015
33005	20.10	5.57E-07	-3.25	7606	19.82	0.39	39.9	1.60	0.031	0.015
34000	20.77	6.72E-07	-3.17	7606	20.43	0.40	41.2	1.61	0.030	0.016
34503	21.19	8.46E-07	-3.07	7606	20.98	0.41	42.4	1.63	0.030	0.017
35004	21.56	7.30E-07	-3.14	7606	21.37	0.42	43.3	1.64	0.029	0.018
35502	22.08	1.05E-06	-2.98	7606	21.82	0.43	44.3	1.65	0.029	0.019
36004	22.40	6.45E-07	-3.19	7606	22.24	0.44	45.3	1.66	0.028	0.020
36507	23.08	1.35E-06	-2.87	7606	22.74	0.45	46.6	1.67	0.028	0.021
37001	23.61	1.06E-06	-2.98	7606	23.35	0.46	48.2	1.68	0.027	0.022
37304	23.85	8.10E-07	-3.09	7606	23.73	0.47	49.3	1.69	0.027	0.023
37601	24.35	1.67E-06	-2.78	7606	24.10	0.47	50.3	1.70	0.026	0.024
38001	24.91	1.39E-06	-2.86	7606	24.63	0.48	51.9	1.71	0.026	0.026
38301	25.61	2.36E-06	-2.63	7606	25.26	0.50	53.9	1.73	0.025	0.028
38604	26.28	2.21E-06	-2.65	7606	25.95	0.51	56.2	1.75	0.025	0.031
38902	27.36	3.63E-06	-2.44	7606	26.82	0.53	59.4	1.77	0.023	0.034
39220	29.48	6.64E-06	-2.18	7606	28.42	0.56	66.1	1.82	0.021	0.042
39261	30.68	2.93E-05	-1.53	7606	30.08	0.59	74.5	1.87	0.020	0.054

Table H.4. Fatigue crack growth data for test Specimen #82 – ASTM A36, R=0.05, 25Hz.

Fatigue Crack Growth Rate Calculations

Secant Method

Specimen 82 - ASTM A36, R=0.05, 25Hz

B (m)	0.0061
W (m)	0.0507
a_0 (mm)	12.5

N (cycles)	a (mm)	da/dN (m/cycle)	log(da/dN)	ΔP (N)	a_{avg} (mm)	$\alpha = a_{avg}/W$ (≥0.2)	ΔK (MPa√m)	log (ΔK) (MPa√m)	W-a	$(4/\pi)*(K_{max}/\sigma_F)^2$
0	12.5			0						
374593	14.61	5.62E-09	-5.25	3043	13.55	0.27	11.4	1.06	0.036	0.012
394732	14.94	1.64E-08	-4.79	3043	14.77	0.29	12.2	1.09	0.036	0.014
414027	15.01	3.63E-09	-5.44	3043	14.97	0.30	12.3	1.09	0.036	0.014
429712	15.14	8.61E-09	-5.07	3043	15.07	0.30	12.4	1.09	0.036	0.015
450454	15.17	1.45E-09	-5.84	3043	15.16	0.30	12.4	1.09	0.036	0.015
470893	15.20	1.22E-09	-5.91	2740	15.18	0.30	11.2	1.05	0.036	0.012
522548	15.25	1.06E-09	-5.97	2740	15.22	0.30	11.2	1.05	0.035	0.012
545838	16.42	5.02E-08	-4.30	2740	15.84	0.31	11.6	1.06	0.034	0.013
560410	16.52	6.52E-09	-5.19	2740	16.47	0.32	12.0	1.08	0.034	0.014
581659	16.83	1.46E-08	-4.84	2464	16.67	0.33	10.9	1.04	0.034	0.011
610063	16.90	2.46E-09	-5.61	2464	16.86	0.33	11.0	1.04	0.034	0.011
640892	16.97	2.27E-09	-5.64	2464	16.93	0.33	11.0	1.04	0.034	0.012
672603	17.09	3.78E-09	-5.42	2464	17.03	0.34	11.1	1.04	0.034	0.012
701598	17.18	3.28E-09	-5.48	2464	17.13	0.34	11.1	1.05	0.034	0.012
736839	17.25	1.84E-09	-5.73	2464	17.21	0.34	11.2	1.05	0.033	0.012
770148	17.49	7.21E-09	-5.14	2464	17.37	0.34	11.2	1.05	0.033	0.012
786843	17.50	5.99E-10	-6.22	2464	17.49	0.34	11.3	1.05	0.033	0.012
800361	17.53	2.59E-09	-5.59	2464	17.51	0.35	11.3	1.05	0.033	0.012
831995	17.57	1.26E-09	-5.90	2220	17.55	0.35	10.2	1.01	0.033	0.010
860530	17.74	5.96E-09	-5.22	2220	17.66	0.35	10.3	1.01	0.033	0.010
879953	17.85	5.41E-09	-5.27	2220	17.79	0.35	10.4	1.02	0.033	0.010
889593	17.91	6.22E-09	-5.21	2220	17.88	0.35	10.4	1.02	0.033	0.010
921166	17.95	1.27E-09	-5.90	2220	17.93	0.35	10.4	1.02	0.033	0.010
953556	18.10	4.79E-09	-5.32	2220	18.02	0.36	10.5	1.02	0.033	0.010
979924	18.24	5.12E-09	-5.29	2220	18.17	0.36	10.6	1.02	0.032	0.011
1000259	18.27	1.72E-09	-5.76	2220	18.25	0.36	10.6	1.03	0.032	0.011
1028851	19.57	4.55E-08	-4.34	2220	18.92	0.37	11.0	1.04	0.031	0.011
1056475	19.62	1.63E-09	-5.79	1993	19.59	0.39	10.2	1.01	0.031	0.010
1075441	19.64	1.32E-09	-5.88	1993	19.63	0.39	10.2	1.01	0.031	0.010
1097677	19.70	2.47E-09	-5.61	1993	19.67	0.39	10.2	1.01	0.031	0.010
1117091	19.74	2.32E-09	-5.63	1993	19.72	0.39	10.3	1.01	0.031	0.010
1158218	19.90	3.89E-09	-5.41	1993	19.82	0.39	10.3	1.01	0.031	0.010
1197647	20.09	4.82E-09	-5.32	1993	20.00	0.39	10.4	1.02	0.031	0.010
1215652	20.23	7.50E-09	-5.13	1993	20.16	0.40	10.5	1.02	0.030	0.011
1229893	20.32	6.67E-09	-5.18	1993	20.27	0.40	10.6	1.02	0.030	0.011
1245343	20.46	9.06E-09	-5.04	1993	20.39	0.40	10.6	1.03	0.030	0.011
1259932	20.60	9.25E-09	-5.03	1993	20.53	0.40	10.7	1.03	0.030	0.011
1317912	20.97	6.38E-09	-5.20	1797	20.78	0.41	9.8	0.99	0.030	0.009
1361211	21.36	9.12E-09	-5.04	1797	21.16	0.42	10.0	1.00	0.029	0.009
1366669	21.37	9.16E-10	-6.04	1797	21.36	0.42	10.1	1.00	0.029	0.010
1403965	21.46	2.55E-09	-5.59	1619	21.41	0.42	9.1	0.96	0.029	0.008
1444682	21.54	1.96E-09	-5.71	1619	21.50	0.42	9.2	0.96	0.029	0.008
1473373	21.65	3.66E-09	-5.44	1619	21.59	0.43	9.2	0.96	0.029	0.008
1497325	21.81	6.89E-09	-5.16	1619	21.73	0.43	9.3	0.97	0.029	0.008
1547530	21.89	1.59E-09	-5.80	1459	21.85	0.43	8.4	0.92	0.029	0.007
1585802	21.94	1.18E-09	-5.93	1459	21.91	0.43	8.4	0.93	0.029	0.007
1644547	22.04	1.79E-09	-5.75	1459	21.99	0.43	8.5	0.93	0.029	0.007
1691342	22.09	1.07E-09	-5.97	1459	22.07	0.44	8.5	0.93	0.029	0.007
1737143	22.17	1.75E-09	-5.76	1459	22.13	0.44	8.5	0.93	0.029	0.007
1755092	22.19	8.36E-10	-6.08	1459	22.18	0.44	8.6	0.93	0.029	0.007

Table H.5. Fatigue crack growth data for test Specimen #83 – ASTM A36, R=0.05, 25Hz.

Fatigue Crack Growth Rate Calculations

Secant Method

Specimen 83 - ASTM A36, R=0.05, 25Hz

B (m)	0.00593
W (m)	0.051
a_0 (mm)	12.45

N (cycles)	a (mm)	da/dN (m/cycle)	log(da/dN)	ΔP (N)	a_{avg} (mm)	$\alpha = a_{avg}/W$ (≥0.2)	ΔK (MPa√m)	log (ΔK) (MPa√m)	W-a	$(4/\pi)*(K_{max}/\sigma_F)^2$
	12.45			0						
376355	13.04	1.55E-09	-5.81	2639	12.74	0.25	9.7	0.99	0.038	0.001
474827	13.52	4.87E-09	-5.31	2639	13.28	0.26	10.0	1.00	0.037	0.001
577384	13.79	2.63E-09	-5.58	2375	13.65	0.27	9.2	0.96	0.037	0.001
650022	13.94	2.13E-09	-5.67	2375	13.86	0.27	9.3	0.97	0.037	0.001
710740	14.02	1.32E-09	-5.88	2375	13.98	0.27	9.3	0.97	0.037	0.001
823293	14.13	9.77E-10	-6.01	2138	14.08	0.28	8.4	0.93	0.037	0.001
925740	14.52	3.81E-09	-5.42	2138	14.33	0.28	8.5	0.93	0.036	0.001
1048510	14.70	1.43E-09	-5.85	1922	14.61	0.29	7.8	0.89	0.036	0.001
1128989	14.81	1.37E-09	-5.86	1922	14.75	0.29	7.8	0.89	0.036	0.001
1229055	15.02	2.15E-09	-5.67	1922	14.91	0.29	7.9	0.90	0.036	0.001
1326178	15.11	9.27E-10	-6.03	1728	15.07	0.30	7.2	0.86	0.036	0.000
1438979	15.14	2.66E-10	-6.58	1728	15.13	0.30	7.2	0.86	0.036	0.000
1543375	15.26	1.15E-09	-5.94	1728	15.20	0.30	7.2	0.86	0.036	0.001
1636534	15.37	1.18E-09	-5.93	1728	15.32	0.30	7.3	0.86	0.036	0.001
1740701	15.48	1.01E-09	-6.00	1728	15.42	0.30	7.3	0.86	0.036	0.001
1767835	15.52	1.66E-09	-5.78	1728	15.50	0.30	7.3	0.86	0.035	0.001
1924678	15.61	5.42E-10	-6.27	1558	15.56	0.31	6.6	0.82	0.035	0.000
2027029	15.75	1.37E-09	-5.86	1558	15.68	0.31	6.7	0.82	0.035	0.000
2192350	15.77	1.21E-10	-6.92	1558	15.76	0.31	6.7	0.83	0.035	0.000
2332091	15.81	2.86E-10	-6.54	1558	15.79	0.31	6.7	0.83	0.035	0.000
2477342	15.85	3.10E-10	-6.51	1558	15.83	0.31	6.7	0.83	0.035	0.000
2627784	15.95	6.31E-10	-6.20	1558	15.90	0.31	6.7	0.83	0.035	0.000
2776575	16.03	5.38E-10	-6.27	1558	15.99	0.31	6.8	0.83	0.035	0.000
2927943	16.17	9.25E-10	-6.03	1558	16.10	0.32	6.8	0.83	0.035	0.000
3076020	16.29	8.10E-10	-6.09	1558	16.23	0.32	6.9	0.84	0.035	0.000
3227144	16.41	8.27E-10	-6.08	1558	16.35	0.32	6.9	0.84	0.035	0.000
3377322	16.55	8.99E-10	-6.05	1558	16.48	0.32	6.9	0.84	0.034	0.000
3527444	16.68	8.66E-10	-6.06	1558	16.61	0.33	7.0	0.84	0.034	0.000
3679819	16.81	8.86E-10	-6.05	1558	16.74	0.33	7.0	0.85	0.034	0.000
4096292	17.16	8.28E-10	-6.08	1403	16.98	0.33	6.4	0.81	0.034	0.000
4406658	17.38	7.25E-10	-6.14	1403	17.27	0.34	6.5	0.81	0.034	0.000
4581704	17.51	7.43E-10	-6.13	1403	17.45	0.34	6.6	0.82	0.033	0.000
4756207	17.64	7.45E-10	-6.13	1403	17.58	0.34	6.6	0.82	0.033	0.000
5128270	17.74	2.55E-10	-6.59	1263	17.69	0.35	6.0	0.78	0.033	0.000
5430923	17.97	7.76E-10	-6.11	1263	17.85	0.35	6.0	0.78	0.033	0.000
6314499	18.57	6.73E-10	-6.17	1263	18.27	0.36	6.2	0.79	0.032	0.000
7528832	19.23	5.48E-10	-6.26	1263	18.90	0.37	6.4	0.80	0.032	0.000
9032936	19.74	3.36E-10	-6.47	1263	19.48	0.38	6.5	0.82	0.031	0.000

Table H.6. Fatigue crack growth data for test Specimen #85 – ASTM A36, R=0.05, 25Hz.

Fatigue Crack Growth Rate Calculations
Secant Method
Specimen 85 - ASTM A36, R=0.05, 25Hz

B (m)	0.0061
W (m)	0.0508
a_0 (mm)	12

N (cycles)	a (mm)	da/dN (m/cycle)	log(da/dN)	ΔP (N)	a_{avg} (mm)	$\alpha = a_{avg}/W$ (≥0.2)	ΔK (MPa√m)	log (ΔK) (MPa√m)	W-a	$(4/\pi)*(K_{max}/\sigma_F)^2$
	12			0						
328096	12.47	1.43E-09	-5.84	3381	12.24	0.24	11.8	1.07	0.038	0.013
405076	13.45	1.27E-08	-4.90	3381	12.96	0.26	12.3	1.09	0.037	0.014
419446	13.61	1.11E-08	-4.95	3043	13.53	0.27	11.4	1.06	0.037	0.012
468120	13.78	3.49E-09	-5.46	3043	13.69	0.27	11.5	1.06	0.037	0.013
482786	13.95	1.16E-08	-4.94	3043	13.86	0.27	11.6	1.06	0.037	0.013
503963	14.05	4.96E-09	-5.30	3043	14.00	0.28	11.7	1.07	0.037	0.013
509765	14.08	5.17E-09	-5.29	3043	14.07	0.28	11.7	1.07	0.037	0.013
516427	14.12	5.25E-09	-5.28	3043	14.10	0.28	11.7	1.07	0.037	0.013
524827	14.32	2.38E-08	-4.62	3043	14.22	0.28	11.8	1.07	0.036	0.013
536317	14.45	1.17E-08	-4.93	3043	14.38	0.28	11.9	1.08	0.036	0.014
543695	14.69	3.19E-08	-4.50	3043	14.57	0.29	12.0	1.08	0.036	0.014
553415	15.02	3.40E-08	-4.47	3043	14.85	0.29	12.2	1.09	0.036	0.014
564603	15.10	7.15E-09	-5.15	3043	15.06	0.30	12.3	1.09	0.036	0.014
573635	15.15	5.54E-09	-5.26	3043	15.12	0.30	12.4	1.09	0.036	0.015
585427	15.37	1.91E-08	-4.72	3043	15.26	0.30	12.5	1.10	0.035	0.015
593990	15.50	1.52E-08	-4.82	3043	15.44	0.30	12.6	1.10	0.035	0.015
603217	15.71	2.22E-08	-4.65	3043	15.60	0.31	12.7	1.10	0.035	0.015
613225	15.89	1.85E-08	-4.73	3043	15.80	0.31	12.8	1.11	0.035	0.016
623128	16.00	1.11E-08	-4.95	3043	15.95	0.31	12.9	1.11	0.035	0.016
633319	16.17	1.62E-08	-4.79	3043	16.08	0.32	13.0	1.11	0.035	0.016
643459	16.26	9.37E-09	-5.03	3043	16.21	0.32	13.1	1.12	0.035	0.016
654448	16.36	8.65E-09	-5.06	3043	16.31	0.32	13.1	1.12	0.034	0.016
663978	16.42	6.30E-09	-5.20	3043	16.39	0.32	13.2	1.12	0.034	0.017
673927	16.51	9.05E-09	-5.04	3043	16.46	0.32	13.2	1.12	0.034	0.017
684846	16.63	1.14E-08	-4.94	3043	16.57	0.33	13.3	1.12	0.034	0.017
693766	16.82	2.07E-08	-4.68	3043	16.72	0.33	13.4	1.13	0.034	0.017
703656	16.99	1.77E-08	-4.75	3043	16.90	0.33	13.5	1.13	0.034	0.017
713281	17.16	1.77E-08	-4.75	3043	17.08	0.34	13.7	1.14	0.034	0.018
723218	17.34	1.76E-08	-4.75	3043	17.25	0.34	13.8	1.14	0.033	0.018
733166	17.45	1.16E-08	-4.94	3043	17.39	0.34	13.9	1.14	0.033	0.018
743242	17.62	1.64E-08	-4.79	3043	17.53	0.35	14.0	1.15	0.033	0.019
753461	17.79	1.71E-08	-4.77	3043	17.70	0.35	14.1	1.15	0.033	0.019
763476	17.92	1.30E-08	-4.89	3043	17.86	0.35	14.2	1.15	0.033	0.019
772202	18.10	2.06E-08	-4.69	3043	18.01	0.35	14.3	1.16	0.033	0.020
783287	18.38	2.53E-08	-4.60	3381	18.24	0.36	16.1	1.21	0.032	0.025
788197	18.46	1.63E-08	-4.79	3381	18.42	0.36	16.2	1.21	0.032	0.025
795334	18.60	1.89E-08	-4.72	3381	18.53	0.36	16.3	1.21	0.032	0.025
802504	18.70	1.39E-08	-4.86	3381	18.65	0.37	16.4	1.22	0.032	0.026
809302	19.03	4.85E-08	-4.31	3381	18.86	0.37	16.6	1.22	0.032	0.026
820080	19.29	2.41E-08	-4.62	3381	19.16	0.38	16.9	1.23	0.032	0.027
829400	19.76	5.04E-08	-4.30	3381	19.52	0.38	17.2	1.23	0.031	0.028
833237	19.82	1.69E-08	-4.77	3381	19.79	0.39	17.4	1.24	0.031	0.029
843353	20.02	1.93E-08	-4.71	3381	19.92	0.39	17.5	1.24	0.031	0.029
854138	20.20	1.72E-08	-4.77	3381	20.11	0.40	17.7	1.25	0.031	0.030
864114	20.55	3.51E-08	-4.45	3381	20.38	0.40	17.9	1.25	0.030	0.031

Table H.7. Fatigue crack growth data for test Specimen #85 – ASTM A36, R=0.05, 25Hz. (continued)

Fatigue Crack Growth Rate Calculations

Secant Method

Specimen 85 - ASTM A36, R=0.05, 25Hz

B (m)	0.0061
W (m)	0.0508
a_0 (mm)	20.95

N (cycles)	a (mm)	da/dN (m/cycle)	log(da/dN)	ΔP (N)	a_{avg} (mm)	$\alpha = a_{avg}/W$ (≥0.2)	ΔK (MPa√m)	log (ΔK) (MPa√m)	W-a	$(4/\pi)*(K_{max}/\sigma_F)^2$
876326	20.95	3.28E-08	-4.48	3381	20.75	0.41	18.3	1.26	0.030	0.032
886832	21.49	5.14E-08	-4.29	3381	21.22	0.42	18.8	1.27	0.029	0.034
898456	21.98	4.17E-08	-4.38	3381	21.73	0.43	19.3	1.29	0.029	0.035
908456	22.70	7.20E-08	-4.14	3381	22.34	0.44	19.9	1.30	0.028	0.038
918646	22.87	1.72E-08	-4.77	3381	22.78	0.45	20.4	1.31	0.028	0.040
929049	23.57	6.68E-08	-4.18	3381	23.22	0.46	20.9	1.32	0.027	0.042
939607	24.26	6.54E-08	-4.18	3381	23.91	0.47	21.8	1.34	0.027	0.045
948531	24.76	5.66E-08	-4.25	3381	24.51	0.48	22.5	1.35	0.026	0.048
954429	25.41	1.10E-07	-3.96	3381	25.09	0.49	23.3	1.37	0.025	0.052
958179	25.69	7.33E-08	-4.13	3381	25.55	0.50	24.0	1.38	0.025	0.055
963491	26.64	1.79E-07	-3.75	3381	26.16	0.51	24.9	1.40	0.024	0.059
968269	27.12	1.02E-07	-3.99	3381	26.88	0.53	26.0	1.42	0.024	0.065
973512	28.04	1.75E-07	-3.76	3381	27.58	0.54	27.3	1.44	0.023	0.071
976419	28.74	2.41E-07	-3.62	3381	28.39	0.56	28.8	1.46	0.022	0.079
980151	29.61	2.34E-07	-3.63	3381	29.17	0.57	30.5	1.48	0.021	0.089
982891	30.34	2.66E-07	-3.57	3381	29.98	0.59	32.3	1.51	0.020	0.100
984678	31.23	4.95E-07	-3.31	3381	30.78	0.61	34.4	1.54	0.020	0.113
985549	31.53	3.50E-07	-3.46	3381	31.38	0.62	36.0	1.56	0.019	0.124
988348	33.15	5.77E-07	-3.24	3381	32.34	0.64	39.0	1.59	0.018	0.145
989092	33.72	7.66E-07	-3.12	3381	33.43	0.66	43.0	1.63	0.017	0.177
989523	34.47	1.75E-06	-2.76	3381	34.09	0.67	45.8	1.66	0.016	0.200

Table H.8. Fatigue crack growth data for test Specimen #91 – ASTM A36, R=0.6, 60Hz.

Fatigue Crack Growth Rate Calculations

Secant Method

Specimen 91 – ASTM A36, 60Hz, R=0.6

B (m)	0.0059
W (m)	0.05109
a_0 (mm)	12.49

N (cycles)	a (mm)	da/dN (m/cycle)	log(da/dN)	ΔP (N)	a_{avg} (mm)	$\alpha = a_{avg}/W$ (≥0.2)	ΔK (MPa√m)	log (ΔK) (MPa√m)	W-a	$(4/\pi)*(K_{max}/\sigma_F)^2$
	12.49			0						
150000	14.37	1.25E-08	-4.90	3914	13.43	0.26	15.0	1.18	0.037	0.012
160000	14.61	2.44E-08	-4.61	3914	14.49	0.28	15.8	1.20	0.036	0.013
220000	15.60	1.64E-08	-4.78	3523	15.11	0.30	14.7	1.17	0.035	0.012
230000	15.86	2.65E-08	-4.58	3523	15.73	0.31	15.2	1.18	0.035	0.012
235000	15.91	9.40E-09	-5.03	3523	15.89	0.31	15.3	1.18	0.035	0.012
240000	16.12	4.20E-08	-4.38	3523	16.02	0.31	15.4	1.19	0.035	0.013
280000	16.71	1.47E-08	-4.83	3203	16.42	0.32	14.3	1.15	0.034	0.011
290000	16.86	1.46E-08	-4.84	3203	16.78	0.33	14.5	1.16	0.034	0.011
300000	17.05	1.93E-08	-4.71	3203	16.95	0.33	14.7	1.17	0.034	0.011
350000	17.57	1.05E-08	-4.98	2882	17.31	0.34	13.4	1.13	0.034	0.010
360000	17.73	1.54E-08	-4.81	2882	17.65	0.35	13.7	1.14	0.033	0.010
370000	17.91	1.83E-08	-4.74	2882	17.82	0.35	13.8	1.14	0.033	0.010
430000	18.49	9.68E-09	-5.01	2597	18.20	0.36	12.6	1.10	0.033	0.009
440000	18.66	1.64E-08	-4.79	2597	18.57	0.36	12.9	1.11	0.032	0.009
450000	18.76	1.03E-08	-4.99	2597	18.71	0.37	13.0	1.11	0.032	0.009
520000	19.26	7.10E-09	-5.15	2349	19.01	0.37	11.9	1.08	0.032	0.008
530000	19.35	9.20E-09	-5.04	2349	19.30	0.38	12.1	1.08	0.032	0.008
540000	19.47	1.21E-08	-4.92	2349	19.41	0.38	12.2	1.08	0.032	0.008
620000	20.05	7.21E-09	-5.14	2117	19.76	0.39	11.2	1.05	0.031	0.007
640000	20.19	7.35E-09	-5.13	2117	20.12	0.39	11.4	1.06	0.031	0.007
660000	20.33	6.80E-09	-5.17	2117	20.26	0.40	11.5	1.06	0.031	0.007
760000	20.98	6.51E-09	-5.19	1922	20.65	0.40	10.6	1.03	0.030	0.006
780000	21.07	4.35E-09	-5.36	1922	21.02	0.41	10.8	1.03	0.030	0.006
800000	21.15	4.25E-09	-5.37	1922	21.11	0.41	10.9	1.04	0.030	0.006
900000	21.79	6.34E-09	-5.20	1743	21.47	0.42	10.0	1.00	0.029	0.005
920000	21.91	6.10E-09	-5.21	1743	21.85	0.43	10.2	1.01	0.029	0.006
940000	22.09	8.90E-09	-5.05	1743	22.00	0.43	10.3	1.01	0.029	0.006
1060000	22.59	4.21E-09	-5.38	1584	22.34	0.44	9.6	0.98	0.029	0.005
1080000	22.74	7.60E-09	-5.12	1584	22.67	0.44	9.7	0.99	0.028	0.005
1100000	22.86	5.70E-09	-5.24	1584	22.80	0.45	9.8	0.99	0.028	0.005
1250000	23.41	3.70E-09	-5.43	1441	23.13	0.45	9.1	0.96	0.028	0.004
1270000	23.51	4.95E-09	-5.31	1441	23.46	0.46	9.2	0.97	0.028	0.005
1290000	23.59	3.80E-09	-5.42	1441	23.55	0.46	9.3	0.97	0.028	0.005
1490000	24.13	2.74E-09	-5.56	1299	23.86	0.47	8.5	0.93	0.027	0.004
1520000	24.32	6.20E-09	-5.21	1299	24.23	0.47	8.7	0.94	0.027	0.004
1550000	24.44	3.90E-09	-5.41	1299	24.38	0.48	8.8	0.94	0.027	0.004
1580000	24.55	3.67E-09	-5.44	1299	24.49	0.48	8.8	0.95	0.027	0.004
1780000	25.07	2.62E-09	-5.58	1175	24.81	0.49	8.1	0.91	0.026	0.004
1810000	25.17	3.37E-09	-5.47	1175	25.12	0.49	8.3	0.92	0.026	0.004
2060000	25.72	2.18E-09	-5.66	1068	25.44	0.50	7.7	0.89	0.025	0.003
2090000	25.82	3.40E-09	-5.47	1068	25.77	0.50	7.8	0.89	0.025	0.003

Table H.9. Fatigue crack growth data for test Specimen #91 – ASTM A36, R=0.6, 60Hz. (continued)

Fatigue Crack Growth Rate Calculations

Secant Method

Specimen 91 – ASTM A36, 60Hz, R=0.6

B (m)	0.0059
W (m)	0.05109
a_0 (mm)	12.49

N (cycles)	a (mm)	da/dN (m/cycle)	log(da/dN)	ΔP (N)	a_{avg} (mm)	$\alpha = a_{avg}/W$ (≥0.2)	ΔK (MPa√m)	log (ΔK) (MPa√m)	W-a	$(4/\pi)^*(K_{max}/\sigma_F)^2$
2120000	25.94	4.07E-09	-5.39	1068	25.88	0.51	7.9	0.90	0.025	0.003
2420000	26.45	1.70E-09	-5.77	961	26.19	0.51	7.2	0.86	0.025	0.003
2450000	26.52	2.20E-09	-5.66	961	26.48	0.52	7.4	0.87	0.025	0.003
2480000	26.58	2.07E-09	-5.68	961	26.55	0.52	7.4	0.87	0.025	0.003
2880000	27.13	1.37E-09	-5.86	872	26.85	0.53	6.8	0.84	0.024	0.003
2910000	27.20	2.47E-09	-5.61	872	27.16	0.53	7.0	0.84	0.024	0.003
2940000	27.28	2.57E-09	-5.59	872	27.24	0.53	7.0	0.85	0.024	0.003
3360000	27.88	1.44E-09	-5.84	801	27.58	0.54	6.6	0.82	0.023	0.002
3420000	27.94	1.00E-09	-6.00	801	27.91	0.55	6.7	0.83	0.023	0.002
4020000	28.51	9.57E-10	-6.02	730	28.23	0.55	6.3	0.80	0.023	0.002
4120000	28.61	9.60E-10	-6.02	730	28.56	0.56	6.4	0.81	0.022	0.002
4820000	29.15	7.73E-10	-6.11	658	28.88	0.57	5.9	0.77	0.022	0.002
4920000	29.23	8.20E-10	-6.09	658	29.19	0.57	6.0	0.78	0.022	0.002
6120000	29.77	4.44E-10	-6.35	605	29.50	0.58	5.7	0.75	0.021	0.002
6270000	29.86	6.40E-10	-6.19	605	29.81	0.58	5.8	0.76	0.021	0.002
7770000	30.63	5.13E-10	-6.29	543	30.25	0.59	5.4	0.73	0.020	0.002
7970000	30.70	3.40E-10	-6.47	543	30.67	0.60	5.6	0.75	0.020	0.002
8170000	30.79	4.60E-10	-6.34	543	30.75	0.60	5.6	0.75	0.020	0.002
8370000	30.92	6.45E-10	-6.19	543	30.86	0.60	5.6	0.75	0.020	0.002
8570000	31.09	8.40E-10	-6.08	543	31.01	0.61	5.7	0.76	0.020	0.002

Table H.10. Fatigue crack growth data for test Specimen #94 – ASTM A36, R=0.6, 60Hz.

Fatigue Crack Growth Rate Calculations

Secant Method

Specimen 94 – ASTM A36, 60Hz, R=0.6

B (m)	0.0059
W (m)	0.05078
a_0 (mm)	12.5

N (cycles)	a (mm)	da/dN (m/cycle)	log(da/dN)	ΔP (N)	a_{avg} (mm)	$\alpha = a_{avg}/W$ (≥0.2)	ΔK (MPa√m)	log (ΔK) (MPa√m)	W-a	$(4/\pi)*(K_{max}/\sigma_F)^2$
	12.5			0						
350000	13.58	3.08E-09	-5.51	2669	13.04	0.26	10.1	1.00	0.037	0.005
380000	13.89	1.03E-08	-4.99	2669	13.73	0.27	10.4	1.02	0.037	0.006
400000	14.03	7.05E-09	-5.15	2669	13.96	0.27	10.6	1.02	0.037	0.006
440000	14.32	7.23E-09	-5.14	2758	14.17	0.28	11.0	1.04	0.036	0.007
460000	14.46	6.95E-09	-5.16	2758	14.39	0.28	11.2	1.05	0.036	0.007
480000	14.64	9.05E-09	-5.04	2758	14.55	0.29	11.3	1.05	0.036	0.007
510000	14.98	1.14E-08	-4.94	2847	14.81	0.29	11.8	1.07	0.036	0.007
520000	15.11	1.27E-08	-4.90	2847	15.04	0.30	11.9	1.08	0.036	0.008
530000	15.18	7.00E-09	-5.15	2847	15.14	0.30	12.0	1.08	0.036	0.008
550000	15.33	7.75E-09	-5.11	2936	15.25	0.30	12.4	1.09	0.035	0.008
560000	15.48	1.46E-08	-4.84	2936	15.40	0.30	12.5	1.10	0.035	0.008
570000	15.62	1.46E-08	-4.84	2936	15.55	0.31	12.6	1.10	0.035	0.008
590000	15.98	1.77E-08	-4.75	3025	15.80	0.31	13.2	1.12	0.035	0.009
600000	16.09	1.12E-08	-4.95	3025	16.03	0.32	13.3	1.12	0.035	0.009
610000	16.28	1.89E-08	-4.72	3025	16.18	0.32	13.4	1.13	0.035	0.010
630000	16.56	1.44E-08	-4.84	3113	16.42	0.32	14.0	1.15	0.034	0.010
638000	16.84	3.44E-08	-4.46	3113	16.70	0.33	14.2	1.15	0.034	0.011
646000	17.09	3.10E-08	-4.51	3113	16.96	0.33	14.4	1.16	0.034	0.011
661000	17.22	9.07E-09	-5.04	3203	17.16	0.34	14.9	1.17	0.034	0.012
666000	17.29	1.32E-08	-4.88	3203	17.26	0.34	15.0	1.18	0.033	0.012
671000	17.45	3.12E-08	-4.51	3203	17.37	0.34	15.1	1.18	0.033	0.012
686000	17.73	1.91E-08	-4.72	3291	17.59	0.35	15.7	1.20	0.033	0.013
691000	17.87	2.70E-08	-4.57	3291	17.80	0.35	15.8	1.20	0.033	0.013
696000	18.07	4.10E-08	-4.39	3291	17.97	0.35	16.0	1.20	0.033	0.014
711000	18.41	2.25E-08	-4.65	3381	18.24	0.36	16.6	1.22	0.032	0.015
719000	18.60	2.31E-08	-4.64	3381	18.50	0.36	16.9	1.23	0.032	0.015
727000	18.84	3.01E-08	-4.52	3381	18.72	0.37	17.1	1.23	0.032	0.016
737000	19.20	3.61E-08	-4.44	3470	19.02	0.37	17.8	1.25	0.032	0.017
742000	19.44	4.78E-08	-4.32	3470	19.32	0.38	18.0	1.26	0.031	0.017
747000	19.69	5.00E-08	-4.30	3470	19.56	0.39	18.3	1.26	0.031	0.018
755000	20.02	4.20E-08	-4.38	3558	19.85	0.39	19.0	1.28	0.031	0.019
758000	20.15	4.23E-08	-4.37	3558	20.09	0.40	19.3	1.28	0.031	0.020
761000	20.27	4.10E-08	-4.39	3558	20.21	0.40	19.4	1.29	0.031	0.020
769000	20.92	8.04E-08	-4.09	3914	20.59	0.41	21.7	1.34	0.030	0.025
771000	21.00	4.15E-08	-4.38	3914	20.96	0.41	22.2	1.35	0.030	0.026
775000	21.29	7.22E-08	-4.14	3914	21.14	0.42	22.4	1.35	0.029	0.027
777000	21.54	1.29E-07	-3.89	4271	21.42	0.42	24.8	1.39	0.029	0.033

Table H.11. Fatigue crack growth data for test Specimen #14-10 - AWS A5.18, R=0.05, 60Hz.

Fatigue Crack Growth Rate Calculations
Secant Method
Specimen 14-10 - AWS 5.18, R=0.05

B (m)	0.00611
W (m)	0.05095
a_0 (mm)	12.51

N (cycles)	a (mm)	da/dN (m/cycle)	log(da/dN)	ΔP (N)	a_{avg} (mm)	$\alpha = a_{avg}/W$ (≥0.2)	ΔK (MPa√m)	log (ΔK) (MPa√m)	W-a	$(4/\pi)*(K_{max}/\sigma_{YS})^2$
	12.51			0						
150000	14.14	1.09E-08	-4.96	5111	13.33	0.26	18.8	1.27	0.037	0.002
165000	14.42	1.85E-08	-4.73	5111	14.28	0.28	19.8	1.30	0.037	0.002
180000	14.99	3.83E-08	-4.42	5111	14.71	0.29	20.2	1.31	0.036	0.003
205000	15.47	1.90E-08	-4.72	4648	15.23	0.30	18.9	1.28	0.035	0.002
215000	15.70	2.31E-08	-4.64	4648	15.58	0.31	19.2	1.28	0.035	0.002
220000	15.80	2.08E-08	-4.68	4648	15.75	0.31	19.4	1.29	0.035	0.002
260000	16.37	1.40E-08	-4.85	4182	16.08	0.32	17.7	1.25	0.035	0.002
275000	16.67	2.06E-08	-4.69	4182	16.52	0.32	18.1	1.26	0.034	0.002
290000	16.88	1.38E-08	-4.86	4182	16.78	0.33	18.4	1.26	0.034	0.002
350000	17.68	1.33E-08	-4.88	3803	17.28	0.34	17.1	1.23	0.033	0.002
370000	17.90	1.14E-08	-4.95	3803	17.79	0.35	17.6	1.25	0.033	0.002
390000	18.44	2.69E-08	-4.57	3803	18.17	0.36	17.9	1.25	0.033	0.002
450000	19.03	9.78E-09	-5.01	3421	18.74	0.37	16.6	1.22	0.032	0.002
465000	19.15	8.13E-09	-5.09	3421	19.09	0.37	16.9	1.23	0.032	0.002
480000	19.45	2.00E-08	-4.70	3421	19.30	0.38	17.1	1.23	0.031	0.002
550000	19.95	7.14E-09	-5.15	3082	19.70	0.39	15.7	1.20	0.031	0.002
565000	20.12	1.09E-08	-4.96	3082	20.03	0.39	16.0	1.20	0.031	0.002
580000	20.31	1.31E-08	-4.88	3082	20.21	0.40	16.1	1.21	0.031	0.002
660000	20.81	6.26E-09	-5.20	2789	20.56	0.40	14.9	1.17	0.030	0.001
690000	21.01	6.43E-09	-5.19	2789	20.91	0.41	15.1	1.18	0.030	0.001
710000	21.16	7.45E-09	-5.13	2789	21.08	0.41	15.3	1.18	0.030	0.001
830000	21.81	5.43E-09	-5.26	2536	21.48	0.42	14.2	1.15	0.029	0.001
850000	21.90	4.85E-09	-5.31	2536	21.86	0.43	14.5	1.16	0.029	0.001
870000	22.05	7.10E-09	-5.15	2536	21.98	0.43	14.6	1.16	0.029	0.001
1030000	22.59	3.42E-09	-5.47	2282	22.32	0.44	13.3	1.13	0.028	0.001
1060000	22.73	4.70E-09	-5.33	2282	22.66	0.44	13.6	1.13	0.028	0.001
1090000	22.83	3.13E-09	-5.50	2282	22.78	0.45	13.7	1.14	0.028	0.001
1310000	23.35	2.35E-09	-5.63	2069	23.09	0.45	12.6	1.10	0.028	0.001
1340000	23.46	3.90E-09	-5.41	2069	23.40	0.46	12.8	1.11	0.027	0.001
1370000	23.55	3.03E-09	-5.52	2069	23.51	0.46	12.9	1.11	0.027	0.001
1820000	24.06	1.14E-09	-5.94	1900	23.81	0.47	12.1	1.08	0.027	0.001
1870000	24.12	1.10E-09	-5.96	1900	24.09	0.47	12.3	1.09	0.027	0.001
1920000	24.21	1.80E-09	-5.74	1900	24.16	0.47	12.3	1.09	0.027	0.001
5170000	24.82	1.87E-10	-6.73	1731	24.51	0.48	11.5	1.06	0.026	0.001
5370000	24.94	5.95E-10	-6.23	1731	24.88	0.49	11.7	1.07	0.026	0.001
5570000	25.07	6.90E-10	-6.16	1731	25.00	0.49	11.8	1.07	0.026	0.001
7420000	25.74	3.59E-10	-6.44	1561	25.41	0.50	10.9	1.04	0.025	0.001
7620000	25.79	2.60E-10	-6.59	1561	25.76	0.51	11.1	1.05	0.025	0.001
7820000	25.90	5.30E-10	-6.28	1561	25.84	0.51	11.2	1.05	0.025	0.001
9970000	26.41	2.39E-10	-6.62	1405	26.15	0.51	10.3	1.01	0.025	0.001
10270000	26.48	2.47E-10	-6.61	1405	26.45	0.52	10.4	1.02	0.024	0.001
10570000	26.60	3.97E-10	-6.40	1405	26.54	0.52	10.5	1.02	0.024	0.001
10670000	26.68	7.70E-10	-6.11	1405	26.64	0.52	10.6	1.02	0.024	0.001
10770000	26.83	1.51E-09	-5.82	1405	26.76	0.53	10.7	1.03	0.024	0.001
10820000	26.90	1.38E-09	-5.86	1405	26.87	0.53	10.7	1.03	0.024	0.001
10870000	26.98	1.54E-09	-5.81	1405	26.94	0.53	10.8	1.03	0.024	0.001

Table H.12. Fatigue crack growth data for test Specimen #23-42 - AWS A5.18, R=0.05, 60Hz.

Fatigue Crack Growth Rate Calculations
Secant Method
Specimen 23-42 - AWS 5.18, R=0.05

B (m)	0.0061
W (m)	0.0508
a_0 (mm)	12.58

Cycles	a (mm)	da/dN (m/cycle)	log(da/dN)	ΔP (N)	a_{avg} (mm)	$\alpha = a_{avg}/W$ (≥0.2)	ΔK (MPa√m)	log (ΔK) (MPa√m)	W-a	$(4/\pi)*(K_{max}/\sigma_{YS})^2$
	12.58			0						
160000	16.47	2.43E-08	-4.61	6846	14.53	0.29	27.0	1.43	0.034	0.006
165000	17.13	1.32E-07	-3.88	6846	16.80	0.33	30.3	1.48	0.034	0.007
180000	17.91	5.17E-08	-4.29	6170	17.52	0.34	28.3	1.45	0.033	0.006
182000	18.17	1.30E-07	-3.89	6170	18.04	0.36	29.1	1.46	0.033	0.006
195000	18.67	3.87E-08	-4.41	5551	18.42	0.36	26.7	1.43	0.032	0.005
203000	18.92	3.08E-08	-4.51	5551	18.79	0.37	27.2	1.43	0.032	0.006
220000	19.45	3.14E-08	-4.50	5000	19.18	0.38	25.0	1.40	0.031	0.005
222000	19.57	5.90E-08	-4.23	5000	19.51	0.38	25.4	1.40	0.031	0.005
260000	20.26	1.81E-08	-4.74	4502	19.91	0.39	23.3	1.37	0.031	0.004
264000	20.43	4.32E-08	-4.36	4502	20.34	0.40	23.9	1.38	0.030	0.004
305000	21.05	1.51E-08	-4.82	4052	20.74	0.41	21.9	1.34	0.030	0.004
310000	21.17	2.48E-08	-4.61	4052	21.11	0.42	22.4	1.35	0.030	0.004
390000	21.91	9.23E-09	-5.04	3652	21.54	0.42	20.6	1.31	0.029	0.003
400000	22.17	2.55E-08	-4.59	3652	22.04	0.43	21.2	1.33	0.029	0.003
450000	23.03	1.72E-08	-4.76	3287	22.60	0.44	19.7	1.29	0.028	0.003
455000	23.09	1.30E-08	-4.89	3287	23.06	0.45	20.2	1.30	0.028	0.003
560000	23.85	7.21E-09	-5.14	2958	23.47	0.46	18.6	1.27	0.027	0.003
570000	23.97	1.19E-08	-4.92	2958	23.91	0.47	19.0	1.28	0.027	0.003
700000	24.72	5.78E-09	-5.24	2660	24.34	0.48	17.6	1.24	0.026	0.002
720000	25.02	1.50E-08	-4.82	2660	24.87	0.49	18.1	1.26	0.026	0.003
850000	25.56	4.14E-09	-5.38	2406	25.29	0.50	16.8	1.23	0.025	0.002
880000	25.76	6.57E-09	-5.18	2406	25.66	0.51	17.2	1.23	0.025	0.002
1030000	26.33	3.84E-09	-5.42	2175	26.04	0.51	15.9	1.20	0.024	0.002
1060000	26.46	4.30E-09	-5.37	2175	26.40	0.52	16.3	1.21	0.024	0.002
1360000	27.13	2.22E-09	-5.65	1966	26.79	0.53	15.1	1.18	0.024	0.002
1380000	27.30	8.75E-09	-5.06	1966	27.21	0.54	15.5	1.19	0.023	0.002
1400000	27.38	4.05E-09	-5.39	1966	27.34	0.54	15.6	1.19	0.023	0.002
1630000	27.95	2.47E-09	-5.61	1793	27.67	0.54	14.5	1.16	0.023	0.002
1670000	28.04	2.33E-09	-5.63	1793	28.00	0.55	14.9	1.17	0.023	0.002
1710000	28.16	2.82E-09	-5.55	1793	28.10	0.55	15.0	1.18	0.023	0.002
1960000	28.70	2.19E-09	-5.66	1628	28.43	0.56	13.9	1.14	0.022	0.001
1990000	28.78	2.50E-09	-5.60	1628	28.74	0.57	14.2	1.15	0.022	0.002
2700000	29.28	7.11E-10	-6.15	1477	29.03	0.57	13.2	1.12	0.022	0.001
2800000	29.37	9.00E-10	-6.05	1477	29.33	0.58	13.5	1.13	0.021	0.001
3600000	30.17	9.89E-10	-6.00	1330	29.77	0.59	12.5	1.10	0.021	0.001
3700000	30.24	7.70E-10	-6.11	1330	30.20	0.59	12.9	1.11	0.021	0.001
4300000	30.74	8.33E-10	-6.08	1205	30.49	0.60	12.0	1.08	0.020	0.001
4500000	30.86	5.75E-10	-6.24	1205	30.80	0.61	12.3	1.09	0.020	0.001
5600000	31.40	4.92E-10	-6.31	1099	31.13	0.61	11.5	1.06	0.019	0.001
5800000	31.48	3.95E-10	-6.40	1099	31.44	0.62	11.8	1.07	0.019	0.001
9250000	32.10	1.81E-10	-6.74	1015	31.79	0.63	11.2	1.05	0.019	0.001
9500000	32.16	2.40E-10	-6.62	1014	32.13	0.63	11.5	1.06	0.019	0.001
9700000	32.26	4.75E-10	-6.32	1014	32.21	0.63	11.6	1.06	0.019	0.001
9900000	32.35	4.80E-10	-6.32	1014	32.30	0.64	11.7	1.07	0.018	0.001
10050000	32.44	5.73E-10	-6.24	1014	32.40	0.64	11.8	1.07	0.018	0.001

Table H.13. Fatigue crack growth data for test Specimen #13-0 - AWS A5.18, R=0.05, 60Hz.

Fatigue Crack Growth Rate Calculations

Secant Method

Specimen 13-0 - AWS 5.18, R=0.05

B (m)	0.00612
W (m)	0.05087
a_0 (mm)	12.58

N (cycles)	a (mm)	da/dN (m/cycle)	log(da/dN)	ΔP (N)	a_{avg} (mm)	$\alpha = a_{avg}/W$ (≥0.2)	ΔK (MPa√m)	log (ΔK) (MPa√m)	W-a	$(4/\pi)*(K_{max}/\sigma_{YS})^2$
	12.58			0						
300000	13.52	3.13E-09	-5.50	3381	13.05	0.26	12.3	1.09	0.037	0.001
350000	13.81	5.70E-09	-5.24	3381	13.66	0.27	12.7	1.10	0.037	0.001
375000	14.10	1.20E-08	-4.92	3381	13.95	0.27	12.9	1.11	0.037	0.001
390000	14.22	7.53E-09	-5.12	3381	14.16	0.28	13.0	1.11	0.037	0.001
405000	14.41	1.32E-08	-4.88	3381	14.32	0.28	13.1	1.12	0.036	0.001
415000	14.58	1.67E-08	-4.78	3550	14.50	0.29	13.9	1.14	0.036	0.001
425000	14.74	1.61E-08	-4.79	3550	14.66	0.29	14.0	1.15	0.036	0.001
435000	14.87	1.23E-08	-4.91	3621	14.80	0.29	14.4	1.16	0.036	0.001
440000	14.97	2.10E-08	-4.68	3621	14.92	0.29	14.5	1.16	0.036	0.001
445000	15.03	1.26E-08	-4.90	3621	15.00	0.29	14.6	1.16	0.036	0.001
450000	15.13	1.84E-08	-4.74	3621	15.08	0.30	14.6	1.16	0.036	0.001
460000	15.24	1.10E-08	-4.96	3696	15.18	0.30	15.0	1.18	0.036	0.001
470000	15.38	1.41E-08	-4.85	3696	15.31	0.30	15.1	1.18	0.035	0.001
480000	15.57	1.96E-08	-4.71	3696	15.47	0.30	15.2	1.18	0.035	0.001
490000	15.72	1.50E-08	-4.82	3696	15.65	0.31	15.3	1.19	0.035	0.001
500000	15.98	2.59E-08	-4.59	4012	15.85	0.31	16.8	1.23	0.035	0.002
505000	16.10	2.32E-08	-4.63	4012	16.04	0.32	17.0	1.23	0.035	0.002
510000	16.26	3.20E-08	-4.49	4012	16.18	0.32	17.1	1.23	0.035	0.002
515000	16.43	3.46E-08	-4.46	4012	16.34	0.32	17.3	1.24	0.034	0.002
525000	16.62	1.90E-08	-4.72	4097	16.52	0.32	17.8	1.25	0.034	0.002
535000	16.89	2.66E-08	-4.58	4097	16.75	0.33	18.0	1.26	0.034	0.002
540000	17.02	2.70E-08	-4.57	4097	16.95	0.33	18.2	1.26	0.034	0.002
550000	17.35	3.31E-08	-4.48	4182	17.19	0.34	18.8	1.27	0.034	0.002
555000	17.53	3.54E-08	-4.45	4182	17.44	0.34	19.0	1.28	0.033	0.002
560000	17.70	3.46E-08	-4.46	4182	17.61	0.35	19.2	1.28	0.033	0.002
570000	18.02	3.23E-08	-4.49	4266	17.86	0.35	19.8	1.30	0.033	0.002
580000	18.38	3.57E-08	-4.45	4266	18.20	0.36	20.2	1.30	0.032	0.002
585000	18.75	7.34E-08	-4.13	4266	18.56	0.36	20.5	1.31	0.032	0.003
590000	18.89	2.92E-08	-4.53	4266	18.82	0.37	20.8	1.32	0.032	0.003
600000	19.13	2.31E-08	-4.64	4266	19.01	0.37	21.0	1.32	0.032	0.003
610000	19.59	4.65E-08	-4.33	4266	19.36	0.38	21.4	1.33	0.031	0.003
615000	19.87	5.62E-08	-4.25	4266	19.73	0.39	21.8	1.34	0.031	0.003
618000	19.97	3.23E-08	-4.49	4266	19.92	0.39	22.0	1.34	0.031	0.003
621000	20.13	5.52E-08	-4.26	4266	20.05	0.39	22.2	1.35	0.031	0.003
626000	20.57	8.77E-08	-4.06	4373	20.35	0.40	23.1	1.36	0.030	0.003
627000	20.65	7.30E-08	-4.14	4373	20.61	0.41	23.4	1.37	0.030	0.003
628000	20.83	1.84E-07	-3.74	4373	20.74	0.41	23.5	1.37	0.030	0.003
629000	20.91	7.60E-08	-4.12	4373	20.87	0.41	23.7	1.37	0.030	0.003
632000	21.07	5.37E-08	-4.27	4373	20.99	0.41	23.8	1.38	0.030	0.003
633000	21.18	1.15E-07	-3.94	4457	21.12	0.42	24.5	1.39	0.030	0.004
634000	21.25	6.60E-08	-4.18	4457	21.21	0.42	24.6	1.39	0.030	0.004
635000	21.35	1.05E-07	-3.98	4457	21.30	0.42	24.7	1.39	0.030	0.004

Table H.14. Fatigue crack growth data for test Specimen #13-0 - AWS A5.18, R=0.05, 60Hz. (continued)

Fatigue Crack Growth Rate Calculations

Secant Method

Specimen 13-0 - AWS 5.18, R=0.05 (continued)

B (m)	0.00612
W (m)	0.05087
a_0 (mm)	12.58

N (cycles)	a (mm)	da/dN (m/cycle)	log(da/dN)	ΔP (N)	a_{avg} (mm)	$\alpha = a_{avg}/W$ (≥0.2)	ΔK (MPa√m)	log (ΔK) (MPa√m)	W-a	$(4/\pi)*(K_{max}/\sigma_{YS})^2$
636000	21.50	1.48E-07	-3.83	4457	21.43	0.42	24.9	1.40	0.029	0.004
637000	21.56	6.30E-08	-4.20	4457	21.53	0.42	25.0	1.40	0.029	0.004
638000	21.69	1.23E-07	-3.91	4457	21.62	0.43	25.1	1.40	0.029	0.004
641000	22.02	1.12E-07	-3.95	4520	21.85	0.43	25.8	1.41	0.029	0.004
642000	22.12	1.00E-07	-4.00	4520	22.07	0.43	26.1	1.42	0.029	0.004
643000	22.26	1.38E-07	-3.86	4520	22.19	0.44	26.3	1.42	0.029	0.004
644000	22.46	2.03E-07	-3.69	4520	22.36	0.44	26.5	1.42	0.028	0.004
647000	22.80	1.12E-07	-3.95	4689	22.63	0.44	27.9	1.45	0.028	0.005
648000	22.95	1.46E-07	-3.84	4689	22.87	0.45	28.3	1.45	0.028	0.005
649000	23.08	1.31E-07	-3.88	4689	23.01	0.45	28.5	1.46	0.028	0.005
650000	23.19	1.17E-07	-3.93	4689	23.13	0.45	28.7	1.46	0.028	0.005
651000	23.33	1.39E-07	-3.86	4689	23.26	0.46	28.9	1.46	0.028	0.005
654000	23.98	2.16E-07	-3.67	4772	23.66	0.47	30.1	1.48	0.027	0.006
655000	24.15	1.73E-07	-3.76	4772	24.07	0.47	30.8	1.49	0.027	0.006
656000	24.27	1.13E-07	-3.95	4772	24.21	0.48	31.1	1.49	0.027	0.006
658000	24.90	3.16E-07	-3.50	4857	24.58	0.48	32.3	1.51	0.026	0.006
659000	25.10	2.03E-07	-3.69	4857	25.00	0.49	33.1	1.52	0.026	0.007
660000	25.62	5.24E-07	-3.28	4857	25.36	0.50	33.8	1.53	0.025	0.007
661000	25.80	1.79E-07	-3.75	4857	25.71	0.51	34.6	1.54	0.025	0.007
662000	26.07	2.68E-07	-3.57	4857	25.94	0.51	35.0	1.54	0.025	0.008
664000	26.72	3.25E-07	-3.49	4942	26.40	0.52	36.7	1.56	0.024	0.008
664500	26.90	3.64E-07	-3.44	4942	26.81	0.53	37.7	1.58	0.024	0.009
665000	27.08	3.44E-07	-3.46	4942	26.99	0.53	38.1	1.58	0.024	0.009
667000	28.14	5.32E-07	-3.27	5026	27.61	0.54	40.4	1.61	0.023	0.010
667500	28.42	5.58E-07	-3.25	5026	28.28	0.56	42.2	1.63	0.022	0.011
668000	28.76	6.76E-07	-3.17	5026	28.59	0.56	43.1	1.63	0.022	0.011
668500	28.96	4.10E-07	-3.39	5026	28.86	0.57	44.0	1.64	0.022	0.012
669500	29.59	6.32E-07	-3.20	5075	29.28	0.58	45.8	1.66	0.021	0.013
670000	30.07	9.56E-07	-3.02	5075	29.83	0.59	47.6	1.68	0.021	0.014
670500	30.41	6.76E-07	-3.17	5075	30.24	0.59	49.1	1.69	0.020	0.015

Table H.15. Fatigue crack growth data for test Specimen #7-15 - AWS A5.18, R=0.05, 60Hz.

Fatigue Crack Growth Rate Calculations

Secant Method

Specimen 7-15 - AWS 5.18, R=0.05

B (m)	0.00613
W (m)	0.05068
a_0 (mm)	12.55

N (cycles)	a (mm)	da/dN (m/cycle)	log(da/dN)	ΔP (N)	a_{avg} (mm)	$\alpha = a_{avg}/W$ (≥0.2)	ΔK (MPa√m)	log (ΔK) (MPa√m)	W-a	$(4/\pi)*(K_{max}/\sigma_{YS})^2$
	12.55			0						
285000	14.10	5.44E-09	-5.26	3803	13.32	0.26	14.1	1.15	0.037	0.001
335000	14.56	9.16E-09	-5.04	3803	14.33	0.28	14.8	1.17	0.036	0.001
420000	15.10	6.33E-09	-5.20	3421	14.83	0.29	13.7	1.14	0.036	0.001
450000	15.36	8.83E-09	-5.05	3421	15.23	0.30	14.0	1.14	0.035	0.001
530000	15.88	6.50E-09	-5.19	3082	15.62	0.31	12.8	1.11	0.035	0.001
570000	16.00	2.87E-09	-5.54	3082	15.94	0.31	13.0	1.11	0.035	0.001
750000	16.50	2.82E-09	-5.55	2789	16.25	0.32	12.0	1.08	0.034	0.001
800000	16.60	1.92E-09	-5.72	2789	16.55	0.33	12.2	1.09	0.034	0.001
1100000	17.40	2.67E-09	-5.57	2536	17.00	0.34	11.3	1.05	0.033	0.001
1200000	17.58	1.76E-09	-5.75	2536	17.49	0.35	11.6	1.06	0.033	0.001
1800000	18.13	9.17E-10	-6.04	2282	17.85	0.35	10.6	1.03	0.033	0.001
2000000	18.38	1.25E-09	-5.90	2282	18.25	0.36	10.8	1.04	0.032	0.001

Table H.16. Fatigue crack growth data for test Specimen #17-24 - AWS A5.18, R=0.05, 60Hz.

Fatigue Crack Growth Rate Calculations

Secant Method

Specimen 17-24 - AWS 5.18, R=0.05

B (m)	0.00608
W (m)	0.05068
a_0 (mm)	12.52

N (cycles)	a (mm)	da/dN (m/cycle)	log(da/dN)	ΔP (N)	a_{avg} (mm)	$\alpha = a_{avg}/W$ (≥0.2)	ΔK (MPa√m)	log (ΔK) (MPa√m)	W-a	$(4/\pi)*(K_{max}/\sigma_{YS})^2$
	12.52			0						
220000	14.01	6.78E-09	-5.17	4648	13.27	0.26	17.3	1.24	0.037	0.002
240000	14.27	1.29E-08	-4.89	4648	14.14	0.28	18.1	1.26	0.036	0.002
260000	14.47	1.01E-08	-5.00	4648	14.37	0.28	18.3	1.26	0.036	0.002
280000	14.72	1.27E-08	-4.90	4648	14.60	0.29	18.5	1.27	0.036	0.002
430000	15.19	3.13E-09	-5.50	4182	14.96	0.30	17.0	1.23	0.035	0.002
450000	15.31	5.95E-09	-5.23	4182	15.25	0.30	17.2	1.24	0.035	0.002
470000	15.80	2.44E-08	-4.61	4182	15.56	0.31	17.5	1.24	0.035	0.002
490000	15.90	5.10E-09	-5.29	4182	15.85	0.31	17.7	1.25	0.035	0.002
580000	16.47	6.36E-09	-5.20	3803	16.19	0.32	16.4	1.22	0.034	0.002
600000	16.54	3.15E-09	-5.50	3803	16.50	0.33	16.7	1.22	0.034	0.002
620000	16.80	1.30E-08	-4.89	3803	16.67	0.33	16.8	1.23	0.034	0.002
640000	16.97	8.95E-09	-5.05	3803	16.88	0.33	17.0	1.23	0.034	0.002
660000	17.12	7.45E-09	-5.13	3803	17.05	0.34	17.2	1.23	0.034	0.002
680000	17.32	9.85E-09	-5.01	3803	17.22	0.34	17.3	1.24	0.033	0.002
700000	17.42	4.95E-09	-5.31	3803	17.37	0.34	17.4	1.24	0.033	0.002
740000	17.61	4.82E-09	-5.32	3803	17.52	0.35	17.6	1.24	0.033	0.002
780000	18.04	1.08E-08	-4.97	3803	17.83	0.35	17.8	1.25	0.033	0.002
860000	18.95	1.14E-08	-4.95	3421	18.50	0.36	16.6	1.22	0.032	0.002
880000	19.15	9.85E-09	-5.01	3421	19.05	0.38	17.1	1.23	0.032	0.002
900000	19.38	1.15E-08	-4.94	3421	19.26	0.38	17.3	1.24	0.031	0.002
1020000	20.07	5.79E-09	-5.24	3082	19.72	0.39	15.9	1.20	0.031	0.002

Table H.17. Fatigue crack growth data for test Specimen #32-36 - AWS A5.18, R=0.6, 60Hz.

Fatigue Crack Growth Rate Calculations

Secant Method

Specimen 32-36 - AWS 5.18, R=0.6

B (m)	0.00605
W (m)	0.0508
a_0 (mm)	12.53

N (cycles)	**a (mm)**	**da/dN (m/cycle)**	**log(da/dN)**	**ΔP (N)**	**a_{avg} (mm)**	**$\alpha = a_{avg}/W$ (≥0.2)**	**ΔK (MPa√m)**	**log (ΔK) (MPa√m)**	**W-a**	**$(4/\pi)*(K_{max}/\sigma_{YS})^2$**
	12.53			0						
176405	13.77	7.05E-09	-5.15	3559	13.15	0.26	13.2	1.12	0.037	0.007
203600	14.02	9.16E-09	-5.04	3559	13.90	0.27	13.7	1.14	0.037	0.008
236312	15.01	3.02E-08	-4.52	3559	14.52	0.29	14.1	1.15	0.036	0.009
276830	16.18	2.88E-08	-4.54	3559	15.59	0.31	14.9	1.17	0.035	0.010
286857	16.40	2.25E-08	-4.65	3559	16.29	0.32	15.5	1.19	0.034	0.010
296857	16.67	2.63E-08	-4.58	3559	16.53	0.33	15.7	1.19	0.034	0.011
306857	16.92	2.50E-08	-4.60	3559	16.79	0.33	15.9	1.20	0.034	0.011
316857	17.29	3.79E-08	-4.42	3594	17.10	0.34	16.3	1.21	0.034	0.011
324857	17.64	4.26E-08	-4.37	3594	17.46	0.34	16.6	1.22	0.033	0.012
330857	17.79	2.58E-08	-4.59	3594	17.71	0.35	16.8	1.23	0.033	0.012
336857	17.96	2.77E-08	-4.56	3594	17.87	0.35	16.9	1.23	0.033	0.012
341857	18.14	3.76E-08	-4.42	3630	18.05	0.36	17.2	1.24	0.033	0.013
346857	18.37	4.42E-08	-4.35	3630	18.25	0.36	17.4	1.24	0.032	0.013
351857	18.56	3.98E-08	-4.40	3630	18.46	0.36	17.6	1.25	0.032	0.013
356857	18.80	4.64E-08	-4.33	3665	18.68	0.37	18.0	1.25	0.032	0.014
361857	18.99	3.82E-08	-4.42	3665	18.89	0.37	18.2	1.26	0.032	0.014
366857	19.34	7.04E-08	-4.15	3665	19.16	0.38	18.4	1.27	0.031	0.015
371857	19.61	5.50E-08	-4.26	3665	19.48	0.38	18.7	1.27	0.031	0.015
376857	19.93	6.30E-08	-4.20	3665	19.77	0.39	19.0	1.28	0.031	0.016
381857	20.21	5.56E-08	-4.25	3719	20.07	0.40	19.6	1.29	0.031	0.017
386857	20.52	6.16E-08	-4.21	3719	20.36	0.40	19.9	1.30	0.030	0.017
391857	20.77	5.06E-08	-4.30	3719	20.64	0.41	20.2	1.31	0.030	0.018
393857	21.04	1.37E-07	-3.86	3825	20.90	0.41	21.1	1.32	0.030	0.019
394857	21.24	2.02E-07	-3.69	3825	21.14	0.42	21.3	1.33	0.030	0.020
395857	21.34	9.60E-08	-4.02	3825	21.29	0.42	21.5	1.33	0.029	0.020
396857	21.48	1.41E-07	-3.85	3825	21.41	0.42	21.6	1.33	0.029	0.020
397857	21.59	1.13E-07	-3.95	3879	21.54	0.42	22.1	1.34	0.029	0.021
398857	21.99	4.01E-07	-3.40	3879	21.79	0.43	22.4	1.35	0.029	0.022
399857	22.18	1.81E-07	-3.74	3879	22.08	0.43	22.7	1.36	0.029	0.022
400857	22.42	2.45E-07	-3.61	3914	22.30	0.44	23.2	1.37	0.028	0.023
401857	22.62	2.03E-07	-3.69	3914	22.52	0.44	23.5	1.37	0.028	0.024
402857	22.75	1.29E-07	-3.89	3914	22.69	0.45	23.7	1.37	0.028	0.024
403857	22.92	1.72E-07	-3.76	3914	22.84	0.45	23.9	1.38	0.028	0.025

Table H.18. Fatigue crack growth data for test Specimen #9-26 - AWS A5.18, R=0.6, 60Hz.

Fatigue Crack Growth Rate Calculations
Secant Method
Specimen 9-26 - AWS 5.18, R=0.6

B (m)	0.00609
W (m)	0.05067
a_0 (mm)	12.43

N (cycles)	a (mm)	da/dN (m/cycle)	log(da/dN)	ΔP (N)	a_{avg} (mm)	$\alpha = a_{avg}/W$ (≥0.2)	ΔK (MPa√m)	log (ΔK) (MPa√m)	W-a	$(4/\pi)*(K_{max}/\sigma_{YS})^2$
	12.43			0						
170000	13.89	8.56E-09	-5.07	3559	13.16	0.26	13.1	1.12	0.037	0.007
190000	14.27	1.93E-08	-4.71	3559	14.08	0.28	13.8	1.14	0.036	0.008
290000	15.52	1.24E-08	-4.91	3203	14.89	0.29	12.9	1.11	0.035	0.007
390000	16.60	1.09E-08	-4.96	2882	16.06	0.32	12.3	1.09	0.034	0.007
465000	17.19	7.87E-09	-5.10	2593	16.90	0.33	11.6	1.06	0.033	0.006
490000	17.38	7.60E-09	-5.12	2593	17.29	0.34	11.8	1.07	0.033	0.006
590000	17.69	3.14E-09	-5.50	2455	17.54	0.35	11.3	1.05	0.033	0.006
620000	18.19	1.64E-08	-4.79	2455	17.94	0.35	11.6	1.06	0.032	0.006
650000	18.50	1.06E-08	-4.97	2455	18.34	0.36	11.8	1.07	0.032	0.006
750000	19.06	5.54E-09	-5.26	2206	18.78	0.37	10.8	1.04	0.032	0.005
780000	19.36	1.02E-08	-4.99	2206	19.21	0.38	11.1	1.04	0.031	0.005
880000	19.99	6.26E-09	-5.20	1993	19.68	0.39	10.3	1.01	0.031	0.005
910000	20.23	8.03E-09	-5.10	1993	20.11	0.40	10.5	1.02	0.030	0.005
1010000	20.81	5.80E-09	-5.24	1797	20.52	0.40	9.7	0.99	0.030	0.004
1040000	20.95	4.47E-09	-5.35	1797	20.88	0.41	9.9	0.99	0.030	0.004
1160000	21.45	4.17E-09	-5.38	1624	21.20	0.42	9.1	0.96	0.029	0.004
1190000	21.55	3.63E-09	-5.44	1624	21.50	0.42	9.2	0.96	0.029	0.004
1490000	22.61	3.51E-09	-5.46	1459	22.08	0.44	8.5	0.93	0.028	0.003
1690000	23.18	2.88E-09	-5.54	1312	22.89	0.45	8.0	0.90	0.027	0.003
1890000	23.68	2.51E-09	-5.60	1183	23.43	0.46	7.5	0.87	0.027	0.002
2190000	24.20	1.71E-09	-5.77	1068	23.94	0.47	6.9	0.84	0.026	0.002
2490000	24.71	1.72E-09	-5.76	961	24.45	0.48	6.4	0.81	0.026	0.002

Table H.19. Fatigue crack growth data for test Specimen #40-44 - AWS A5.18, R=0.6, 60Hz.

Fatigue Crack Growth Rate Calculations
Secant Method
Specimen 40-44 – AWS 5.18, R=0.6

B (m)	0.00606
W (m)	0.05059
a_0 (mm)	12.41

N (cycles)	a (mm)	da/dN (m/cycle)	log(da/dN)	ΔP (N)	a_{avg} (mm)	$\alpha = a_{avg}/W$ (≥0.2)	ΔK (MPa√m)	log (ΔK) (MPa√m)	W-a	$(4/\pi)*(K_{max}/\sigma_{YS})^2$
	12.41			0						
500000	14.58	4.35E-09	-5.36	2669	13.50	0.27	10.1	1.00	0.036	0.004
700000	15.59	5.04E-09	-5.30	2402	15.09	0.30	9.9	0.99	0.035	0.004
800000	16.20	6.13E-09	-5.21	2162	15.90	0.31	9.2	0.97	0.034	0.004
1000000	16.99	3.94E-09	-5.40	1948	16.60	0.33	8.6	0.94	0.034	0.003
1200000	17.71	3.60E-09	-5.44	1753	17.35	0.34	8.1	0.91	0.033	0.003
1400000	18.22	2.53E-09	-5.60	1575	17.97	0.36	7.5	0.87	0.032	0.002
1700000	18.95	2.42E-09	-5.62	1495	18.58	0.37	7.3	0.87	0.032	0.002
1950000	19.46	2.06E-09	-5.69	1343	19.20	0.38	6.8	0.83	0.031	0.002
2360000	20.08	1.51E-09	-5.82	1210	19.77	0.39	6.3	0.80	0.031	0.002
2860000	20.60	1.03E-09	-5.99	1090	20.34	0.40	5.9	0.77	0.030	0.001
3495000	21.24	1.01E-09	-6.00	1090	20.92	0.41	6.0	0.78	0.029	0.002
4195000	21.89	9.36E-10	-6.03	996	21.56	0.43	5.7	0.76	0.029	0.001
4870000	22.76	1.28E-09	-5.89	996	22.32	0.44	5.9	0.77	0.028	0.002
5470000	23.27	8.52E-10	-6.07	899	23.01	0.45	5.6	0.75	0.027	0.001
6000000	23.80	1.01E-09	-6.00	899	23.53	0.47	5.7	0.76	0.027	0.001
6600000	24.32	8.63E-10	-6.06	801	24.06	0.48	5.3	0.72	0.026	0.001
6700000	24.41	9.20E-10	-6.04	801	24.36	0.48	5.4	0.73	0.026	0.001
7500000	24.91	6.26E-10	-6.20	730	24.66	0.49	5.0	0.70	0.026	0.001
7650000	25.01	6.33E-10	-6.20	730	24.96	0.49	5.1	0.70	0.026	0.001
9360000	25.52	3.02E-10	-6.52	658	25.26	0.50	4.7	0.67	0.025	0.001
9760000	25.60	2.02E-10	-6.69	658	25.56	0.51	4.7	0.68	0.025	0.001
10060000	25.79	6.33E-10	-6.20	658	25.70	0.51	4.8	0.68	0.025	0.001
10360000	25.94	4.73E-10	-6.32	658	25.87	0.51	4.8	0.68	0.025	0.001

Table H.20. Fatigue crack growth data for test Specimen #75-60 - AWS A5.28, R=0.05, 60Hz.

Fatigue Crack Growth Rate Calculations

Secant Method

Specimen 75-60 – AWS 5.28, R=0.05

B (m)	0.00581
W (m)	0.0508
a_0 (mm)	12.49

N (cycles)	a (mm)	da/dN (m/cycle)	log(da/dN)	ΔP (N)	a_{avg} (mm)	$\alpha = a_{avg}/W$ (≥0.2)	ΔK (MPa√m)	log (ΔK) (MPa√m)	W-a	$(4/\pi)*(K_{max}/\sigma_{YS})^2$
	12.49			0						
210000	14.18	8.04E-09	-5.09	4226	13.33	0.26	16.4	1.22	0.037	0.001
220000	14.39	2.06E-08	-4.69	4226	14.28	0.28	17.3	1.24	0.036	0.001
230000	14.50	1.18E-08	-4.93	4226	14.44	0.28	17.4	1.24	0.036	0.001
240000	14.66	1.56E-08	-4.81	4226	14.58	0.29	17.5	1.24	0.036	0.001
270000	15.18	1.74E-08	-4.76	3803	14.92	0.29	16.1	1.21	0.036	0.001
290000	15.38	9.80E-09	-5.01	3803	15.28	0.30	16.4	1.21	0.035	0.001
310000	15.65	1.37E-08	-4.86	3803	15.51	0.31	16.6	1.22	0.035	0.001
330000	15.90	1.26E-08	-4.90	3803	15.78	0.31	16.8	1.22	0.035	0.001
380000	16.48	1.16E-08	-4.94	3421	16.19	0.32	15.4	1.19	0.034	0.001
400000	16.86	1.89E-08	-4.72	3421	16.67	0.33	15.8	1.20	0.034	0.001
410000	16.96	1.02E-08	-4.99	3421	16.91	0.33	16.0	1.20	0.034	0.001
490000	17.59	7.88E-09	-5.10	3082	17.28	0.34	14.7	1.17	0.033	0.001
510000	18.01	2.07E-08	-4.68	3082	17.80	0.35	15.1	1.18	0.033	0.001
520000	18.23	2.18E-08	-4.66	3082	18.12	0.36	15.3	1.18	0.033	0.001
580000	18.74	8.52E-09	-5.07	2789	18.48	0.36	14.1	1.15	0.032	0.001
590000	18.86	1.27E-08	-4.90	2789	18.80	0.37	14.3	1.16	0.032	0.001
600000	18.96	9.70E-09	-5.01	2789	18.91	0.37	14.4	1.16	0.032	0.001
680000	19.58	7.73E-09	-5.11	2536	19.27	0.38	13.4	1.13	0.031	0.000
690000	19.68	1.00E-08	-5.00	2536	19.63	0.39	13.6	1.13	0.031	0.000
710000	19.77	4.60E-09	-5.34	2536	19.73	0.39	13.7	1.14	0.031	0.000
790000	20.33	7.00E-09	-5.15	2282	20.05	0.39	12.5	1.10	0.030	0.000
810000	20.49	8.05E-09	-5.09	2282	20.41	0.40	12.7	1.11	0.030	0.000
910000	21.01	5.15E-09	-5.29	2069	20.75	0.41	11.8	1.07	0.030	0.000
940000	21.15	4.73E-09	-5.32	2069	21.08	0.41	12.0	1.08	0.030	0.000
1090000	21.67	3.48E-09	-5.46	1900	21.41	0.42	11.2	1.05	0.029	0.000
1140000	21.89	4.30E-09	-5.37	1900	21.78	0.43	11.4	1.06	0.029	0.000
1340000	22.58	3.48E-09	-5.46	1731	22.23	0.44	10.7	1.03	0.028	0.000
1360000	22.71	6.30E-09	-5.20	1731	22.65	0.45	10.9	1.04	0.028	0.000
1420000	22.85	2.32E-09	-5.64	1731	22.78	0.45	11.0	1.04	0.028	0.000
1450000	22.99	4.87E-09	-5.31	1731	22.92	0.45	11.1	1.04	0.028	0.000
1712000	23.50	1.92E-09	-5.72	1561	23.24	0.46	10.2	1.01	0.027	0.000
1772000	23.67	2.95E-09	-5.53	1561	23.58	0.46	10.4	1.02	0.027	0.000
1832000	23.82	2.47E-09	-5.61	1561	23.75	0.47	10.4	1.02	0.027	0.000
2132000	24.44	2.05E-09	-5.69	1436	24.13	0.47	9.8	0.99	0.026	0.000
2182000	24.54	2.00E-09	-5.70	1436	24.49	0.48	10.0	1.00	0.026	0.000
2532000	25.07	1.51E-09	-5.82	1308	24.80	0.49	9.3	0.97	0.026	0.000
2612000	25.25	2.33E-09	-5.63	1308	25.16	0.50	9.5	0.98	0.026	0.000
2692000	25.38	1.58E-09	-5.80	1308	25.32	0.50	9.6	0.98	0.025	0.000
3192000	26.03	1.30E-09	-5.89	1184	25.70	0.51	8.9	0.95	0.025	0.000
3292000	26.16	1.34E-09	-5.87	1184	26.10	0.51	9.1	0.96	0.025	0.000

Table H.21. Fatigue crack growth data for test Specimen #75-60 - AWS A5.28, R=0.05, 60Hz. (continued)

Fatigue Crack Growth Rate Calculations
Secant Method
Specimen 75-60 – AWS 5.28, R=0.05

B (m)	0.00581
W (m)	0.0508
a_0 (mm)	12.49

N (cycles)	a (mm)	da/dN (m/cycle)	log(da/dN)	ΔP (N)	a_{avg} (mm)	$\alpha = a_{avg}/W$ (≥0.2)	ΔK (MPa√m)	log (ΔK) (MPa√m)	W-a	$(4/\pi)*(K_{max}/\sigma_{YS})^2$
3842000	26.67	9.16E-10	-6.04	1099	26.42	0.52	8.6	0.94	0.024	0.000
3942000	26.76	9.50E-10	-6.02	1099	26.71	0.53	8.8	0.94	0.024	0.000
4742000	27.37	7.55E-10	-6.12	992	27.06	0.53	8.1	0.91	0.023	0.000
4862000	27.43	5.00E-10	-6.30	992	27.40	0.54	8.3	0.92	0.023	0.000
6062000	27.91	4.03E-10	-6.39	952	27.67	0.54	8.1	0.91	0.023	0.000
6162000	27.95	4.00E-10	-6.40	952	27.93	0.55	8.3	0.92	0.023	0.000
7000000	28.32	4.42E-10	-6.36	952	28.14	0.55	8.4	0.92	0.022	0.000
9162000	28.90	2.68E-10	-6.57	863	28.61	0.56	7.8	0.89	0.022	0.000
9722000	29.11	3.73E-10	-6.43	863	29.00	0.57	8.1	0.91	0.022	0.000
10522000	29.70	7.40E-10	-6.13	923	29.41	0.58	8.9	0.95	0.021	0.000
10822000	30.02	1.07E-09	-5.97	923	29.86	0.59	9.2	0.96	0.021	0.000

Table H.22. Fatigue crack growth data for test Specimen #67-76 - AWS A5.28, R=0.05, 60Hz.

Fatigue Crack Growth Rate Calculations

Secant Method

Specimen 67-76 – AWS 5.28, R=0.05

B (m)	0.00583
W (m)	0.05081
a_0 (mm)	12.5

N (cycles)	**a (mm)**	**da/dN (m/cycle)**	**log(da/dN)**	**ΔP (N)**	**a_{avg} (mm)**	**$\alpha = a_{avg}/W$ (≥0.2)**	**ΔK (MPa√m)**	**log (ΔK) (MPa√m)**	**W-a**	**$(4/\pi)*(K_{max}/\sigma_{YS})^2$**
	12.5			0						
350000	14.23	4.93E-09	-5.31	3803	13.36	0.26	14.8	1.17	0.037	0.001
370000	14.47	1.19E-08	-4.92	3803	14.35	0.28	15.5	1.19	0.036	0.001
390000	14.62	7.50E-09	-5.12	3803	14.54	0.29	15.7	1.20	0.036	0.001
420000	15.15	1.78E-08	-4.75	4012	14.88	0.29	16.8	1.23	0.036	0.001
435000	15.38	1.51E-08	-4.82	4012	15.26	0.30	17.2	1.23	0.035	0.001
450000	15.71	2.25E-08	-4.65	4012	15.54	0.31	17.4	1.24	0.035	0.001
460000	15.86	1.49E-08	-4.83	4012	15.79	0.31	17.6	1.25	0.035	0.001
470000	16.03	1.67E-08	-4.78	4012	15.95	0.31	17.8	1.25	0.035	0.001
480000	16.35	3.22E-08	-4.49	4012	16.19	0.32	18.0	1.26	0.034	0.001
490000	16.65	3.01E-08	-4.52	4226	16.50	0.32	19.3	1.28	0.034	0.001
498000	16.92	3.39E-08	-4.47	4226	16.79	0.33	19.5	1.29	0.034	0.001
506000	17.06	1.74E-08	-4.76	4226	16.99	0.33	19.8	1.30	0.034	0.001
514000	17.32	3.19E-08	-4.50	4226	17.19	0.34	19.9	1.30	0.033	0.001
522000	17.57	3.19E-08	-4.50	4226	17.44	0.34	20.2	1.31	0.033	0.001
532000	18.13	5.59E-08	-4.25	4435	17.85	0.35	21.6	1.34	0.033	0.001
537000	18.38	4.90E-08	-4.31	4435	18.25	0.36	22.1	1.34	0.032	0.001
540000	18.48	3.30E-08	-4.48	4435	18.43	0.36	22.3	1.35	0.032	0.001
543000	18.64	5.63E-08	-4.25	4435	18.56	0.37	22.4	1.35	0.032	0.001
546000	18.81	5.67E-08	-4.25	4435	18.73	0.37	22.6	1.35	0.032	0.001
551000	19.21	7.82E-08	-4.11	4648	19.01	0.37	24.1	1.38	0.032	0.002
552000	19.30	9.40E-08	-4.03	4648	19.25	0.38	24.4	1.39	0.032	0.002
553000	19.39	9.10E-08	-4.04	4648	19.34	0.38	24.5	1.39	0.031	0.002
554000	19.45	5.50E-08	-4.26	4648	19.42	0.38	24.6	1.39	0.031	0.002
556000	19.62	8.65E-08	-4.06	4750	19.53	0.38	25.3	1.40	0.031	0.002
557000	19.71	9.00E-08	-4.05	4750	19.66	0.39	25.4	1.41	0.031	0.002
558000	19.77	6.40E-08	-4.19	4750	19.74	0.39	25.5	1.41	0.031	0.002
559000	19.85	7.80E-08	-4.11	4750	19.81	0.39	25.6	1.41	0.031	0.002
561000	20.06	1.05E-07	-3.98	4857	19.96	0.39	26.4	1.42	0.031	0.002
562000	20.19	1.33E-07	-3.88	4857	20.13	0.40	26.6	1.43	0.031	0.002
564000	20.38	9.50E-08	-4.02	4857	20.29	0.40	26.9	1.43	0.030	0.002
565000	20.46	7.50E-08	-4.12	4857	20.42	0.40	27.0	1.43	0.030	0.002
567000	20.71	1.27E-07	-3.90	4965	20.59	0.41	27.9	1.45	0.030	0.002
568000	20.80	8.80E-08	-4.06	4965	20.76	0.41	28.1	1.45	0.030	0.002
569000	20.97	1.72E-07	-3.76	4965	20.89	0.41	28.3	1.45	0.030	0.002
571000	21.25	1.37E-07	-3.86	5071	21.11	0.42	29.3	1.47	0.030	0.002
572000	21.42	1.70E-07	-3.77	5071	21.33	0.42	29.6	1.47	0.029	0.002
573000	21.52	1.07E-07	-3.97	5071	21.47	0.42	29.8	1.47	0.029	0.002
575000	21.78	1.28E-07	-3.89	5173	21.65	0.43	30.7	1.49	0.029	0.003
576000	21.98	1.97E-07	-3.71	5173	21.88	0.43	31.1	1.49	0.029	0.003
577000	22.15	1.74E-07	-3.76	5173	22.07	0.43	31.4	1.50	0.029	0.003

Table H.23. Fatigue crack growth data for test Specimen #67-76 - AWS A5.28, R=0.05, 60Hz. (continued)

Fatigue Crack Growth Rate Calculations

Secant Method

Specimen 67-76 – AWS 5.28, R=0.05

B (m)	0.00583
W (m)	0.05081
a_0 (mm)	12.5

N (cycles)	a (mm)	da/dN (m/cycle)	log(da/dN)	ΔP (N)	a_{avg} (mm)	$\alpha = a_{avg}/W$ (≥0.2)	ΔK (MPa√m)	log (ΔK) (MPa√m)	W-a	$(4/\pi)*(K_{max}/\sigma_{YS})^2$
579000	22.47	1.60E-07	-3.80	5280	22.31	0.44	32.5	1.51	0.028	0.003
580000	22.63	1.57E-07	-3.80	5280	22.55	0.44	32.9	1.52	0.028	0.003
581000	22.78	1.46E-07	-3.84	5280	22.70	0.45	33.2	1.52	0.028	0.003
583000	23.23	2.28E-07	-3.64	5386	23.00	0.45	34.4	1.54	0.028	0.003
584000	23.42	1.86E-07	-3.73	5386	23.32	0.46	35.1	1.54	0.027	0.003
585000	23.60	1.81E-07	-3.74	5386	23.51	0.46	35.4	1.55	0.027	0.003
587000	24.02	2.09E-07	-3.68	5494	23.81	0.47	36.8	1.57	0.027	0.004
588000	24.27	2.58E-07	-3.59	5494	24.15	0.48	37.5	1.57	0.027	0.004
589000	24.58	3.02E-07	-3.52	5494	24.43	0.48	38.1	1.58	0.026	0.004
590000	24.84	2.68E-07	-3.57	5703	24.71	0.49	40.2	1.60	0.026	0.004
590800	25.11	3.35E-07	-3.47	5703	24.98	0.49	40.9	1.61	0.026	0.004
591600	25.35	2.91E-07	-3.54	5703	25.23	0.50	41.5	1.62	0.025	0.005
593000	25.86	3.69E-07	-3.43	5917	25.60	0.50	44.0	1.64	0.025	0.005
593500	26.07	4.12E-07	-3.39	5917	25.96	0.51	45.0	1.65	0.025	0.005
594000	26.33	5.28E-07	-3.28	5917	26.20	0.52	45.7	1.66	0.024	0.006
595000	26.72	3.86E-07	-3.41	6125	26.52	0.52	48.3	1.68	0.024	0.006
595500	27.03	6.16E-07	-3.21	6125	26.87	0.53	49.3	1.69	0.024	0.006
596000	27.27	4.96E-07	-3.30	6125	27.15	0.53	50.2	1.70	0.024	0.007
597000	28.40	1.12E-06	-2.95	6338	27.84	0.55	54.4	1.74	0.022	0.008
597300	28.61	7.13E-07	-3.15	6338	28.50	0.56	57.0	1.76	0.022	0.009
597600	28.90	9.77E-07	-3.01	6338	28.76	0.57	58.0	1.76	0.022	0.009

Table H.24. Fatigue crack growth data for test Specimen #79-59 - AWS A5.28, R=0.6, 60Hz.

Fatigue Crack Growth Rate Calculations
Secant Method
Specimen 79-59 – AWS 5.28, R=0.6

B (m)	0.00583
W (m)	0.0507
a_0 (mm)	12.51

N (cycles)	a (mm)	da/dN (m/cycle)	log(da/dN)	ΔP (N)	a_{avg} (mm)	$\alpha = a_{avg}/W$ (≥0.2)	ΔK (MPa√m)	log (ΔK) (MPa√m)	W-a	$(4/\pi)*(K_{max}/\sigma_{YS})^2$
	12.51			0						
160000	13.88	8.56E-09	-5.07	3914	13.19	0.26	15.1	1.18	0.037	0.003
170000	14.31	4.28E-08	-4.37	3914	14.09	0.28	15.8	1.20	0.036	0.004
180000	14.67	3.59E-08	-4.44	3914	14.49	0.29	16.1	1.21	0.036	0.004
210000	15.28	2.06E-08	-4.69	3523	14.97	0.30	14.9	1.17	0.035	0.003
220000	15.44	1.59E-08	-4.80	3523	15.36	0.30	15.2	1.18	0.035	0.003
230000	15.61	1.69E-08	-4.77	3523	15.53	0.31	15.3	1.19	0.035	0.004
260000	16.12	1.70E-08	-4.77	3203	15.87	0.31	14.2	1.15	0.035	0.003
270000	16.36	2.41E-08	-4.62	3203	16.24	0.32	14.5	1.16	0.034	0.003
280000	16.68	3.18E-08	-4.50	3203	16.52	0.33	14.7	1.17	0.034	0.003
310000	17.19	1.70E-08	-4.77	2882	16.93	0.33	13.5	1.13	0.034	0.003
320000	17.28	9.30E-09	-5.03	2882	17.24	0.34	13.7	1.14	0.033	0.003
330000	17.61	3.24E-08	-4.49	2882	17.44	0.34	13.8	1.14	0.033	0.003
390000	18.18	9.52E-09	-5.02	2597	17.89	0.35	12.7	1.11	0.033	0.002
400000	18.39	2.15E-08	-4.67	2597	18.28	0.36	13.0	1.11	0.032	0.003
410000	18.56	1.68E-08	-4.77	2597	18.48	0.36	13.1	1.12	0.032	0.003
460000	19.09	1.06E-08	-4.98	2349	18.82	0.37	12.1	1.08	0.032	0.002
470000	19.26	1.75E-08	-4.76	2349	19.18	0.38	12.3	1.09	0.031	0.002
480000	19.36	9.90E-09	-5.00	2349	19.31	0.38	12.4	1.09	0.031	0.002
530000	19.87	1.02E-08	-4.99	2117	19.62	0.39	11.3	1.05	0.031	0.002
540000	20.00	1.25E-08	-4.90	2117	19.93	0.39	11.5	1.06	0.031	0.002
550000	20.18	1.86E-08	-4.73	2117	20.09	0.40	11.6	1.07	0.031	0.002
620000	20.70	7.41E-09	-5.13	1922	20.44	0.40	10.7	1.03	0.030	0.002
630000	20.78	7.90E-09	-5.10	1922	20.74	0.41	10.9	1.04	0.030	0.002
640000	20.91	1.31E-08	-4.88	1922	20.84	0.41	11.0	1.04	0.030	0.002
710000	21.48	8.11E-09	-5.09	1743	21.19	0.42	10.1	1.01	0.029	0.002
725000	21.54	3.80E-09	-5.42	1743	21.51	0.42	10.3	1.01	0.029	0.002
740000	21.67	8.73E-09	-5.06	1743	21.60	0.43	10.4	1.02	0.029	0.002
810000	22.18	7.27E-09	-5.14	1584	21.92	0.43	9.6	0.98	0.029	0.001
835000	22.24	2.48E-09	-5.61	1584	22.21	0.44	9.7	0.99	0.028	0.001
850000	22.38	9.27E-09	-5.03	1584	22.31	0.44	9.8	0.99	0.028	0.001
960000	22.98	5.45E-09	-5.26	1441	22.68	0.45	9.1	0.96	0.028	0.001
975000	23.09	7.53E-09	-5.12	1441	23.03	0.45	9.3	0.97	0.028	0.001
990000	23.26	1.11E-08	-4.96	1441	23.17	0.46	9.3	0.97	0.027	0.001
1120000	23.80	4.15E-09	-5.38	1299	23.53	0.46	8.6	0.93	0.027	0.001
1140000	23.89	4.95E-09	-5.31	1299	23.84	0.47	8.7	0.94	0.027	0.001
1160000	24.01	5.85E-09	-5.23	1299	23.95	0.47	8.8	0.94	0.027	0.001
1290000	24.59	4.42E-09	-5.36	1175	24.30	0.48	8.1	0.91	0.026	0.001
1310000	24.65	3.00E-09	-5.52	1175	24.62	0.49	8.3	0.92	0.026	0.001
1440000	25.15	3.90E-09	-5.41	1068	24.90	0.49	7.6	0.88	0.026	0.001
1460000	25.20	2.20E-09	-5.66	1068	25.17	0.50	7.8	0.89	0.026	0.001

Table H.25. Fatigue crack growth data for test Specimen #79-59 - AWS A5.28, R=0.6, 60Hz. (continued)

Fatigue Crack Growth Rate Calculations
Secant Method
Specimen 79-59 – AWS 5.28, R=0.6

B (m)	0.00583
W (m)	0.0507
a_0 (mm)	12.51

N (cycles)	a (mm)	da/dN (m/cycle)	log(da/dN)	ΔP (N)	a_{avg} (mm)	$\alpha = a_{avg}/W$ (≥0.2)	ΔK (MPa√m)	log (ΔK) (MPa√m)	W-a	$(4/\pi)*(K_{max}/\sigma_{YS})^2$
1480000	25.32	6.30E-09	-5.20	1068	25.26	0.50	7.8	0.89	0.025	0.001
1670000	25.87	2.87E-09	-5.54	961	25.60	0.50	7.2	0.86	0.025	0.001
1700000	25.93	2.20E-09	-5.66	961	25.90	0.51	7.3	0.86	0.025	0.001
1730000	26.05	3.77E-09	-5.42	961	25.99	0.51	7.4	0.87	0.025	0.001
1950000	26.63	2.65E-09	-5.58	872	26.34	0.52	6.8	0.83	0.024	0.001
1980000	26.75	3.93E-09	-5.41	872	26.69	0.53	7.0	0.84	0.024	0.001
2230000	27.30	2.20E-09	-5.66	801	27.02	0.53	6.5	0.82	0.023	0.001
2260000	27.40	3.50E-09	-5.46	801	27.35	0.54	6.7	0.83	0.023	0.001
2510000	27.91	2.03E-09	-5.69	730	27.66	0.55	6.2	0.79	0.023	0.001
2540000	27.99	2.53E-09	-5.60	730	27.95	0.55	6.3	0.80	0.023	0.001
2840000	28.56	1.92E-09	-5.72	658	28.28	0.56	5.9	0.77	0.022	0.001
2880000	28.64	2.00E-09	-5.70	658	28.60	0.56	6.0	0.78	0.022	0.001
3230000	29.25	1.73E-09	-5.76	591	28.95	0.57	5.5	0.74	0.021	0.000
3280000	29.36	2.14E-09	-5.67	591	29.30	0.58	5.7	0.75	0.021	0.000
3680000	29.92	1.40E-09	-5.85	533	29.64	0.58	5.2	0.72	0.021	0.000
3730000	30.00	1.76E-09	-5.75	533	29.96	0.59	5.4	0.73	0.021	0.000
4230000	30.51	1.01E-09	-6.00	480	30.26	0.60	4.9	0.69	0.020	0.000
4280000	30.58	1.40E-09	-5.85	480	30.54	0.60	5.0	0.70	0.020	0.000
4830000	31.10	9.47E-10	-6.02	432	30.84	0.61	4.6	0.67	0.020	0.000
4910000	31.17	8.88E-10	-6.05	432	31.13	0.61	4.8	0.68	0.020	0.000
5610000	31.65	6.87E-10	-6.16	391	31.41	0.62	4.4	0.64	0.019	0.000
5710000	31.72	7.10E-10	-6.15	391	31.69	0.62	4.5	0.65	0.019	0.000
6710000	32.25	5.27E-10	-6.28	352	31.99	0.63	4.2	0.62	0.018	0.000
6810000	32.31	6.20E-10	-6.21	352	32.28	0.64	4.3	0.63	0.018	0.000
7860000	32.87	5.31E-10	-6.27	321	32.59	0.64	4.0	0.60	0.018	0.000
8010000	32.94	4.80E-10	-6.32	321	32.91	0.65	4.1	0.61	0.018	0.000
9310000	33.59	4.97E-10	-6.30	290	33.26	0.66	3.8	0.58	0.017	0.000
9510000	33.66	3.60E-10	-6.44	290	33.62	0.66	4.0	0.60	0.017	0.000
11770000	34.17	2.26E-10	-6.65	258	33.91	0.67	3.6	0.56	0.017	0.000
11970000	34.20	1.65E-10	-6.78	258	34.19	0.67	3.7	0.57	0.016	0.000

Table H.26. Fatigue crack growth data for test Specimen #55-66 - AWS A5.28, R=0.6, 60Hz.

Fatigue Crack Growth Rate Calculations

Secant Method

Specimen 55-66 – AWS 5.28, R=0.6

B (m)	0.0058
W (m)	0.05091
a_0 (mm)	12.52

N (cycles)	a (mm)	da/dN (m/cycle)	log(da/dN)	ΔP (N)	a_{avg} (mm)	$\alpha = a_{avg}/W$ (≥0.2)	ΔK (MPa√m)	log (ΔK) (MPa√m)	W-a	$(4/\pi)*(K_{max}/\sigma_{YS})^2$
	12.52			0						
140000	13.74	8.74E-09	-5.06	3914	13.13	0.26	15.0	1.18	0.037	0.003
155000	13.91	1.10E-08	-4.96	3914	13.83	0.27	15.6	1.19	0.037	0.004
170000	14.13	1.46E-08	-4.84	3914	14.02	0.28	15.8	1.20	0.037	0.004
245000	14.70	7.67E-09	-5.12	3523	14.41	0.28	14.5	1.16	0.036	0.003
260000	15.00	2.00E-08	-4.70	3523	14.85	0.29	14.8	1.17	0.036	0.003
275000	15.32	2.13E-08	-4.67	3523	15.16	0.30	15.0	1.18	0.036	0.003
360000	15.95	7.40E-09	-5.13	3203	15.64	0.31	14.0	1.15	0.035	0.003
375000	16.21	1.76E-08	-4.75	3203	16.08	0.32	14.3	1.16	0.035	0.003
390000	16.49	1.82E-08	-4.74	3203	16.35	0.32	14.5	1.16	0.034	0.003
500000	17.14	5.91E-09	-5.23	2882	16.81	0.33	13.4	1.13	0.034	0.003
520000	17.34	1.00E-08	-5.00	2882	17.24	0.34	13.7	1.14	0.034	0.003
540000	17.50	8.30E-09	-5.08	2882	17.42	0.34	13.8	1.14	0.033	0.003
620000	18.05	6.82E-09	-5.17	2597	17.78	0.35	12.7	1.10	0.033	0.002
640000	18.17	5.95E-09	-5.23	2597	18.11	0.36	12.9	1.11	0.033	0.002
660000	18.31	6.90E-09	-5.16	2597	18.24	0.36	13.0	1.11	0.033	0.003
780000	18.84	4.48E-09	-5.35	2349	18.58	0.36	11.9	1.08	0.032	0.002
800000	18.96	5.90E-09	-5.23	2349	18.90	0.37	12.1	1.08	0.032	0.002
820000	19.05	4.50E-09	-5.35	2349	19.01	0.37	12.2	1.09	0.032	0.002
970000	19.58	3.52E-09	-5.45	2117	19.32	0.38	11.2	1.05	0.031	0.002
995000	19.68	4.00E-09	-5.40	2117	19.63	0.39	11.3	1.05	0.031	0.002
1020000	19.80	4.68E-09	-5.33	2117	19.74	0.39	11.4	1.06	0.031	0.002
1220000	20.35	2.78E-09	-5.56	1922	20.08	0.39	10.5	1.02	0.031	0.002
1280000	20.51	2.58E-09	-5.59	1922	20.43	0.40	10.7	1.03	0.030	0.002
1340000	20.66	2.58E-09	-5.59	1922	20.59	0.40	10.8	1.03	0.030	0.002
1590000	21.29	2.50E-09	-5.60	1743	20.98	0.41	10.0	1.00	0.030	0.001
1630000	21.39	2.50E-09	-5.60	1743	21.34	0.42	10.2	1.01	0.030	0.002
1670000	21.49	2.50E-09	-5.60	1743	21.44	0.42	10.3	1.01	0.029	0.002
1990000	22.10	1.91E-09	-5.72	1584	21.79	0.43	9.5	0.98	0.029	0.001
2030000	22.16	1.63E-09	-5.79	1584	22.13	0.43	9.7	0.99	0.029	0.001
2080000	22.28	2.36E-09	-5.63	1584	22.22	0.44	9.7	0.99	0.029	0.001
2680000	23.12	1.39E-09	-5.86	1441	22.70	0.45	9.1	0.96	0.028	0.001
2760000	23.25	1.71E-09	-5.77	1441	23.18	0.46	9.3	0.97	0.028	0.001
2840000	23.41	1.94E-09	-5.71	1441	23.33	0.46	9.4	0.97	0.028	0.001
3340000	24.03	1.25E-09	-5.90	1299	23.72	0.47	8.7	0.94	0.027	0.001
3390000	24.13	2.02E-09	-5.69	1299	24.08	0.47	8.8	0.95	0.027	0.001
3440000	24.30	3.32E-09	-5.48	1299	24.22	0.48	8.9	0.95	0.027	0.001
3710000	25.18	3.26E-09	-5.49	1175	24.74	0.49	8.3	0.92	0.026	0.001
3760000	25.39	4.08E-09	-5.39	1175	25.28	0.50	8.6	0.93	0.026	0.001
3930000	25.96	3.41E-09	-5.47	1068	25.67	0.50	8.0	0.90	0.025	0.001
3960000	26.15	6.20E-09	-5.21	1068	26.06	0.51	8.2	0.91	0.025	0.001
4000000	26.37	5.38E-09	-5.27	1068	26.26	0.52	8.3	0.92	0.025	0.001

Table H.27. Fatigue crack growth data for test Specimen #55-66 - AWS A5.28, R=0.6, 60Hz. (continued)

Fatigue Crack Growth Rate Calculations
Secant Method
Specimen 55-66 – AWS 5.28, R=0.6

B (m)	0.0058
W (m)	0.05091
a_0 (mm)	12.52

N (cycles)	a (mm)	da/dN (m/cycle)	log(da/dN)	ΔP (N)	a_{avg} (mm)	$\alpha = a_{avg}/W$ (≥0.2)	ΔK (MPa√m)	log (ΔK) (MPa√m)	W-a	$(4/\pi)*(K_{max}/\sigma_{YS})^2$
4200000	27.00	3.20E-09	-5.50	961	26.68	0.52	7.7	0.88	0.024	0.001
4235000	27.09	2.31E-09	-5.64	961	27.04	0.53	7.8	0.89	0.024	0.001
4260000	27.21	4.96E-09	-5.30	961	27.15	0.53	7.9	0.90	0.024	0.001
4520000	27.90	2.67E-09	-5.57	872	27.56	0.54	7.4	0.87	0.023	0.001
4560000	28.10	4.95E-09	-5.31	872	28.00	0.55	7.6	0.88	0.023	0.001
4760000	28.67	2.85E-09	-5.55	801	28.38	0.56	7.1	0.85	0.022	0.001
4800000	28.77	2.45E-09	-5.61	801	28.72	0.56	7.3	0.86	0.022	0.001
5000000	29.27	2.51E-09	-5.60	730	29.02	0.57	6.8	0.83	0.022	0.001
5050000	29.40	2.54E-09	-5.60	730	29.33	0.58	7.0	0.84	0.022	0.001
5300000	29.98	2.33E-09	-5.63	658	29.69	0.58	6.4	0.81	0.021	0.001
5340000	30.04	1.50E-09	-5.82	658	30.01	0.59	6.6	0.82	0.021	0.001
5640000	30.55	1.70E-09	-5.77	605	30.29	0.60	6.2	0.79	0.020	0.001
5690000	30.65	1.94E-09	-5.71	605	30.60	0.60	6.3	0.80	0.020	0.001
5990000	31.18	1.77E-09	-5.75	552	30.91	0.61	5.9	0.77	0.020	0.001
6040000	31.28	2.16E-09	-5.67	552	31.23	0.61	6.1	0.78	0.020	0.001
6540000	31.86	1.15E-09	-5.94	499	31.57	0.62	5.6	0.75	0.019	0.000
6590000	31.98	2.42E-09	-5.62	499	31.92	0.63	5.8	0.76	0.019	0.001
6640000	32.11	2.56E-09	-5.59	499	32.04	0.63	5.9	0.77	0.019	0.001
7140000	32.80	1.40E-09	-5.86	463	32.45	0.64	5.6	0.75	0.018	0.000
7240000	32.92	1.19E-09	-5.92	463	32.86	0.65	5.8	0.77	0.018	0.001
7740000	33.66	1.48E-09	-5.83	427	33.29	0.65	5.6	0.75	0.017	0.000
7790000	33.72	1.13E-09	-5.95	427	33.69	0.66	5.8	0.76	0.017	0.001
8290000	34.37	1.29E-09	-5.89	392	34.04	0.67	5.5	0.74	0.017	0.000
8655000	34.87	1.39E-09	-5.86	356	34.62	0.68	5.3	0.72	0.016	0.000
9205000	35.41	9.71E-10	-6.01	321	35.14	0.69	5.0	0.70	0.016	0.000
9265000	35.47	9.67E-10	-6.01	321	35.44	0.70	5.2	0.71	0.015	0.000
9885000	35.97	8.11E-10	-6.09	290	35.72	0.70	4.8	0.68	0.015	0.000
9945000	36.03	9.83E-10	-6.01	290	36.00	0.71	5.0	0.70	0.015	0.000
10545000	36.54	8.58E-10	-6.07	258	36.29	0.71	4.6	0.66	0.014	0.000
10645000	36.58	4.10E-10	-6.39	258	36.56	0.72	4.7	0.67	0.014	0.000
10745000	36.65	6.90E-10	-6.16	258	36.62	0.72	4.7	0.67	0.014	0.000
11345000	37.16	8.40E-10	-6.08	236	36.91	0.72	4.5	0.65	0.014	0.000
12145000	37.72	6.99E-10	-6.16	213	37.44	0.74	4.3	0.63	0.013	0.000
12224500	37.77	6.79E-10	-6.17	213	37.74	0.74	4.4	0.65	0.013	0.000
13145000	38.31	5.86E-10	-6.23	191	38.04	0.75	4.1	0.62	0.013	0.000
14945000	38.88	3.17E-10	-6.50	169	38.59	0.76	3.9	0.59	0.012	0.000
15154500	38.95	3.20E-10	-6.50	169	38.91	0.76	4.1	0.61	0.012	0.000
15345000	39.06	5.88E-10	-6.23	169	39.00	0.77	4.1	0.62	0.012	0.000
15545000	39.23	8.35E-10	-6.08	169	39.14	0.77	4.2	0.63	0.012	0.000
15645000	39.32	9.10E-10	-6.04	169	39.27	0.77	4.3	0.63	0.012	0.000

Table H.28. Fatigue crack growth data for test Specimen #73-4 - AWS A5.28, R=0.6, 60Hz.

Fatigue Crack Growth Rate Calculations

Secant Method

Specimen 73-4 – AWS 5.28, R=0.6

B (m)	0.0058
W (m)	0.05071
a_0 (mm)	12.56

N (cycles)	a (mm)	da/dN (m/cycle)	log(da/dN)	ΔP (N)	a_{avg} (mm)	$\alpha = a_{avg}/W$ (≥0.2)	log (ΔK) (Pa√m)	ΔK (MPa√m)	log (ΔK) (MPa√m)	W-a	$(4/\pi)*(K_{max}/\sigma_{YS})^2$
	12.56			0							
300000	14.08	5.05E-09	-5.30	3203	13.32	0.26	7.097	12.5	1.10	0.037	0.002
330000	14.31	7.90E-09	-5.10	3203	14.19	0.28	7.117	13.1	1.12	0.036	0.003
430000	14.83	5.13E-09	-5.29	2882	14.57	0.29	7.079	12.0	1.08	0.036	0.002
460000	15.02	6.30E-09	-5.20	2882	14.92	0.29	7.087	12.2	1.09	0.036	0.002
590000	15.53	3.98E-09	-5.40	2597	15.27	0.30	7.050	11.2	1.05	0.035	0.002
620000	15.66	4.27E-09	-5.37	2597	15.60	0.31	7.057	11.4	1.06	0.035	0.002
770000	16.17	3.42E-09	-5.47	2349	15.92	0.31	7.020	10.5	1.02	0.035	0.002
800000	16.28	3.40E-09	-5.47	2349	16.22	0.32	7.027	10.6	1.03	0.034	0.002
1030000	16.78	2.17E-09	-5.66	2117	16.53	0.33	6.988	9.7	0.99	0.034	0.001
1070000	16.88	2.50E-09	-5.60	2117	16.83	0.33	6.995	9.9	1.00	0.034	0.001
1100000	16.96	2.77E-09	-5.56	2117	16.92	0.33	6.997	9.9	1.00	0.034	0.001
1150000	17.16	4.08E-09	-5.39	2224	17.06	0.34	7.022	10.5	1.02	0.034	0.002
1190000	17.28	2.82E-09	-5.55	2224	17.22	0.34	7.025	10.6	1.03	0.033	0.002
1230000	17.39	2.88E-09	-5.54	2224	17.33	0.34	7.028	10.7	1.03	0.033	0.002
1270000	17.59	5.05E-09	-5.30	2402	17.49	0.34	7.065	11.6	1.06	0.033	0.002
1290000	17.67	4.10E-09	-5.39	2402	17.63	0.35	7.068	11.7	1.07	0.033	0.002
1310000	17.85	8.55E-09	-5.07	2402	17.76	0.35	7.070	11.8	1.07	0.033	0.002
1330000	18.26	2.09E-08	-4.68	2580	18.05	0.36	7.108	12.8	1.11	0.032	0.002
1340000	18.35	8.70E-09	-5.06	2580	18.31	0.36	7.114	13.0	1.11	0.032	0.003
1350000	18.47	1.15E-08	-4.94	2580	18.41	0.36	7.116	13.1	1.12	0.032	0.003
1370000	18.77	1.55E-08	-4.81	2669	18.62	0.37	7.135	13.7	1.14	0.032	0.003
1380000	18.96	1.89E-08	-4.72	2669	18.87	0.37	7.141	13.8	1.14	0.032	0.003
1390000	19.10	1.34E-08	-4.87	2669	19.03	0.38	7.144	13.9	1.14	0.032	0.003
1400000	19.33	2.30E-08	-4.64	2669	19.21	0.38	7.148	14.1	1.15	0.031	0.003
1420000	19.69	1.83E-08	-4.74	2758	19.51	0.38	7.169	14.8	1.17	0.031	0.003
1425000	19.96	5.22E-08	-4.28	2758	19.82	0.39	7.176	15.0	1.18	0.031	0.003
1430000	20.01	1.16E-08	-4.94	2758	19.98	0.39	7.180	15.1	1.18	0.031	0.003
1445000	20.33	2.14E-08	-4.67	2847	20.17	0.40	7.198	15.8	1.20	0.030	0.004
1450000	20.44	2.04E-08	-4.69	2847	20.39	0.40	7.203	15.9	1.20	0.030	0.004
1455000	20.61	3.46E-08	-4.46	2847	20.52	0.40	7.206	16.1	1.21	0.030	0.004
1465000	20.89	2.83E-08	-4.55	2936	20.75	0.41	7.224	16.8	1.22	0.030	0.004
1468000	21.03	4.43E-08	-4.35	2936	20.96	0.41	7.229	17.0	1.23	0.030	0.004
1471000	21.18	5.10E-08	-4.29	2936	21.10	0.42	7.232	17.1	1.23	0.030	0.004
1481000	21.52	3.38E-08	-4.47	3025	21.35	0.42	7.251	17.8	1.25	0.029	0.005
1484000	21.68	5.30E-08	-4.28	3025	21.60	0.43	7.257	18.1	1.26	0.029	0.005
1487000	21.78	3.37E-08	-4.47	3025	21.73	0.43	7.260	18.2	1.26	0.029	0.005
1495000	22.20	5.29E-08	-4.28	3113	21.99	0.43	7.279	19.0	1.28	0.029	0.005
1498000	22.33	4.30E-08	-4.37	3113	22.26	0.44	7.285	19.3	1.29	0.028	0.006
1501000	22.53	6.67E-08	-4.18	3113	22.43	0.44	7.289	19.5	1.29	0.028	0.006
1509000	23.06	6.64E-08	-4.18	3203	22.79	0.45	7.310	20.4	1.31	0.028	0.006

Table H.29. Fatigue crack growth data for test Specimen #73-4 - AWS A5.28, R=0.6, 60Hz. (continued)

Fatigue Crack Growth Rate Calculations

Secant Method

Specimen 73-4 – AWS 5.28, R=0.6

B (m)	0.0058
W (m)	0.05071
a_0 (mm)	12.56

N (cycles)	a (mm)	da/dN (m/cycle)	log(da/dN)	ΔP (N)	a_{avg} (mm)	$\alpha = a_{avg}/W$ (≥0.2)	log (ΔK) (Pa√m)	ΔK (MPa√m)	log (ΔK) (MPa√m)	W-a	$(4/\pi)*(K_{max}/\sigma_{YS})^2$
1512000	23.18	4.03E-08	-4.39	3203	23.12	0.46	7.318	20.8	1.32	0.028	0.006
1515000	23.41	7.67E-08	-4.12	3203	23.30	0.46	7.322	21.0	1.32	0.027	0.007
1523000	24.02	7.60E-08	-4.12	3291	23.71	0.47	7.344	22.1	1.34	0.027	0.007
1525000	24.22	1.00E-07	-4.00	3291	24.12	0.48	7.354	22.6	1.35	0.026	0.008
1527000	24.46	1.20E-07	-3.92	3291	24.34	0.48	7.360	22.9	1.36	0.026	0.008
1532000	24.86	8.08E-08	-4.09	3381	24.66	0.49	7.380	24.0	1.38	0.026	0.009
1533000	24.99	1.28E-07	-3.89	3381	24.93	0.49	7.387	24.4	1.39	0.026	0.009
1534000	25.12	1.30E-07	-3.89	3381	25.05	0.49	7.390	24.6	1.39	0.026	0.009
1539000	25.75	1.26E-07	-3.90	3470	25.43	0.50	7.411	25.8	1.41	0.025	0.010
1541000	26.00	1.23E-07	-3.91	3470	25.87	0.51	7.423	26.5	1.42	0.025	0.010
1543000	26.26	1.34E-07	-3.87	3470	26.13	0.52	7.430	26.9	1.43	0.024	0.011
1546000	26.73	1.54E-07	-3.81	3558	26.49	0.52	7.451	28.2	1.45	0.024	0.012
1547000	26.91	1.82E-07	-3.74	3558	26.82	0.53	7.460	28.8	1.46	0.024	0.012
1548000	27.09	1.85E-07	-3.73	3558	27.00	0.53	7.465	29.2	1.47	0.024	0.013
1550000	27.45	1.78E-07	-3.75	3648	27.27	0.54	7.484	30.5	1.48	0.023	0.014
1551000	27.62	1.68E-07	-3.77	3648	27.53	0.54	7.491	31.0	1.49	0.023	0.014
1552000	27.79	1.73E-07	-3.76	3648	27.70	0.55	7.496	31.3	1.50	0.023	0.015
1554000	28.15	1.79E-07	-3.75	3736	27.97	0.55	7.514	32.7	1.51	0.023	0.016
1555000	28.34	1.96E-07	-3.71	3736	28.25	0.56	7.523	33.3	1.52	0.022	0.017
1556000	28.62	2.77E-07	-3.56	3736	28.48	0.56	7.530	33.9	1.53	0.022	0.017
1557000	28.85	2.30E-07	-3.64	3914	28.74	0.57	7.558	36.1	1.56	0.022	0.019
1558000	29.17	3.19E-07	-3.50	3914	29.01	0.57	7.566	36.8	1.57	0.022	0.020
1559000	29.39	2.21E-07	-3.66	3914	29.28	0.58	7.575	37.5	1.57	0.021	0.021

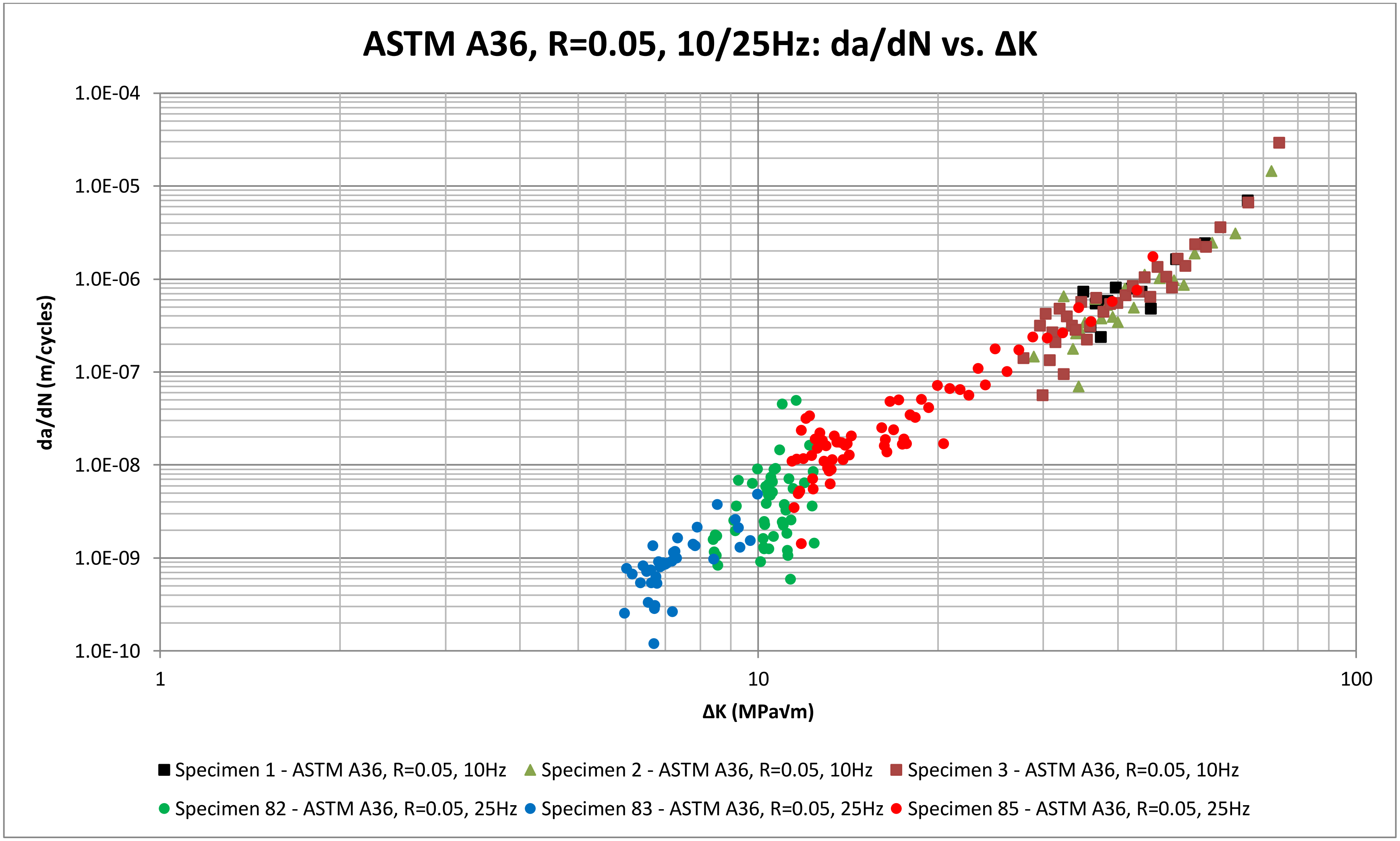

Figure H.1. Fatigue crack growth data for ASTM A36 at stress ratio R=0.05 with a test frequency of 25Hz and 10Hz.

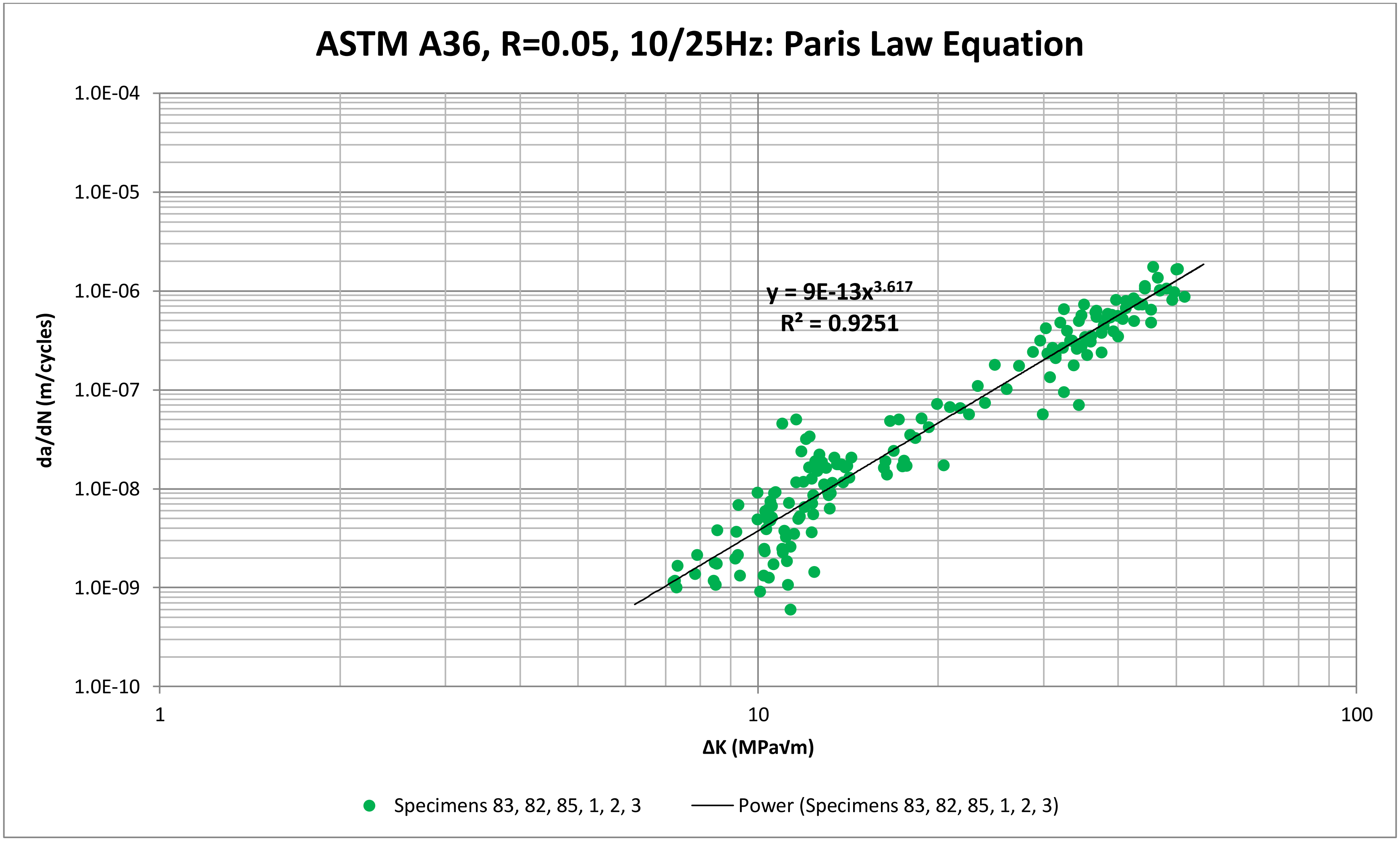

Figure H.2. Crack growth rate data and Paris Equation for ASTM A36 at stress ratio R=0.05 with a test frequency of 10 and 25Hz.

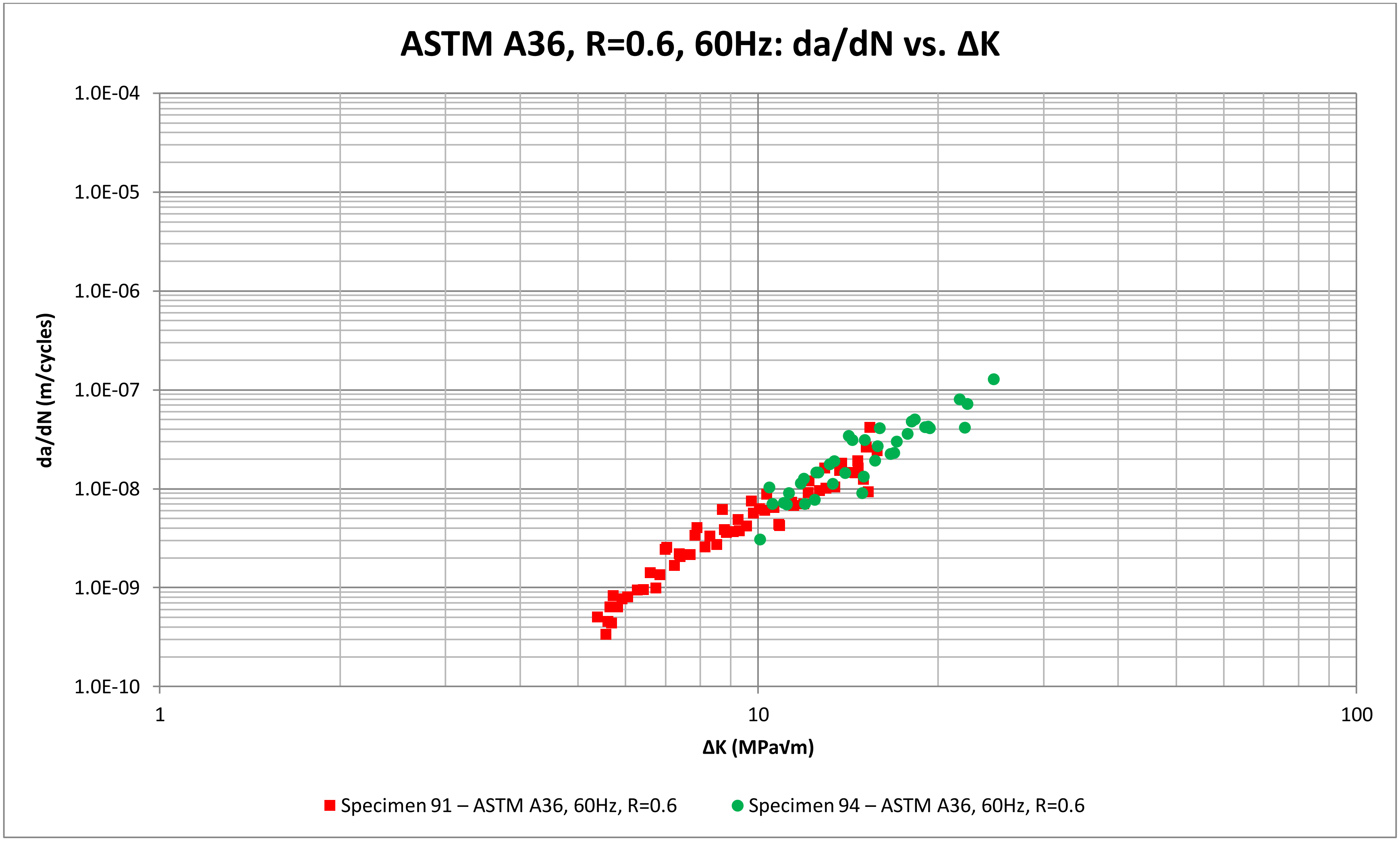

Figure H.3. Fatigue crack growth data for ASTM A36 at stress ratio R=0.6 with a test frequency of 60Hz.

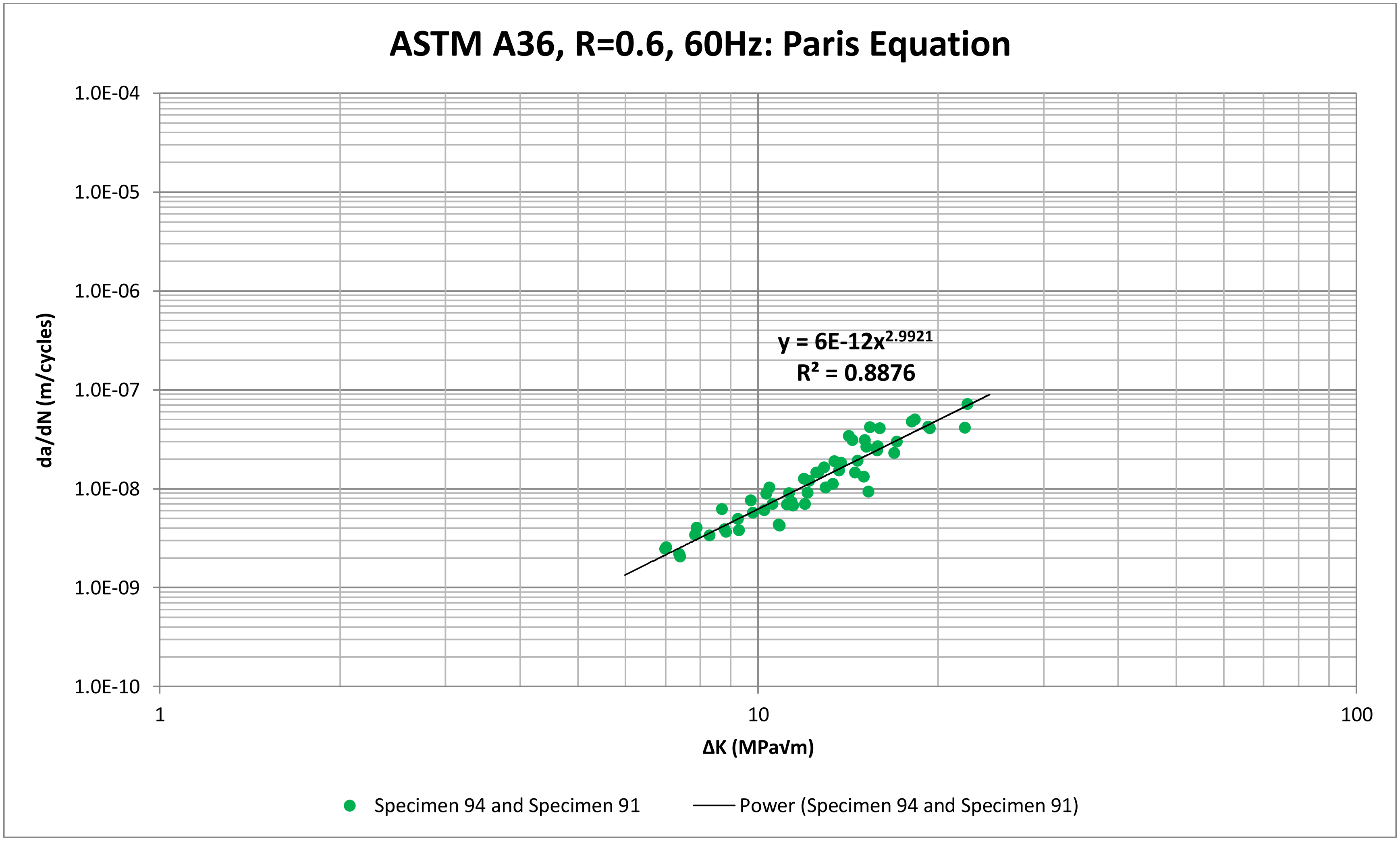

Figure H.4. Fatigue crack growth data and Paris Equation for ASTM A36 at stress ratio R=0.6 with a test frequency of 60Hz.

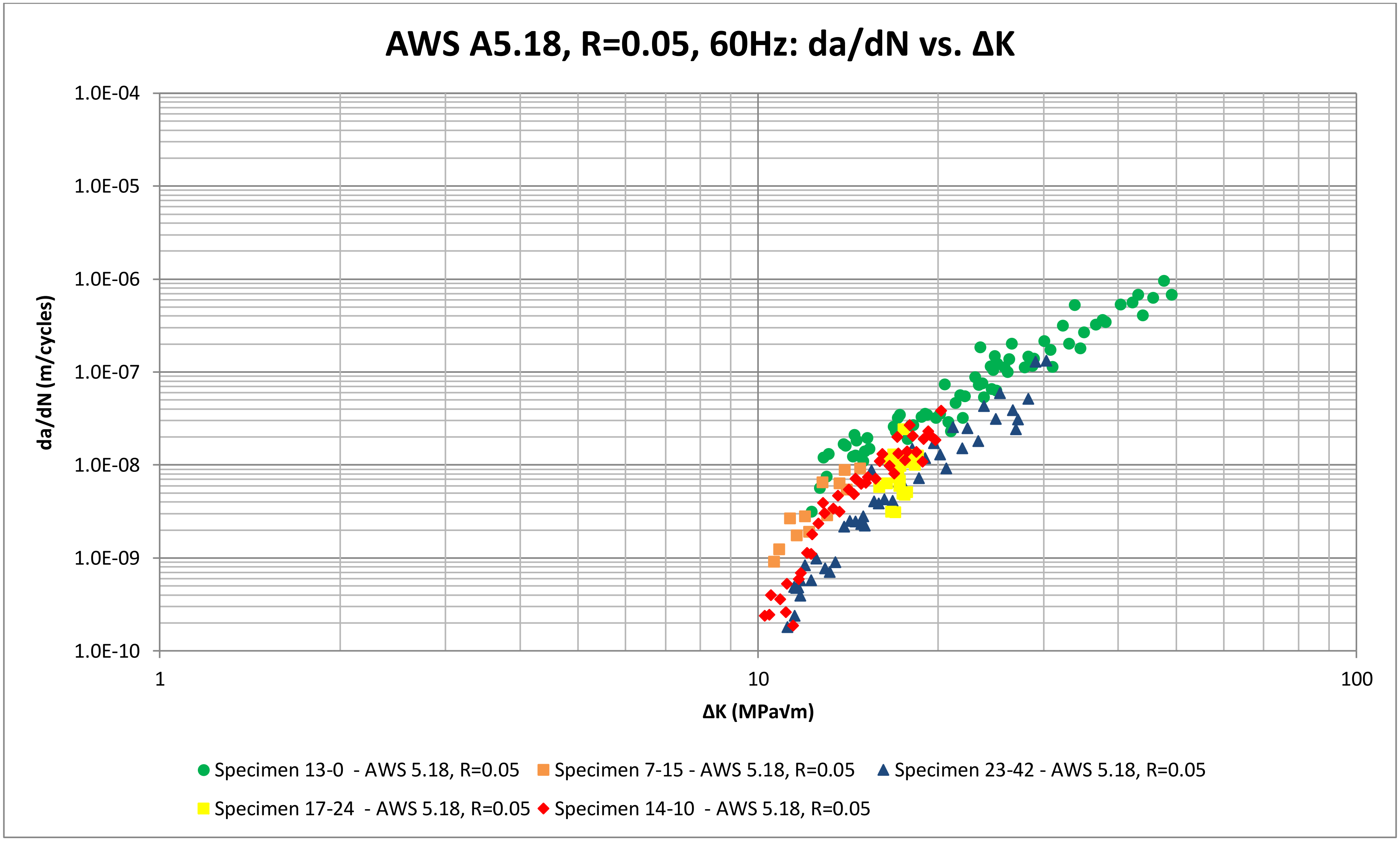

Figure H.5. Fatigue crack growth data for AWS A5.18 at stress ratio R=0.05 with a test frequency of 60Hz.

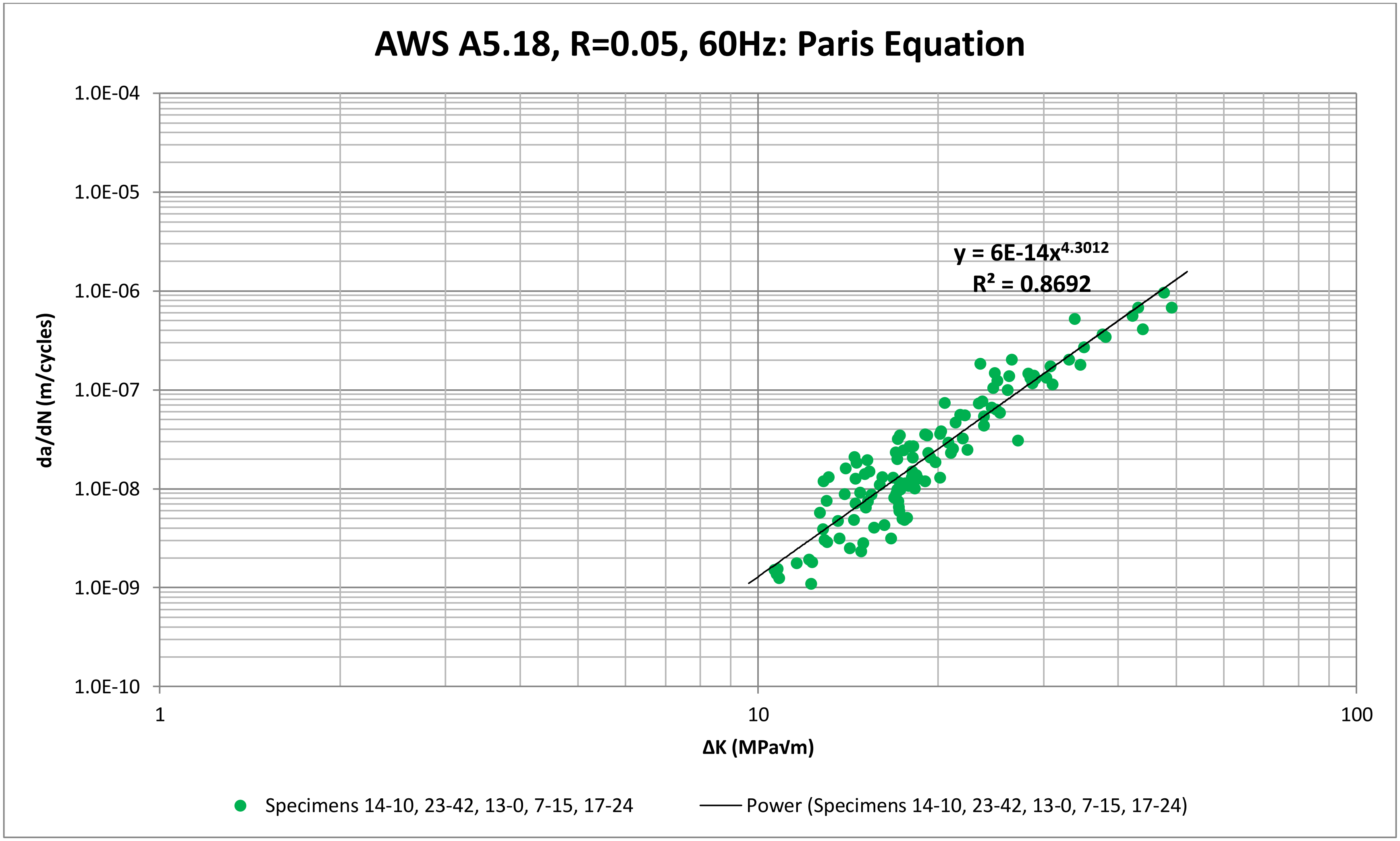

Figure H.6. Crack growth rate data and Paris Equation for AWS A5.18 at stress ratio R=0.6 with a test frequency of 60Hz.

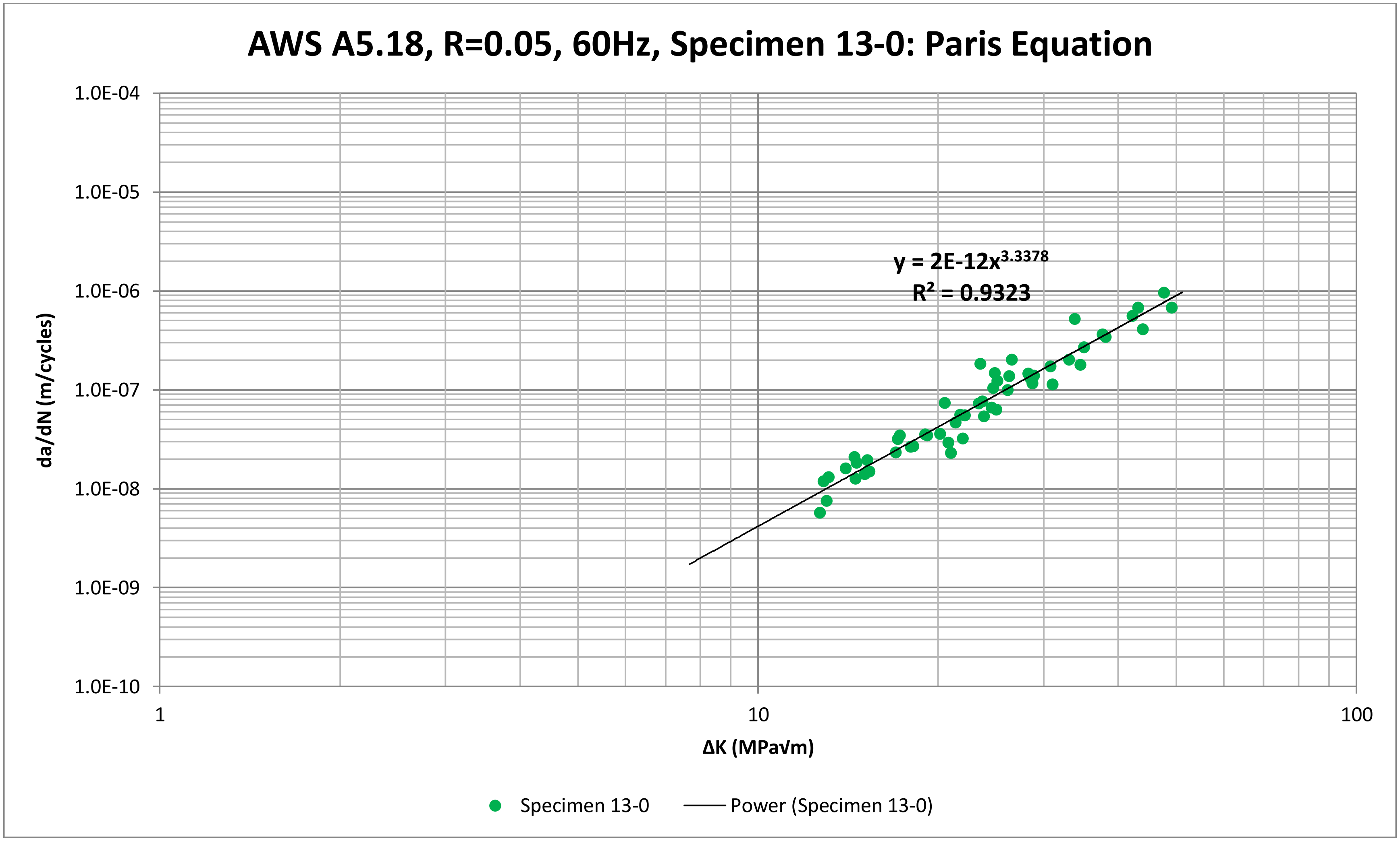

Figure H.7. Paris Equation for Specimen 13-0 AWS A5.18 at stress ratio R=0.6 with a test frequency of 60Hz.

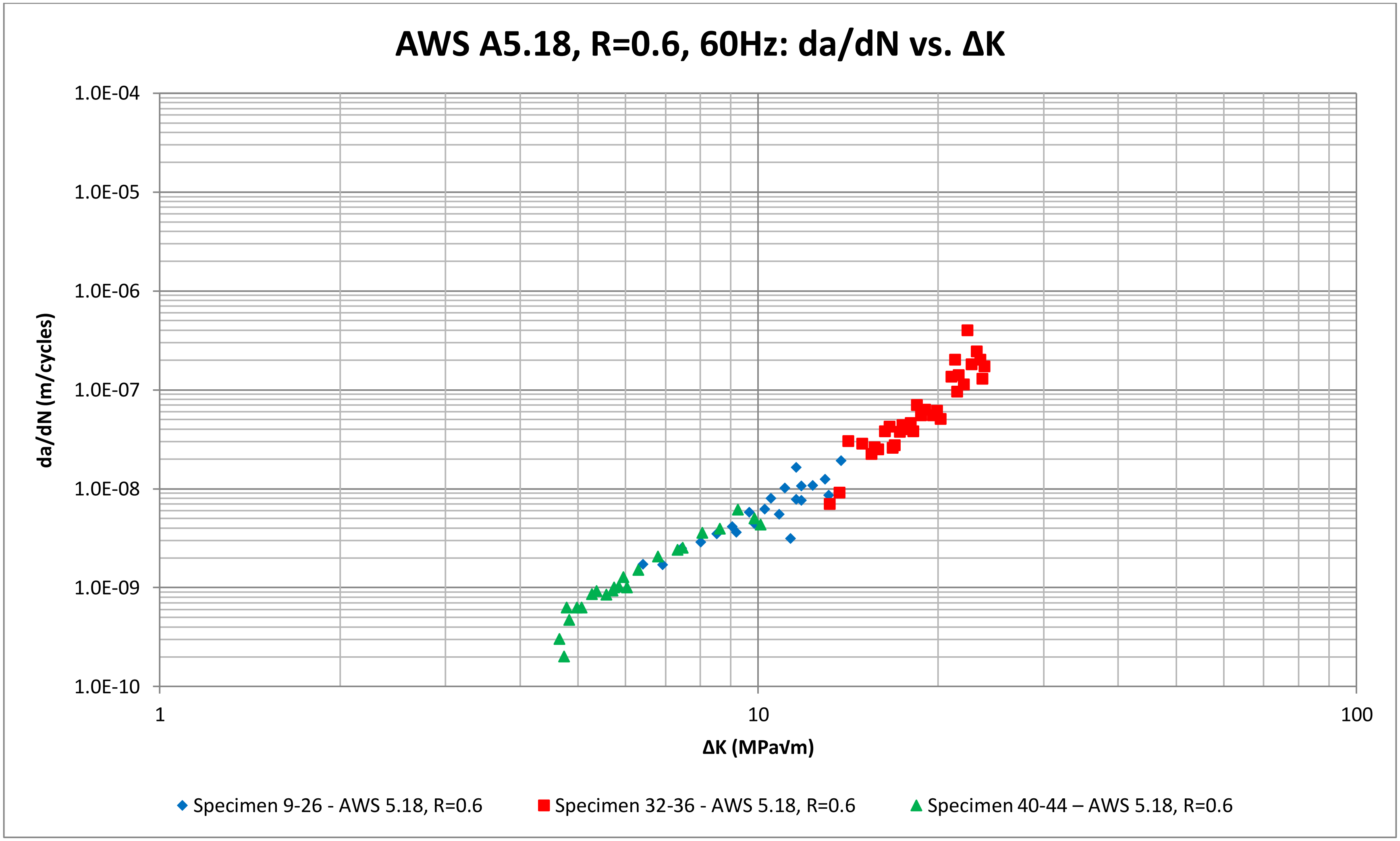

Figure H.8. Fatigue crack growth data for AWS A5.18 at stress ratio R=0.6 with a test frequency of 60Hz.

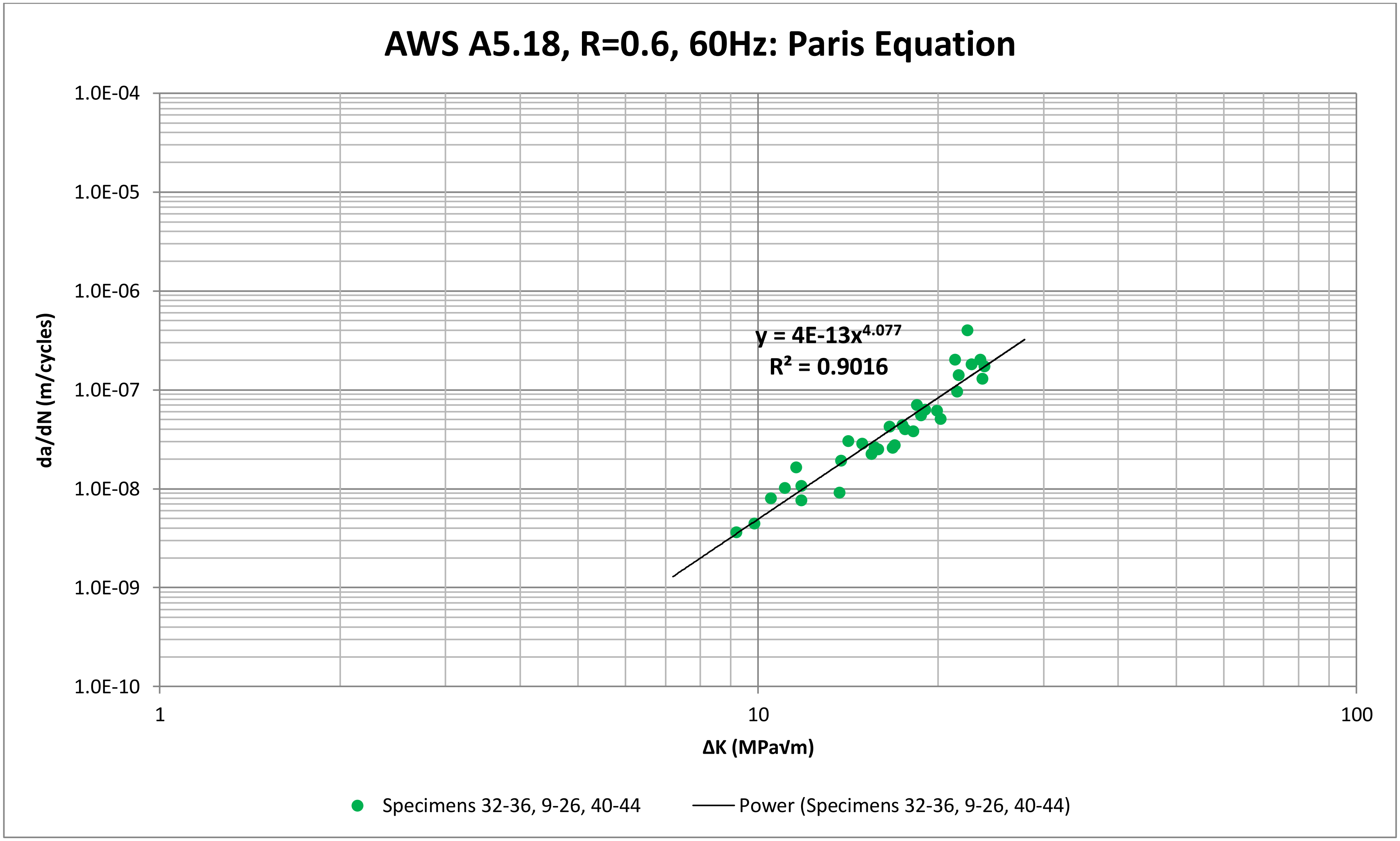

Figure H.9. Crack growth rate data and Paris Equation for AWS A5.18 at stress ratio R=0.6 with a test frequency of 60Hz.

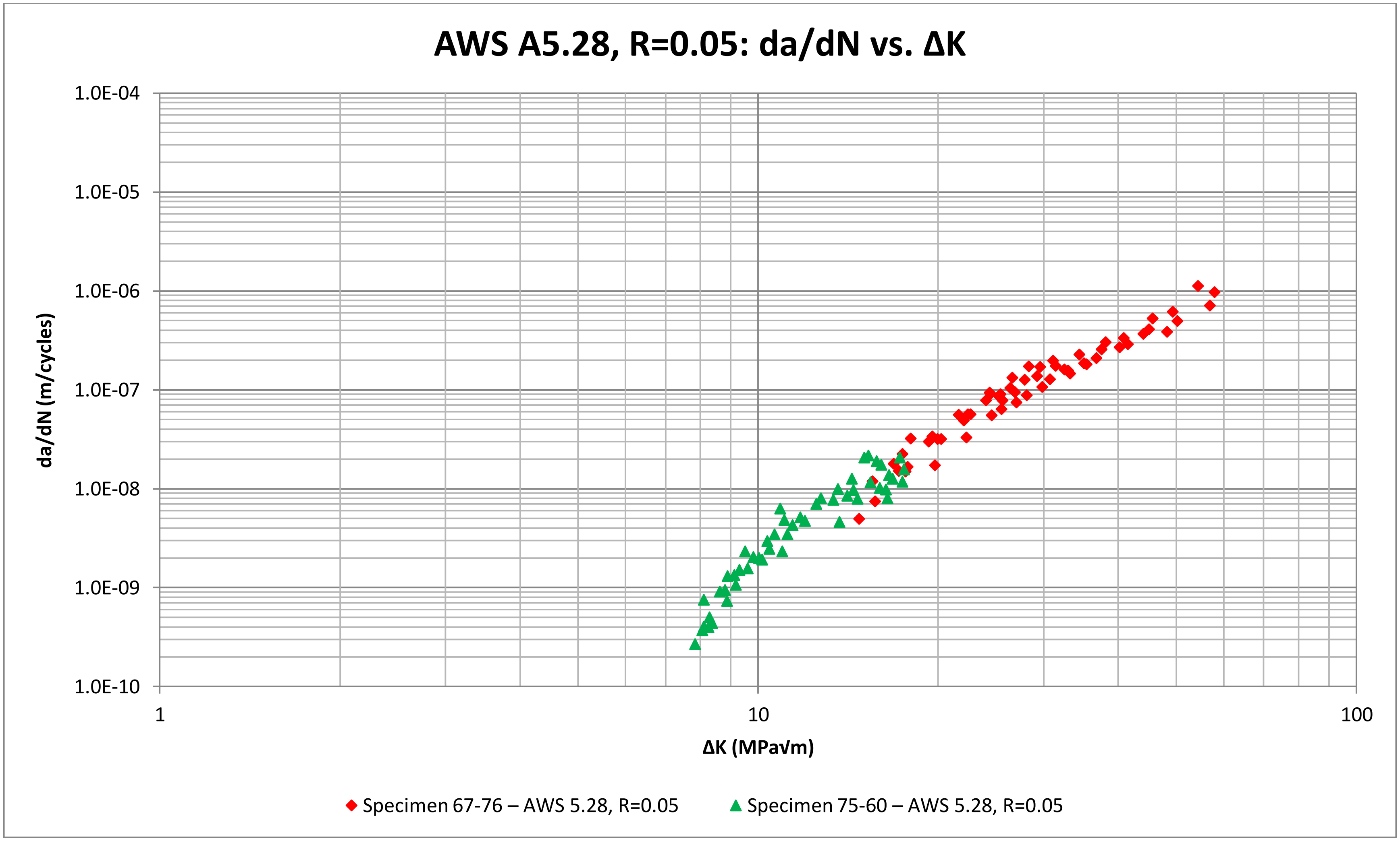

Figure H.10. Fatigue crack growth data for AWS A5.28 at stress ratio R=0.05 with a test frequency of 60Hz.

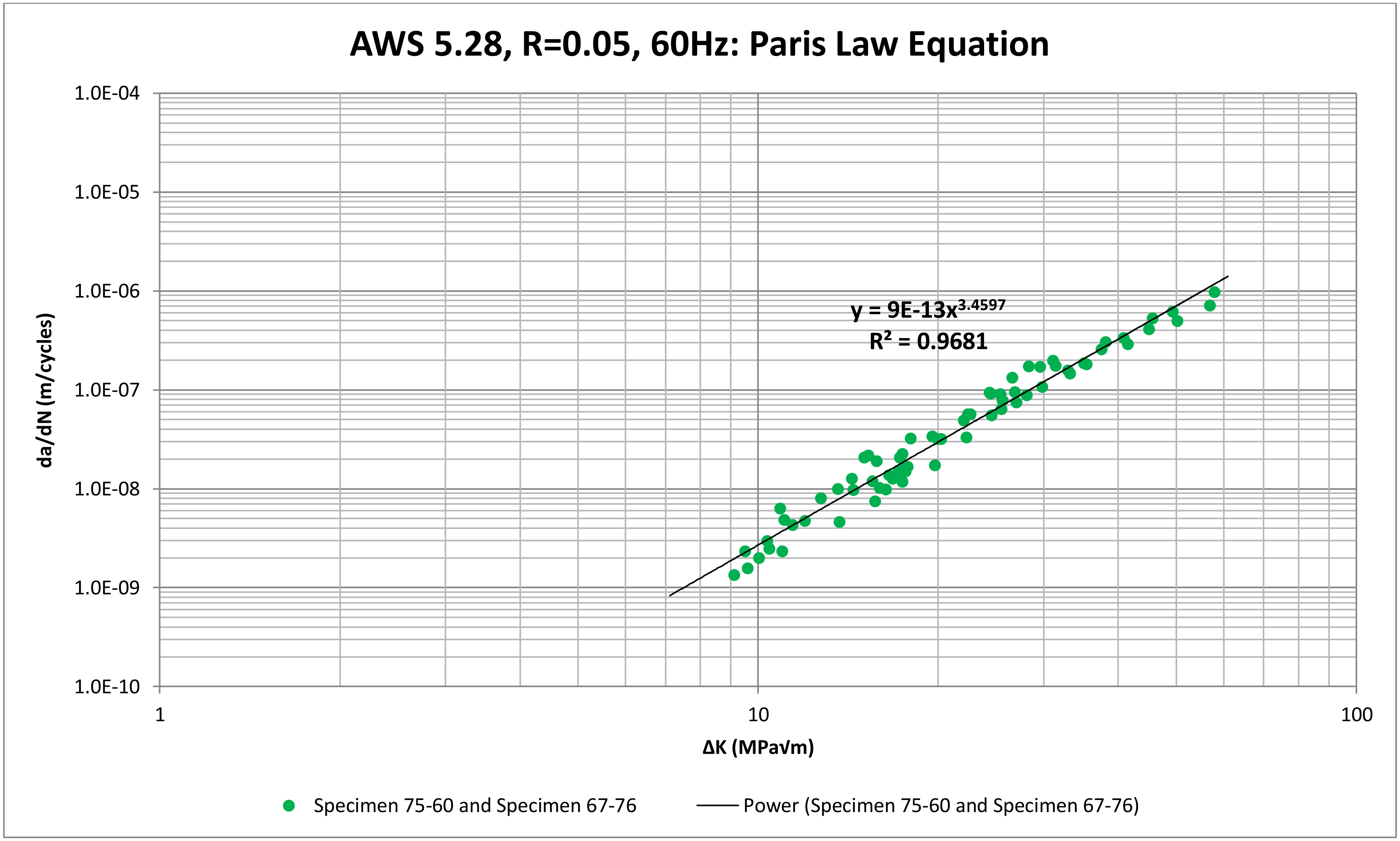

Figure H.11. Crack growth rate data and Paris Equation for AWS A5.28 at stress ratio R=0.05 with a test frequency of 60Hz.

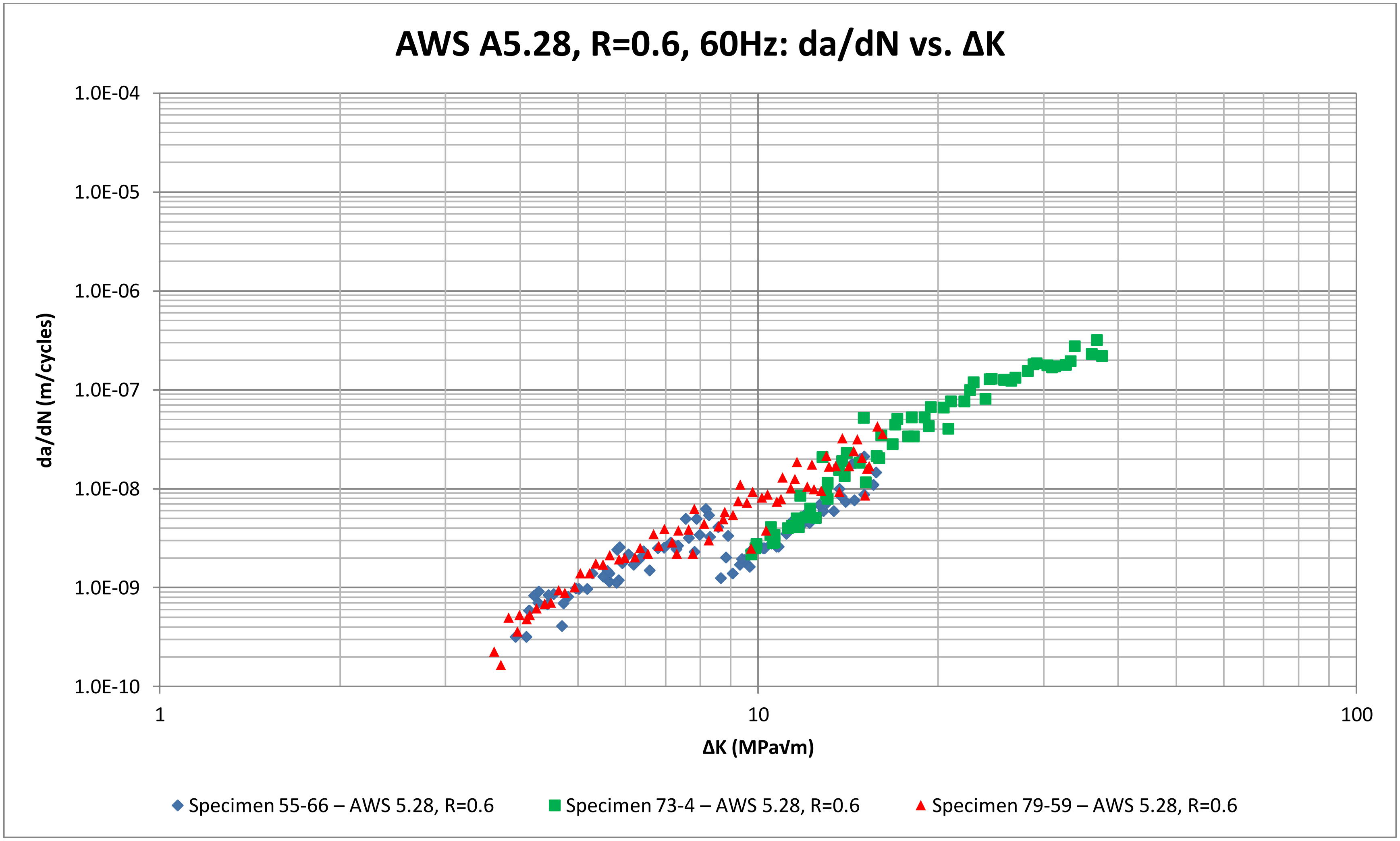

Figure H.12. Fatigue crack growth data for AWS A5.28 at stress ratio R=0.6 with a test frequency of 60Hz.

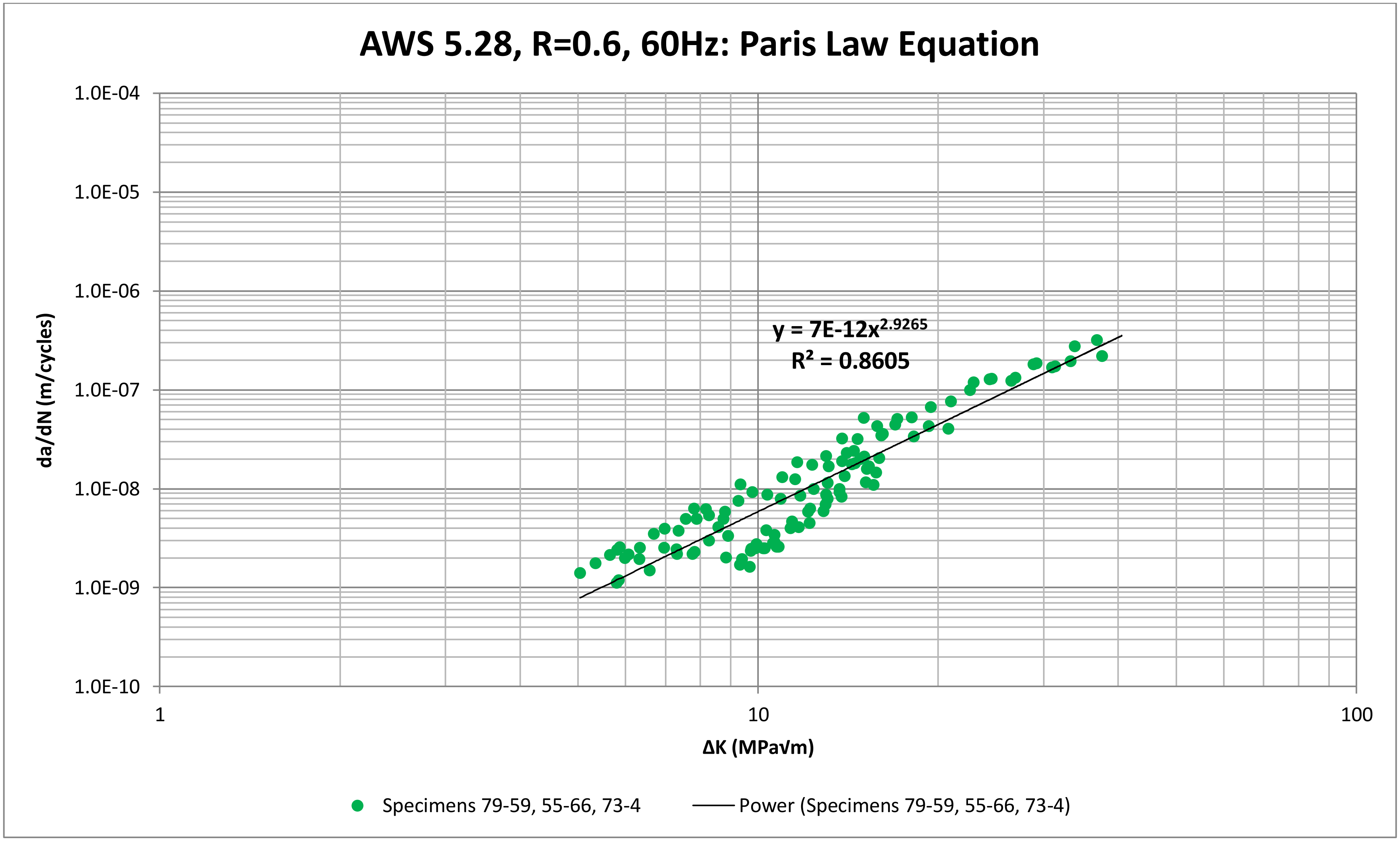

Figure H.13. Crack growth rate data and Paris Equation for AWS A5.28 at stress ratio R=0.6 with a test frequency of 60Hz.

Appendix I: Test Machine Information

Tensile Test Machine

Instron Model 5500R test machine, 44kN (10,000lb_f) load cell, Bluehill 2 Software Version 2.16.

Fatigue Test Machine

MTS Model 312.21 Serial Number 803, MTS 793 Software Version 5.4.

Hardness Test Machine

Wilson/Rockwell Hardness Tester Series 500, Model B523T.

Light Microscope

Olympus DHE3 Metallograph, Spot Insight Camera.

Scanning Electron Microscope

JEOL JSM 6510LV Scanning Electron Microscope.